



Poznan University of Technology

Faculty of Chemical Technology

Institute of Chemistry and Technical Electrochemistry
Division of Applied Electrochemistry



DOCTORAL DISSERTATION

***One-step assembly of metal-ion capacitors using
redox-active electrolytes***

*Jednoetapowy montaż kondensatorów metalo-jonowych
z wykorzystaniem elektrolitów redoks*

Adam Maćkowiak

Scientific discipline: Chemical Sciences

Scientific Supervisor:

Dr. Krzysztof Fic

Poznan, 2024

One-step assembly of metal-ion capacitors using redox-active electrolytes



European Research Council

Established by the European Commission

This thesis research was supported by **The European Research Council** within the **Starting Grant project** titled: *'If immortality unveil...'* – development of the novel types of energy storage systems with excellent long-term performance, (GA 759603) under European Unions' Horizon 2020 research and innovation programme. Also, this thesis research was supported by The European Research Council within the **Proof of Concept project** titled: *'It yet remains to see...'* - Hybrid electrochemical energy storage system of high power and improved cycle life, (GA 101138710) under European Unions' Horizon Europe research and innovation programme.

Principal investigator: Dr. Krzysztof Fic

Badania do niniejszej pracy prowadzone były przy wsparciu **Europejskiej Rady ds. Badań Naukowych** w ramach **projektu Starting Grant** pt.: *'If immortality unveil...'* – development of the novel types of energy storage systems with excellent long-term performance, (GA 759603) w ramach programu badań i innowacji Horizon 2020 Unii Europejskiej. Jednocześnie, badania do niniejszej pracy prowadzone były przy wsparciu Europejskiej Rady ds. Badań Naukowych w ramach **projektu Proof of Concept** pt.: *'It yet remains to see...'* - Hybrid electrochemical energy storage system of high power and improved cycle life, (GA 101138710) w ramach programu badań i innowacji Horizon Europe Unii Europejskiej.

Kierownik projektu: dr hab. inż. Krzysztof Fic, prof. PP



This research work has been partially realized in the frame of **BGF SSHN project** entitled „Metal-ion capacitors as the future of energy storage devices” granted from the **French Government**, France.

Część badań została przeprowadzona w ramach **projektu BGF SSHN** zatytułowanego „Kondensatory metalo-jonowe jako przyszłość urządzeń do magazynowania energii” finansowanego przez **Rząd Francuski**, Francja.



This work has been supported by the Polish National Agency for Academic Exchange (**NAWA**) under the **STER programme**, Towards Internationalization of Poznan University of Technology Doctoral School (2022-2024).

Praca ta została wsparta przez Narodową Agencję Wymiany Akademickiej (**NAWA**) w ramach **programu STER**, Towards Internationalization of Poznan University of Technology Doctoral School (2022-2024).

*“Be brave, be curious, be determined,
overcome the odds. It can be done.”*

Stephen Hawking

Acknowledgments

First of all, I would like to thank my wife, **Zuzanna**, for her constant support and great belief in me. Many times we fought, and many times I was late because I had to assemble cells but you were always there for me and supported me. Thank you, my love.

I am deeply grateful to my supervisor, **Dr. Krzysztof Fic**, for his unwavering belief and his investment in my both academic and personal development. His guidance has provided invaluable lessons in both academia and life, for which I am immensely grateful.

I would also like to extend my gratitude to **Dr. Paweł Jeżowski** for his academic guidance and mental support throughout my doctoral studies. Thank you for showing me the 'hybrid way' and for your assistance with my research work.

Deepest thanks to **Dr. Camelia Matei Ghimbeu** and **Prof. Dominic Rochefort** for allowing me to work in their teams in Mulhouse and Montreal. Both experiences were unforgettable adventures during which I learned a great deal.

Moreover, many thanks to all members of the **PowerSourcesGroup**, and especially **Maciej** (for our hours-long conversations about science, business, and life), **Przemek** (for our thorough investigations of CV figures), **Kuba** (for his frequent visits and life advice during conferences), **Paulina** (for always making the workday brighter), **Bartosz G.** (for enriching my vocabulary with many interesting phrases), **Anetta** (for always finding time to talk even when she was far away), **Justyna** (for our shared gelato moments and kitten photos), and **Adam** (for never saying 'I don't have time now', that I could always count on your support). Thanks to you, it was a wonderful time in my life!

I would like to thank my parents, **Anna** and **Romuald**, for their love, eternal support and wonderful upbringing that I have received from them. I would also like to thank **Adrian** and **Justyna** for always being there to lend a helping hand. Additionally, I want to express my gratitude to my **family in Kaczki** and **Łęgowo** for their support, faith, and for always providing a warm and welcoming environment where I could spend quality time.

Lastly, I would like to thank **Mikołaj** for always being there for me, and for sharing his honest opinions and abundance of joy with me.

In memory of

Danuta and Bernard Maćkowiak

Table of contents

Acknowledgments	5
Table of contents	6
Abstract	8
Abbreviations and symbols	10
Chapter I – Literature review	15
1. Motivation of the research	16
2. Electrochemical energy storage systems	18
3. Electrical double-layer capacitors (EDLCs)	23
3.1. The electric double-layer (EDL)	24
3.2. Cell construction and applications	26
3.3. Electrode materials	27
3.4. Electrolytes	30
4. Lithium-ion batteries (LIBs)	34
4.1. Principle of operation	35
4.2. Electrode materials	38
4.3. Electrolytes	41
4.4. SEI formation	43
5. Metal-ion capacitors (MICs)	45
5.1. Principle of operation	46
5.2. Lithium-ion capacitors (LICs)	47
5.3. Sodium-ion capacitors (NICs)	48
5.4. Potassium-ion capacitors (KICs)	50
5.5. Pre-insertion techniques	51
6. Electrochemical research techniques	56

**One-step assembly of metal-ion capacitors using
redox-active electrolytes**

7. Summary	59
Chapter II – Dissertation aims and outline	61
Chapter III – One-step assembly approach using thiocyanate additive	65
1. Context of the research and summary	68
2. Article 1	74
3. Manuscript 1	98
Chapter IV – Investigation of lithium intercalation process using SPECS	126
1. Context of the research and summary	129
2. Article 2	134
3. Manuscript 2	149
Chapter V – Redox-active additives to electrolyte for metal-ion capacitors	171
1. Context of the research and summary	173
2. Article 3	178
Chapter VI – Summary of the results	189
Articles not included in the dissertation	193
List of figures and tables	196
Scientific accomplishments	198
1. Publications	198
2. Patents and patent applications	200
3. Scientific conferences	202
4. Awards	205
5. Research projects	207
6. Memberships and trainings	208
Literature	209
Copyrights	222
Co-authorship statements	223

Abstract

The first chapter of the dissertation is dedicated to the literature review. It begins with an introduction to the motivation behind the conducted scientific research and a general overview of electrical energy storage systems. Subsequently, it highlights three main energy storage systems: electrical double-layer capacitors, lithium-ion batteries, and hybrid metal-ion capacitors. Each section focuses on describing the energy storage mechanism in the respective device, the electrode materials used, and the electrolytes employed. The advantages and disadvantages are emphasized, applications are listed, and the characteristic parameters of these devices are presented. The formation of the solid electrolyte interphase layer is also described, along with a discussion of the most popular hybrid capacitors: lithium-ion, sodium-ion, and potassium-ion. Current pre-insertion techniques used by researchers are also presented. The next part of the review describes the electrochemical techniques used, with particular emphasis on the step potential electrochemical spectroscopy (SPECS) method utilized in this dissertation. The entire review concludes with a summary.

The second chapter of the dissertation outlines the aims and objectives of the work, which are intended to help verify the proposed hypothesis. The hypothesis assumes the use of redox-active salt additives in the electrolyte to conduct a one-step assembly approach for metal-ion capacitors. The third chapter presents two studies (**A1** and **M1**) that confirm the hypothesis by demonstrating that redox electrolyte containing thiocyanate anions enable insertion of metal ions into the structure of the negative electrode in lithium-ion, sodium-ion, and potassium-ion capacitors. The fourth chapter of the dissertation presents two studies (**A2** and **M2**) that describe the use of the SPECS technique to study the intercalation of lithium ions into the graphite and the influence of an additional redox reaction on this process. The fifth chapter presents study **A3**, which discusses the use of redox additives other than thiocyanate salts in the electrolyte. The sixth chapter summarizes the results obtained from the research conducted for the dissertation. The final part presents the achievements of the dissertation author, along with a list of references and statements from co-authors.

Streszczenie

Rozdział pierwszy dysertacji jest poświęcony przeglądowi literatury. Rozpoczyna się od przedstawienia motywacji przeprowadzonych badań oraz ogólnego przeglądu systemów magazynowania energii elektrycznej. W dalszej części wyróżniono trzy główne systemy magazynowania energii: kondensatory podwójnej warstwy elektrycznej, ogniwa litowo-jonowe oraz hybrydowe kondensatory metalo-jonowe. W każdym rozdziale skupiono się na opisie mechanizmu magazynowania energii w danym urządzeniu, stosowanych materiałach elektrodowych oraz wykorzystywanych elektrolitach. Podkreślono wady i zalety, wymieniono zastosowania oraz przedstawiono charakterystyczne parametry tych urządzeń. Opisano również tworzenie się warstwy ochronnej elektrody ujemnej oraz omówiono najpopularniejsze hybrydowe kondensatory: litowo-jonowe, sodowo-jonowe i potasowo-jonowe. Przedstawiono także znane w literaturze techniki preinsercji. Kolejna część przeglądu opisuje stosowane techniki elektrochemiczne, ze szczególnym uwzględnieniem metody SPECS wykorzystanej w tej dysertacji. Całość wieńczy podsumowanie przeglądu literatury.

Rozdział drugi dysertacji opisuje cele i zadania pracy, które mają pomóc w weryfikacji założonej hipotezy. Hipoteza zakłada wykorzystanie dodatku soli redoks do elektrolitu w celu przeprowadzenia jednoetapowej metody montażu kondensatorów metalo-jonowych. W trzecim rozdziale zaprezentowano dwie prace (**A1** i **M1**), w których potwierdzono postawioną hipotezę, wykazując, że dzięki elektrolitowi redoks zawierającemu aniony rodankowe można zainsertować jony metalu w strukturę elektrody ujemnej w kondensatorach litowo-jonowych, sodowo-jonowych i potasowo-jonowych. Czwarta część dysertacji przedstawia dwie prace (**A2** i **M2**), które opisują wykorzystanie techniki SPECS do badań interkalacji jonów litu w strukturę grafitu oraz wpływ dodatkowej reakcji redoks na ten proces. Piąty rozdział przedstawia pracę **A3**, która omawia wykorzystanie innych niż sole rodankowe dodatków redoks do elektrolitu. Rozdział szósty podsumowuje wyniki otrzymane w ramach badań wykonanych do dysertacji. W ostatniej części przedstawione zostały osiągnięcia autora, wraz z wykazem literatury i oświadczeniami współautorów.

Abbreviations and symbols

Abbreviation	Description
A	– Surface area, m ²
AC	– Activated carbon
ACN	– Acetonitrile
Ag ₂ S	– Silver sulfide
Al	– Aluminium
B	– Diffusion parameter, A s ^{0.5}
BET	– Brunauer-Emmett-Teller isotherm
BMIMBF ₄	– 1-Butyl-3-methylimidazolium tetrafluoroborate
C	– Capacitance, F
C	– Theoretical graphite capacity (372 mAh g ⁻¹)
C ₂ H ₂ S	– Thiirene
C ₂ H ₄	– Ethylene
C ₂ H ₆	– Ethane
C ₆	– Carbon (graphite)
CE	– Counter electrode
C _{EDL}	– Capacitance from EDL, F
CNTs	– Carbon nanotubes
CO	– Carbon monoxide
CO ₂	– Carbon dioxide
COS	– Carbonyl sulfide
CS	– Carbon monosulfide
CS ₂	– Carbon disulfide
CsF	– Caesium fluoride
Cu	– Copper
CV	– Cyclic voltammetry
CVD	– Chemical vapour deposition
\tilde{D}	– Diffusion coefficient, m ² s ⁻¹
DEC	– Diethyl carbonate
DEG	– Diethylene glycol
DMC	– Dimethyl carbonate

**One-step assembly of metal-ion capacitors using
redox-active electrolytes**

DME	–	Dimethyl ether
E	–	Energy, Wh
ΔE	–	Potential change
EC	–	Ethylene carbonate
EDL	–	Electric double-layer capacitor
EDLC	–	Electrical double-layer capacitor
EDR	–	Equivalent distributed resistance
EDS	–	Energy dispersive spectroscopy
EES	–	Electrical energy storage system
EMIMBF ₄	–	1-Ethyl-3-methylimidazolium tetrafluoroborate
ESR	–	Equivalent series resistance
FEC	–	Fluoroethylene carbonate
GCPL	–	Galvanostatic cycling with potential limitation
GITT	–	Galvanostatic intermittent titration technique
I	–	Current, A
I _D	–	Diffusive current, A
I _{EDL}	–	EDL current, A
IL	–	Ionic liquid
I _R	–	Residual current, A
I _T	–	Total current, A
KERS	–	Kinetic energy recovery system
KIC	–	Potassium-ion capacitor
KPF ₆	–	Potassium hexafluorophosphate
L	–	Sample thickness, m
LCO	–	Lithium cobalt oxide, LiCoO ₂
LEDC	–	Lithium ethylene decarbonate
LFP	–	Lithium iron phosphate, LiFePO ₄
LIB	–	Lithium-ion battery
LiBF ₄	–	Lithium tetrafluoroborate
LiBOB	–	Lithium bis(oxalato)borate
LiBr	–	Lithium bromide
LIC	–	Lithium-ion capacitor
LiF	–	Lithium fluoride

**One-step assembly of metal-ion capacitors using
redox-active electrolytes**

LiNO ₃	–	Lithium nitrate
LiOAc	–	Lithium acetate
LiOH	–	Lithium hydroxide
LiOR	–	Lithium alkyl carbonate
LiPF ₆	–	Lithium hexafluorophosphate
LiSCN	–	Lithium thiocyanate
LiTFSI	–	Lithium bis(trifluoromethanesulfonyl)imide
Li ₂ CO ₃	–	Lithium carbonate
Li ₂ C ₄ O ₄	–	Lithium squarate
Li ₂ MnO ₃	–	Lithium manganite
Li ₂ O	–	Lithium oxide
Li ₂ RuO ₃	–	Lithium ruthenate
Li ₂ S	–	Lithium sulfide
Li ₅ FeO ₄	–	LFO, Lithium rich lithium ion
Li ₆ CoO ₄	–	Lithium cobalt oxide
LLTO	–	Lithium lanthanum titanium oxide
LLZO	–	Lithium lanthanum zirconium oxide
LMO	–	Lithium manganese oxide, LiMn ₂ O ₄
LTO	–	Lithium titanate, Li ₄ Ti ₅ O ₁₂
MIC	–	Metal-ion capacitor
MnO ₂	–	Manganese dioxide
MoS ₂	–	Molybdenum disulfide
MWCNTs	–	Multi-walled carbon nanotubes
NaClO ₄	–	Sodium perchlorate
NaOAc	–	Sodium acetate
NCA	–	Lithium nickel-cobalt-aluminum oxide, LiNiCoAlO ₂
NEC	–	Nippon Electric Company
Ni-Cd	–	Nickel-cadmium battery
Ni-MH	–	Nickel-hydrogen battery
NiC	–	Sodium-ion capacitor
NMP	–	N-Methyl-2-pyrrolidone
NMC	–	Lithium nickel-manganese-cobalt oxide, LiNiMnCoO ₂
OCV	–	Open circuit voltage, V

**One-step assembly of metal-ion capacitors using
redox-active electrolytes**

PAN	–	Polyacrylonitrile
PANI	–	Polyaniline
PAS	–	Polyacenic semiconductive
PbO ₂	–	Lead (IV) oxide
PC	–	Propylene carbonate
PE	–	Polyethylene
PEG	–	Polyethylene glycol
PEIS	–	Potentiostatic electrochemical impedance spectroscopy
PEO	–	Polyethylene oxide
PP	–	Polypropylene
PTFE	–	Poly(tetrafluoroethylene)
PVDF	–	Poly(vinylidene fluoride)
RE	–	Reference electrode
R _{EDL}	–	Resistance of EDL, Ohm
r _p	–	Particle radius, m
RT	–	Room temperature, 21°C
RuO ₂	–	Ruthenium dioxide
SCN ⁻	–	Thiocyanate anion
SEI	–	Solid electrolyte interphase
SEM	–	Scanning electron microscopy
SHE	–	Standard hydrogen electrode
SO	–	Sulfur monoxide
SOHIO	–	Standard Oil Company of Ohio
SPECS	–	Step potential electrochemical spectroscopy
SWCNTs	–	Single-walled carbon nanotubes
t	–	Rest time, s
τ	–	Time interval, s
TEABF ₄	–	Tetraethylammonium tetrafluoroborate
TEM	–	Transmission electron microscopy
TiN	–	Titanium nitride
Ti ₂ S	–	Titanium sulfide
TMP	–	Trimethyl phosphate
t _p	–	Pulse duration, s

**One-step assembly of metal-ion capacitors using
redox-active electrolytes**

TPP	–	Triphenyl phosphate
U	–	Voltage, V
UPS	–	Uninterruptible power supply
V	–	Volume, dm ³
VC	–	Vinylene carbonate
VEC	–	Vinyl ethylene carbonate
WE	–	Working electrode
X	–	% of 1 mol lithium ions intercalated into graphite structure
XPS	–	X-ray photoelectron spectroscopy
XRD	–	X-ray diffraction

Chapter I

Literature review

1. Motivation of the research

Currently, life in the world has accelerated to an incredible level. Each of us uses an alarming amount of electricity daily, which we once did not need at all [1]. Every day we turn on lights, watch television, use smartphones and computers, drive cars or use public transportation. People often do not realize how dependent they are on electricity. In addition to these activities, there are also small everyday items that we take for granted, such as wireless headphones, electric toothbrushes, coffee machines, or induction cooktops. Can anyone today imagine life without a refrigerator? Without electricity, humanity would regress significantly in development, which is why it is so important to take care of the privilege of having access to it [2].

However, continuous technological development and consumerism have caused the demand for electricity to become unimaginably high and constantly growing. Popular nonrenewable fossil fuels, such as coal, natural gas, and oil, are depleting at an alarming rate [3]. Their continued use also has a negative impact on the environment, which is why there is increasing talk about global warming, the destruction of the ozone layer, and the doomsday clock, which indicates how close we are to midnight [4].

Scientists are trying to initiate innovative solutions to obtain green energy, aiming at a more ecological approach to environmental protection [4]. Geothermal, nuclear, solar, wind, and tidal energies are often utilized. All of these solutions generate energy in a more environmentally friendly process, but there are always downsides. For example, geothermal energy cannot be produced everywhere, wind farms take up a lot of space and pose a threat to birds, and nuclear energy, although it provides a huge amount of energy, carries the risk of radioactive waste and nuclear plant failures [5-7].

Therefore, local production of electricity is becoming increasingly popular. This involves, for example, photovoltaic panels on roofs of houses or electrolyzers that produce hydrogen [8]. Despite still high costs, these solutions are beginning to prove effective locally in meeting electricity demand and are also ecologically beneficial. This is evidenced by the large number of households that have decided to install photovoltaic panels on their roofs and the growing number

One-step assembly of metal-ion capacitors using redox-active electrolytes

of hydrogen-powered vehicles (e.g., Solaris 18 Urbino Hydrogen) [9] [10]. However, these solutions show that humanity is moving toward renewable energy sources that are environmentally friendly and inexpensive to obtain, which is undoubtedly the right direction, although it will take time.

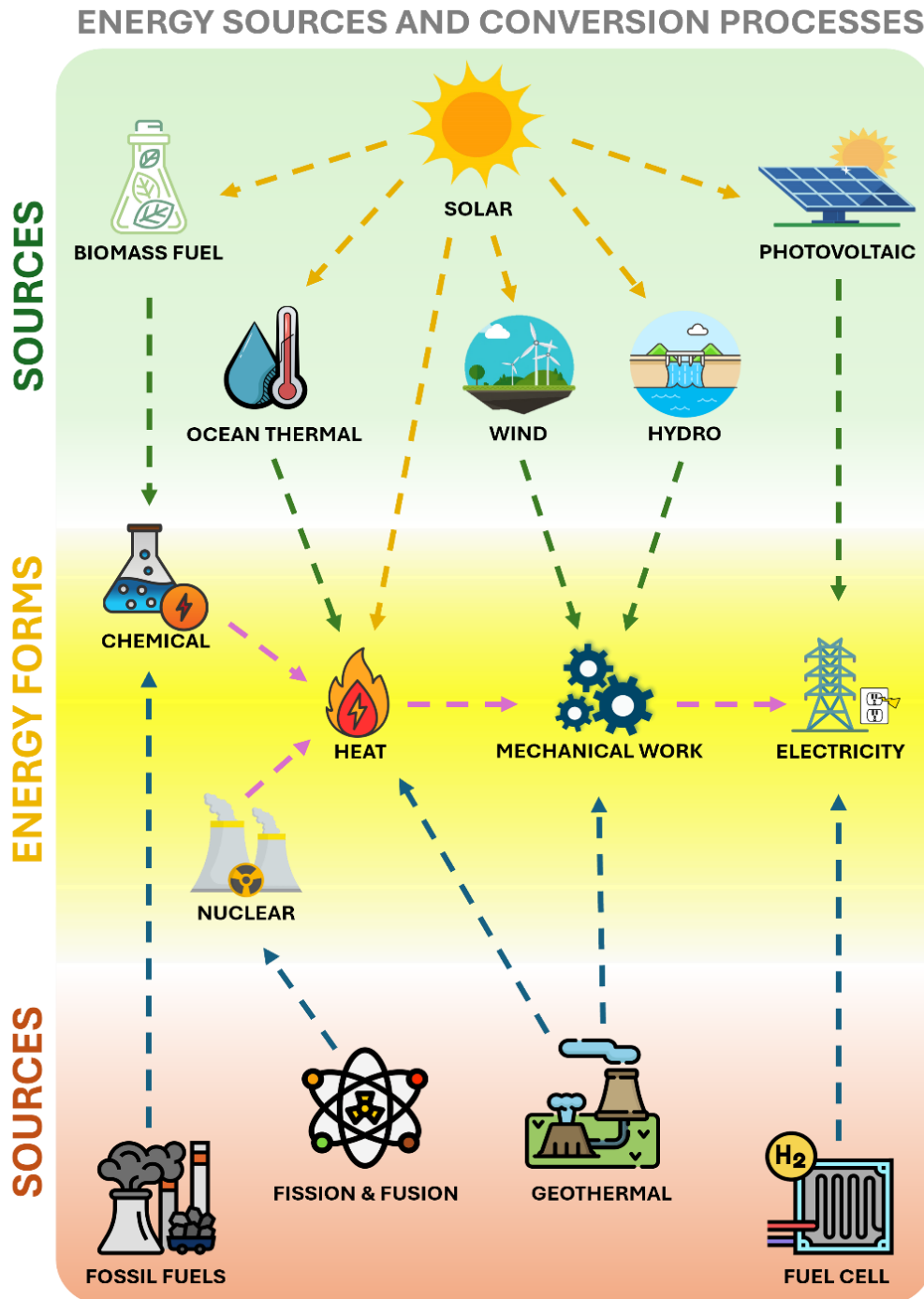


Figure 1. Energy sources and methods used for its conversion [11].

2. Electrochemical energy storage systems

Electrical energy storage systems (EESS) play a crucial role in the energy transition, enabling the management of renewable energy and ensuring the stabilization of power grids [12, 13]. Given the ever-growing demand for electricity, the development of EESS seems to be a necessity. EESS and conversion systems can be divided into three main groups: fuel cells, batteries, and capacitors.

Fuel cells

Fuel cells are devices that, in fact, convert chemical energy directly into electrical energy [14]. This occurs through an electrochemical reaction between a fuel, which can be hydrogen, methanol, or ethanol, and an oxidizer, most commonly oxygen. A typical fuel cell has a nominal voltage of approximately 0.7 V with an efficiency of approximately 60% [15]. The operating principle involves supplying hydrogen, its oxidation on an electrode usually coated with platinum black, followed by the transport of H^+ ions through an ion-exchange membrane to reduced oxygen at the cathode. Fuel cells are characterized by high operational purity due to green reaction products, which are electrical energy, heat, and water (in the case of the most popular hydrogen cells) [16].

Hydrogen fuel cells have a specific energy of approximately 1000 Wh kg^{-1} , specific power around 2 W kg^{-1} , and a lifespan of about 10 000 operational hours [17]. However, these cells have their drawbacks. Despite high initial efficiency, it rapidly declines, mainly due to impurities in the fuel supplied (hydrogen or oxygen) [18]. Additionally, the production of these cells is relatively expensive, and the storage of hydrogen raises many safety concerns [19]. Nevertheless, many see them as the future, primarily due to the simple reaction, which does not produce any highly harmful by-products for the environment. The main areas of application for hydrogen cells include backup storage systems in factories, cogeneration devices for electricity production (e.g., in combined heat and power plants), and increasingly in hydrogen-powered vehicles (such as the mentioned hydrogen-powered buses) [20].

Batteries

The most common group of EESS is batteries, as they are used literally everywhere energy storage is needed: laptops, wireless headphones, smartphones, electric vehicles, small electronic devices, and as large-scale electrical energy storage systems. There are many types and classifications of batteries based on their operating principle or the materials used in their production.

One of the most popular batteries is the nickel-metal hydride (Ni-MH) battery, where the cathode is a nickel plate, and the anode is a metal alloy that reacts with the hydrogen released during charging to form a metal hydride [21]. These batteries can achieve power ($250 - 1000 \text{ W kg}^{-1}$) and energy of about (70 Wh kg^{-1}), maintaining a lifespan of approximately 500 charge and discharge cycles [22]. Ni-MH batteries have completely replaced the previously used nickel-cadmium (Ni-Cd) cells, mainly due to their higher specific energy and environmental aspect (absence of cadmium) [23]. Ni-MH batteries are most often used in a range of devices that require longer operating times and relatively fast charging and discharging parameters, such as power tools, medical devices, UPS systems, the lighting industry, radio-controlled toys, and alarm and measurement devices [24]. The disadvantages of Ni-MH cells include their high self-discharge rate and their susceptibility to damage caused by deep discharge or overcharging.

The next group of batteries consists of zinc-air batteries. This type of battery is constructed with a zinc anode and a cathode with a large surface area (e.g., activated carbon, denoted further as AC) [25]. The electrolyte in these cells is usually a concentrated potassium hydroxide solution [26]. These cells are mainly used in electric fences and hearing aids due to their high specific energy (470 Wh kg^{-1}), inexpensive raw materials for production, and low self-discharge rate [27]. The nominal voltage of the cell is around 1.5 V. However, drawbacks such as poor resistance to high and low temperatures, hygroscopicity, and the negative impact of CO_2 significantly limit the application of zinc-air cells [28]. Moreover, these batteries belong to the group of primary cells, meaning that they can only be recharged through mechanical electrode replacement.

Another important group of batteries is lead-acid batteries. In these batteries, the negative electrode is made of a lead grid, while the positive electrode is made of lead dioxide (PbO_2) [29]. The electrolyte is a 37% sulfuric acid solution [30]. The nominal voltage of a single cell is 2.1 V. Lead-acid cells are characterized by high energy (approximately 40 Wh kg^{-1}), a low self-discharge rate, and an average lifespan of 500 – 800 charge and discharge cycles [31]. Lead-acid batteries are known for their low cost, high efficiency, and, above all, reliability, which allows them to be widely used in most combustion engine vehicles [32]. However, because of the challenges of recycling caused by toxic components such as lead and sulfuric acid, they are increasingly being replaced by other energy storage solutions.

Currently, the most popular group of both batteries and the entire EESS are lithium-ion batteries [33]. They have gained immense popularity due to their energy values being more than twice that of Ni-MH batteries ($100 - 250 \text{ Wh kg}^{-1}$), and also because they do not suffer from the memory effect or the lazy battery effect [34, 35]. One of the electrodes in a Li-ion cell is made of carbon (mainly graphite), while the other is made of lithiated metal oxides, with an organic solution of lithium salts serving as the electrolyte [36]. These types of batteries can reach voltages as high as 3.8 V, maintain a lifespan of approximately 1000 charge and discharge cycles, and have very low self-discharge [37]. However, the production of these cells is relatively expensive, the components are not environmentally friendly, and the availability of lithium on Earth is decreasing at an alarming rate [38]. Therefore, cheaper alternatives such as sodium-ion cells, which are currently gaining popularity, are being sought [39]. Li-ion cells are discussed in more detail in section 4 of chapter I.

Capacitors

The last group of EESS consists of electrochemical capacitors. Capacitors are devices that store electrical energy by accumulating electric charges on the surfaces of electrodes separated by a dielectric layer [40]. Initially, they were constructed with two metal plates with air between them, but with time, this concept was improved by creating electrolytic capacitors [41]. In these capacitors, one of the electrodes is an electrolyte, allowing much higher specific

One-step assembly of metal-ion capacitors using redox-active electrolytes

energy values (approximately 0.02 Wh kg^{-1}) [42]. Interestingly, the main advantage of capacitors is their ability to operate at high power values (up to 1000 kW kg^{-1}) [43]. Over time, electrodes with a large specific surface area were used, allowing capacitors to store ten times more energy ($0.2 - 5 \text{ Wh kg}^{-1}$) [44]. In these devices, the phenomenon of the formation of an electric double-layer was observed, hence the later name electrical double-layer capacitors (EDLCs). These devices often use an organic electrolyte, which allows for a nominal voltage of around 2.7 V [45]. A characteristic feature of capacitors is their very long lifespan, capable of reaching millions of charge and discharge cycles [46]. However, due to their low specific energy and high self-discharge [47], their application is limited to scenarios that require high power but low energy, such as computer memory, digital communication devices, or regenerative braking processes (KERS) [48]. A summary of the most important EESS is presented in **Figure 2**.

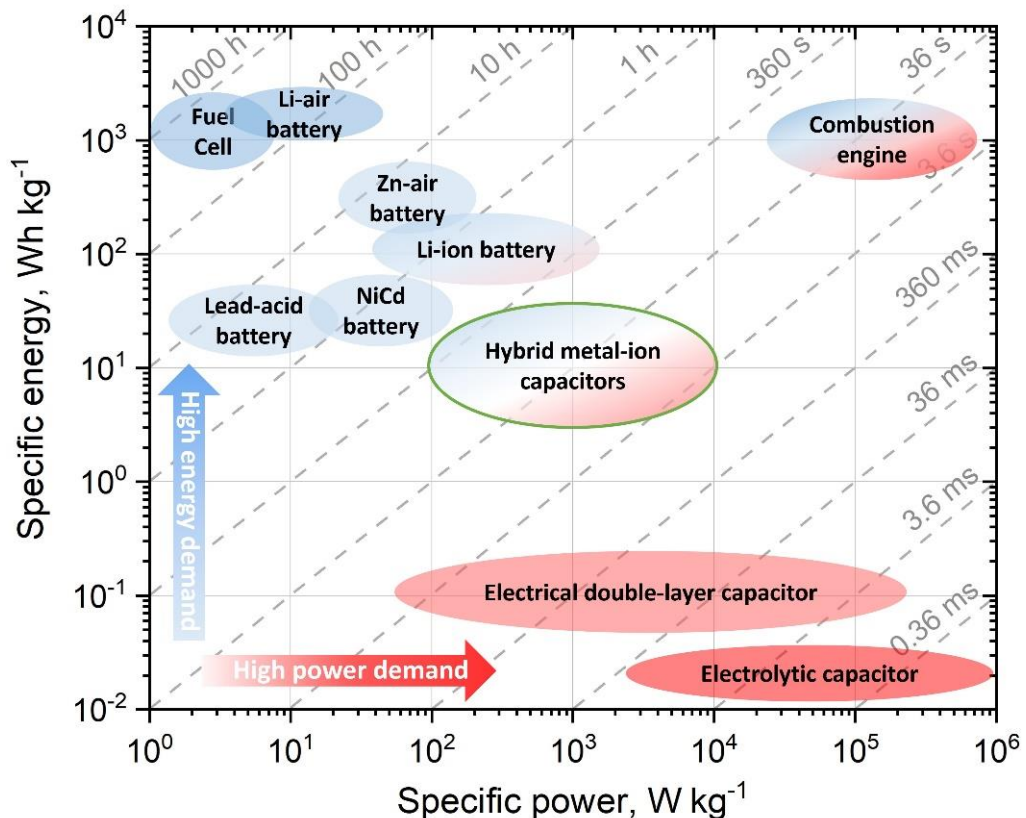


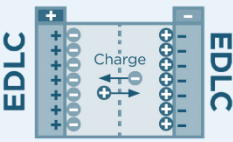
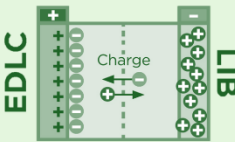
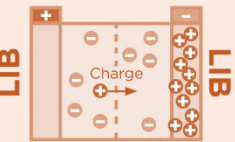
Figure 2. Ragone plot of popular energy storage systems [49, 50].

The main goal and challenge facing researchers around the world is to construct the ideal energy storage device that is cheap to produce, made of environmentally friendly materials, and capable of achieving high energy and power values while maintaining long cycle life and low self-discharge [51]. This task is exceptionally demanding, but quite achievable. By improving existing solutions and likely combining them into a single device, it will be possible to enjoy the benefits of an ideal energy storage system. However, many years of research will unfortunately be needed before this happens.

Currently, the best energy storage devices are lithium-ion batteries, mainly due to their high specific energy values [52]. Years of research, starting from 1974 by Stanley Whittingham to the Nobel Prize in 2019, suggest that much has already been achieved in their development, and further improvements seem marginal [53]. Therefore, more novel breakthrough solutions must be sought. One of the most promising solutions is the combination of lithium-ion batteries with electrical double-layer capacitors, creating entirely new devices known as hybrid lithium-ion capacitors (LIC) [54]. Their inception is estimated to have been in the 1980s, but in reality, they appeared at the beginning of this century. These devices have graphite as negative electrode like lithium-ion batteries, while the positive electrode is usually activated carbon, as in the case of EDLCs [55]. The organic electrolyte allows the intercalation process and high operating voltage (even up to 4.2 V), preserving the high specific energy of these systems (up to 70 Wh kg⁻¹) [56]. Furthermore, by combining with capacitors, the hybrid system gains in power values (>10 000 W kg⁻¹) and system lifetime (up to 100,000 charge and discharge cycles) [57]. However, the disadvantage of these systems is the need for the pre-intercalation process of the graphite electrode [58]. Unfortunately, despite their unique properties, hybrid capacitors are not widely used due to the high production costs associated with the complex assembly of these devices. But what if scientists could streamline the pre-intercalation process? **Table 1** shows the comparison of most important parameters of EDLCs, LICs and LIBs.

**One-step assembly of metal-ion capacitors using
redox-active electrolytes**

Table 1. Comparison of EDLC, LIC and LIB [59].

Parameter	Electrical double-layer capacitor	Lithium-ion capacitor	Lithium-ion battery
Principal operation			
Internal resistance	Low	Medium	High
Operating temperature (°C)	-40 to +70	-25 to +85	-25 to +60
Maximum operating voltage (V)	2.3 to 2.7	3.8 to 4.2	3.8 to 4.2
Minimum operating voltage (V)	0	2.2	2.5
Specific energy (Wh kg ⁻¹)	0.2 - 5	10 - 70	100 - 250
Specific power (W kg ⁻¹)	> 100 000	> 10 000	> 1 000
Recharge cycles	> 1 000 000	> 100 000	> 3 000
Self-discharge time at room temperature	Short (week)	Medium (weeks)	Long (month)
Working life at room temperature	> 20 years	5 - 10 years	3 - 5 years

3. Electrical double-layer capacitors (EDLCs)

Since the 1950s, engineers from General Electric have been experimenting with electrodes made of porous activated carbon primarily for fuel cell and battery application [60]. In 1957, H. I. Becker patented the first electrochemical capacitor. Becker's invention demonstrated that the use of activated carbon allowed very high capacitance in the capacitor [61].

The shape of supercapacitors as we know today was invented by Robert A. Rightmire, a chemist at Standard Oil Company of Ohio (SOHIO) [62]. However, SOHIO did not find a practical application for the invention and licensed the product to the Nippon Electric Company (NEC). NEC commercialized the technology in 1975 [63]. Later, alternative technologies emerged. Between 1975 and 1981, the concept of pseudocapacitance was developed by Brian Evans Conway, leading to the creation of capacitors exploiting pseudocapacitance effect at the device level. In 1994, the electrochemical-electrolytic hybrid capacitor was developed with two different electrodes used. In 1999 Conway defined a term “supercapacitor” [64]. In the early 2000s, the lithium-ion capacitor was invented [65]. Currently, work continues to improve the parameters of supercapacitors, with a major focus on specific energy.

3.1. The electric double-layer (EDL)

To begin considerations on EDLCs, one must begin by understanding the operation and mechanism of the electric double-layer (EDL). The electric double-layer is a term for the model of the structure that appears at the interface of two phases [66]. It is fundamentally important to describe commonly encountered structures of matter. The distribution of electric charges in the layer is largely determined by the electrical conductivity of the bordering phases, that is, the type, mobility, and concentration of electric charges present or potentially forming in both phases. Furthermore, the adsorption and orientation of polar molecules and the induction of charges within them affect the potential distribution in interfacial areas.

The first model of the electric double-layer was presented by Hermann von Helmholtz in 1879 [67]. Helmholtz believed that at the solid/liquid interface, the electric charge on the surface of the metal is neutralized by ions forming a layer closely adhering to the metal surface. This theory was refined by Louis Gouy and David Chapman, incorporating the diffuse nature of charges in the double-layer [68]. In 1910, Gouy observed that the thermal motion of ions in solution counteracts the ideal arrangement of ions in the electrochemical layer, causing its diffuse structure. In 1913, Chapman calculated the potential distribution as a

function of the distance from the metal (electrical surface). Later, in 1924, the German physicist Otto Stern seemed to combine the two previous EDL models [69]. He distinguished a stiff layer, i.e., ions directly adhered to the metal surface, and a diffuse layer, formed by ions further from the metal, performing chaotic thermal motions, yet simultaneously in a specific electrostatic order between the ionic charge and the charge on the metal surface. Ultimately, in 1947, David Grahame modified Stern's model by dividing the double-layer area with two planes parallel to the metal surface [70]. Grahame's model of the electric double-layer remains valid to this day and is presented in **Figure 3**.

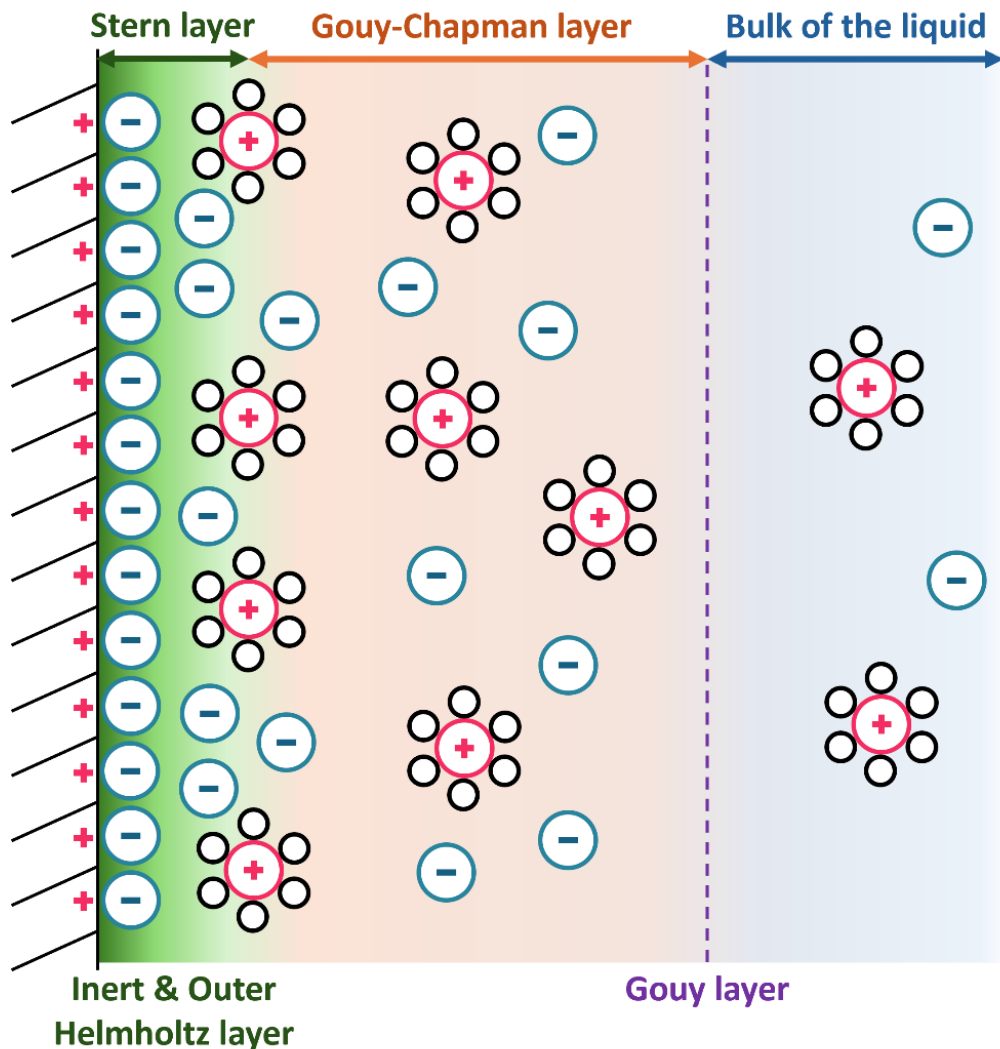


Figure 3. Scheme of the electric double-layer formed at the solid state – liquid interface [70].

3.2. Cell construction and applications

Electrical double-layer capacitors (EDLCs) are a type of electrolytic capacitor with a specific design that exhibits much greater electrical capacitance compared to a classic capacitor. This is due to the use of symmetrical carbon electrodes with a highly developed surface area, where the charge is stored through the separation of ions in the Helmholtz double-layer between the electrode surface and the electrolyte (**Figure 4**) [71]. The main advantage of using EDLCs is their high specific power ($>100,000 \text{ W kg}^{-1}$), which allows for rapid charging and quick release of electrical energy [72]. Another benefit is their longevity, which can last uninterruptedly through even a million charge and discharge cycles [73]. Additionally, the "clean" electrochemical storage process results in very low energy losses during individual charge and discharge cycles. EDLCs can operate over a wide temperature range and, compared to other energy storage systems, are much more environmentally friendly.

Unfortunately, EDLCs are characterized by a lower specific energy ($0.2 - 5 \text{ Wh kg}^{-1}$) compared to batteries, which is due to the low maximum operating voltage ($< 2.7 \text{ V}$). This relationship is explained by the equation for the energy of an electrochemical capacitor presented in **Equation 1** [74].

$$E = \frac{1}{2} C U^2 \quad (1)$$

Another limitation of EDLCs is their high self-discharge rate. Therefore, these devices are most commonly used when a small amount of energy is needed quickly. EDLCs can be used in energy storage systems to smooth power fluctuations and for short-term buffering. Additionally, they can be utilized in hybrid and electric vehicles to support regenerative braking systems and increase power, as emergency power supplies in UPS systems, and even in trams and buses for rapid charging at stops [75].

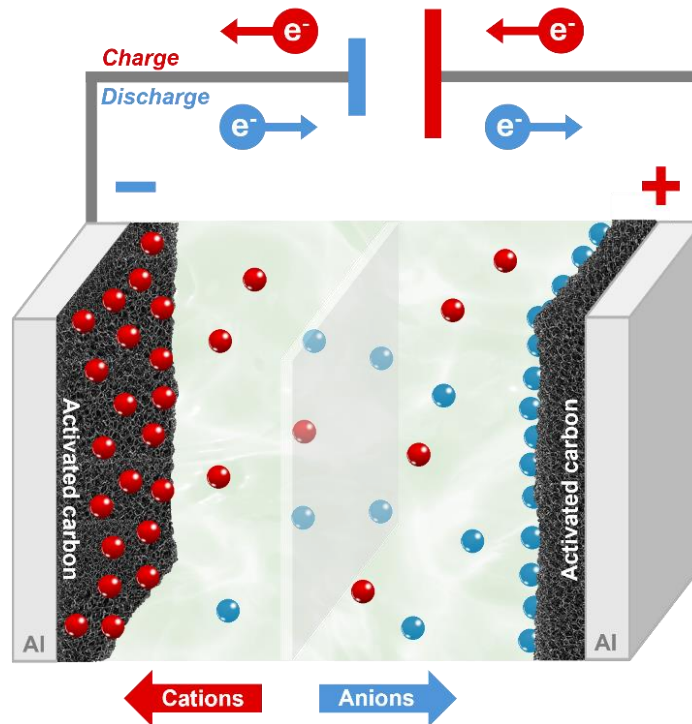


Figure 4. Schematic construction of EDLC.

3.3. Electrode materials

The electrode material together with the electrolyte constitutes the most important part of an electrochemical capacitor. The type of electrode used, its porosity, density, and the presence of heteroatoms or other functional groups determine the proper functioning and characteristics of EDLCs [76]. Electrode materials are usually applied to a metal current collector in the form of thin coatings. Electrodes must exhibit excellent conductivity, high electrochemical and thermal stability, as well as corrosion resistance, and most importantly, a large active surface area [77]. Of course, they should also be environmentally friendly and inexpensive to produce. Theoretically, the larger the active surface area, the larger the resulting electric double-layer. However, in practice, this is not always advantageous. It is believed that the smaller the pores, the greater the capacitance of the EDLC and, consequently, the specific energy [78]. However, small pores cause an increase in equivalent series resistance (ESR), thereby reducing the specific power of the system [79]. Therefore, the pore size must be adjusted to the desired application.

One-step assembly of metal-ion capacitors using redox-active electrolytes

Electrodes used in EDLCs can be divided into two main groups: carbon materials and pseudocapacitive materials (**Figure 5**).

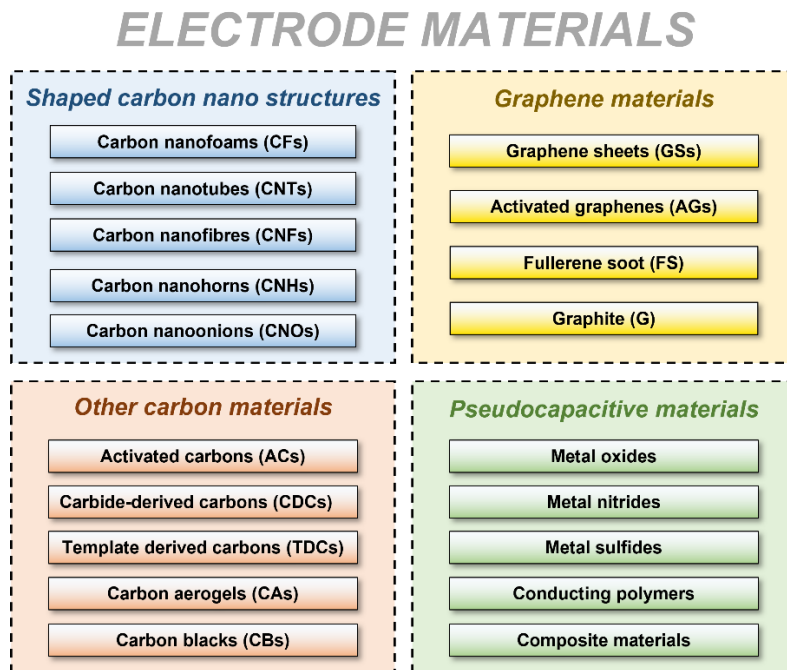


Figure 5. Electrode materials for electrochemical capacitors.

Among pseudocapacitive materials, which in addition to non-faradaic charge attraction in the double-layer also exhibit redox activity, one can mention metal oxides (e.g., MnO_2 [80], RuO_2 [81]), metal nitrides (TiN [82]), metal sulfides (MoS_2 [83]), conducting polymers (PANI [84]), and composite materials, which usually consist of a mixture of pseudocapacitive material with carbon material [85]. Despite the increased capacitance of such capacitors due to the additional redox reaction, they often face the problem of reduced number of charge and discharge cycles as well as higher production costs.

Carbon materials can be divided into shaped carbon nano structures, graphene materials, and other carbon materials (**Figure 5**). The group of shaped carbon nanostructures includes nanofoams [86], nanofibers [87], nanohorns [88], nanooxions [89], and the most popular electrode materials for EDLCs – nanotubes (CNTs) [90]. CNTs consist of a hollow cylindrical tube made of one-atom-thick sheets of graphene. Nanotubes can be divided into single-walled (SWNTs) nanotubes or multi-walled nanotubes (MWNTs). MWNTs are simply additional graphene walls built up, each larger than the previous one [91].

Nanotubes typically have a diameter of 1 to 3 nm. They have a moderately high specific surface area, about $\sim 800 \text{ m}^2 \text{ g}^{-1}$. Their advantage as a capacitor material is their increased wettability and conductivity compared to activated carbon [92]. Nevertheless, more charge can be stored in activated carbon because of its larger specific surface area. Additionally, the use of nanotubes results in EDLCs being over ten times more expensive compared to using activated carbon. However, the high conductivity and wettability of nanotubes are often utilized in composite materials with activated carbon.

The second group of carbon electrodes consists of materials made from graphene, such as graphene sheets [93], activated graphenes [94], fullerene soots [95], and graphite [96]. Graphite is composed of graphene layers arranged parallel to each other, with weak Van der Waals interactions between them [97]. It is the cheapest material due to the lack of a complicated production process. However, because of its low specific surface area, it does not find significant application in EDLCs. Graphite is better suited for lithium-ion batteries because of its layered structure and ability to intercalate metal ions. Graphene, as a 2D structure, is a one-atom-thick sheet made of hexagonally shaped carbon atoms. It has an excellent theoretical specific surface area of $2630 \text{ m}^2 \text{ g}^{-1}$, which theoretically leads to a capacitance of 550 F g^{-1} [98]. Its advantages over activated carbon include excellent wettability and significantly better electrical conductivity. Unfortunately, the use of graphene comes with several challenges. Graphene sheets tend to restack and aggregate due to Van der Waals forces, leading to a significant loss of accessible surface area [99]. This reduces the effective surface area available for charge storage, diminishing the performance of the electrode. Maintaining the mechanical integrity of graphene-based electrodes over long cycles can be challenging. The electrodes can suffer from structural degradation during many charge-discharge cycles, which affects the long-term stability and performance of the EDLCs. Lastly, high-quality graphene is expensive to produce. Methods for producing graphene, such as chemical vapor deposition (CVD) or graphite exfoliation, are complex and costly, making it difficult to scale up for commercial applications [100].

The last group consists of other carbon materials. The main representatives

include carbide-derived carbons [101], template-derived carbons [102], carbon aerogels [103], carbon blacks [104], and the most popular carbon material for capacitors, activated carbons. Activated carbon (AC) is unique due to the network of micro and mesopores created during activation [105]. Activated carbon can be obtained through physical or chemical activation. Physical activation, also known as thermal activation, is carried out at a temperature of 400 – 1000°C in a continuous flow of carbon dioxide [106]. Chemical activation involves treating carbon at a temperature of 400 – 700°C in the presence of an activating agent such as H₂SO₄, KOH, or H₃PO₄ [107]. As a result of activation, a material with small pores and volume, high microporosity, and above all, a high active surface area exceeding 2000 m² g⁻¹ is obtained. By changing the temperature, pressure, activation time, or activating agents, the parameters of the activated carbon obtained can be controlled. Currently, EDLCs with activated carbon can achieve even 100 – 200 F g⁻¹ with a specific energy of 1 – 2 Wh kg⁻¹ at a given power of 10 000 W kg⁻¹ [108]. Physical activation is commercially used because of the increased cost of chemical activation.

3.4. Electrolytes

The electrolyte in EDLCs is a very important component that significantly impacts the overall performance of the electrochemical capacitor. Aside from the type and porosity of the electrode, the composition of the electrolyte (salt and solvent) determines the formation of the electric double-layer. The most critical parameters appear to be ionic conductivity and viscosity, which influence how much charge can be stored and how quickly this process can occur [109]. Of course, the thermal and electrochemical stability of the electrolyte is also important, because the higher the voltage that can be applied to the cell, the higher its energy, according to **Equation 1** [110]. Another characteristic feature of electrolytes is hydrophilicity, which can affect the composition of the electrolyte and complicate its storage. Environmental impact and safety are also important, with a focus on the explosiveness and flammability of the electrolytes. Corrosiveness is also significant, as the electrolyte can greatly affect the cyclic performance of the cell. All these features are ultimately topped by cost, as the electrolyte must be economically viable. **Table 2** summarizes the mentioned

One-step assembly of metal-ion capacitors using redox-active electrolytes

electrolyte characteristics and shows their importance in relation to aqueous, organic, ionic liquid, and solid-state electrolytes.

Table 2. Advantages and disadvantages of the electrolytes used in the ECs [111].

Criteria	Aqueous 	Organic 	Ionic liquids 	Solid-state 
Ionic conductivity	High (100 – 1000 mS cm ⁻¹)	Moderate (1 – 10 mS cm ⁻¹)	Moderate (1 – 10 mS cm ⁻¹)	Low to moderate (0.1 – 10 mS cm ⁻¹)
Overall energy	Moderate (limited voltage window)	High (broad voltage window)	High (broad voltage window)	Moderate to high
Overall power	High (high ionic conductivity)	Moderate	Moderate	Low to moderate
Viscosity	Low	Moderate	High	N/A
Hydrophilicity	High	Low	Moderate	N/A
Flammability	Low	High	Low	Low
Corrosivity	High	Low to moderate	Low	Low
Electrochemical stability	Low to moderate (1 – 2 V)	High (2.5 – 3 V)	High (4 – 5 V)	High
Price	Low	Moderate to high	High	Moderate to high
Impact on environment	Moderate	High	Moderate	Low to moderate
Storage	Good (stable at RT)	Moderate (sensitive to moisture)	Moderate (sensitive to impurities)	Good (stable at RT)

Aqueous electrolytes

Aqueous electrolytes are classified primarily into acidic, alkaline and neutral solutions, the most common being the solutions of KOH [112], NaCl [113], KCl [114], H₂SO₄ [115], and Na₂SO₄ [116] solutions. These electrolytes are used in applications requiring higher power outputs. Research on these electrolytes mainly focuses on increasing the stability of the electrochemical window. Water decomposition results in the release of oxygen at the positive electrode and hydrogen evolution at the negatively polarized electrode at just 1.23 V [117]. Therefore, moderate specific energy can be obtained. The advantage of aqueous electrolytes is their high ionic conductivity (100 – 1000 mS cm⁻¹), which goes hand in hand with low viscosity and the ability to use high current regimes, resulting in

high specific power [118]. Typically, aqueous electrolytes are less flammable and explosive, making them suitable for everyday use. They are also easy to store because they are usually stable in air at room temperature, and their high hydrophilicity does not significantly affect them. Unfortunately, their downside is the high corrosiveness to steel systems, often due to the extreme pH levels used. Poorly chosen materials can cause corrosion, which can reduce the lifespan of the system. Additionally, aqueous electrolytes are not always environmentally friendly, as additives and extreme pH levels can alter the environmental water balance [119]. Nevertheless, the production of these electrolytes is very simple and cheap, which contributes to their popularity.

Recently, an interesting option to increase the specific energy of EDLCs with aqueous electrolytes is the "water-in-salt" concept [120]. This concept involves increasing the concentration of conducting salt in water to the extent that there is more salt than water by volume and weight. An example is the use of cesium fluoride (CsF), where this solution can increase the electrochemical stability of the electrolyte even up to 2 V, as the remaining water is strongly bound to the salt and does not have direct contact with the electrode [121]. Unfortunately, this approach reduces the ionic conductivity of the electrolyte, leading to a decrease in specific power. Therefore, the solution must be tailored to the specific application. Another way to increase the specific energy in EDLCs is by using redox salt additives [122]. In this case, the use of iodides [123], bromides [124], or thiocyanates [125] causes an additional faradaic reaction at the electrode, increasing the working capacitance of the electrochemical capacitor. However, such a solution also reduces the specific power of the system due to the slower redox reaction process. Additionally, the redox reaction usually negatively affects the cycling performance of the entire cell.

Organic electrolytes

Organic electrolytes are currently the most widely used electrolytes in the industry for EDLCs, and tetraethylammonium tetrafluoroborate (TEABF₄) in acetonitrile (ACN) is the most prevalent solution [126]. They are popular due to their high electrochemical stability (2.5 – 3 V), which translates into higher specific energy values compared to other types of electrolytes [127]. Additionally, their

moderate viscosity and ionic conductivity ($1 - 10 \text{ mS cm}^{-1}$) allow for decent specific power values. Organic electrolytes have little impact on the corrosiveness of systems; only additives to the electrolytes may cause issues in this regard. Unfortunately, organic electrolytes need to be stored in special chambers that maintain an inert environment, as they can evaporate, and despite their low hydrophilicity, any addition of water deteriorates their electrochemical stability. Furthermore, organic electrolytes are generally flammable and harmful to the environment, so safety precautions must be taken when working with these cells, primarily to prevent overheating [52]. The cost of organic electrolytes is moderate, which makes them attractive to industrial companies despite their numerous environmental drawbacks. The most commonly used organic solvents include ACN [128], propylene carbonate (PC) [129], ethylene carbonate (EC) [130], and dimethyl carbonate (DMC) [131]. Conductive salts used include TEABF₄ [126] and lithium bis(trifluoromethanesulfonyl)imide (LiTFSI) [132].

Ionic liquids

Due to the ability to design ionic liquids, there is increasing discussion about new compounds that improve the electrochemical performance of electrochemical capacitors [133]. Nevertheless, most ionic liquids (i.e., salts composed entirely of ions, often considered as salts with melting points below 100°C) share common characteristics. Firstly, they have high viscosity, which affects their ionic conductivity, resulting in lower specific power values [134]. Ionic liquids are generally hydrophilic, and the presence of water decreases their electrochemical stability, which is their main advantage (4 – 5 V) [135]. Another drawback of ionic liquids is their high cost, because of the complex synthesis process, which often leaves substrates or byproducts that reduce the stability of the electrolyte. Additionally, the still-unknown environmental impact makes scientists cautious of these "green electrolytes". However, their low corrosiveness, lack of flammability, and explosiveness, and especially wide electrochemical stability window, make them an interesting and continuously evolving group of electrolytes. The most commonly used ionic liquids include 1-Ethyl-3-methylimidazolium Tetrafluoroborate ([EMIM]BF₄) [136], 1-Butyl-3-methylimidazolium Tetrafluoroborate ([BMIM]BF₄) [137], and 1-Ethyl-3-

methylimidazolium Bis(trifluoromethanesulfonyl)imide ([EMIM]TFSI) [138].

Solid-state electrolytes

Solid-state electrolytes are solid ionic conductors that are also electrically insulating materials [139]. The first inorganic solid-state electrolyte was discovered by Michael Faraday in the 19th century, and it was silver sulfide (Ag_2S) [140]. Currently, the most popular group of solid-state electrolytes consists of conductive polymers, with the first of them, polyethylene oxide (PEO), being invented in the 1970s by V. Wright [141]. Other popular polymer electrolytes include polyvinylidene fluoride (PVDF) [142], polyacrylonitrile (PAN) [143], and polyethylene glycol (PEG) [144]. Solid-state electrolytes have many advantages, such as high electrochemical stability, nonflammability, low corrosiveness, easy and stable storage at room temperature and reduced negative environmental impact. All these factors contribute to decent specific energy values. However, reduced ionic conductivity (ranging from 0.1 to 10 mS cm^{-1}) makes these systems inefficient for applications requiring higher current regimes [145]. In such cases, it is better to use a lithium-ion battery, which will provide more energy.

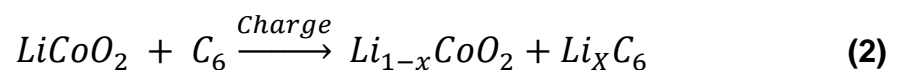
4. Lithium-ion batteries (LIBs)

At the beginning of the twentieth century, the enormous potential of lithium as a battery material was recognized. It is a metal with the lowest density, low electrochemical potential (around -3.05 V vs. SHE), and a high energy-to-mass ratio [146]. The American physical chemist George Newton Lewis began experiments with lithium batteries as early as 1912, but real work on lithium-ion batteries only emerged in the 1970s [147]. The breakthrough occurred in 1974 when Stanley Whittingham first used titanium disulfide (TiS_2) as a cathode material, which had a layered structure and could accommodate lithium ions without significant changes in its crystal structure [148]. Another important step toward lithium-ion cells occurred in 1979. Professor John Goodenough at the University of Oxford replaced TiS_2 with another cathode material – LiCoO_2 [149]. They created a new type of lithium battery, where lithium could travel through the battery from one electrode to the other in the form of ions. This solution forms the basis for current lithium-ion batteries. Then, in 1985, Akira Yoshino used

petroleum coke as an anode material for batteries, where molecular-level spaces were observed that could host lithium ions [150]. Following this discovery, the first commercial lithium-ion battery appeared in 1991. It was introduced by Sony to their cameras, and other companies soon followed the Japanese giant's lead [147]. The great advantage of lithium-ion technology over then dominant nickel-cadmium was quickly recognized. The advantages were not only the high density, allowing one to store twice the charge in a battery of the same size, but also the high cell voltage at 3.6 V. Whittingham, Goodenough, and Yoshino were awarded a Nobel prize in 2019 [151].

4.1. Principle of operation

Lithium-ion batteries are made up of an anode (mainly graphite) and a cathode made of a lithiated metal oxide (e.g., LiCoO_2), which are separated by a membrane soaked in an organic electrolyte (mainly LiPF_6 salt dissolved in an EC:DMC mixture) (**Figure 6**) [152]. A characteristic feature of lithium-ion cells is their high specific energy (up to 250 Wh kg^{-1}), which is due to the high capacity of the electrodes as well as the wide operating voltage range of the cell (3.6 – 3.8 V) [153]. The cathode operates in a potential range up to 4.3 V vs. Li/Li^+ , while the anode can operate at a potential close to 0 vs. Li/Li^+ [154]. The anode can operate at such a low potential due to a phenomenon called intercalation. The intercalation mechanism involves the reversible incorporation of lithium ions into the structure of transition metal compounds (which make up the cathode material) and graphite (which is usually the anode material) without fundamentally changing the crystal structural parameters of these substances [155]. The basic elements of the intercalated material unit cell remain unchanged except for minor, reversible distortions of the structure. The overall reaction that occurs during the charging of a lithium-ion cell is presented in **Equation 2** [156], where x is the percentage of 1 mol of lithium ions intercalated into the graphite structure.



One-step assembly of metal-ion capacitors using redox-active electrolytes

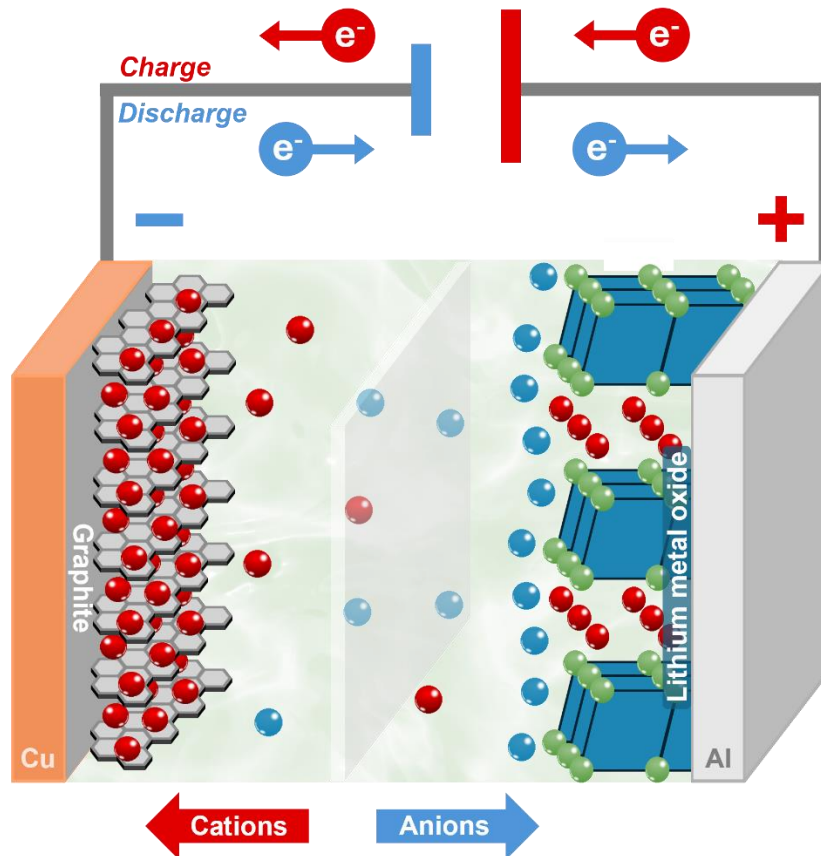


Figure 6. Lithium-ion battery construction.

When a closer look at the curve (**Figure 7**) representing the galvanostatic charging of a graphite electrode is taken, one can observe that at a potential of about 1 V vs. Li/Li⁺, capacitive processes related to the formation of the SEI layer begin. Subsequently, the intercalation process occurs until the system reaches the theoretical value for graphite (372 mAh g⁻¹) at a potential close to 0 vs. Li/Li⁺ [157]. However, this curve has a characteristic shape, indicating that the intercalation of lithium ions into the graphite electrode structure occurs gradually. The characteristic drop followed by a plateau in potential values is the result of progressing through successive stages of intercalation. Initially, there are no lithium atoms in graphite (C₆), but upon reaching the stage 4, lithium enters the structure with ratio of one lithium atom for every 72 carbon atoms. In stage 3, there is already twice as much lithium (LiC₃₆). In the second stage of intercalation, every other graphene layer is filled with lithium (LiC₁₂). After reaching the first stage, all interlayer spaces in the graphite structure are filled with lithium, meaning one lithium atom for every 6 carbon atoms (**Figure 8**) [158]. Prolonged

One-step assembly of metal-ion capacitors using redox-active electrolytes

charging of the system may cause lithium to deposit on the surface of the graphite (known as lithium plating), which is a highly undesirable phenomenon as it can lead to the formation of metal dendrites and poses a risk of short-circuiting the system [159].

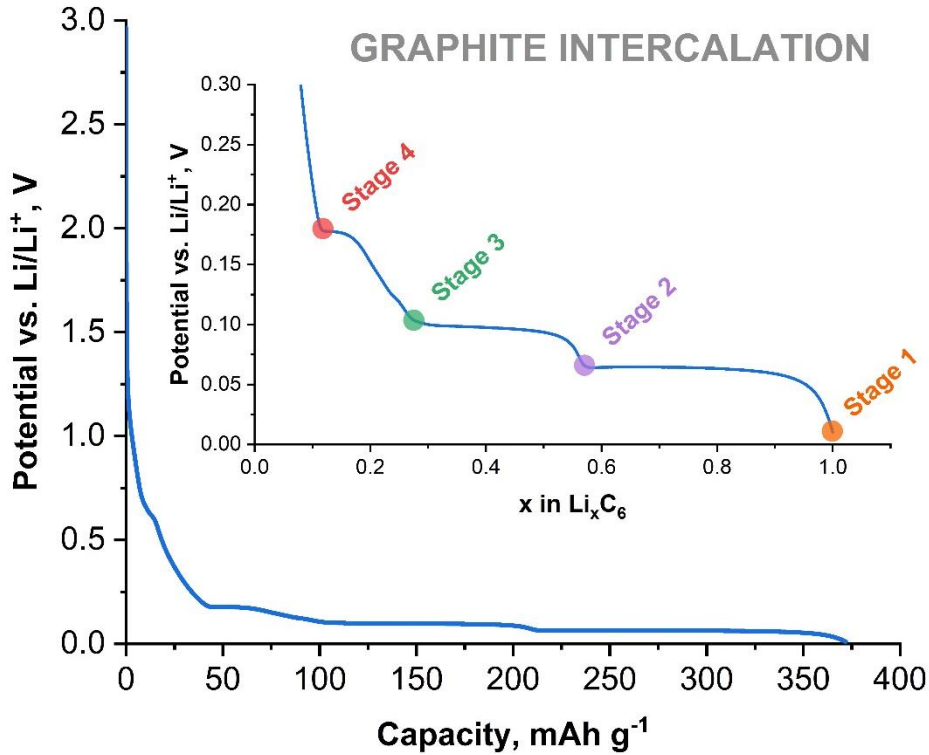


Figure 7. Galvanostatic charging of the graphite electrode [158].

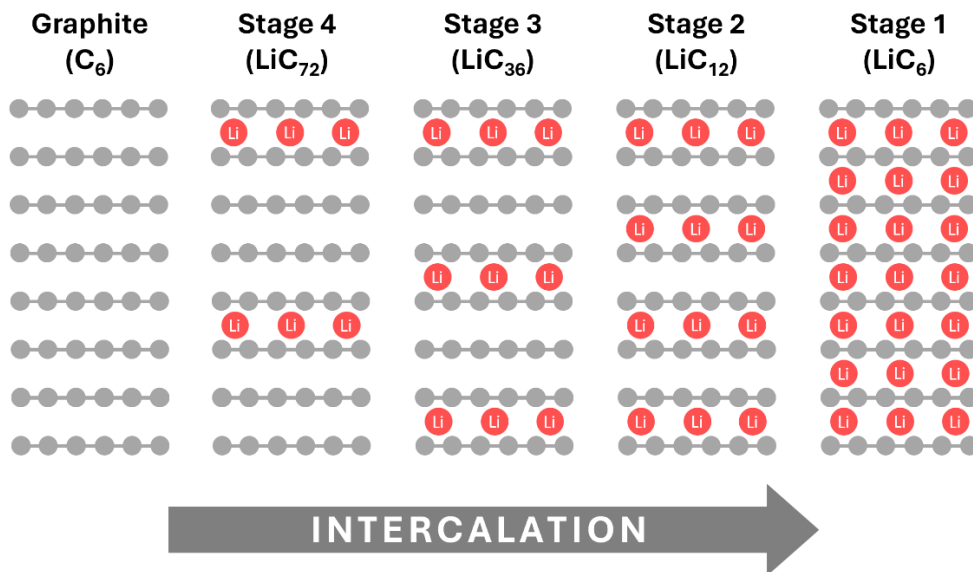


Figure 8. Schematic representation of each stage during the graphite intercalation process [158].

Lithium-ion batteries have several advantages and disadvantages. The most important advantage is their high specific energy, which means that they can store a large amount of energy per unit mass of the system. This makes them ideal for portable devices such as electronics, electric vehicles, and other applications where weight and space are critical factors. Another advantage is their long lifespan (up to 2000 cycles with NMC cathode) compared to other energy storage technologies. They also have a very low self-discharge rate, which means that once charged, they maintain their charge level for a long time [160]. In addition, these batteries can be charged relatively quickly and do not suffer from memory effect or lazy battery issues. However, their disadvantages include the high production cost (both for individual components and for the assembly process). There are also safety concerns, as they can potentially explode or catch fire in the case of overcharging or overheating. Furthermore, they are not environmentally friendly due to the use of organic solvents and rare metals in the cathodes [161]. Another significant issue is the decreasing availability of lithium worldwide, which will make these batteries increasingly expensive. In general, lithium-ion batteries offer a combination of benefits that make them suitable for many modern applications, but they also come with challenges that need to be managed effectively.

4.2. Electrode materials

The selection of electrode materials for lithium-ion batteries is complex and significant. The choice of cathode and anode materials impacts the final performance of the battery [162]. Each material comes with its unique benefits and drawbacks, making it appropriate for various applications depending on the needs for specific energy, specific power, safety, lifetime, and cost.

Cathodes

There are several main cathode materials available on the market (**Figure 9**). One of them is lithium cobalt oxide (LCO) [163]. LiCoO_2 is characterized by a high capacity of approximately 150 mAh g^{-1} and good cycle stability (500 – 1000 cycles). The working plateau of the cathode is in the range of 3.8 volts - 4.3 volts vs. Li/Li^+ . However, the LCO electrode has poor thermal

One-step assembly of metal-ion capacitors using redox-active electrolytes

stability (around 150°C) and is relatively expensive. In addition, there are environmental and ethical concerns with respect to the use and extraction of cobalt [164]. Despite these numerous drawbacks, cathode material is used in batteries for small electronics, smartphones, and laptops.

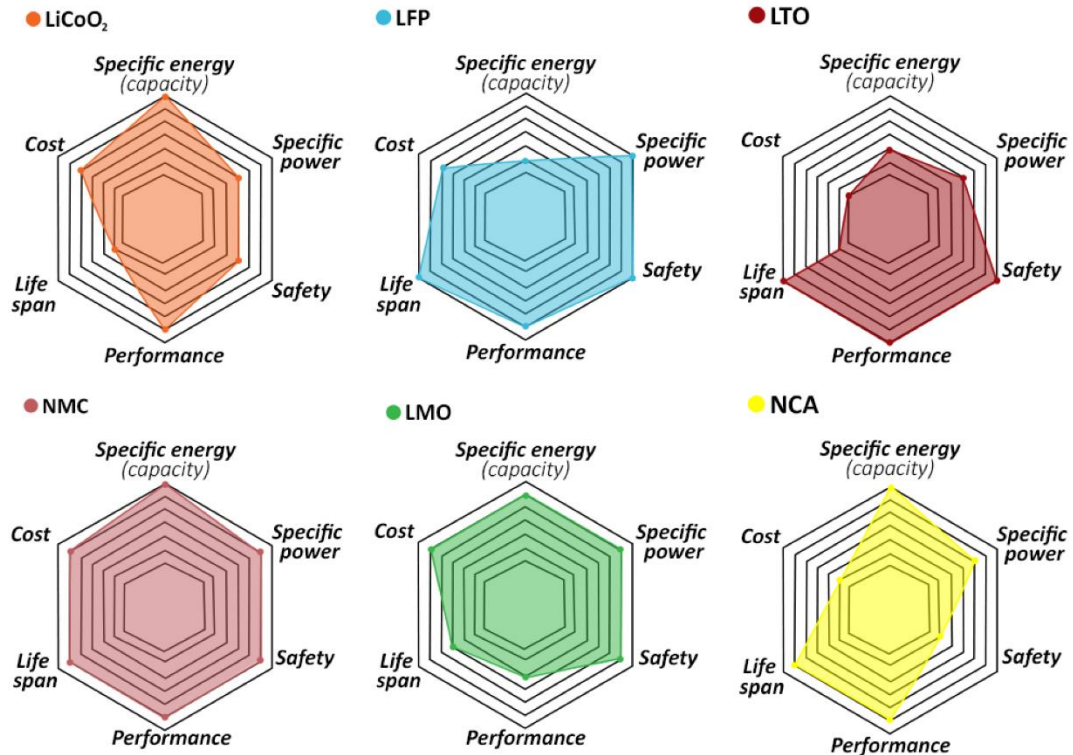


Figure 9. Comparison of Li-ion batteries with different cathode materials and LTO anode material [165].

The next cathode material is lithium iron phosphate (LFP) [166]. LiFePO_4 is characterized by a special olivine structure that provides excellent thermal resistance and safety. This electrode can operate for a very long time without signs of damage (over 2000 cycles). LFP also has a great capacity (160 – 170 mAh g^{-1}), but the low working plateau of the electrode (around 3.3 V vs. Li/Li^+) means that the overall energy stored by batteries with this cathode is lower compared to other cathode materials. Batteries with LFP are used as energy storage systems and in electric vehicles specifically, where the lifespan of the cell is more important than the stored energy [167].

Another cathode material is lithium manganese oxide (LMO) [168]. LiMn_2O_4 has a characteristic 3D spinel structure, which provides good thermal stability and

high-rate capability. Furthermore, this material is quite safe and relatively inexpensive. It has a slightly lower capacity compared to other materials (120 – 130 mAh g⁻¹), but with a working potential of 3.8 – 4.3 V vs. Li/Li⁺, it can remain competitive. However, cells with LMO cathodes quickly lose capacity over time, remaining effective for only about 300 – 700 cycles [169]. The short lifespan significantly limits their use to power tools and small medical devices.

The next cathode material is lithium nickel cobalt aluminum oxide (NCA) [170]. LiNiCoAlO₂ is primarily characterized by high specific energy and long lifespan. The capacity of the material is 175 mAh g⁻¹, with a working plateau potential of 3.5 – 4.3 V vs. Li/Li⁺. Unfortunately, poor thermal stability (up to 150°C), high electrode cost, and high safety concerns make this material rarely used in the current industry (primarily used in Tesla cars) [171].

The most versatile and currently the most widely used cathode material is lithium nickel manganese cobalt oxide (NMC) [172]. LiNiMnCoO₂ is the most balanced cathode material, providing good thermal stability (210°C), long lifespan (1000 – 2000 cycles), and high capacity (150 mAh g⁻¹ with a working potential of 3.7 – 4.3 V vs. Li/Li⁺). NMC is used in most electronic devices and electric vehicles [165]. Nevertheless, because of the high production cost and the use of cobalt, a better alternative to NMC is still being sought.

Anodes

Anode technology has remained relatively consistent over the years, but advances in Li-ion cathodes, new materials, coatings, and manufacturing processes require ongoing research. Given the anode, enhancing the anode component is crucial for creating long-lasting batteries [173].

Currently, most commercially available batteries for mobile phones or laptops are lithium-ion batteries with a graphite anode. The graphite anode has the best compatibility with the cathodes used in Li-ion [157]. With its layered structure, low working potential (0.15 – 0.25 V vs. Li/Li⁺), good electrical conductivity, low cost, and stable cycling performance, graphite has dominated as anode materials for years. However, with its limited theoretical capacity (372 mAh g⁻¹) and high potential for lithium plating at high charge rates, it is still far from a perfect solution.

Another solution that is currently gaining popularity among scientists is silicon-based anodes [174, 175]. Their distinguishing feature is an enormous theoretical capacity (4200 mAh g^{-1}), which is more than 10 times greater than that of the graphite currently used [176]. The operating potential of such electrodes is also very low (around $0.4 \text{ V vs. Li/Li}^+$), allowing for a huge amount of specific energy to be obtained. Unfortunately, significant volume expansion during cycling leads to mechanical degradation and reduced lifespan. However, if the volumetric expansion of the electrode could be controlled, silicon-based electrodes would likely replace graphite electrodes [177].

The last anode material is lithium titanate (LTO) [178]. $\text{Li}_4\text{Ti}_5\text{O}_{12}$ is characterized by a distinctive spinel structure, exceptional safety, and a long cycle life. Batteries with LTO anodes have been known since the 1980s. They are most commonly paired with NMC, allowing charging even at a 5C current rate [179]. The lifespan of cells with this electrode is estimated to be up to 7000 charge and discharge cycles [180]. Additionally, LTO is safe and performs well even at low temperatures up to -30°C . The use of LTO eliminates the formation of the SEI layer and the phenomenon of lithium plating on the electrode surface during fast charging. The thermal stability is also significantly better than that of other materials. Despite its numerous advantages, this material has a low capacity of 175 mAh g^{-1} and operates at a potential of $1.5 \text{ V vs. Li/Li}^+$, which results in a very low specific energy compared to graphite (around 65 Wh kg^{-1}), making it more of a competitor to nickel-cadmium batteries [181].

4.3. Electrolytes

The electrolyte in lithium-ion batteries is responsible for ionic conductivity between the cathode and anode during charging and discharging [182]. The choice of electrolyte affects the overall performance of the battery, its safety, and its longevity. A good electrolyte should provide high ionic conductivity while maintaining electronic insulation; additionally, it should be stable within the operating range of the cell, preferably nonflammable and nontoxic, and compatible with electrode materials [183]. Due to the high operating voltage of lithium-ion cells ($3.6 - 3.8 \text{ V}$), aqueous electrolytes are disqualified in favor of

organic electrolytes. Currently, various electrolytes are used with different compositions and ratios of compounds. The most common electrolyte ensuring stability and high ionic conductivity is LP30, which is 1M LiPF₆ in EC:DMC (1:1, V:V) solution [184].

Ethylene carbonate (EC) has a high dielectric constant and forms a stable SEI layer on the surface of the anode [185]. Dimethyl carbonate (DMC) has low viscosity and improves ionic conductivity [186]. Other commonly used solvents include diethyl carbonate (DEC) [187], which is very similar to DMC but has a slightly higher boiling point (126°C), and propylene carbonate (PC), which is rarely used due to the formation of an unstable SEI layer with graphite. However, PC is used much more frequently in sodium-ion cells [188].

Among the salts dissolved in organic solvents, lithium hexafluorophosphate (LiPF₆) is often used [189]. It is characterized by balanced conductivity, stability, and safety. During its decomposition, a protective film is formed on the electrode. However, this salt is very sensitive to the presence of water, as it can react to form strong hydrofluoric acid [190]. Another salt used in electrolytes is lithium tetrafluoroborate (LiBF₄), which provides good stability and safety but has slightly lower ionic conductivity than LiPF₆ [191]. Another salt is lithium bis(trifluoromethanesulfonyl)imide (LiTFSI), with very high thermal stability and high ionic conductivity [192]. However, due to higher production costs and the potential for corrosion of aluminium current collectors, it is less commonly used in industry. The last salt is lithium bis(oxalato)borate (LiBOB), which forms a stable SEI on the surface of the anode and also improves the battery life [193].

In addition to organic liquid electrolytes, solid electrolytes are also used, such as polyethylene oxide (PEO), which is flexible and can form thin films, but has lower ionic conductivity at room temperature [194]. Another type of solid electrolyte is ceramic electrolytes, which provide high ionic conductivity and excellent thermal stability. Examples of such electrolytes are LLZO [195], which has high conductivity and stability against lithium metal, and LLTO [196], which has moderate ionic conductivity but very high chemical stability. In addition, there are gel electrolytes, which are a hybrid between liquid and solid electrolytes. Here, polyethylene glycol (PEG) [197] is used, offering flexibility and ease of

processing, as well as polyacrylonitrile (PAN) [198], used in some gel formulations for its mechanical properties and compatibility with lithium salts.

To boost battery performance, additives are often introduced into the electrolytes. The selection and combination of these additives depend on the specific needs of the battery, such as high specific energy, extended cycle life, safety, and operational conditions. Vinylene carbonate (VC) and fluoroethylene carbonate (FEC) are commonly used to enhance the stability of the SEI layer, extend the life cycle, and minimize capacity loss [199, 200]. Lithium bis(oxalate)borate (LiBOB) is added to enhance cathode stability, reduce decomposition at high voltages, and improve battery safety [201]. Triphenyl phosphate (TPP) and trimethyl phosphate (TMP) are employed to improve thermal stability and safety [202, 203]. Lithium bis(trifluoromethanesulfonyl)imide (LiTFSI) is used as a high voltage stabilizer to prevent oxidation [192]. Vinyl ethylene carbonate (VEC) helps reduce gas formation during cycling, preventing swelling, while lithium fluoride (LiF) is often used to enhance the ionic conductivity of the SEI layer [204, 205].

4.4. SEI formation

The Solid Electrolyte Interphase (SEI) is a thin layer of chemical compounds formed on the surface of the anode material (mainly the graphite electrode) during the electrochemical reduction of the electrolyte [206]. This layer is usually about 100 – 120 nm thick and is responsible for the stability of the electrode and the transfer of lithium ions into and out of the graphite structure [207]. At the same time, the SEI blocks the movement of anions and other compounds into the anode electrode. This layer plays an important role in the longevity of the entire battery system [208].

The SEI layer is mainly formed during the first charge-discharge cycle of a lithium-ion battery, where the electrode material reacts with the electrolyte at the solid/liquid interphase. At a potential between 1.2 V and 0.8 V vs. Li/Li⁺, the electrochemical reduction of the electrolyte occurs, leading to the formation of chemical compounds such as lithium fluoride (LiF) and lithium ethylene dicarbonate (LEDC) [209]. The formation of these compounds is accompanied

One-step assembly of metal-ion capacitors using redox-active electrolytes

by a considerable volume of organic gases as by-products of this reaction. Gases emitted are mainly ethylene and ethane [210]. The released gases can pose a problem in the long term, as they increase the pressure in the system. In the production process of lithium-ion batteries, the gases released during SEI formation are removed using various techniques. For example, during the assembly of pouch cells, a special "pocket" is created, which is cut off after several charging cycles, and the generated gases are being removed [211].

During subsequent charge-discharge cycles, further reduction reactions of the electrolyte and the previously formed compounds occur. Here, LEDC is mainly further decomposed, forming additional compounds, both inorganic (lithium carbonate (Li_2CO_3), lithium oxide (Li_2O), lithium hydroxide (LiOH)) and organic (lithium alkyl carbonates (LiOR) and polyethylene oxide (PEO)) [212]. During the cyclic operation of the system, gases are still released, but in much smaller quantities, and their composition is mainly limited to carbon dioxide (CO_2) [213].

The breakdown of LEDC somewhat reduces the tightness of the SEI layer, which is why the so-called cycling formation of the system is important. In subsequent cycles, the SEI is resealed with additional decomposition products, building successive SEI layers and forming a stable structure (**Figure 10**).

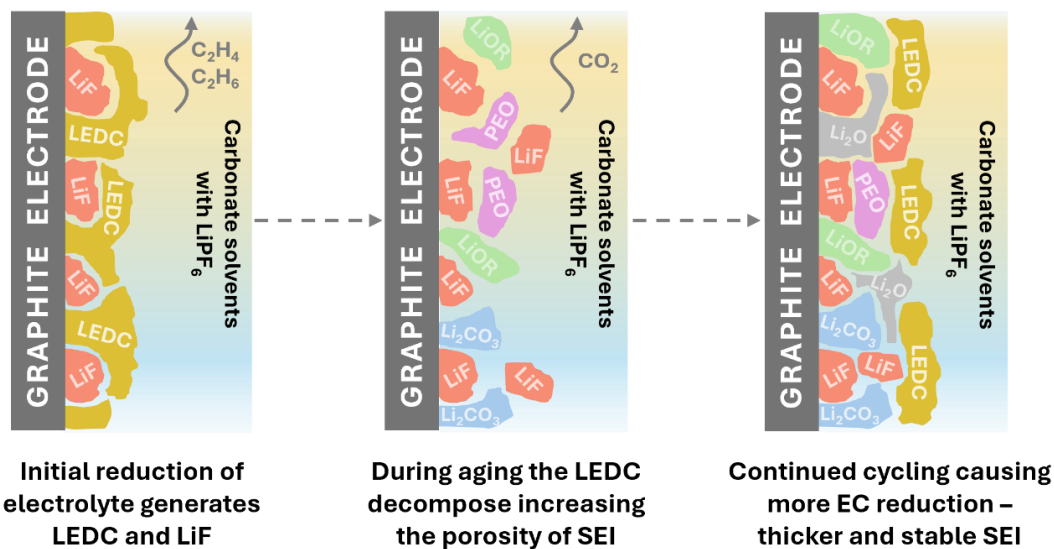


Figure 10. Stages of formation of the SEI layer on the graphite electrode using a conventional electrolyte (LiPF_6 in EC:DMC, 1:1, v:v) [212].

Several important factors influence the formation of the SEI. One of them is, of course, the electrolyte used (lithium salts with solvents and organic additives). The choice of electrolyte determines the composition and thickness of the SEI layer, which can ultimately affect its stability [214]. Furthermore, the rate of the SEI formation process depends on the applied current regime. A higher applied current will result in a thinner and more cracked SEI layer, whereas a slower charging current will result in a thick, tight, but more resistive SEI. Therefore, it is crucial to find the optimal solution for the system being used. Temperature is also a very important factor, since it influences the rate of chemical reactions and the solubility of salts in the organic electrolyte. The type of negative electrode, whether graphite, LTO, or silicon-based mixtures, will also affect the final composition of the SEI layer.

As already mentioned, the formation of the SEI layer has a significant impact on the cyclic operation of the entire electrode. On the one hand, the process of SEI formation may seem unfavorable because part of the lithium is consumed, which increases the irreversible capacity of the system and also increases the resistance in the system, thereby lowering the ionic conductivity of the electrolyte. On the other hand, the SEI layer, which is insoluble in the organic electrolyte, protects the negative electrode from the continuous decomposition of solvents and also allows the unobstructed flow of lithium ions to and from the anode electrode, maintaining the operating potential of the electrode and significantly improving the cyclic performance and lifespan of the entire battery [215].

5. Metal-ion capacitors (MICs)

The development of hybrid metal-ion capacitors began in 1981 with Dr. Yamabe and Dr. Yata, who pyrolyzed phenolic resin at 400 – 700°C to synthesize polyacenic semiconductive (PAS) [216]. This material was explored for its high specific energy and commercialized by Kanebo Co. The PAS capacitor was first used in 1986, and by 1991, a similar material was used in the concept of LICs. Among various possible electrode material combinations, the pairing of an activated carbon positive electrode with a lithium intercalation negative electrode has proven to be the most effective so far. Consequently, the first LIC is considered to have been introduced in 2001 by Amatucci et al., introducing

activated carbon as the positive electrode, LTO as the negative electrode, and 1M LiPF₆ in EC:DMC as the electrolyte [65]. Since then, anode materials such as graphite and hard carbon have been tested to enhance energy capacity while maintaining power output comparable to that of EDLCs. As a relatively new energy storage technology, the research on lithium-ion capacitors is not as extensive as that on LIBs or EDLCs but is rapidly increasing each year [217].

5.1. Principle of operation

Metal-ion capacitors are a class of hybrid electrochemical energy storage devices that combine the charge storage mechanism characteristic of EDLCs (charging electric double-layer) and Li-ion batteries (intercalation/deintercalation of lithium ions) [218]. They use a high specific surface area carbon material (characteristic of EDLCs) as the positive electrode and an intercalation material (mainly graphite, characteristic of Li-ion batteries) as the negative electrode, which undergoes reversible lithium-ion intercalation reactions. During charging and discharging, lithium ion intercalation and deintercalation occur within the negative electrode material, while on the positive electrode, ions are adsorbed and desorbed in the pores of the carbon material [219]. Since the process on the positive electrode is non-faradaic (no redox reactions or structural changes occur), it is relatively fast compared to the ion intercalation process occurring on the opposite electrode, limiting the power of such a lithium-ion capacitor to the negative electrode [54]. However, faradaic reactions that occur on the negative electrode result in a higher capacity on the anode, so the positive electrode limits the specific energy of the capacitor. Doping the anode lowers its potential, thereby achieving a higher output voltage for the capacitor. Typically, the output voltage for lithium-ion capacitors ranges from 3.8 to 4.0 V [56]. However, they are limited by a minimum voltage of 1.8 to 2.2 V because if the voltage drops below these values, lithium ions deintercalate faster than they can be restored during normal use. Lithium-ion capacitors can store 5-10 times more energy (up to 70 Wh kg⁻¹) than conventional electrical double-layer capacitors, and unlike batteries, they have a relatively higher specific power (up to 10 000 W kg⁻¹) and longer lifespan (up to 100 000 cycles) [220]. The self-discharge rates for hybrid capacitors range between those of lithium-ion batteries and EDLCs because of

the use of activated carbon electrodes, which is the main cause of this undesirable process.

5.2. Lithium-ion capacitors (LICs)

Lithium-ion capacitors (LICs) are the leading hybrid metal-ion capacitors today, largely due to the distinctive electrochemical properties of lithium and the technological success of lithium-ion batteries [221]. LICs feature a negative electrode made from graphite or LTO, facilitating the intercalation process (**Figure 11**). The positive electrode typically consists of activated carbon or mixtures of activated carbon with lithiated salts or conductive polymers. A membrane made from fiberglass or polymers (PE, PP), saturated with an organic electrolyte (commonly 1M LiPF₆ in EC:DMC), separates the electrodes [57]. This design offers several benefits discussed above, but there are notable drawbacks, mainly the high production cost. This cost is driven by the complex assembly and balancing procedures, including a pre-insertion phase and meticulous charge balancing between electrodes. Consequently, the high production cost confines its use to applications that require high power and energy [222].

LICs find applications in electric and hybrid vehicles, particularly in regenerative braking systems, enabling rapid energy capture and release [223]. They are also utilized in start-stop systems and as auxiliary power sources. LICs are beneficial for charge leveling and energy storage in renewable energy systems, such as solar and wind power, helping to balance supply and demand [224, 225]. In the industrial sector, LICs are used in equipment that requires dependable, high-power energy storage, such as backup power supplies and uninterruptible power systems (UPS). They also provide backup power for telecommunication systems, ensuring consistent performance during power outages. In addition, LICs are used in railway systems for power management, supporting auxiliary power units, and energy recovery during braking [226].

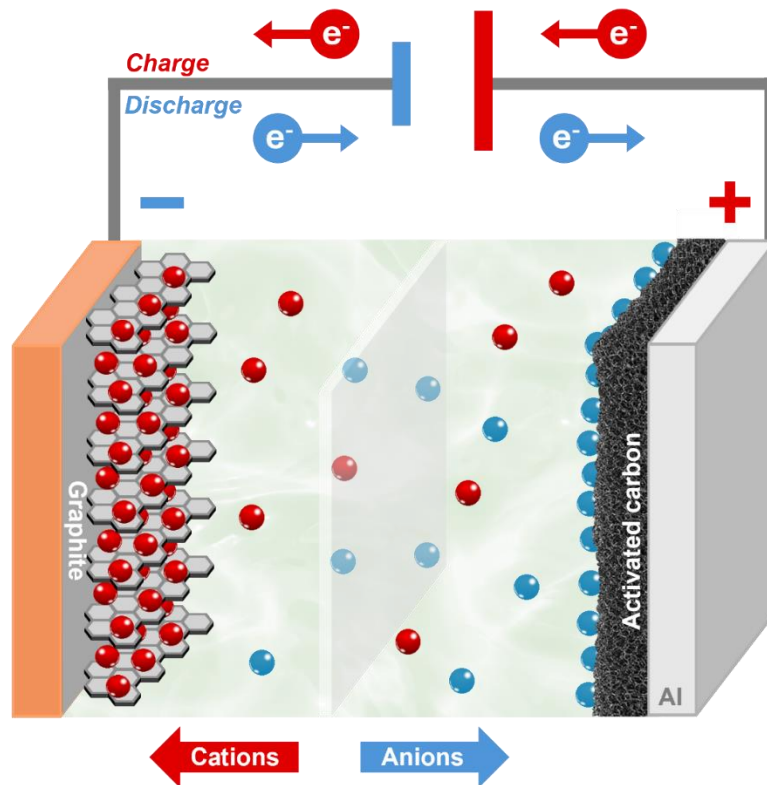


Figure 11. Schematic construction of the lithium-ion capacitor [54].

5.3. Sodium-ion capacitors (NICs)

Due to concerns about lithium availability, recent scientific research has turned to exploring sodium as a more cost-effective alternative [227]. Consequently, there has been an increase yearly in the number of articles on sodium-ion technology [228-230]. Activated carbon is used as the positive electrode in the construction of NICs (**Figure 12**). However, unlike lithium technology, graphite cannot serve as a negative electrode because sodium cannot form graphite intercalation compounds [231]. Initially, this was believed to be due to the larger size of sodium ions (0.95 nm) compared to lithium ions (0.6 nm), making it difficult for sodium to fit into graphene structures. However, the main reason is the alteration in the chemical bond between alkali metal ions and carbon atoms [232, 233]. Therefore, hard carbon is frequently used as the negative electrode in sodium-ion systems, resulting in a more stable anode when sodium is inserted [234]. Unfortunately, hard carbon has a notable disadvantage compared to graphite: it has a higher irreversible capacity due to a different SEI

One-step assembly of metal-ion capacitors using redox-active electrolytes

formation mechanism, giving it a theoretical capacity of about 320 mAh g^{-1} , which is lower than graphite (372 mAh g^{-1}), leading to a lower specific energy of the device [235]. Additionally, because of the different negative electrodes, other electrolyte solvents are used. The most common electrolyte is 1M NaPF_6 in a mixture of EC:PC [236]. However, studies indicate that using NaClO_4 in the same solvent mixture can improve NIC performance [237]. While the solvent mixture with PC provides stable SEI, it has lower ionic conductivity ($\sim 9 \text{ mS cm}^{-1}$) compared to lithium electrolytes ($\sim 13 \text{ mS cm}^{-1}$).

Sodium-ion capacitors are intended to be a more affordable alternative to LICs but come with several disadvantages. The most significant is the reduced specific energy due to the lower capacity of the hard carbon electrode. Furthermore, the lower conductivity of the electrolyte and the different SEI formation mechanisms also make lithium-ion technology superior. Additionally, the negative electrode is less stable, resulting in a shorter lifespan for NICs compared to LICs. Despite these drawbacks, sodium-ion technology offers lower production costs, no problem with sodium availability, and higher specific power values, as hard carbon electrodes handle higher current regimes better than graphite electrodes [238].

One-step assembly of metal-ion capacitors using redox-active electrolytes

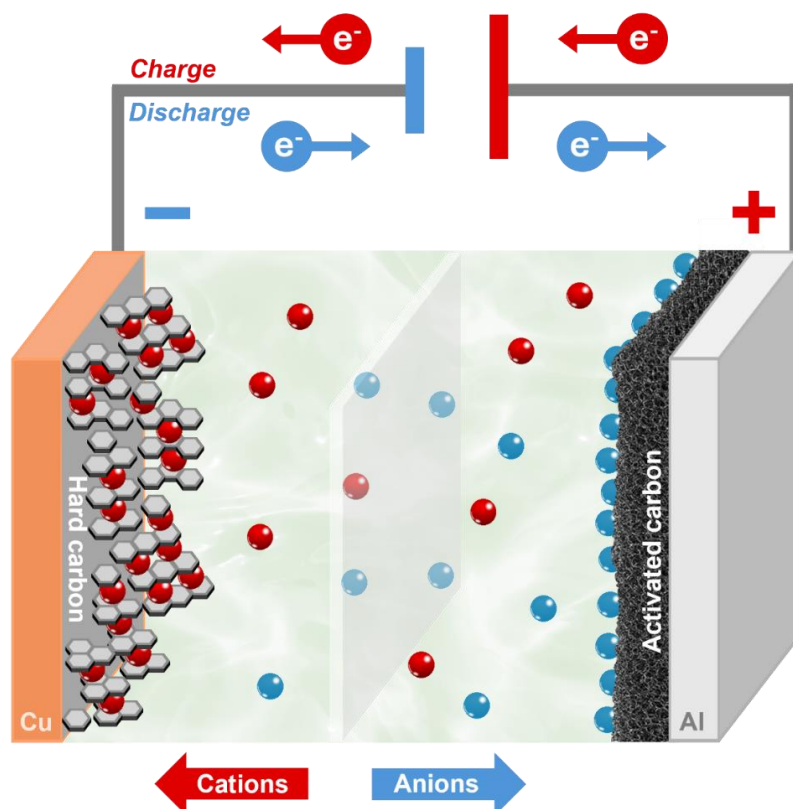


Figure 12. Schematic construction of the sodium-ion capacitor.

5.4. Potassium-ion capacitors (KICs)

Potassium ion capacitors (KICs) utilize potassium ions for storing charge and have a construction similar to lithium-ion capacitors (LICs) [239]. In KICs, graphite is typically used as the negative electrode and activated carbon is used as the positive electrode. The key difference lies in the electrolyte, which contains potassium ions instead of lithium ions, with 1M KPF₆ in EC:DMC being the most common choice [240]. Recently, diethylene glycol dimethyl ether (Diglyme, DEG DME) has become increasingly popular as a solvent, as it enhances the performance of potassium-ion cells by reducing self-discharge rates and improving the cyclability [241]. The process of inserting potassium ions into graphite is well-documented, involving the melting of potassium over graphite powder to form a KC₈ structure [242]. This process results in the potassium being inserted into the graphite, changing its color from black to bronze. The structure is characterized by the potassium ions being twice the distance between the hexagons in the carbon framework. However, fully intercalated graphite

electrodes are pyrophoric, which poses safety risks for potassium-ion systems. Despite these challenges, potassium-ion capacitors are a promising area of research in energy storage due to their potential cost benefits, abundance, and favorable electrochemical properties, although they still face significant challenges in materials development and long-term stability [243].

5.5. Pre-insertion techniques

Unlike lithium-ion batteries, metal-ion capacitors require a stage called pre-intercalation or pre-insertion [244]. This stage involves intercalating/inserting metal ions into the structure of the negative electrode during first charging cycle, so it gains the characteristics of a battery-type electrode. In LIBs, lithium ions come from the cathode; in the case of hybrid capacitors, it is activated carbon, and the lithium ions in the electrolyte are insufficient to intercalate the negative electrode. Unfortunately, the pre-insertion process is an additional step that needs to be performed during cell preparation, which significantly impacts the production costs of metal-ion capacitors. That is how it is so important to find a solution to the pre-insertion process to reduce the time, and cost of LICs assembly. Currently, four pre-insertion methods are known in the literature: using an auxiliary metallic electrode [245], using a positive composite electrode [246], using a concentrated (lithiated) electrolyte [247], and using a thicker positive electrode [248].

The first pre-insertion technique was proposed in 2006 by Fuji Heavy Industry and Aida et al., where they used an auxiliary metallic electrode [249]. Initially, this process involved first the assembly of a half-cell of lithium versus graphite, intercalation of the graphite, disassembling the cell and reassembling it with activated carbon (**Figure 13**). Later, the process was improved by introducing a small amount of metallic lithium into the assembled hybrid, which is intended to be entirely used for the graphite intercalation process in the first charging cycle. This solution was described by JM Energy in their ULTIMO systems [250]. Nevertheless, the construction of such a cell was very complicated, and there was a high risk of short-circuiting due to the lithium electrode. In addition, the use of lithium raised safety concerns. Another problem

One-step assembly of metal-ion capacitors using redox-active electrolytes

was that lithium was often not fully used up in the intercalation process, and its residues quickly formed dendrites, causing system short circuits and, consequently, short lifespan of the hybrid capacitors.

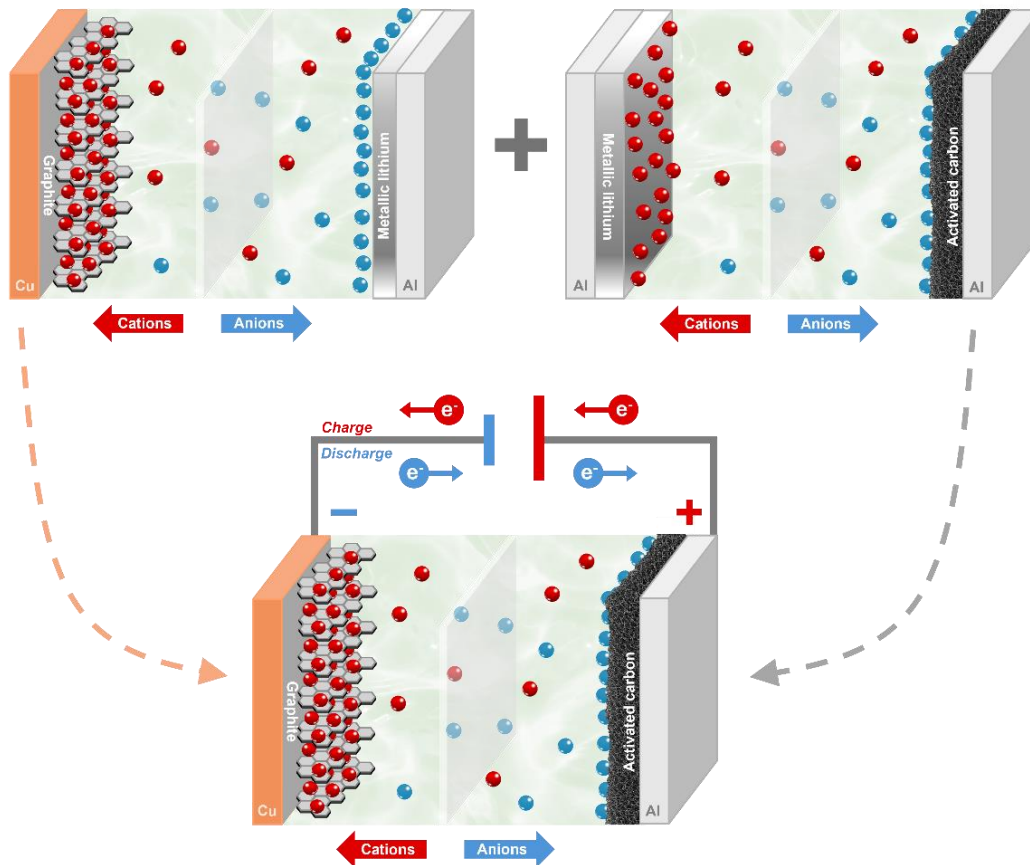


Figure 13. Assembly of lithium-ion capacitor using an auxiliary metallic electrode approach for pre-insertion.

Another pre-insertion technique is the use of a composite positive electrode (**Figure 14**) [244]. In this case, the positive electrode of such a cell consists of a mixture of activated carbon with lithium metal oxide. The purpose of adding this to activated carbon is to conduct an irreversible chemical reaction that supplies the charge necessary to balance the capacity of the negative electrode and enable its intercalation. Additionally, during the reaction, lithium ions are released, which are essential for proper pre-insertion. The first composite material used was a mixture of activated carbon with lithium molybdate (Li_2MoO_3), with a total capacity of 207 mAh g^{-1} [246]. Unfortunately, the lithium molybdate oxidation reaction occurs at a potential of $4.7 \text{ V vs. Li/Li}^+$, which

exceeds the electrolyte decomposition potential (for 1M LiPF₆ in EC:DMC it is about 4.5 V vs. Li/Li⁺). Furthermore, approximately 30% of lithium is reinserted into the structure of the composite material, which is an undesirable phenomenon. In subsequent years, other additives were tried to increase capacity, such as Li₂RuO₃ [251] and Li₅FeO₄ [252], but only the use of lithium metal oxide (Li₆CoO₄) provided a lower reaction potential (4.3 V vs. Li/Li⁺) than the electrolyte decomposition potential [253]. However, this solution still did not solve the reversibility issues of the reaction.

Therefore, over time, a new group of sacrificial materials was developed, designed to undergo electrochemical oxidation during the first charging cycle, rendering the compound inactive [254]. One example of such a salt is Li₂DHBN, presented by Jeżowski et al. This salt, being of organic origin, was not only expected to completely decompose during the first charging cycle but also to have a positive environmental impact [255]. Despite excellent electrochemical performance and system longevity, the final oxidation product still remained in the electrolyte/electrode, making it a dead mass that degraded the performance of the LIC. Recently, attempts have been made to add compounds to the electrode that evolve to a gaseous state after electrochemical oxidation. An example of such a compound is dilithium squarate (Li₂C₄O₄), which oxidizes to CO₂, which can then be easily removed from the system [256]. Nevertheless, the increase in pressure and gas release causes irreversible changes in the positive electrode, leading to the search for other pre-insertion methods.

One-step assembly of metal-ion capacitors using redox-active electrolytes

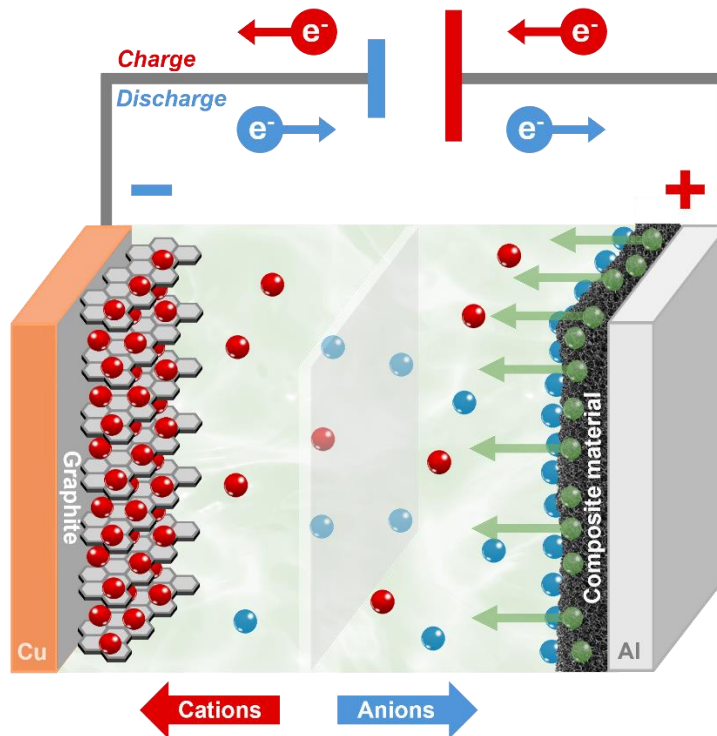


Figure 14. Assembly of a lithium-ion capacitor using a composite materials approach for pre-insertion.

Another method of pre-inserting metal ions into the structure of the negative electrode is the use of a concentrated electrolyte [247]. In 2012, Decaux et al. proposed a pre-insertion method in which, using 10 successive charge/self-discharge pulses, they pushed the lithium ions from the electrolyte (2M LiTFSI in EC:DMC) to the graphite electrode (**Figure 15**). However, this technique only partially intercalated the negative electrode, resulting in a reduced electrode capacity and consequently lower energy of the entire cell. Additionally, the presence of a very concentrated electrolyte negatively affects the viscosity parameter and, most importantly, reduces the ionic conductivity of the electrolyte. The use of this technique is also economically unfeasible because of the use of very large amounts of expensive LiTFSI salt.

The last pre-intercalation method is using a thicker positive electrode. This method, known as mass balancing, aims to equalize the capacity between the positive and negative electrodes by increasing the mass of one of the electrodes [248]. Due to the higher theoretical capacity of graphite (372 mAh g⁻¹) compared to activated carbon (about 70 mAh g⁻¹), a larger positive electrode is used to

One-step assembly of metal-ion capacitors using redox-active electrolytes

balance the charge between the electrodes. Unfortunately, this method often proves ineffective, and additionally, the resistance resulting from using such a thick electrode negatively impacts the performance parameters of the entire cell. Moreover, the very heavy positive electrode adversely affects the specific energy values, which are calculated based on the mass of the entire system.

The presented pre-insertion methods allow for effective pre-insertion of metal ions into the structure of the negative electrode; however, each of them has its drawbacks and risks, making metal-ion capacitors still an unpopular and unprofitable device on the market. Therefore, new solutions that will contribute to the popularization of metal-ion capacitors are crucial.

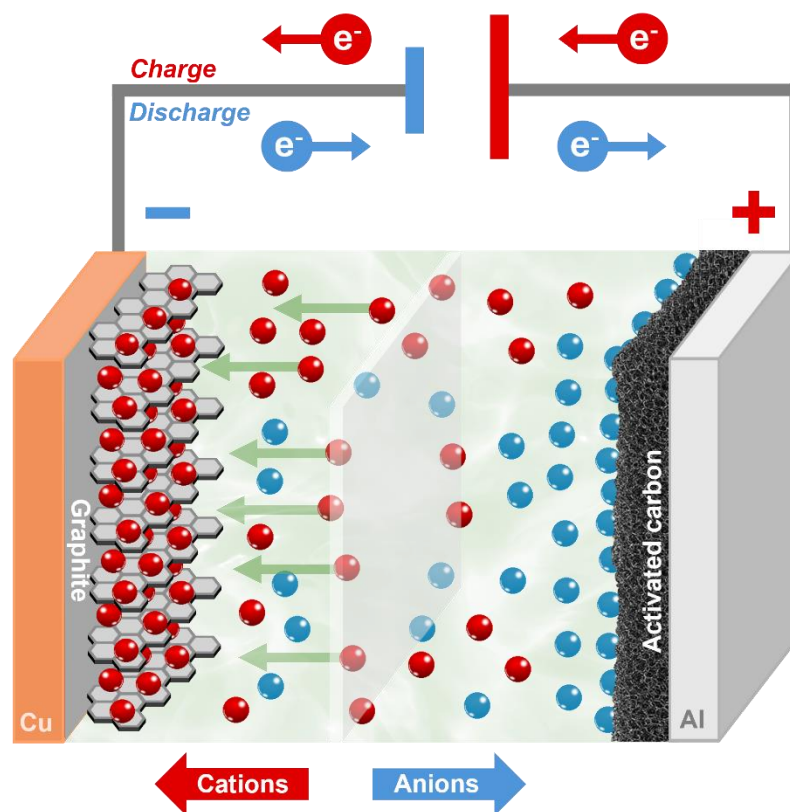


Figure 15. Pre-insertion of graphite electrode using concentrated electrolyte approach.

6. Electrochemical research techniques

There are many known electrochemical techniques in the literature that are commonly used in laboratories. These methods are used to study the behavior of electrochemical systems such as capacitors, batteries, fuel cells, single cells, and sensors. These techniques help to understand the properties of materials, electrolytes, and reactions at the electrode-electrolyte interface. Techniques are often divided based on whether the surface or the bulk of the electrolyte, collector, or electrode is being studied (**Figure 16**). Often, the potential or voltage of the cell is checked with an external current of zero (OCV). However, the most popular are dynamic techniques, in which the parameters of the components remain constant except for one, which is the subject of the study.

Research can be conducted using either a two- or three-electrode setup. Two-electrode studies are typically used for full cells, industrial cells, where there are only two electrodes: the working electrode (WE) and the counter electrode (CE). Typically, these are the anode and cathode or positive and negative electrodes. However, in preliminary scientific research or fundamental studies, three-electrode studies are often used, where, in addition to the WE and CE, there is also a reference electrode (RE). The reference electrode has a known, stable working potential (e.g., metallic lithium, whose working potential in an organic environment is -3.05 V vs. SHE [257]), which allows the study of not only the entire system but also individual electrodes.

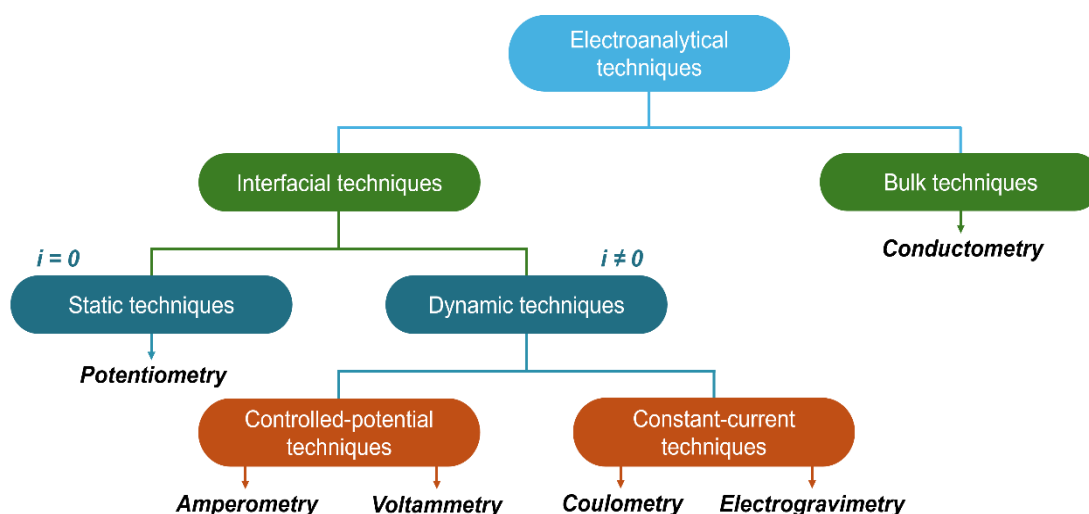


Figure 16. Scheme of electroanalytical techniques [258].

Cyclic voltammetry (CV)

Cyclic voltammetry is one of the voltametric techniques in which a linearly variable potential is applied to the working electrode during measurement [259]. The term "cyclic" comes from the measurement method, where in the electrolyte a reaction $X \rightarrow Y$, such as an electrooxidation reaction, is directly followed by the reverse process, i.e., an electroreduction reaction $Y \rightarrow X$. This allows for obtaining information about the kinetics and mechanisms of electrode processes. The potential starts from a minimum value to a maximum value - the anodic cycle, after which the polarization direction of the electrode changes from the maximum value back to the minimum. Oxidation processes occur during the anodic cycle, whereas reduction processes occur during the cathodic cycle. Such a polarization cycle of the working electrode can be repeated multiple times.

Galvanostatic cycling with potential limitation (GCPL)

Using the GCPL technique, the changing potential of a cell is studied over time while a constant current value is applied [260]. Naturally, the study is limited by specified potential limits (upper and lower) to prevent cell damage. GCPL is the most standard tool for studying the cyclic operation of cells. The dependence C/h is often used, where C is the maximum theoretical capacity of the cell, and h is the time in which the user wants the cell to be charged to capacity C . The study of galvanostatic charging and discharging can be repeated many times; it is often performed until the cell exceeds 80% of its initial capacity. Such an exceedance suggests cell deterioration, and the number of charging and discharging cycles performed is often an indicator of the cell's lifespan.

Potentiostatic electrochemical impedance spectroscopy (PEIS)

The electrochemical impedance spectroscopy has many applications in corrosion, battery, fuel cell development, sensors, and physical electrochemistry. It can provide information on reaction parameters, corrosion rates, porosity of the electrode surfaces, coating, mass transport, interfacial capacitance measurements [261]. The PEIS experiment performs impedance measurements in potentiostatic mode by applying a sinus around the DC potential that can be set to a fixed value. For very capacitive or low impedance electrochemical

systems, the potential amplitude can lead to a current overflow that can stop the experiment in order to protect the unit from overheating.

Step-Potential Electrochemical Spectroscopy (SPECS)

The SPECS technique is a relatively new method for characterizing energy storage systems. It was first introduced in 2015 [262], where it was used to describe electrode materials in electrical double-layer capacitors. This technique involves applying a series of gradual potential changes (called potential steps) to the system, which are separated by a rest time [263]. During these potential steps, the current response is measured. In this technique, it is very important that the potential steps are as small as possible, making the technique more precise. However, it is even more important that the rest time is long enough for the current response to stabilize. The total current response (I_T) after each potential step is then thoroughly analyzed and separated into three components: I_{EDL} , associated with the formation of the electric double-layer; I_D , associated with diffusion processes; and I_R , associated with additional redox reactions occurring in the system (**Equation 3**) [264].

$$I_T = I_{EDL} + I_D + I_R \quad (3)$$

To calculate each of the individual parameters, their components must be taken into account. It is important to note that during the formation of the electric double-layer, there are processes occurring on the porous surface of the electrode, as well as processes occurring in the bulk of the electrode. Therefore, considering the influence of the rest time (t) and the potential step (ΔE), it becomes feasible to compute additional components such as resistance (R_{EDL}), differential capacitance (C_{EDL}), diffusion parameter (B) and residual current (I_R), resulting in the formulation of the final equation (**Equation 4**) [265].

$$I_T = \frac{\Delta E}{R_{EDL}} \exp\left(-\frac{t}{R_{EDL} + C_{EDL}}\right) + \frac{B}{t^{0.5}} + I_R \quad (4)$$

By combining the calculated system components, a thorough illustration of the performance of the system can be explained. Therefore, SPECS is a quick and effective method for determining the stability of electrode materials, evaluating ionic mobility within the electrolyte, measuring the equivalent series

resistance (ESR) of electrode materials, and optimizing cell engineering [266].

Galvanostatic intermittent titration technique (GITT)

Unlike SPECS, GITT involves applying a current pulse to the system and measuring its potential response. GITT is a widely recognized and frequently utilized method, mainly for determining the diffusion coefficient in energy storage systems. The Weppner and Huggins equation is typically used to calculate diffusion values [267]. However, to accurately determine the diffusion coefficient in systems with a graphite electrode, a modified version of the equation is used [268]:

$$\tilde{D} = \frac{4}{9\pi} \left(\frac{E_4 - E_0}{E_2 - E_1} \right)^2 \frac{r_p^2}{t_p} \text{ for } \left(\tau \ll \frac{L^2}{\tilde{D}} \right) \quad (5)$$

symbol \tilde{D} represents the diffusion coefficient [$\text{m}^2 \text{s}^{-1}$], τ is the interval time from charging to discharging (excluding relaxation phase) [s], and L is the sample thickness [m] in **Equation 5**. The potential response observed during GITT comprises five distinct phases: starting from the initial potential (E_0), transitioning through the voltage jump (IR drop, $E_1 - E_0$), progressing to the increment phase ($E_2 - E_1$), further proceeding through the subsequent IR drop ($E_3 - E_2$), and ultimately reaching the phase of final resting potential (E_4) (Fig. 1). Using this equation, along with the potential response data, the values of t_p (pulse duration) and r_p (particle radius), allow the determination of the diffusion coefficient.

7. Summary

Currently, people are increasingly using electronic devices, creating a continuously growing need for energy storage systems. However, the solutions currently in use are no longer sufficient. When people buy devices such as laptops or cell phones, the battery lasts for a few hours of intensive work and then needs to be recharged. After about two years, the battery is usually damaged and needs to be replaced. Therefore, it is crucial to develop new technologies that meet consumer needs and contribute to environmental protection.

The most commonly used energy storage system today is lithium-ion batteries, which consist of a lithium-intercalated layered anode and a lithiated metal oxide as the cathode immersed in an organic solution. Li-ion batteries

One-step assembly of metal-ion capacitors using redox-active electrolytes

currently provide the best specific energy relative to moderate power. For applications where rapid use of stored energy is required, EDLCs perform best. The absence of Faradaic reactions, which store energy solely based on electrostatic attraction, makes them well-suited for high-power applications.

However, much has already been achieved in the development of both EDLCs and Li-ion batteries, so new solutions such as hybrid metal-ion capacitors are being sought. These combine both energy storage mechanisms – electrostatic attraction and the anode intercalation process. Hybrid capacitors have many advantages and represent an optimal solution where high power and high specific energy are needed, but they are limited by the necessary pre-insertion stage. Currently, there are several pre-insertion techniques, but none can provide comprehensive lithium-ion insertion with an economic approach. Solving this problem could be a breakthrough in energy storage systems and, who knows, might one day replace the currently used batteries.

Chapter II

Dissertation aims and outline

Aim and scope of thesis

The main problem aimed to be solved during the dissertation is to optimize the assembling of metal-ion capacitors. The use of auxiliary metallic lithium electrodes is somehow dangerous for the working environment and expensive for industrial use. Furthermore, the presence of a dead mass on the positive electrode in sacrificial composites and the loss of conductivity during intercalation of concentrated electrolytes are issues that require further optimization [269]. At the same time, all of these problems might be solved using redox-active electrolytes. Therefore, the following hypothesis is proposed:

*In hybrid metal-ion capacitors, a **redox-active** electrolyte can work as a **charge balancer** and facilitate the insertion of metal ions from the electrolyte into the anode structure.*

The research concept is to dissolve the calculated number of electroactive species (namely thiocyanate salt) in common electrolytes used for Li-ion, Na-ion, and K-ion capacitors, which will allow for the full insertion of metal ions into the graphite or hard carbon electrode structure. During charging, redox reactions related to the dissolved compound in the electrolyte will take place at the positive electrode. The potential of the positive electrode should remain constant (plateau) or slope slowly, until the redox reaction is exhausted. During this time, metal ions (lithium or sodium or potassium from the electroactive compound) will intercalate into a carbon structure at the negative electrode. The cell charged in this way will be examined in terms of determining the operating voltage, self-discharge, ageing or power/energy values. Then, detailed tests of both the electrolyte and electrode materials after electrochemical work will be carried out with the use of spectroscopic analyses. After understanding the processes in the cell and selecting the optimal conditions, electrolyte and electrode materials of the hybrid capacitor, the system will be assembled to compare the values with commercial systems. Finally, other redox-active additives will be searched that could find an application in the one-step assembly approach.

The scientific novelty of the work is the approach of one-step pre-insertion of the carbon-negative electrode in metal-ion capacitors.

Nevertheless, the pre-insertion process from the electrolyte is already described in the literature; however, it is not with the redox-active electrolyte and not with a completed full insertion process. This solution brings many advantages and solves problems encountered with the previous methods, especially the problem of the loss of electrical conductivity by the electrolyte and the cost of the cell assembly. The cell obtained by this method may additionally have higher power and energy values than the commercially used metal-ion capacitors and may constitute a breakthrough in energy storage devices. Further developments of the system could bring the Li-ion capacitors above those currently used Li-ion batteries, but this is still a far-reaching conclusion. Additionally, the SPECS technique was employed in the research, which so far has only been used to describe the operation of electrical double-layer capacitors. By utilizing the SPECS technique in systems with Faradaic reactions, it was possible to accurately describe important parameters like capacity, resistance, or diffusion coefficient during electrochemical operation. The SPECS technique may become a powerful tool for research on not only electrochemical capacitors but also battery cells.

Structure of the thesis

The doctoral thesis consists of **three published scientific articles (A)** and **two manuscripts (M)** submitted to peer-reviewed scientific journals, considered as unpublished results on the thesis submission date. The thesis is divided into six chapters. The first chapter describes a literature review regarding energy storage systems: electrical double-layer capacitors, lithium-ion batteries, and hybrid metal-ion capacitors. The second chapter presents the aim of the work with the research hypothesis highlighted, the main assumptions, and the structure of the entire dissertation. In the third chapter, article **(A1)** and manuscript **(M1)** are presented, which confirm the previously stated hypothesis regarding the use of redox electrolytes for conducting a one-step pre-metalation method for metal-ion capacitors. For this purpose, an electrolyte with the addition of thiocyanate salt was used. The fourth chapter presents article **(A2)** and manuscript **(M2)**, which introduce the SPECS technique, as a comprehensive tool

One-step assembly of metal-ion capacitors using redox-active electrolytes

for studying the intercalation process of graphite anodes and allows for the assessment of the impact of redox-active salt additives in the electrolyte. The fifth chapter describes attempts to use other redox-active salts instead of thiocyanate salts, which can be utilized in the one-step pre-metalation approach in metal-ion capacitors, with an example of acetate salts presented in article **A3**. The final, sixth chapter of the thesis is a description of the obtained results and a summary of the conducted research. At the end of the work, a list of the candidate's achievements is included, along with statements from co-authors about their contributions to the conducted research.

Chapter III

One-step assembly approach using thiocyanate additive

Article 1: *Redox-active electrolytes as a viable approach for the one-step assembly of metal-ion capacitors*

Manuscript 1: *Li-ion capacitor exploiting a redox-active electrolyte*

Article 1:

Redox-active electrolytes as a viable approach for the one-step assembly of metal-ion capacitors

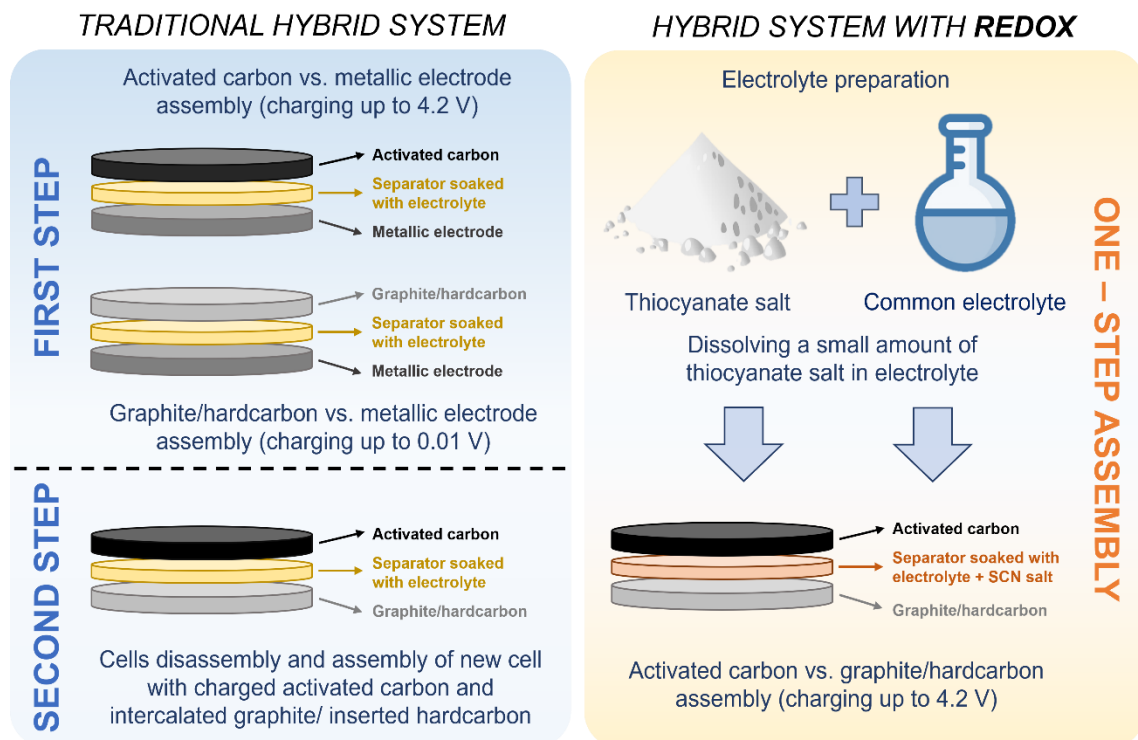
Authors: Adam Maćkowiak, Paweł Jeżowski, Yukiko Matsui, Masashi Ishikawa, Krzysztof Fic

Journal: Energy Storage Materials, 2024, 65, 103163

DOI: doi.org/10.1016/j.ensm.2023.103163

Licence: The content is available under CC BY 4.0

Contribution: Conceptualization, data curation, formal analysis, investigation, methodology, visualization, writing – original draft.



Manuscript 1:

Li-ion capacitor exploiting a redox-active electrolyte

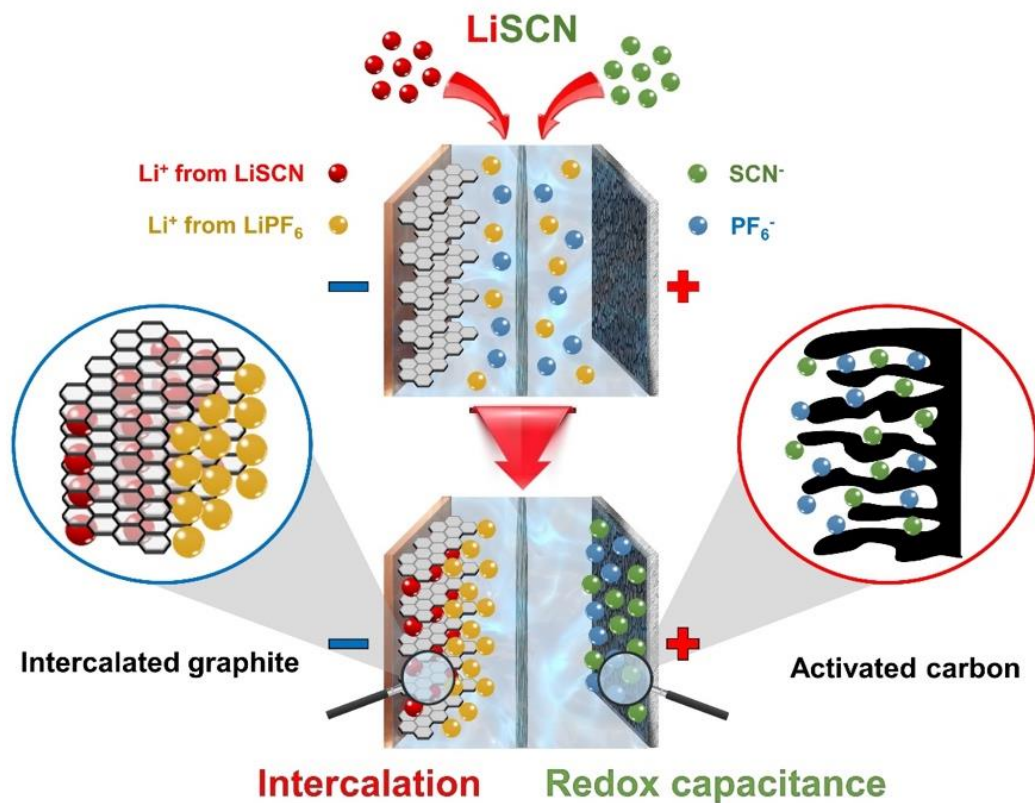
Authors: **Adam Maćkowiak**, Paweł Jeżowski, Adam Ślesiński, Yukiko Matsui, Kazunari Soeda, Masashi Ishikawa, Krzysztof Fic

Journal: Unpublished data

DOI: -

Licence: Restricted data

Contribution: Conceptualization, data curation, formal analysis, investigation, methodology, visualization, writing – original draft.



Context of the research and summary

The motivation for conducting the research in the first two works is to solve the problem of assembling metal-ion capacitors. Current techniques make the construction of metal-ion capacitors expensive, time-consuming, dangerous, and often result in reduced cyclic performance of the cell. Based on a literature review [124, 125, 247, 270] and preliminary research, it was hypothesized that it is possible to insert metal ions into the structure of the negative electrode using a redox-active electrolyte. Naturally, this hypothesis needs to be confirmed, which is why the first two papers focus on attempting to insert metal ions into the structure of negative electrodes using the addition of thiocyanate salts to popular electrolytes. A series of electrochemical and spectroscopic studies were conducted to confirm the hypothesis and explain the changes occurring in hybrid capacitors.

Article 1 focused on the insertion of lithium, sodium, and potassium ions in lithium-ion, sodium-ion, and potassium-ion capacitors, respectively. At the very beginning of the supplementary information, the exact procedure for calculating the addition of thiocyanates to the electrolyte is provided, along with instructions on how to assemble a hybrid capacitor with this electrolyte. Subsequently, tests were conducted in half-cells with activated carbon vs. metal (lithium, sodium, or potassium). Initially, cyclic voltammetry tests were performed, where irreversible activity of thiocyanate salts was observed. Furthermore, voltammograms for sodium, lithium, and potassium were compared, showing that despite very similar chemical composition, the activity of thiocyanates in each system is different. This is likely due to the size of the cation and its solvation shell, which causes charge storage in the pores at the electrode/electrolyte interface to vary. Additionally, galvanostatic charge and discharge tests were conducted in the same system, confirming the irreversibility of the thiocyanate reaction. It was observed that in a single charging cycle at a C/10 current, capacities of about 200 mAh g⁻¹ could be obtained from the reaction. Adding the capacity of activated carbon can balance the capacities of the positive and negative electrodes.

One-step assembly of metal-ion capacitors using redox-active electrolytes

Next, to confirm the hypothesis, a full system of graphite (or hard carbon) vs. activated carbon was assembled, with metal (lithium, sodium, or potassium) added as a reference electrode. In this system, a successful attempt was made to insert metal ions into the structure of the negative electrode. A plateau of the potential on the positive electrode was observed, allowing for the insertion of metal ions into the negative electrode. In the case of the graphite electrode, all stages of intercalation were observed. A comparative study was also conducted by assembling the same system without the addition of thiocyanates - this system, of course, did not allow for intercalation, and the potential of the positive electrode quickly reached the cut-off limit. Furthermore, cyclic studies were conducted in a three-electrode system to compare the performance of individual electrodes during cyclic operation, where gradual degradation of the negative electrode was observed. Electrochemical impedance spectroscopy studies were then conducted, comparing the resistance of a hybrid Li-ion capacitor assembled using the traditional method (with metallic lithium) and one assembled using the one-step assembly method with a redox-active electrolyte. Despite similar ESR values, the diffusive layer resistance for the system with SCN^- was significantly lower, translating to lower resistance values in systems assembled with the redox electrolyte. PEIS also examined the conductivity of the electrolytes, suggesting that the addition of SCN^- slightly lowers ionic conductivity (from 13 to 11 mS cm^{-1}), but after extraction, the conductivity value returns to the optimal value used in conventional electrolytes.

Subsequently, the specific power and energy of five systems were calculated: a lithium hybrid assembled using the traditional method (71 Wh kg^{-1} , 130 W kg^{-1}), a hybrid with the addition of LiSCN (115 Wh kg^{-1} , 125 W kg^{-1}), a hybrid with the addition of NaSCN (91 Wh kg^{-1} , 156 W kg^{-1}), a hybrid with the addition of KSCN (78 Wh kg^{-1} , 130 W kg^{-1}), and a hybrid assembled with a ten times heavier positive electrode (27 Wh kg^{-1} , 179 W kg^{-1}) to compare the charge balancing and mass-balancing techniques. It is evident that mass balancing is not effective, as adding mass to the system reduces the specific energy values. The values obtained using the one-step assembly technique with the redox electrolyte are higher than the energy values obtained using the traditional

technique. Even for the sodium system, which is limited by the lower capacity of hard carbon, higher specific energy was obtained.

A series of spectroscopic studies were then conducted to examine both the electrolyte and the electrodes before and after electrochemical operation. FTIR studies showed that for the electrolyte before electrochemical operation, a signal from thiocyanates at a wavelength of 2072 cm^{-1} can be observed. However, this signal disappears after the first extraction and completely vanishes after a few cycles of system operation. Raman spectroscopy, X-ray diffraction (XRD), X-ray photoelectron spectroscopy (XPS), transmission electron microscopy (TEM), High-Angle Annular Dark-Field Scanning Transmission Electron Microscopy (HAADF-STEM), and Energy Dispersive X-ray Spectroscopy (EDS) studies were also conducted. Unfortunately, none of the techniques used provided a definitive answer about the composition of the final product of thiocyanate oxidation in an organic medium. It is likely that thiocyanate oxidation follows multiple pathways. However, the data suggests that the final product is still a mixture of sulfur and carbon precipitated on the surface of the positive electrode. The last study conducted in this article is gas chromatography with mass spectrometry to identify gases emitted during the first charging cycle of the system. It was observed that in addition to the characteristic gases released during the formation of the SEI layer, a large volume of gases with $m/z = 44$ and 76 are emitted. Mass 44 is responsible for the formation of an intermediate oxidation product of SCN to the unstable compound CS, which then transitions to the more stable form of CS₂ with a mass of 76 . The conducted studies do not establish a uniform reaction for the thiocyanate anion, but they show that it may not be linear and can lead to the formation of several different products. Nevertheless, the hypothesis was confirmed, as it was successfully possible to insert metal ions into the structure of the negative electrode using a redox-active electrolyte in metal-ion capacitors.

In **Manuscript 1**, the focus was on improving the process of lithium-ion intercalation into graphite structures in lithium-ion capacitors, then identifying the reaction mechanism of the thiocyanate anion, followed by optimizing the assembly process and comparing the obtained results with commercial systems. The main goal was to determine whether the one-step assembly approach has

One-step assembly of metal-ion capacitors using redox-active electrolytes

marketable potential and how a system assembled this way compares to commercial cells, as well as to investigate what exactly happens with thiocyanates during pre-intercalation.

The research began with a half-cell of activated carbon vs. metallic lithium in an organic electrolyte with added LiSCN to study the activity of the additive. Two reactions were observed, the first at a potential of about 3.5 V and the second at about 4.1 V vs. Li/Li⁺. The two oxidation reactions suggest the formation of an intermediate product and its subsequent oxidation to the final form. The reaction is also slightly reversible. However, after just 6 cycles, the redox activity completely disappeared, and the positive electrode exhibited only capacitive behavior. Next, the negative electrode was examined in a half-cell with and without LiSCN addition using galvanostatic charging and discharging. No significant difference was observed in the performance of the negative electrode, only a slightly higher capacity was used for SEI layer formation in the system with lithium thiocyanate, indicating an increase in the system's irreversible capacity. This observation suggests that SCN⁻ ions may affect the thickness and integrity of the SEI layer.

Subsequently, a three-electrode one-step pre-insertion was conducted with and without thiocyanate salt. In the setup, besides the negative electrode (graphite) and the positive electrode (activated carbon), metallic lithium was used as the reference electrode. LiSCN salt delivered additional capacity, allowing full intercalation of the graphite electrode. Without the thiocyanate salt, intercalation was not possible, and the positive electrode quickly reached the electrolyte decomposition potential. Then, the performance of both electrodes was examined during cycling tests in the voltage range of 2.2 V to 4.2 V. The positive electrode operated in a capacitive manner, characteristic of electrochemical capacitors, while the negative electrode maintained potential through redox reactions (intercalation). Over time, the negative electrode began to degrade. The system was then analyzed using impedance spectroscopy, and Nyquist and Bode plots were obtained for pre- and post-cycling operation. The equivalent distributed resistance (EDR) improves after cycling due to better intercalation of

the graphite; however, the curve shape indicates issues with the diffusive layer resistance during electrochemical operation.

Next, the obtained cycling results were compared with a commercial system. The system with LiSCN recorded about 2400 cycles at a higher operating voltage, while the commercial system operated for tens of thousands of cycles at a voltage range of 2.2 V to 3.8 V. Additionally, self-discharge of the commercial LIC, a hybrid capacitor with LiSCN, and a commercial EDL capacitor was compared. Generally, EDL capacitors exhibit high self-discharge, which was also observed in this case. For the LIC with SCN, the voltage dropped by about 0.2 V after 12 hours, still giving a higher voltage than the commercial capacitor. However, the precise construction of the commercial capacitor results in minimal self-discharge (0.02 V after 12 hours) and contributes to improved system cyclability. Therefore, the next step was to compare the energy and power of the system. A Ragone plot was created to show the importance of the mass of individual components on the specific energy and power of the system. Specific energy was determined for the following components: active electrode mass, total electrode mass, current collector mass, separator mass, CR2032 casing mass, and electrolyte mass. The hybrid capacitor with LiSCN achieved better energy values (9 Wh kg⁻¹) compared to the commercial LiC (7 Wh kg⁻¹) when both systems exhibited a capacity of about 20 F and energy values were calculated based on all components. This result indicates that, besides effective charging, the one-step assembly technique allows for better specific energy values.

Further studies aimed at identifying thiocyanate reactions were initiated. FTIR studies showed the disappearance of the signal at a wavelength of 2072 cm⁻¹, characteristic of SCN. Raman spectroscopy, SEM with EDS, XPS, and tomography images were also conducted, revealing the cracking of the negative electrode after cycling. GCMS was used to identify gases produced during the operation of the system with SCN. Characteristic gases for the SEI layer with masses 24, 25, 26 and 27 were observed from compounds C₂H₂, C₂H₄. Additionally, other masses not present in the system without SCN were identified: 48 (SO), 58 (C₂H₂S), and 60 (COS). A sharp increase in mass 44 (CS, CO₂) and 76 (CS₂) was also noted. The multitude of obtained masses suggests the

formation of many reaction products. Initially, an unstable CS compound likely forms, which can then react, mainly producing CS₂ but also SO and COS, as confirmed by gas chromatography. **Manuscript 1** presented a series of possible reactions and highlighted one with the highest probability, where ethylene carbonate reacts with LiSCN, yielding lithium cyanate and thiirane, with carbon dioxide as an intermediate product. The most important conclusion is that no harmful hydrogen cyanide is formed during oxidation, therefore LiSCN are safe to use as an electrolyte additive.

In summary, both works present an effective one-step assembly pre-insertion approach for metal-ion capacitors using redox-active electrolyte with thiocyanate salts. This technique saves time and money during the assembly of metal-ion capacitors and increases their specific energy. Of course, the solution has some issues, such as lower cyclability and higher self-discharge compared to commercial cells, but these can be addressed with proper electrode balance and better cell construction.

Article 1

One-step assembly of metal-ion capacitors using redox-active electrolytes

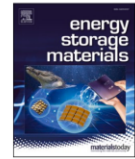
Energy Storage Materials 65 (2024) 103163



Contents lists available at ScienceDirect

Energy Storage Materials

journal homepage: www.elsevier.com/locate/ensm



Redox-active electrolytes as a viable approach for the one-step assembly of metal-ion capacitors

Adam Maćkowiak^a, Paweł Jeżowski^a, Yukiko Matsui^b, Masashi Ishikawa^{b,*}, Krzysztof Fic^{a,b,*}

^a Institute of Chemistry and Technical Electrochemistry, Poznan University of Technology, Berdychowo 4, Poznan 60-965, Poland

^b Department of Chemistry and Materials Engineering, Faculty of Chemistry, Materials and Bioengineering, Kansai University, 3-3-35 Yamate-cho, Suita 564-8680, Japan

ARTICLE INFO

Keywords:

Lithium-ion capacitor
Sodium-ion capacitor
Potassium-ion capacitor
One-step preintercalation
Redox-active electrolyte
Metal-ion capacitor

ABSTRACT

The assembly of metal-ion capacitors is a very challenging task; the use of traditional metallic electrodes or sacrificial materials induces technical problems during cell assembly or affects its normal operation. Here, we report an efficient, one-step method for assembling metal-ion capacitors using redox-active electrolytes with thiocyanate-based salts. The addition of a redox-active salt compensates for the charge on the positive electrode while enabling the insertion of metal ions into the structure of the negative electrode. The proposed approach reduces assembly time and cost and results in increased specific energy compared to that from the traditional two-step assembled hybrid systems. Furthermore, we demonstrate that the proposed approach can be successfully implemented for sodium-ion and potassium-ion hybrid capacitors. Our results are supported by operando techniques and can potentially facilitate further research on metal-ion capacitors and applications of these devices.

1. Introduction

Currently, secondary batteries (especially lithium-ion batteries; LIBs) [1–3] and electrochemical capacitors (ECs) [4–7] are the two main technologies used for electrochemical energy storage. On the one hand, the storage of electrical energy in LIBs is based on slow redox reactions in the electrode bulk [8,9]; on the other hand, the energy storage in ECs is related to the formation of an electric double-layer (EDL) at the surface of electrodes [10,11]. Although LIBs can store more energy ($\sim 250 \text{ Wh kg}^{-1}$) than ECs ($\sim 10 \text{ Wh kg}^{-1}$), their power rarely exceeds 1 kW kg^{-1} , and their lifespan is limited to approximately 1000 cycles. In contrast, ECs can reach a power of 10 kW kg^{-1} and store energy continuously for millions of cycles due to the capacitive storage mechanism [12,13]. However, in recent years, a novel hybrid energy storage system that combines the features of LIBs and ECs, namely, lithium-ion capacitors (LICs) has emerged [14–17].

LIC construction is very similar to all energy storage devices; there are two electrodes, separated by a porous membrane, soaked in the electrolyte. The main difference, compared to other devices, is that the energy storage mechanism for each electrode is different. The positive electrode is most often similar to the one in ECs (porous electrodes such as activated carbon) and stores energy in the form of EDL [18], while the

negative electrode is characteristic of LIBs (for example, graphite), which undergoes continuous intercalation and deintercalation of lithium ions from its structure [19]. This internal combination of two completely different mechanisms enables the attainment of energy and power that cannot be achieved by traditional ECs and LIBs, respectively. However, to obtain a fully functional LIC, it is usually necessary to prelithiate the negative graphite electrode, and thus far, there are three available methods for successful prelithiation [20]. The first method uses metallic lithium introduced as an auxiliary electrode. When the prelithiation of graphite is performed in one cell, the intercalated graphite electrode is removed and placed in the second cell with a positive activated carbon electrode [21]. The use of metallic lithium is considered rather unsafe because it can lead to the formation of dendrites, which can further cause internal short-circuiting [22]. To avoid the mentioned issues, it is possible to incorporate lithium-rich salts into the composition of the positive activated carbon electrode and create a composite electrode [15,23,24]. During the initial polarization, the lithium salt releases lithium ions and compensates for the charge necessary for the intercalation of the negative electrode, and afterwards, the oxidized form of lithium salt is no longer electrochemically active. Nevertheless, in most cases, the oxidized salt is present in the electrode composition (forming so-called dead mass), which can significantly

* Corresponding author at: Institute of Chemistry and Technical Electrochemistry, Poznan University of Technology, Berdychowo 4, Poznan 60-965, Poland.
E-mail addresses: masaishi@kansai-u.ac.jp (M. Ishikawa), krzysztof.fic@put.poznan.pl (K. Fic).

<https://doi.org/10.1016/j.ensm.2023.103163>

Received 20 August 2023; Received in revised form 18 December 2023; Accepted 24 December 2023

Available online 26 December 2023

2405-8297/© 2023 The Authors. Published by Elsevier B.V. This is an open access article under the CC BY license (<http://creativecommons.org/licenses/by/4.0/>).

One-step assembly of metal-ion capacitors using redox-active electrolytes

A. Maćkowiak et al.

Energy Storage Materials 65 (2024) 103163

decrease the overall electrochemical performance of the cell [25]; However, recent studies show that during oxidation of the lithium salt, the product can dissolve in the electrolyte [15] or be in a gaseous state [26]. Finally, the last method uses a highly concentrated electrolyte that plays the role of a lithium-ion reservoir. However, the data presented show that the drop in lithium-ion concentration is so significant that the lifespan of this device is less than 500 cycles [27].

Our study presents an original approach to the preintercalation/preinsertion of lithium-, sodium-, and potassium-ion capacitors, called metal-ion capacitors (MICs); we propose the addition of soluble redox-active salt to the electrolyte (Fig. 1).

2. Results and discussion

2.1. Redox activity of the electrolyte

Based on previous considerations, we aimed to intercalate a graphite electrode using lithium ions from the electrolyte. The current literature reports certain concepts using concentrated electrolytes, but all were unsuccessful in certain aspects [27]. The charge necessary to intercalate a negative electrode often exceeded the charge accumulated by a positive electrode. Therefore, our first approach was to balance the charge using a much larger positive electrode (10 times heavier than the negative electrode). Notably, the intercalation using only lithium ions from the electrolyte was possible if the charge of the positive electrode was properly balanced (Supplementary Fig. S1a). However, a problem developed during cycling because the large mass of the positive electrode caused the applied current to be devastating for the negative electrode (Supplementary Fig. S1b). Finally, this approach reduces the power and energy of the system [28].

To mitigate this issue, we proposed a different approach using a redox-active additive to the electrolyte. Additional redox reactions could balance the charge between the positive and negative electrodes as well as provide the necessary metal ions for preintercalation/preinsertion. For this reason, thiocyanate salts were selected as the redox-active additives because of their expected solubility in organic solvents and known redox activity in aqueous electrolytes [29]. To investigate the redox activity of SCN^- anions in an organic medium, they were studied as electrolytes in lithium-ion, sodium-ion, and potassium-ion capacitors.

Thiocyanate salts were found to be easily dissolved in organic electrolytes (carbonates) and demonstrate a redox response at ca. 3.5 V vs. metallic reference, as shown in Fig. 2a. The redox potential strongly

depended on the applied current density; thus, it was decided to use C/10 current density for the first charging process (C – theoretical capacity of graphite, 372 mAh g^{-1}). With the NaSCN system, a different solvent was used (ethylene carbonate (EC):propylene carbonate (PC) mixture, optimal for sodium-ion capacitors [30], which reduced the operational voltage window (the signal from the electrolyte decomposition). This solvent was used due to the reaction of metallic sodium with the electrolyte $1 \text{ mol L}^{-1} \text{ NaPF}_6 \text{ EC:dimethyl carbonate (DMC)}$ containing SCN^- ions (Supplementary Fig. S2a,b). Based on the cyclic voltammetry profiles, each system was characterized by two oxidation reactions of the thiocyanates. Notably, despite the presence of the SCN^- anion, which was responsible for the redox reaction, the current response differed between each system. For the sodium-ion cell, the different responses could be due to different solvent interactions [31]. However, between the lithium- and potassium-containing cells, the only difference in the cell composition was the cation, which apparently plays a significant and often underestimated role in charge storage. Another important advantage of thiocyanate salts was the irreversibility of their electrochemical reactions - reversible redox reaction could lessen the work of the positive electrode, which could affect the voltage of the entire system and, as a result, cause the energy decrease.

In practice, thiocyanate reactions were slightly reversible, as shown in Fig. 2b. The obtained capacity did not reflect the theoretical capacity (for detailed calculations for the theoretical capacity, please see the supplementary description). With each cycle, the capacity from the SCN^- reaction decreased, and it could provide the calculated value. However, the capacity obtained in the first cycle was the most important from the preinsertion process point of view. Therefore, the redox activity of thiocyanate salts fulfilled all the necessary requirements for their possible implementation in metal-ion capacitors.

2.2. Metal-ion capacitors assembled in one step

In the previous section, it was confirmed that the redox reaction occurs at well-defined electrode potentials. Next, it was necessary to determine whether the redox reaction enabled the intercalation/insertion of cations into the structure of the negative electrode without the use of a metallic electrode or sacrificial materials. For this purpose, a cell with a negative electrode (graphite) and a positive electrode (activated carbon) was assembled. Salt containing the SCN^- anion was added to the electrolyte, and the cell was charged with a C/10 current (Fig. 3a). The addition of a thiocyanate salt changed the potential slope of the response from the positive electrode, which enabled full intercalation of the

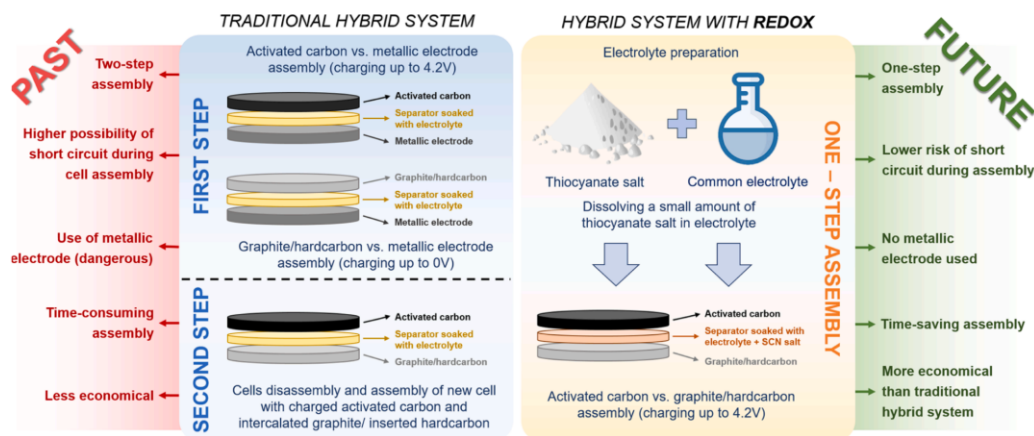


Fig. 1. Schematic representation of the assembly of a traditional hybrid metal-ion capacitor and hybrid system with redox-active electrolyte.

2

One-step assembly of metal-ion capacitors using redox-active electrolytes

A. Maćkowiak et al.

Energy Storage Materials 65 (2024) 103163

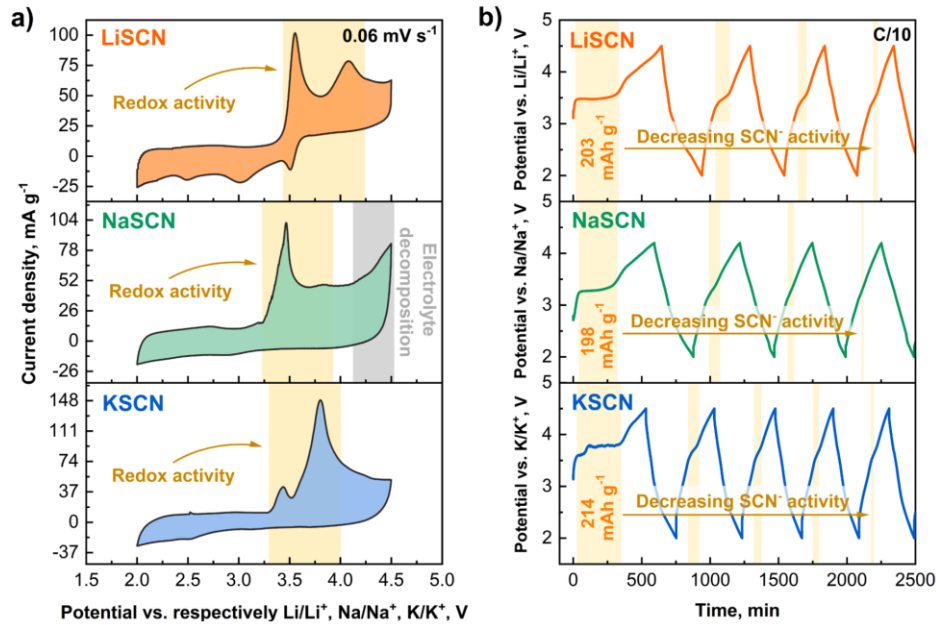


Fig. 2. Redox activity of thiocyanate anions during the half-cell assembly for the activated carbon vs. the metallic electrode with lithium, sodium and potassium: (a) cyclic voltammetry with scan rate 0.06 mV s^{-1} (calculated from current C/10) and (b) galvanostatic charge/discharge with potential limitation with current equal to C/10.

negative electrode. For comparison, another system that did not contain thiocyanate ions was constructed. In this case, the lack of a plateau region from the response of the positive electrode caused the voltage cutoff limit to be quickly reached, which did not enable the negative electrode to even reach the second stage of intercalation. The cell was then run for cycling (Fig. 3b). The system worked very effectively; even after 1000 cycles, it maintained an efficiency above 80 % of the initial capacitance. A slight degradation of the negative electrode was observed.

The previous experiment was then repeated with the sodium-ion capacitor (Fig. 3c). In this case, the graphite was replaced with hard-carbon because of the inability of sodium to form graphite intercalation compounds. Generally, this was considered to be caused by the size mismatch between Na and the graphite interlayer spacings, but the major reason was the change in the chemical bonding between the alkali metal ions and carbon atoms [32,33]. Sodium-ion capacitors are characterized by a different mechanism of solid-electrolyte interphase (SEI) formation with the insertion of sodium ions into the structure of hard-carbon. Nevertheless, the presented approach was successful since the full insertion of sodium ions into hardcarbon was obtained. In Fig. 3d, the first and 20th cycles of the system are shown. Despite the high resistance, the system retained acceptable capacitance.

Following the success of lithium- and sodium-ion systems, the technique was also tested on potassium-ion capacitors. Since potassium could react with the styrene-butadiene rubber present in the graphite electrode (Supplementary Fig. S3), the material was changed to one that did not have this additive. Fig. 3e presents the insertion of potassium ions during the initial charge of the potassium-ion capacitor. However, during cycling (Fig. 3f), problems were encountered, showing the devastating effect of potassium ions on the graphite structure. The high current forced the rapid evacuation of large potassium ions from the graphite, causing its destruction. Reducing the current (e.g., C/10) could help; however, the system would still significantly lose capacitance, and

the negative electrode potential was heading toward a zero value, i.e., the plating of metallic potassium. To improve the operation of the potassium system, a different electrolyte or negative electrode could be used; despite this, the proposed one-step assembly technique was also applicable to potassium-ion capacitors.

2.3. Comparison with traditional hybrid Li-ion capacitor

To compare hybrid one-step assembly capacitors, a traditional two-step hybrid lithium-ion capacitor was constructed. Both cells were characterized with electrochemical impedance spectroscopy (Fig. 4a). The equivalent series resistance (ESR) values were similar for both hybrid systems, as they were constructed with the same electrode materials. The response from the Stern layer on the spectra for both systems was comparable; the size of additional SCN^- ions did not impact the Stern layer thickness. The electric double-layer response was also similar for both hybrid systems. However, small deviations were visible for the thiocyanate-containing system, which meant that some of them were still active in the system and produced a redox response. The diffusive layer resistance (characterized by the second semicircle, Fig. 4a $\text{Re}(Z)$ ca. 16Ω) for the one-step assembly hybrid was much lower than for the traditional hybrid (21Ω) likely due to the precipitation of conductive salt on the electrode/electrolyte interphase. Therefore, the product of SCN^- oxidation did not negatively affect the resistance of the materials.

In the next step, the resistance was compared for both systems at a minimum (2.2 V), medium (3.2 V), and maximum (4.2 V) working voltage. The resistance curves for one-step and two-step assembly hybrids were very similar; however, for the SCN^- -containing system, the lower diffusive resistance enabled improved charge propagation. Additionally, it was changing with continuous working; thus, it could be concluded that certain chemical processes were ongoing in the electrolyte. In the beginning, these processes appeared beneficial for the system, but the final product of the reaction could still be a concern. The

3

One-step assembly of metal-ion capacitors using redox-active electrolytes

A. Maćkowiak et al.

Energy Storage Materials 65 (2024) 103163

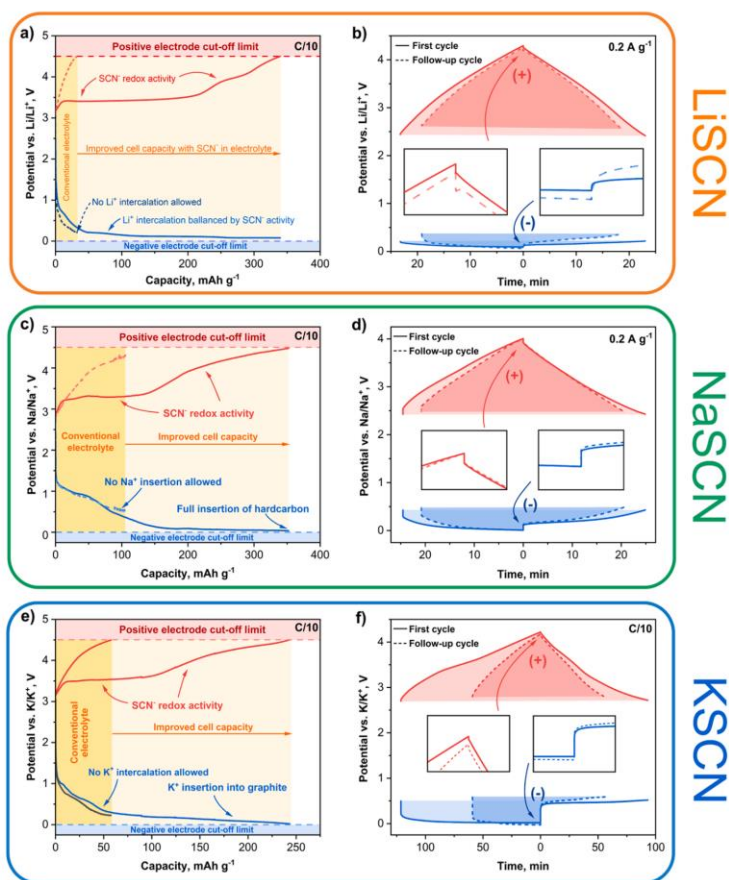


Fig. 3. Three-electrode measurements using redox-active thiocyanates to balance the negative electrode: (a), (c), (e) first galvanostatic charging of the positive and negative electrodes using C/10 enabling preintercalation/preinsertion of cations into the structure of the negative electrode and (b), (d), (f) galvanostatic charging/discharging of the full cell; first cycle and last cycle.

equivalent distribution resistance (EDR) value for the one-step assembly hybrid was smaller, meaning that the charge was better distributed and that the maximum power of the device was higher than that for the two-step assembly system.

Comparing first charging and discharging curves for one-step and two-step assembled systems it should be noted that they are not the same (Supplementary Fig. S4). For the lithium-ion capacitor, the increased capacity of the positive electrode for the SCN-based system is notable, which affects further the energy value. In the case of the sodium-ion capacitor, there are no significant differences between the results of different construction techniques. However, in the case of a potassium-ion capacitor, the system using the two-step technique can store much more charge, which indicates that the electrolyte premetalation technique for potassium-ion capacitors should be further improved, as it is very sensitive to the given current density and potassium cations diffusion.

Subsequently, the specific power and energy of the system with the redox reactions were investigated. Fig. 5 shows the dependence of the specific power and energy of the tested systems during the first cycles of their operation. The worst energy (27 Wh kg^{-1}) properties were found in the system with a large positive electrode, which was explained earlier in the article. A hybrid potassium-ion capacitor also provided an

insufficient amount of energy (60 Wh kg^{-1}) due to the destruction of the graphite structure from large potassium ions. The sodium system was limited by hardcarbon, had a smaller capacity compared to graphite and demonstrated high energy (92 Wh kg^{-1}) and power. Moreover, the lithium-ion capacitor with redox-active electrolyte produced a very high energy (115 Wh kg^{-1}) that was comparable to lithium-ion batteries and completely outperformed the traditional hybrid capacitor (71 Wh kg^{-1}). This result was very promising because it demonstrated a lithium-ion capacitor that could offer higher power and, especially, a long life cycle.

2.4. Spectroscopic and operando GCMS investigation

To determine whether the thiocyanate anion is stable after dissolving in the electrolyte, Fourier-transform infrared (FT-IR) spectra were obtained (Fig. 6a). Signals from the solvents and conductive salts were observed, as well as a strong signal from the SCN^- anion at a wavelength of 2072 cm^{-1} . After confirmation of the SCN^- anions stability in the solution, a comparison of the electrolyte with SCN^- after extraction was performed. The signal from SCN decreased; however, it did not disappear completely, which confirmed that the thiocyanates were still active even after the extraction; this result agreed with electrochemical tests (Fig. 2b). A similar relationship was observed for systems with sodium

4

One-step assembly of metal-ion capacitors using redox-active electrolytes

A. Maćkowiak et al.

Energy Storage Materials 65 (2024) 103163

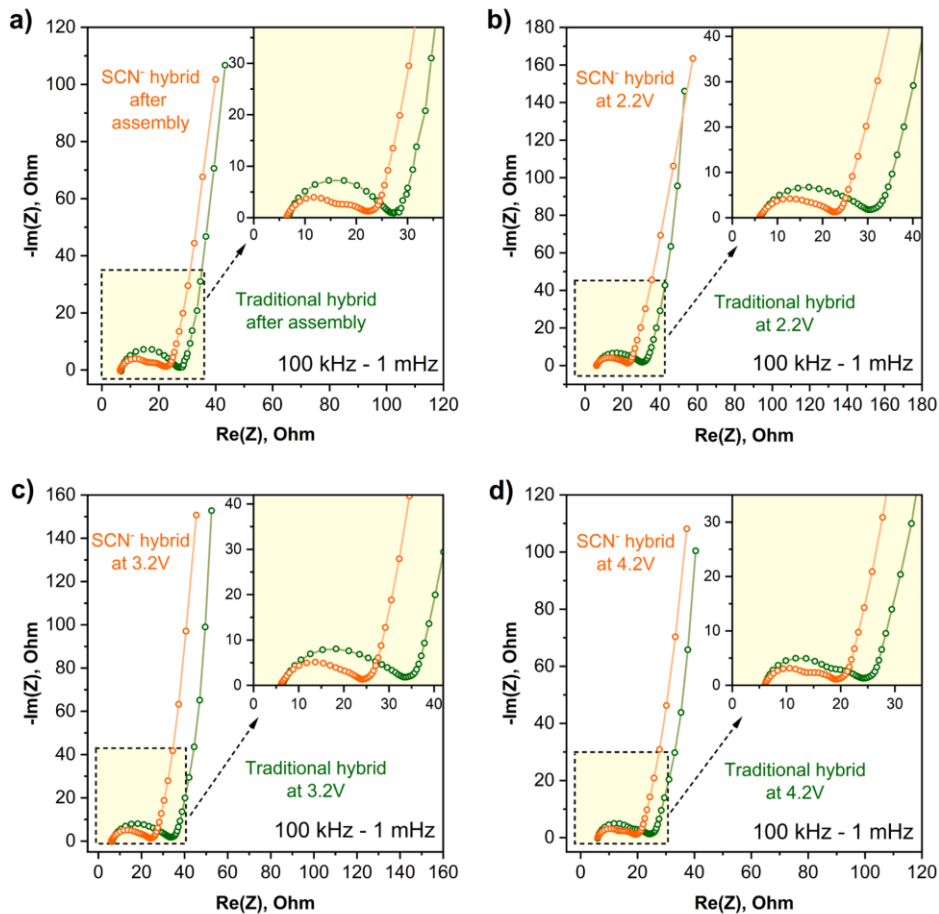


Fig. 4. Comparison of the hybrid systems assembled in one step and two steps using electrochemical impedance spectroscopy: (a) after cell assembly, (b) at minimum working voltage (2.2 V), (c) at medium working voltage (3.2 V), and (d) at maximum working voltage (4.2 V).

and potassium (Supplementary Fig. S6a,b). Proper development of the SEI was very important for the operation of the cell [34], and in the LiSCN system, the signals coming from the solvent (especially from DMC, 2965 cm^{-1} and 1605 cm^{-1}) decreased after the first charging cycle.

Raman spectra were obtained to determine the change in electrode material before and after electrochemical work (Fig. 6b and c; Supplementary Figs. S8a,b, and S9a,b). Using a microscope, small local areas could be found where a yellow precipitate appears (Supplementary Fig. S7a,b). Preliminary analysis showed that it was a complex compound of sulfur with carbon, oxygen and likely lithium. The presence of this yellow precipitate might not be beneficial for the longer cycling of the system since it could clog the pores of the activated carbon. Nevertheless, this small amount of conductive salt did not significantly affect the first cycles of the electrochemical work. To describe the precipitated compound in more detail, an analysis was performed using an X-ray diffractometer (Supplementary Figs. S10–S12). Unfortunately, the small amount of the obtained compound or its lack of crystallographic structure did not enable an accurate description of the obtained structure. Also, to extend the characterization of the system with thiocyanate anion additional experiments were performed: X-ray

Photoelectron Spectroscopy (XPS) (Supplementary Fig. S13), Transmission Electron Microscopy (TEM), High-Angle Annular Dark-Field Scanning Transmission Electron Microscopy (HAADF-STEM) and Energy Dispersive X-ray Spectroscopy (EDS) (Supplementary Figs. S14–S16). Unfortunately, all performed techniques did not provide clear answer about the composition of the final product of the thiocyanate oxidation in organic medium. Probably, there are several pathways of thiocyanate oxidation. However, based on the obtained data, the final product must be still the combination of sulfur and carbon.

To investigate the SCN reaction in more detail, the system was studied using operando gas chromatography coupled with mass spectrometry (GCMS). The results presented in Fig. 7a showed the most important masses formed during the first charging of the system. The collected results were compared with those from a traditional hybrid containing no thiocyanate anions. In both cases, gases from SEI formation were visible (signals for $m/z = 24\text{--}27$); these were mostly responsible for the evolution of ethylene [35]. However, the signals obtained from the hybrid were weaker, which could mean that the SEI composition was potentially different. The main compounds that were formed during electrochemical work were ethylene (C_2H_4), carbon monosulfide (CS), carbon dioxide (CO_2), sulfur monoxide (SO), thiirene ($\text{C}_2\text{H}_2\text{S}$),

5

One-step assembly of metal-ion capacitors using redox-active electrolytes

A. Maćkowiak et al.

Energy Storage Materials 65 (2024) 103163

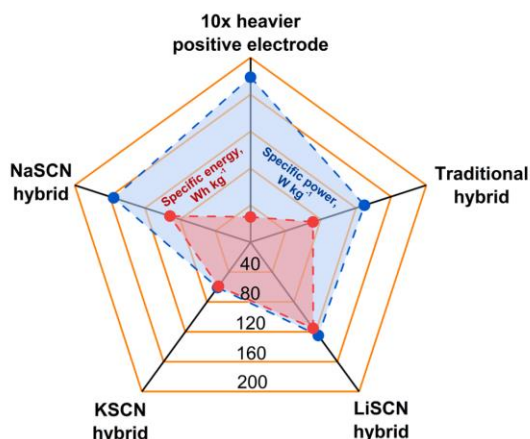


Fig. 5. Specific power and energy dependence chart of all assembled and discussed hybrid-ion capacitors (for different graph representation, please see Supplementary Fig. S5).

carbonyl sulfide (COS) and carbon disulfide (CS₂). Notably, no toxic hydrogen cyanide (HCN) was released. This result was also confirmed by performing operando GCMS for the sodium-ion capacitor (Supplementary Fig. S17a).

Based on the obtained data and previous research, a potential explanation of the reactions taking place in the system is provided. Quantitatively, the strongest signals come from $m/z = 44$ and 76 (Fig. 7b). Therefore, thiocyanate is unstable under an applied voltage, undergoes an irreversible reaction, and mainly reacts with the carbon present in the electrode material. In the first phase, the thiocyanate anion polymerizes to (SCN)₂ [29]. In the second part, the polymer is oxidized to CS [36]. During this process, elemental sulfur is also formed, deposited on the carbon, and further reacts to form CS or a substrate for the obtained precipitate. CS is an unstable compound; therefore, it reacts quickly with carbon on the surface to form CS₂ [37] or oxidizes from electrolyte decomposition products to form COS [38]. A carbon disulfate product is formed on the surface of the positive electrode made of carbon, after which it is probably also oxidized. The resulting product is noticeable on the surface of the electrode (Supplementary Fig. S7a,b).

3. Conclusion

The successful use of thiocyanate salts as a redox-active addition to the electrolyte allowed for the compensation of the charge on the positive electrode, enabling the intercalation/insertion process on the negative electrode. This provided a completely new and interesting assembly of metal-ion capacitors in just one step. First, the one-step assembled systems had lower resistance than two-step systems (16 Ω compared to 21 Ω), resulting in better diffusion and charge propagation. This was reflected in the obtained specific energy values (115 Wh kg⁻¹ compared to 71 Wh kg⁻¹). Moreover, it was shown that SCN⁻ anions underwent an irreversible reaction, which was confirmed by the signal at 2072 cm⁻¹ in the FT-IR spectra. Operando GCMS measurements indicated that the main reaction of thiocyanates was associated with the formation of CS and at a later stage, CS₂ and other oxidized species, such as COS.

One-step assembly has many advantages compared to the traditional method: lower production costs, no use of an expensive and dangerous metallic electrode, faster assembly time, and higher energy density compared to the currently used lithium-ion capacitors. Although the technique itself appears to work flawlessly, the use of thiocyanate salts has certain limitations. The complicated reaction process at high

potential causes the formation of small amounts of conductive salt on the surface of the positive electrode; noticeable volume of gases has been also observed. Nevertheless, these issues do not discredit the concept, as they can be easily solved at the device processing level (e.g., primary gas evacuation); of course, changing the redox additive can potentially solve these issues too; however, this is a challenging task for future research.

Proposed approach could close the gap between lithium-ion batteries and metal-ion capacitors. We believe that this concept could revolutionize the metal-ion capacitor market and facilitate the development of sustainable energy storage devices.

4. Experimental section

Electrolyte: Salts: lithium hexafluorophosphate (LiPF₆), potassium hexafluorophosphate (KPF₆), sodium perchlorate (NaClO₄), lithium thiocyanate hydrate (LiSCN xH₂O), sodium thiocyanate (NaSCN) and potassium thiocyanate (KSCN) were purchased from Sigma-Aldrich (Merck). Before use, all salts were dried under a vacuum at 120°C for one week to remove water contamination. Lithium thiocyanate hydrate salt was predried at 100°C using a liquid nitrogen cold trap to remove excess water. Anhydrous solvents: ethylene carbonate (EC), propylene carbonate (PC), and dimethyl carbonate (DMC) were purchased from Sigma-Aldrich (Merck). The electrolyte preparation for lithium cell investigations consisted of preparing a 1 molar solution of LiPF₆ in ethylene carbonate and dimethyl carbonate mixed in a volumetric ratio of 1:1 with an addition of a calculated amount of dissolved LiSCN salt. The same approach was used for the potassium cells, but instead of LiPF₆ and LiSCN, KPF₆ and KSCN salts were used. The electrolyte preparation for sodium investigations consisted of preparing a 1 molar solution of NaClO₄ in ethylene carbonate and propylene carbonate mixed in a volumetric ratio of 1:1 with an addition of a calculated amount of NaSCN salt. The mass of thiocyanate salts added to each electrolyte was determined by the mass of each negative electrode and its theoretical capacity (Supplementary description). Then, 600 μL of the electrolytes received were added to soak the separators during electrochemical cell preparation. All reagents were stored in the MBraun glovebox, which ensured inert environmental conditions. The conductivity values of the electrolytes obtained are shown in Supplementary Information Fig. S19. The conductivity measurement was performed at 25°C using a 2-electrode Swagelok system with a spacer, and the impedance spectroscopy method was used to calculate the conductivity from the resistance.

Electrode material: The negative electrode of the hybrid Li-ion capacitor was made of copper foil covered with a mixture of graphite, styrene-butadiene rubber (SBR), carboxymethyl cellulose (CMC) and carbon black (total thickness = 57 μm) provided by the MTI corporation (Supplementary Fig. S20a). The negative electrode of the hybrid Na-ion capacitor was a laboratory-prepared electrode made of copper foil coated with a mixture of hardcarbon (Carbotron P, Kureha), polyvinylidene fluoride (PVDF) and carbon black (total thickness = 93 μm) (Supplementary Fig. S20b). The negative electrode of the hybrid K-ion capacitor was graphite mixed with CMC and coated on copper foil (total thickness = 100 μm) and was provided by Customcells® (Supplementary Fig. S20c). The positive electrode of all metal-ion capacitors was a self-standing electrode made of Kuraray YP80F (80 %), polytetrafluoroethylene (PTFE) (10 %) and carbon black C65 (10 %) (total thickness = 114 μm). The microtextural characteristics of the positive electrode were determined by using the Brunauer-Emmett-Teller (BET) isotherm method (77 K) with N₂ as an adsorbate (ASAP 2460, Micromeritics, USA). 1558 m² g⁻¹ was the surface area of the positive electrode [6]. Before the adsorption/desorption steps, samples were flushed at 350°C for 12 h under continuous helium flow and further degassed at 25°C for 5 h (vacuum). The reference electrodes were made from metallic lithium, sodium and potassium (all purchased from Sigma-Aldrich). During half-cell measurements, the counter electrode and reference electrode were shaped as metallic discs (d = 16 mm).

Cell assembly: First, round electrodes (d = 16 mm, A = 2 cm²) were

6

One-step assembly of metal-ion capacitors using redox-active electrolytes

A. Maćkowiak et al.

Energy Storage Materials 65 (2024) 103163

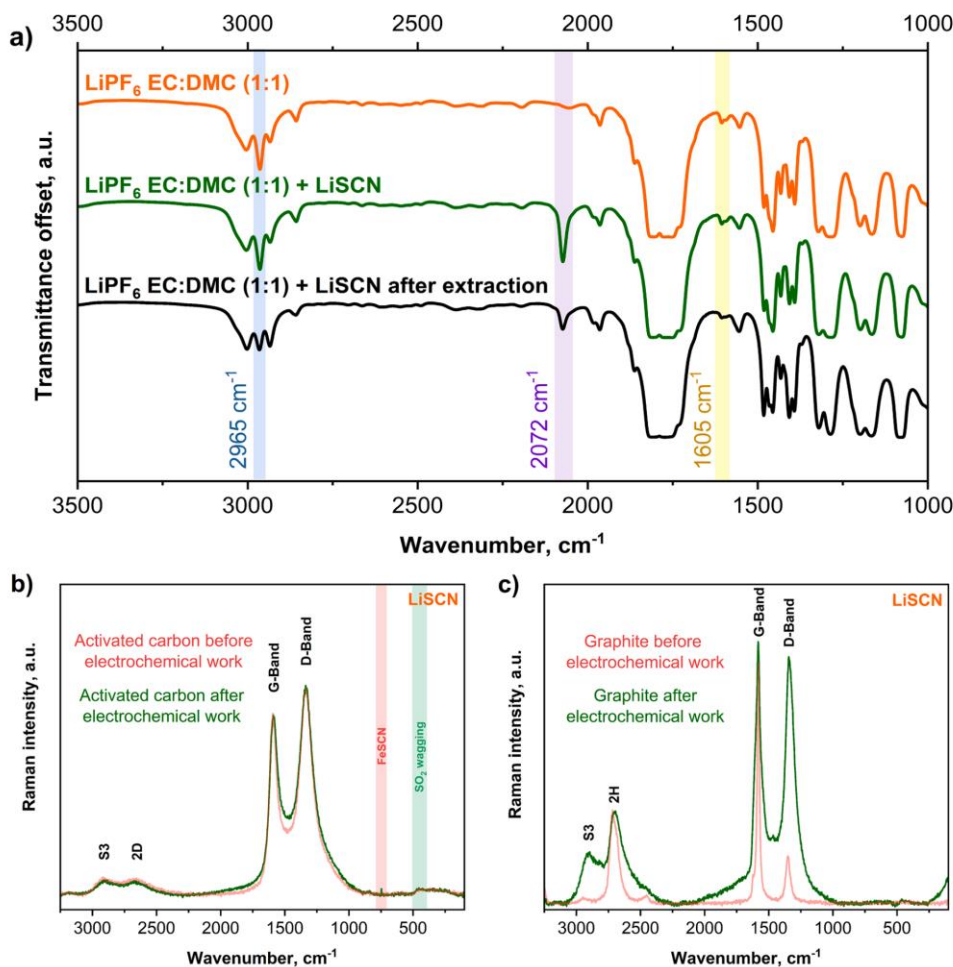


Fig. 6. (a) FT-IR spectra of the electrolyte with thiocyanate anions and the electrolyte after extraction in a lithium-ion capacitor assembled using a one-step approach; Raman spectra of the (b) positive electrode and (c) negative electrodes before and after lithium-ion capacitor electrochemical work (1000 cycles).

cut from positive and negative electrode materials using EL-Cut provided by EL-CELL®. The active mass ratio of the electrodes was approximately 1:1. Then, the electrolyte was prepared. Before each cell was assembled, the electrolyte was freshly prepared. After, the positive and negative electrodes were placed in the ECC-REF electrochemical cell (provided by EL-CELL®) and separated using two glass fibre discs ($d = 18$ mm, GF/D, Whatman®) soaked with 600 μ L of electrolyte. The reference electrode was inserted as metal pieces in the reference pinhole using an ECC loader (provided by EL-CELL®). All cells were prepared in a glovebox (MBraun) to ensure negligible amounts of water and oxygen (<0.1 ppm). For a detailed specification of cell assembly, see the description in Supplementary Information.

Spectroscopic investigation: Infrared spectra of the electrolyte were obtained using an infrared spectrometer (Nicolet™ iS5 FT-IR) in the 1000–3500 cm^{-1} wavenumber range. Electrode materials were tested before and after electrochemical work with a Raman DXR microscope (Thermo Fischer Scientific). Special closed cuvettes with Kapton tape were used to prevent precipitation from oxidization. The laser power (DXR 532 nm) was 0.5 to 5 mW, and the exposure time was 8×20 s using

a pinhole of 50 μ m. X-ray diffractograms were obtained from a BRUKER D8 Advanced apparatus equipped with a Johansson monochromator using Cu K α radiation (Cu K α , $\lambda = 1.5406$ Å) and a LynxEye silicon strip detector. The measurement angle was between 5 and 100 2θ deg. Gas chromatography with mass spectrometry (GC–MS) analysis was conducted using EVOQ GC-TQ™ MS, Bruker. The apparatus was connected to PAT-Cell-Gas made by EL-CELL®. The electrochemical cell was inserted into the thermostatic chamber (25°C). The temperature of the injector was 190°C, the column was 170°C and the mass spectrometer was 220°C.

Electrochemical investigation: Electrochemical measurements were performed in the ECC-Ref and PAT-Cell-Gas (in the case of GCMS measurement) systems provided by the EL-CELL®. The reference metallic lithium pin was introduced to ECC-Ref by using ECC-Load. Electrochemical measurements (cyclic voltammetry, galvanostatic charge/discharge with potential limitations, and impedance spectroscopy) were performed via a multichannel galvanostat/potentiostat (VMP-3 BioLogic®). Temperature control was provided by a thermostatic chamber.

7

One-step assembly of metal-ion capacitors using redox-active electrolytes

A. Maćkowiak et al.

Energy Storage Materials 65 (2024) 103163

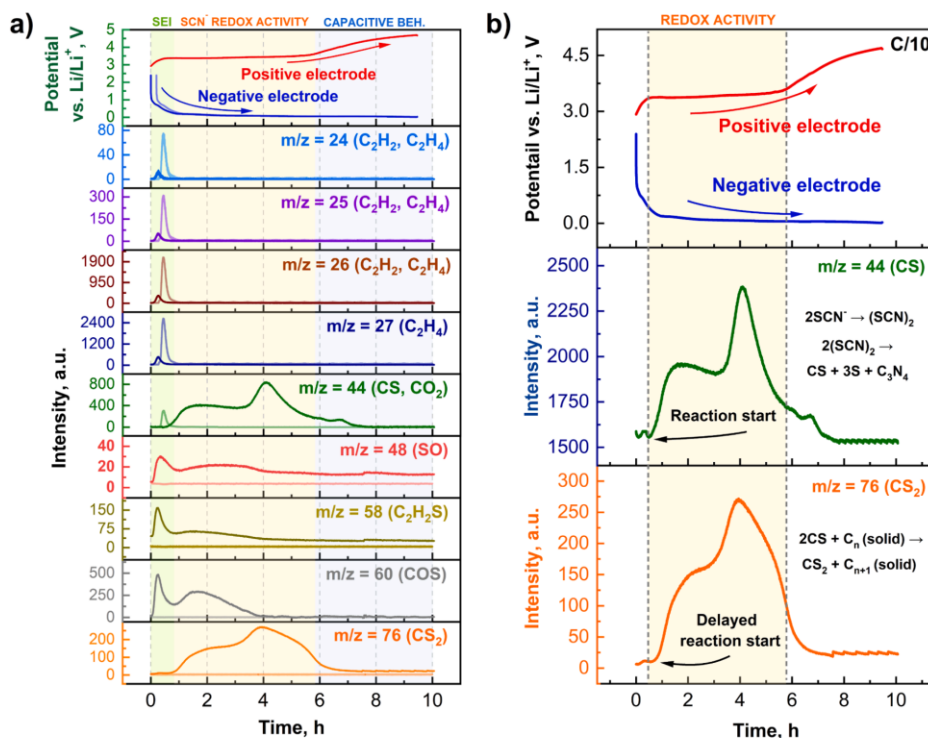


Fig. 7. (a) Comparison of operando GCMS results of lithium-ion capacitors assembled using a one-step (darker line) and a two-step (lighter line) approach (b) only masses used for the main SCN^- reaction in one-step approach.

CRediT authorship contribution statement

Adam Maćkowiak: Conceptualization, Data curation, Formal analysis, Investigation, Methodology, Visualization, Writing – original draft. **Paweł Jezowski:** Conceptualization, Funding acquisition, Investigation, Methodology, Supervision, Validation, Writing – original draft. **Yukiko Matsui:** Writing – original draft, Supervision, Methodology, Formal analysis, Writing – review & editing. **Masashi Ishikawa:** Writing – review & editing, Writing – original draft, Supervision, Methodology, Funding acquisition, Conceptualization. **Krzysztof Fic:** Writing – review & editing, Writing – original draft, Supervision, Project administration, Methodology, Funding acquisition, Conceptualization, Formal analysis, Investigation, Resources, Software.

Declaration of Competing Interest

The authors declare that they have no known competing financial interests or personal relationships that could have appeared to influence the work reported in this paper.

Data availability

Data will be made available on request.

Acknowledgements

This work was financially supported by the European Research Council within the Starting Grant project (GA 759603) under European

Union Horizon 2020 research and innovation programme. KF would like to acknowledge the funding received from the Polish Ministry for Science and Higher Education for a research stay at Kansai University (JP) (contract No. 1718/1/MOB/V/2018/0). PJ would also like to acknowledge the Foundation for Polish Science and the START 2019 programme.

Supplementary materials

Supplementary material associated with this article can be found, in the online version, at [doi:10.1016/j.ensm.2023.103163](https://doi.org/10.1016/j.ensm.2023.103163).

References

- [1] C. Sun, X. Zhang, C. Li, K. Wang, X. Sun, Y. Ma, Fast charging of energy-dense lithium-ion batteries, *Energy Storage Mater.* 32 (2020) 497–516.
- [2] J.T. Frith, M.J. Lacey, U. Ulissi, A non-academic perspective on the future of lithium-based batteries, *Nat. Commun.* 14 (2023) 420.
- [3] I. Konuma, D. Goonetilleke, N. Sharma, T. Miyuki, S. Hiroi, K. Ohara, Y. Yamakawa, Y. Morino, H.B. Rajendra, T. Ishigaki, N. Yabuuchi, A near dimensionally invariable high-capacity positive electrode material, *Nat. Mater.* 22 (2023) 225–234.
- [4] P. Simon, Y. Gogotsi, Perspectives for electrochemical capacitors and related devices, *Nat. Mater.* 19 (2020) 1151–1163.
- [5] J.B. Goodenough, K.S. Park, The Li-ion rechargeable battery: a perspective, *J. Am. Chem. Soc.* 135 (2013) 1167–1176.
- [6] K. Fic, A. Platek, J. Piwek, E. Frackowiak, Sustainable materials for electrochemical capacitors, *Mater. Today* 21 (2018) 437–454.
- [7] S.E.M. Pourhosseini, A. Bothe, A. Balducci, F. Beguin, P. Ratajczak, Strategy to assess the carbon electrode modifications associated with the high voltage ageing of electrochemical capacitors in organic electrolyte, *Energy Storage Mater.* 38 (2021) 17–19.
- [8] J.W. Choi, D. Aurbach, Promise and reality of post-lithium-ion batteries with high energy densities, *Nat. Rev. Mater.* 1 (2016) 16013.

One-step assembly of metal-ion capacitors using redox-active electrolytes

A. Maćkowiak et al.

Energy Storage Materials 65 (2024) 103163

- [9] J.M. Tarascon, Material science as a cornerstone driving battery research, *Nat. Mater.* 21 (2022) 979–982.
- [10] P. Simon, Y. Gogotsi, Materials for electrochemical capacitors, *Nat. Mater.* 7 (2008) 845–854.
- [11] M. Salanne, B. Rotenberg, K. Naoi, K. Kaneko, P.L. Taberna, C.P. Grey, B. Dunn, P. Simon, Efficient storage mechanisms for building better supercapacitors, *Nat. Energy* 1 (2016) 16070.
- [12] W. Cao, J. Zhang, H. Li, Batteries with high theoretical energy densities, *Energy Storage Mater.* 26 (2020) 46.
- [13] J. Zhao, A.F. Burke, Electrochemical capacitors: performance metrics and evaluation by testing and analysis, *Adv. Energy Mater.* 11 (2021) 2002192.
- [14] M.R. Lukatskaya, B. Dunn, Y. Gogotsi, Multidimensional materials and device architectures for future hybrid energy storage, *Nat. Commun.* 7 (2016) 12647.
- [15] P. Jeżowski, O. Crosnier, E. Deumf, P. Poizot, F. Béguin, T. Brousse, Safe and recyclable lithium-ion capacitors using sacrificial organic lithium salt, *Nat. Mater.* 17 (2018) 167–173.
- [16] X. Yang, F. Cheng, O. Ka, L. Wen, X. Gu, W. Hou, W. Lu, L. Dai, High-voltage lithium-ion capacitors enabled by a multifunctional phosphite electrolyte additive, *Energy Storage Mater.* 46 (2022) 431–442.
- [17] M. Soltani, S.H. Beheshti, A comprehensive review of lithium ion capacitor: development, modelling, thermal management and applications, *J. Energy Storage* 34 (2021) 102019.
- [18] K. Kato, M.T.F. Rodrigues, G. Babu, P.M. Ajayan, Revealing anion chemistry above 3V in Li-ion capacitors, *Electrochim. Acta* 324 (2019) 134871.
- [19] N. Ogihara, M. Hasegawa, H. Kumagai, R. Mikita, N. Nagasako, Heterogeneous intercalated metal-organic framework active materials for fast-charging non-aqueous Li-ion capacitors, *Nat. Commun.* 14 (2023) 1472.
- [20] L. Jin, C. Shen, A. Shellikeri, Q. Wu, J. Zheng, P. Andrei, J.G. Zhang, J.P. Zheng, Progress and perspectives on pre-lithiation technologies for lithium ion capacitors, *Energy Environ. Sci.* 13 (2020) 2341–2362.
- [21] T. Aida, K. Yamada, M. Morita, An advanced hybrid electrochemical capacitor that uses a wide potential range at the positive electrode, *Electrochim. Solid-State Lett.* 9 (2006) A534.
- [22] W. Li, H. Yao, K. Yan, G. Zheng, Z. Liang, Y.M. Chiang, Y. Cui, The synergetic effect of lithium polysulfide and lithium nitrate to prevent lithium dendrite growth, *Nat. Commun.* 6 (2015) 7436.
- [23] X. Wang, L. Liu, Z. Niu, Carbon-based materials for lithium-ion capacitors, *Mater. Chem. Front.* 3 (2019) 1265–1279.
- [24] P. Jeżowski, K. Fic, O. Crosnier, T. Brousse, F. Béguin, Lithium rhenium(VII) oxide as a novel material for graphite pre-lithiation in high performance lithium-ion capacitors, *J. Mater. Chem. A* 4 (2016) 12609–12615.
- [25] P. Jeżowski, K. Fic, O. Crosnier, T. Brousse, F. Béguin, Use of sacrificial lithium nickel oxide for loading graphitic anode in Li-ion capacitors, *Electrochim. Acta* 206 (2016) 440–445.
- [26] P. Jeżowski, A. Chojnacka, X. Pan, F. Béguin, Sodium amide as a “zero dead mass” sacrificial material for the pre-sodiation of the negative electrode in sodium-ion capacitors, *Electrochim. Acta* 375 (2021) 137980.
- [27] C. Decaux, G. Lota, E. Raymundo-Piñero, E. Frackowiak, F. Béguin, Electrochemical performance of a hybrid lithium-ion capacitor with a graphite anode preloaded from lithium bis(trifluoromethane)sulfonamide-based electrolyte, *Electrochim. Acta* 86 (2012) 282–286.
- [28] V. Khomenko, E. Raymundo-Piñero, F. Béguin, High-energy density graphite/AC capacitor in organic electrolyte, *J. Power Sources* 177 (2008) 643–651.
- [29] B. Gorska, P. Bujewska, K. Fic, Thiocyanates as attractive redox-active electrolytes for high-energy and environmentally-friendly electrochemical capacitors, *Phys. Chem. Chem. Phys.* 19 (2017) 7923–7935.
- [30] A. Ponrouch, E. Marchante, M. Courty, J.-M. Tarascon, M.R. Palacín, In search of an optimized electrolyte for Na-ion batteries, *Energy Environ. Sci.* 5 (2012) 8572–8583.
- [31] X. Pan, A. Chojnacka, P. Jeżowski, F. Béguin, Na₂S sacrificial cathodic material for high performance sodium-ion capacitors, *Electrochim. Acta* 318 (2019) 471–478.
- [32] H. Moriwake, A. Kuwabara, C.A.J. Fisher, Y. Ikuhara, Why is sodium-intercalated graphite unstable? *RSC Adv.* 7 (2017) 3655–36554.
- [33] J.Y. Hwang, S.T. Myung, Y.K. Sun, Sodium-ion batteries: present and future, *Chem. Soc. Rev.* 46 (2017) 3529–3614.
- [34] J.E.N. Swallow, M.W. Fraser, N.J.H. Kneusels, J.F. Charlton, C.G. Sole, C.M. E. Phelan, E. Björklund, P. Bencok, C. Escudero, V. Pérez-Dieste, C.P. Grey, R. J. Nicholls, R.S. Weatherup, Revealing solid electrolyte interphase formation through interface-sensitive Operando X-ray absorption spectroscopy, *Nat. Commun.* 13 (2022) 6070.
- [35] T. Liu, L. Lin, X. Bi, L. Tian, K. Yang, J. Liu, M. Li, Z. Chen, J. Lu, K. Amine, K. Xu, F. Pan, In situ quantification of interphasial chemistry in Li-ion battery, *Nat. Nanotechnol.* 14 (2019) 50–56.
- [36] T.S. Miller, A. d’Aleo, T. Suter, A.E. Aliev, A. Sella, P.F. McMillan, Pharaoh’s serpents: new insights into a classic carbon nitride material, *Z. Anorg. Allg. Chem.* 643 (2017) 1572–1580.
- [37] E.K. Moltzen, K.J. Klabunde, A. Senning, Carbon monosulfide: a review, *Chem. Rev.* 88 (1988) 391–406.
- [38] M. Abián, M. Cebrián, Á. Millera, R. Bilbao, M.U. Alzueta, CS₂ and COS conversion under different combustion conditions, *Combust. Flame* 162 (2015) 2119–2127.

Supporting Information for

Redox-active electrolytes as a viable approach for the one-step assembly of metal-ion capacitors

Detailed calculations of used thiocyanate salt addition to the electrolyte

The theoretical capacity of the lithium thiocyanate (LiSCN) salt was calculated using Faraday's equation (**Equation S1**):

$$m = \frac{MIT}{Fz}$$

Where,

m = mass of the substance, g

M = molar mass of the substance, g mol⁻¹

I = applied current, A

T = time, s

F = Faraday's constant, C mol⁻¹

z = number of electrons used in single reaction, -

The molar mass of the lithium thiocyanate salt equals 65.02 mol g⁻¹. Putting this value into the equation and changing the units it is possible to obtain capacity about 412 mAh g⁻¹. Because the exact active mass of the graphite and its theoretical capacity (372 mAh g⁻¹) are well known, it is possible to calculate the amount of LiSCN addition to balance the positive electrode.

For further calculations, the molar mass of sodium thiocyanate (NaSCN) was 81.07 g mol⁻¹ and the molar mass of potassium thiocyanate (KSCN) was 97.18 g mol⁻¹. It can be concluded that the smaller molar mass of the salt is the more theoretical capacity from the reaction will be obtained (per 1 gram of the salt).

Detailed assembly of metal-ion capacitor using one-step approach

Firstly, all electrodes and salts were dried under vacuum for over one week and introduced to the glove box where reduced amount of water and oxygen occurs. In the small vial, the ethylene carbonate was measured, then the same amount of dimethyl carbonate (or propylene carbonate) was added and mixed. A lithium hexafluorophosphate

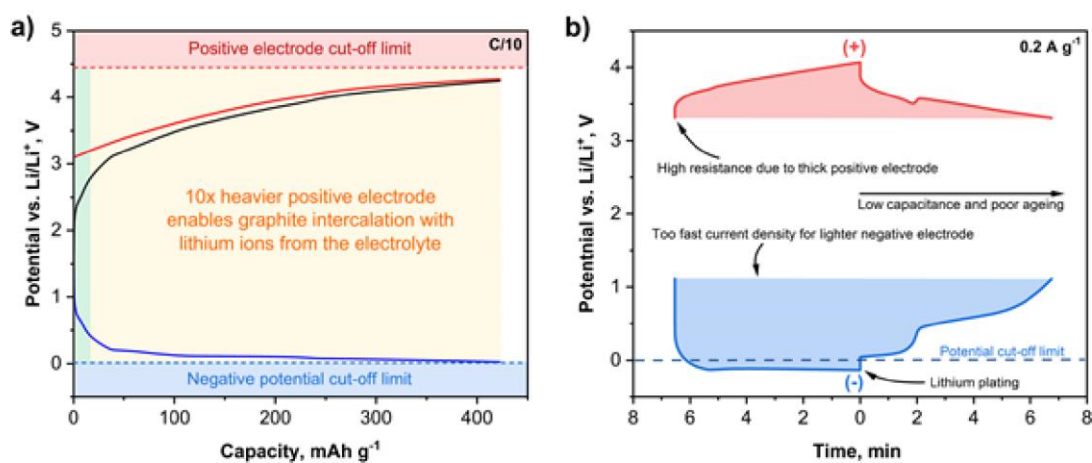
One-step assembly of metal-ion capacitors using redox-active electrolytes

(or potassium hexafluorophosphate, or sodium perchlorate) salt was further added to solvents to obtain one molar solution. From this electrolyte, a 600 μL was taken and added to the small vial with a calculated amount of thiocyanate salt. After 5 minutes of energetic mixing the electrolyte was ready. The cell assembly consisted of placing a negative electrode (16 mm, graphite/hardcarbon) on the bottom of the ECC-Ref cell. Next, two separators Whatman GF/D were placed. After that, a small amount of metallic reference was added to the reference hole. 600 μL of electrolyte was added to soak the separators. In the end, the positive electrode made as a self-standing activated carbon disc (16 mm) was placed on the top and the system was tightly closed.

Detailed assembly of lithium-ion capacitor using two-step approach

The first step of drying electrodes, and salts and then preparing the electrolyte (1 mol L⁻¹ LiPF₆ in EC:DMC, 1:1, v:v) was conducted as described for a one-step approach. Subsequently, two electrochemical cells were assembled. The first one consisted of placing a positive electrode (16 mm, activated carbon) on the bottom of the ECC-Ref cell. Next, two separators (Whatman GF/D) were placed and soaked with 600 μL of the electrolyte. The counter electrode was a metallic electrode (16 mm, lithium disc). After adding the lithium, the system was closed tightly and charged up to 4.2 V. The assembly of the second cell was identical to the abovementioned description, however, the activated carbon electrode was replaced with graphite electrode. The system was then charged up to 0.01 V. After first charging, two cells were disassembled and charged electrodes were taken to assemble a new system (actual lithium-ion capacitor), where intercalated graphite constitutes a negative electrode and activated carbon constitutes a positive electrode.

Supplementary figures



One-step assembly of metal-ion capacitors using redox-active electrolytes

Figure S1. Three-electrode measurements using 10x heavier positive electrode to balance graphite negative electrode a) first galvanostatic charging of positive and negative electrode using C/10 allowing preintercalation of cation into the structure of the negative electrode b) galvanostatic charging/discharging of full cell.

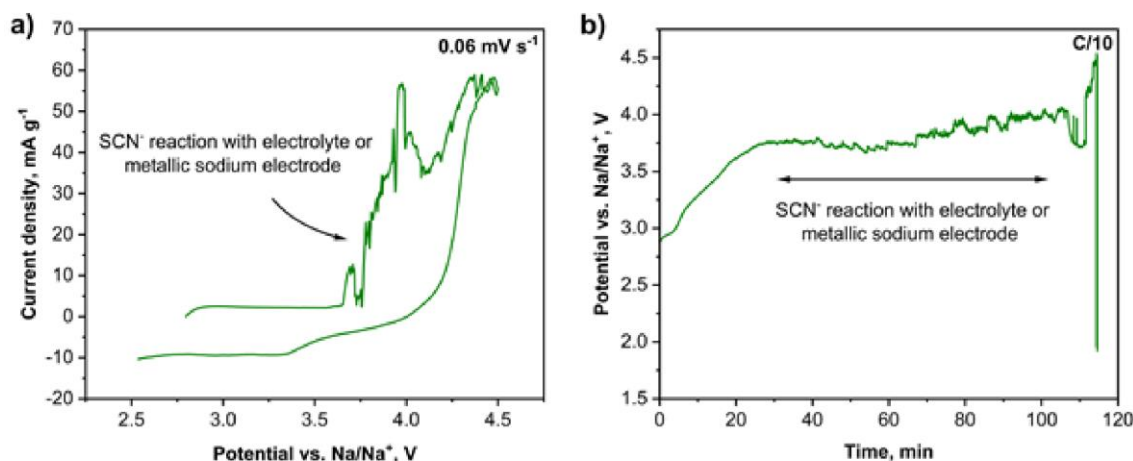


Figure S2. An attempt to use redox-active sodium thiocyanate in 1 mol L⁻¹ sodium hexafluorophosphate in ethylene carbonate and dimethyl carbonate (1 mol L⁻¹ NaPF₆ in EC:DMC) a) cyclic voltammogram with scan rate related to C/10 current b) galvanostatic charging using C/10 current.

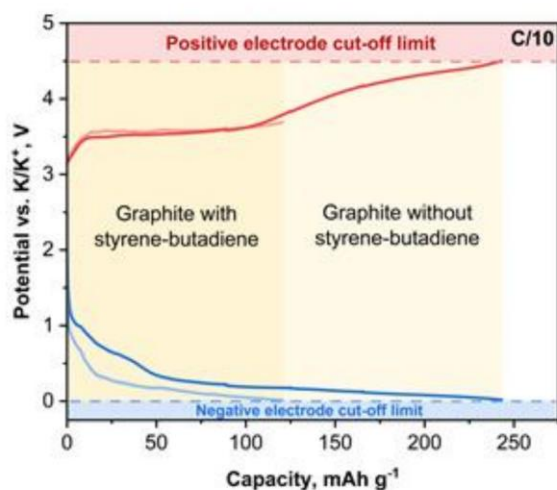


Figure S3. Preintercalation step of two potassium-ion capacitors containing graphite with styrene-butadiene rubber and graphite without the rubber in one-step assembly using redox-active potassium thiocyanate in 1 mol L⁻¹ potassium hexafluorophosphate in ethylene carbonate and dimethyl carbonate (1 mol L⁻¹ NaPF₆ in EC:DMC) with C/10 current.

One-step assembly of metal-ion capacitors using redox-active electrolytes

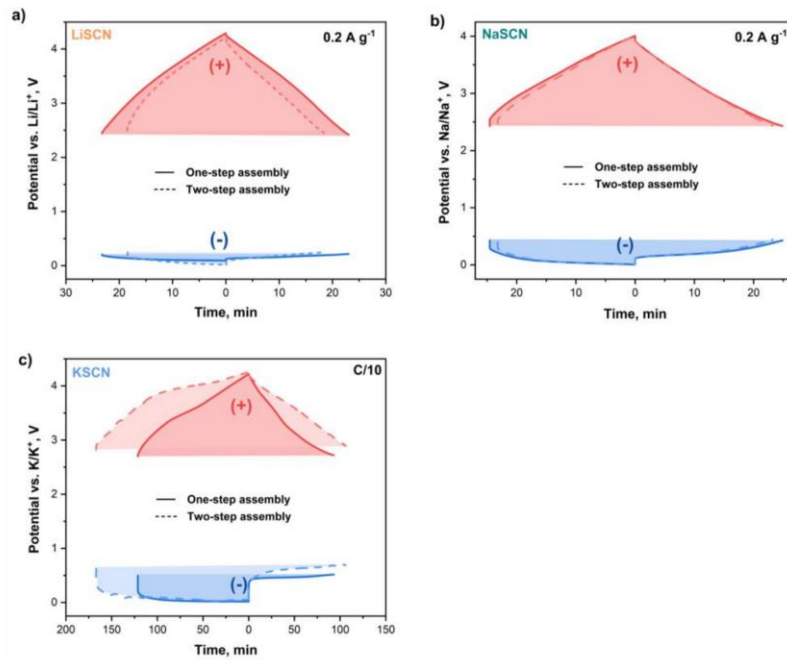


Figure S4. Comparison of first charging and discharging curves for one-step and two-step assembled a) lithium-ion capacitors b) sodium-ion capacitors c) potassium-ion capacitors.

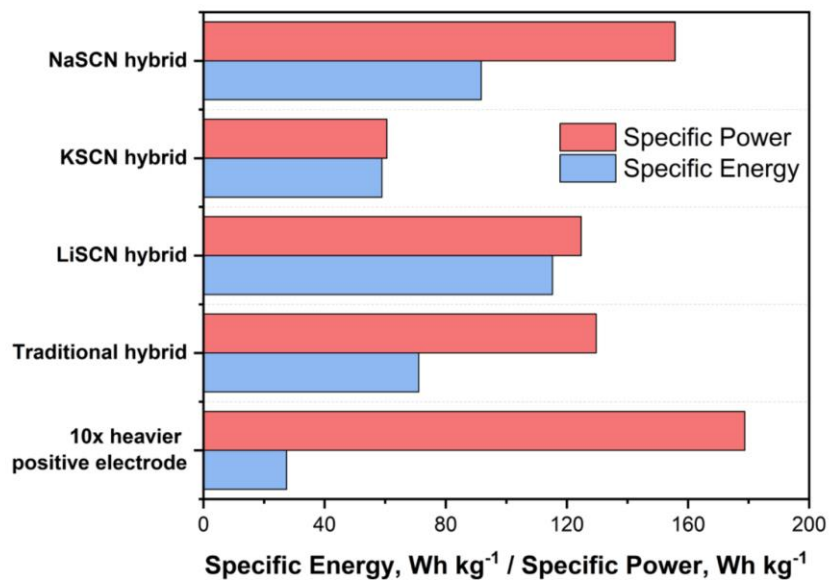


Figure S5. Specific power and energy dependence chart of all assembled and discussed hybrid-ion capacitors.

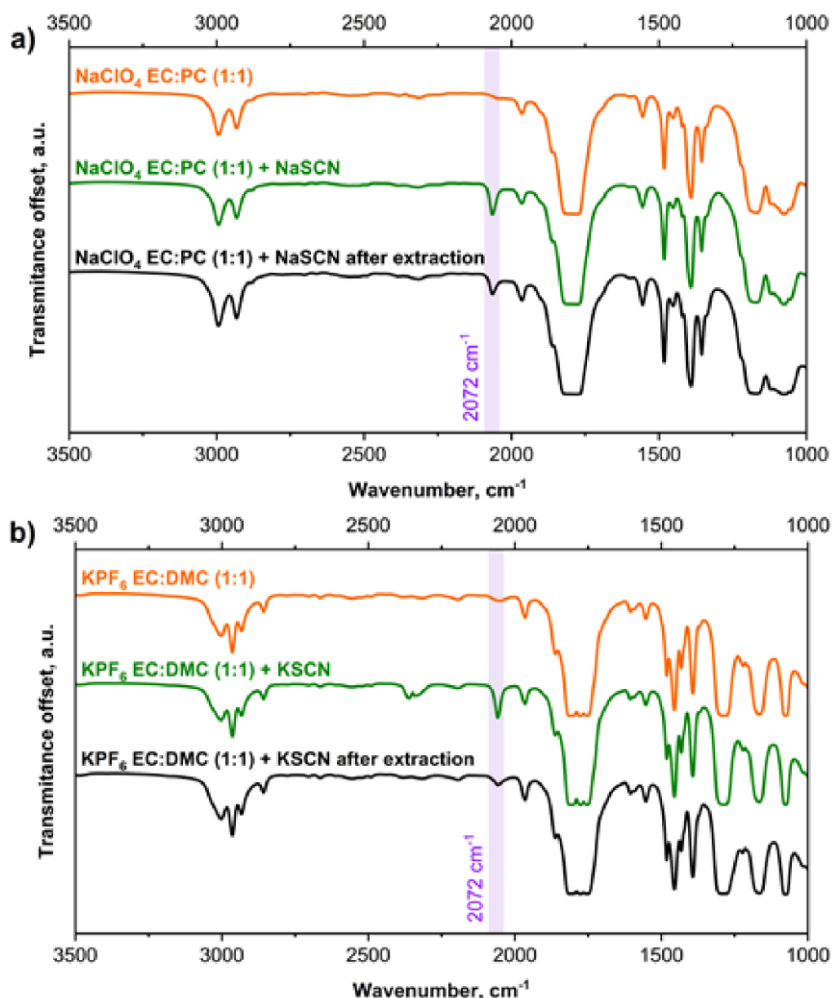


Figure S6. FT-IR spectra of electrolyte with thiocyanate anions and electrolyte after extraction using one-step approach a) in sodium-ion capacitor b) in potassium-ion capacitor.

Raman spectroscopy

To examine the change in the electrode materials before and after electrochemical work, Raman spectroscopy was carried out. At first sight, the positive electrode did not change much (Figure 6b). However, after a closer look, a small signal at 750 cm⁻¹ can be observed. This is due to the use of a steel current collector. Thiocyanates easily react with iron in steel collectors, therefore, to prevent this reaction a different collector material should be applied. Also, using a microscope, small local areas can be found where a yellow precipitate appears. It was very sensitive to the laser beam; however, we managed to obtain a Raman spectrum and an image of this precipitate (Figure S5a,b). Preliminary analysis shows that it

is a complex compound of sulphur with carbon and oxygen and probably lithium. Oxygen might appear because the measurements were taken on air and the sample was oxidising. For sodium- and potassium-ion capacitors (Figure S6a, S7a) this precipitate also appears on the positive electrode. However, in sodium, the composition is different. The S-O stretching bond is more clearly visible, probably because of more oxidising agents in the electrolyte (e.g. NaClO₄). On the negative electrode surface, no precipitation was observed (Figure 6c). However, the structure changed a lot because the disorder band signal strongly increased. This is caused by the continuous intercalation and deintercalation of lithium ions, which causes progressive destruction of the graphite structure. However, this is a natural way to work with graphite. The same phenomenon (increasing of disorder band) was observed for sodium- and potassium-ion capacitors (Figure S6b, S7b). The differences between the graphites can also be seen because they come from different additions to the materials (carbon black or styrene rubber).

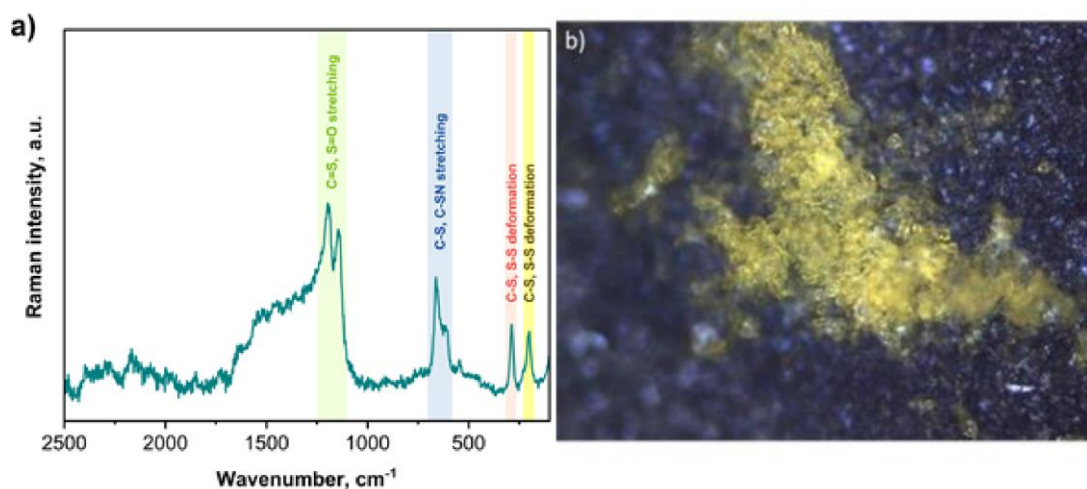


Figure S7. a) Raman spectrum and b) 50x magnification image of yellow precipitate present on the positive electrode after electrochemical work of cell with thiocyanate anion.

One-step assembly of metal-ion capacitors using redox-active electrolytes

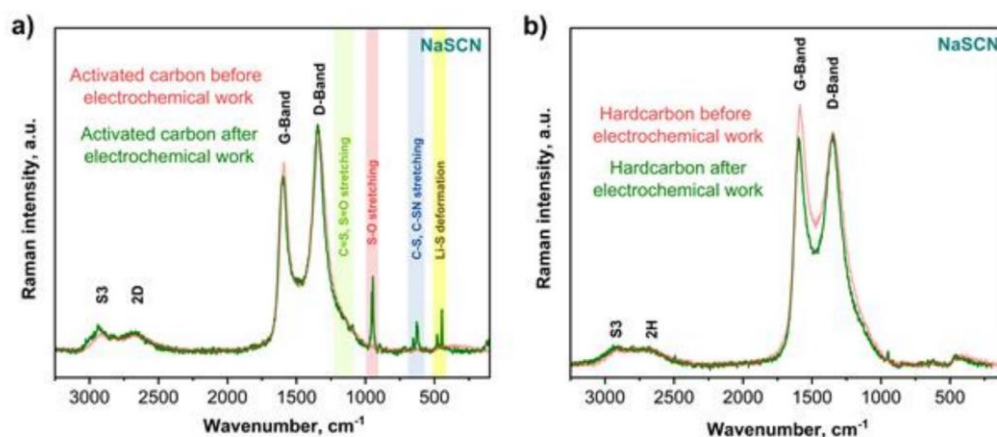


Figure S8. Raman spectra of a) activated carbon b) hardcarbon, before and after electrochemical work (20 cycles) of sodium-ion capacitor assembled using the one-step approach.

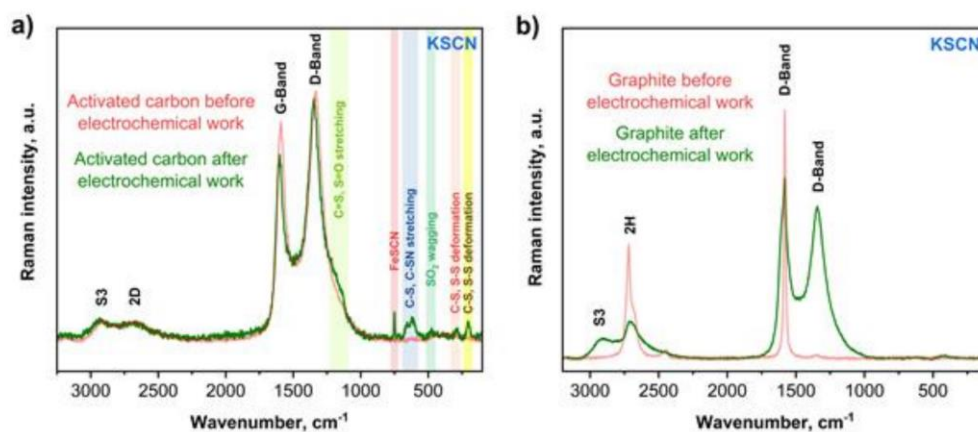


Figure S9. Raman spectra of a) activated carbon b) graphite, before and after electrochemical work (10 cycles) of potassium-ion capacitor assembled using one-step approach.

X-ray diffraction (XRD)

The analysis was performed in closed cuvettes with Kapton foil to prevent further oxidation of the sample. Kapton foil and carbon give strong signals in the range between 12 and 25 degrees, which might also overshadow the signals from the yellow precipitate. Nevertheless, despite the signals from PTFE, copper foil, or used calcite glue, the signals from carbides were visible.

One-step assembly of metal-ion capacitors using redox-active electrolytes

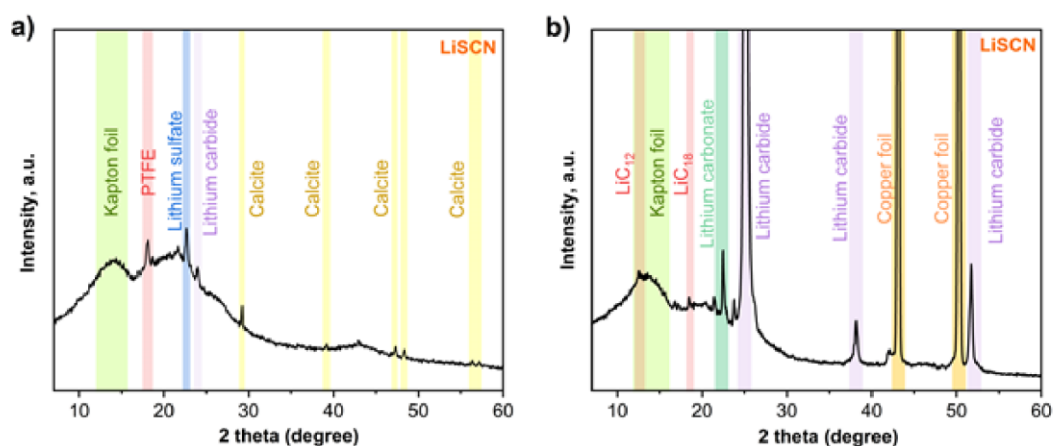


Figure S10. X-ray diffractometer of a) positive and b) negative electrodes, of lithium-ion capacitor assembled using one-step approach after electrochemical work. (1000 cycles)

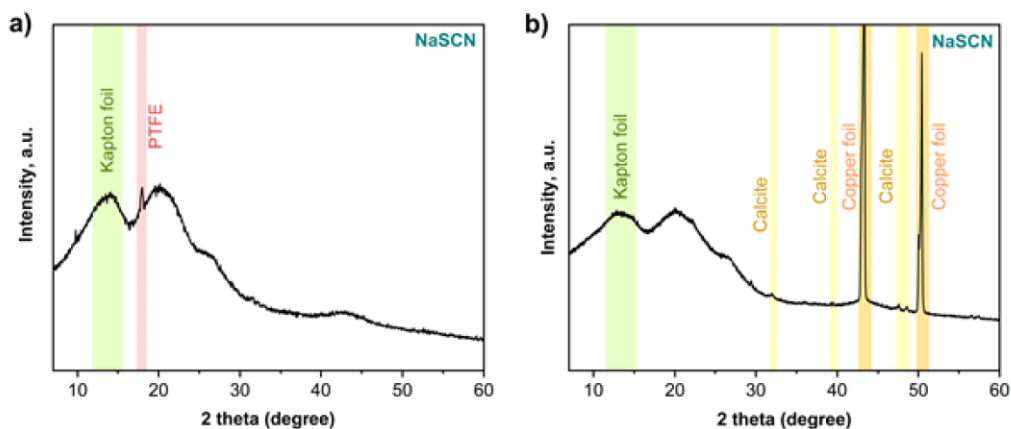


Figure S11. X-ray diffractometer of a) positive and b) negative electrodes, of sodium-ion capacitor assembled using one-step approach after electrochemical work (20 cycles).

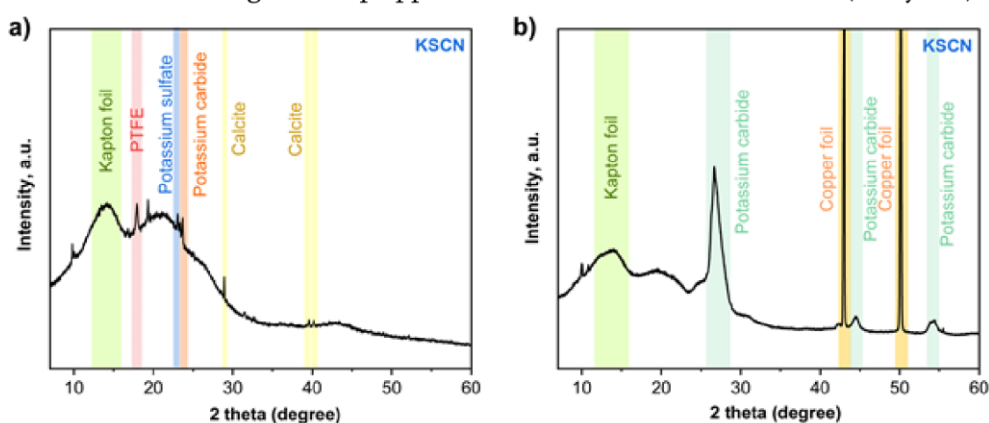


Figure S12. X-ray diffractometer of a) positive and b) negative electrode, of potassium-ion capacitor assembled using the one-step approach after electrochemical work.

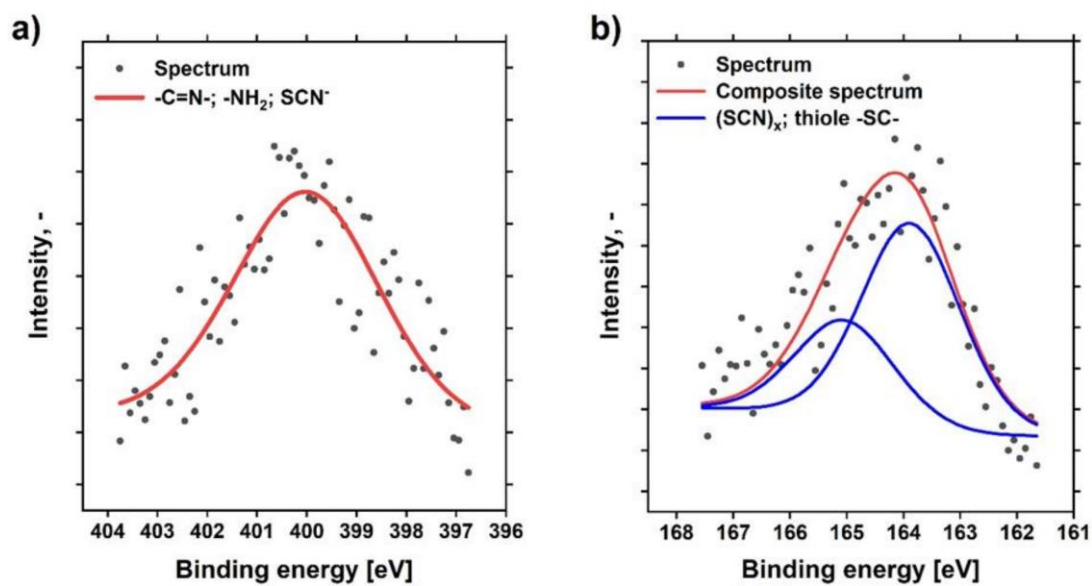
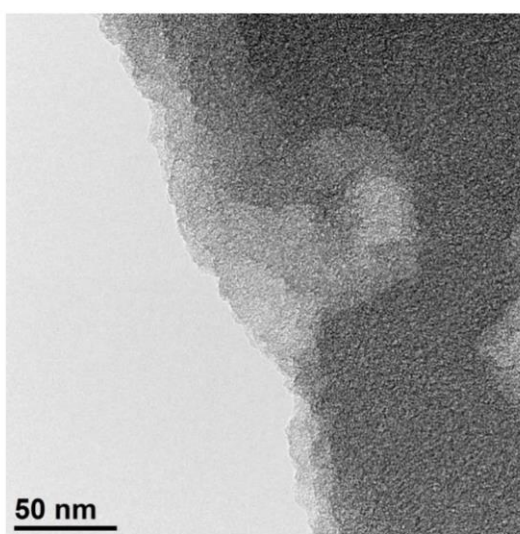
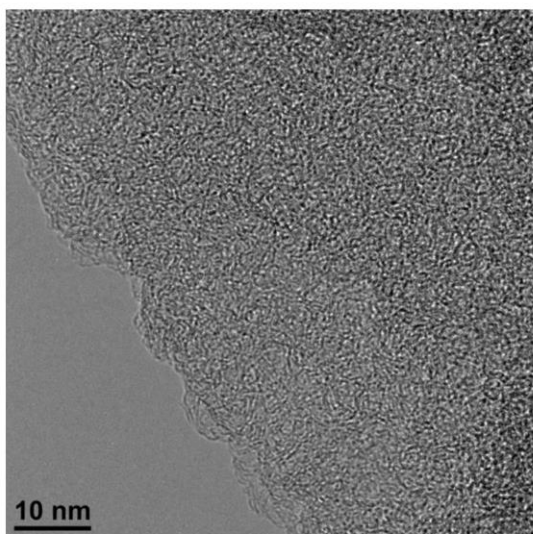


Figure S13. a) Sulfur and b) nitrogen XPS spectra of positive electrode of Li-ion capacitor with LiSCN after 1000 cycles.



One-step assembly of metal-ion capacitors using redox-active electrolytes

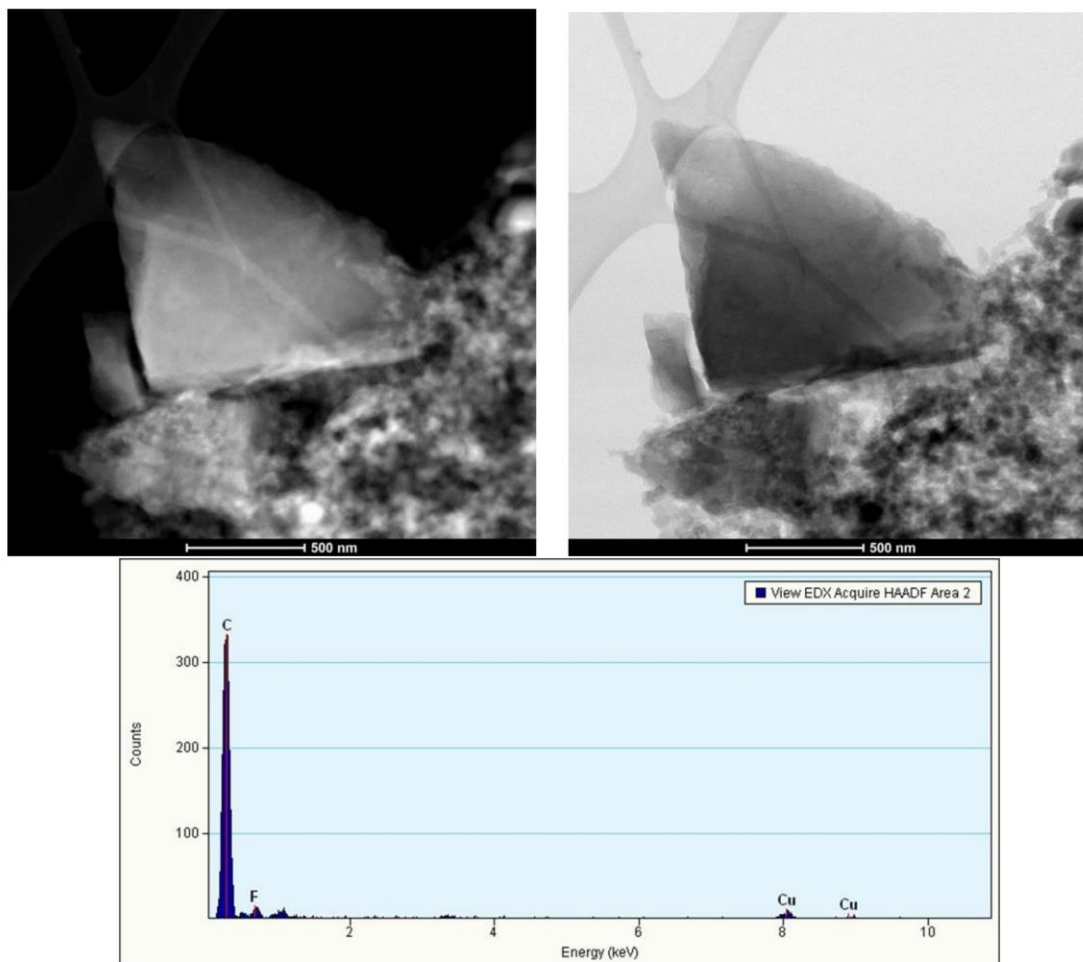


Figure S14. TEM images of positive electrode before electrochemical work with magnification at a) 10 nm b) 50 nm; c) and d) HAADF-STEM images of positive electrode before electrochemical work with magnification at 500 nm; e) Energy dispersive spectrum of positive electrode before electrochemical work.

One-step assembly of metal-ion capacitors using redox-active electrolytes

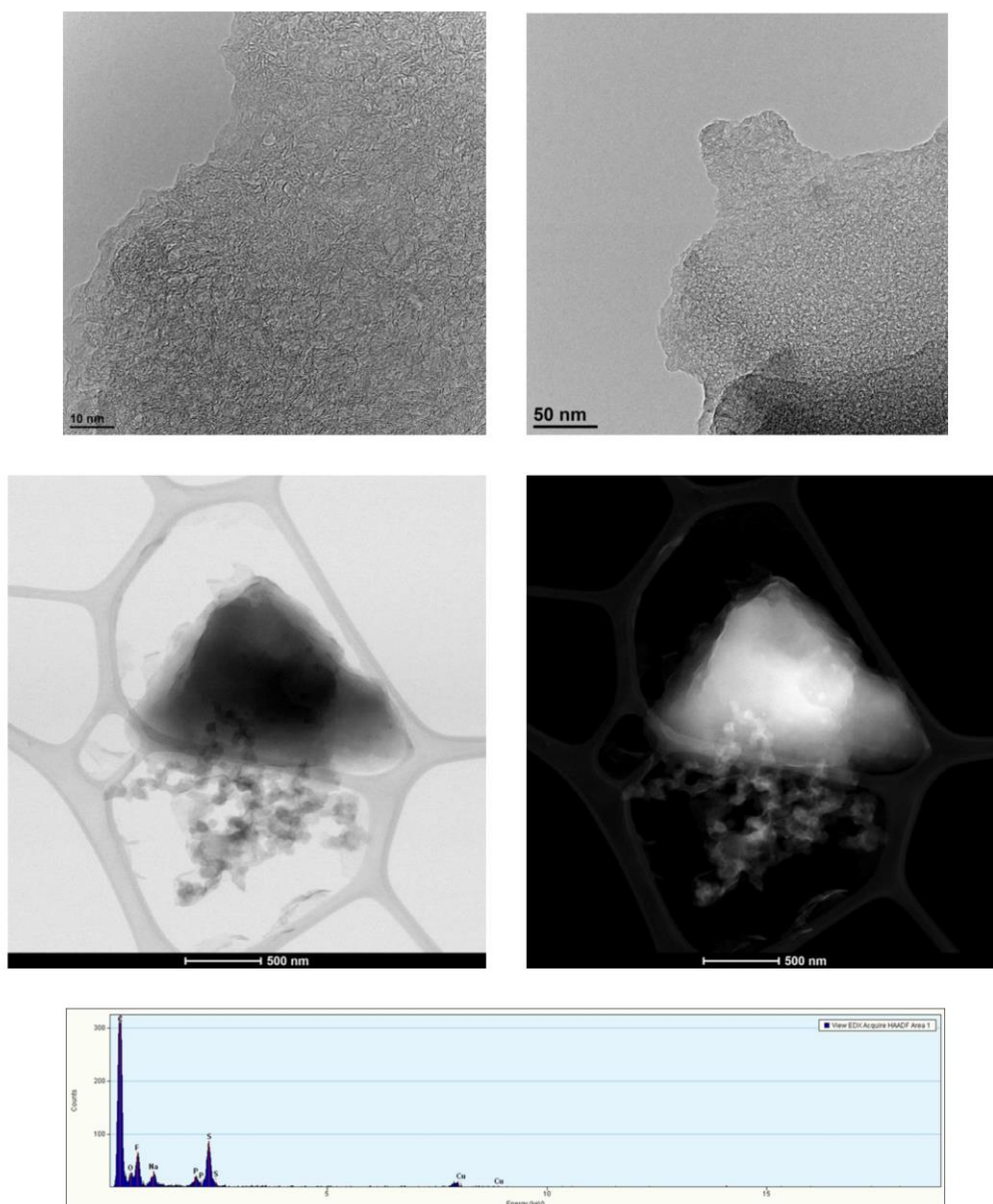


Figure S15. TEM images of positive electrode after 1000 cycles with thiocyanate additive with magnification at a) 10 nm b) 50 nm; c) and d) HAADF-STEM images of the positive electrode after 1000 cycles with thiocyanate additive with magnification at 500 nm; e) Energy dispersive spectrum of the positive electrode after 1000 cycles with thiocyanate additive.

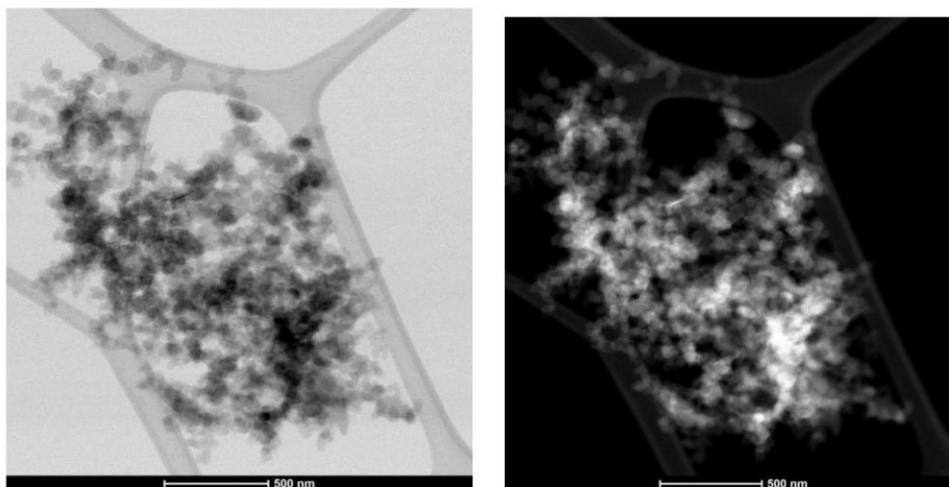


Figure S16. a) and b) HAADF-STEM images of carbon soot at positive electrode after 1000 cycles with thiocyanate additive with magnification at 500 nm;

Gas chromatography with mass spectrometry (GCMS)

The GCMS operando technique was used for the determination of gases that evolve during the operation of sodium-ion and potassium-ion capacitors (Figure S11a,b). In the case of a potassium-ion capacitor, the resulting signals are comparable to those obtained for the lithium-ion system because of the similar composition of the electrolyte. Also, there are signals from the formation of the SEI layer, mainly ethylene, a strong signal from 44 (CO₂ or CS) and of course a signal from the main reaction - 76. In the case of a sodium-ion cell, the SEI formation mechanism is different, therefore, signals from ethylene were not observed. Of course, there are also signals from masses 44 and 76 that suggest that the initial SCN reaction mechanism in each hybrid capacitor is the same. Due to the other electrolyte used in the sodium system, the decomposition of organic solvents occurs at higher voltages (Figure S12). A rapid increase in SO, SO₂, chlorinated hydrocarbons and also other organic sulphur compounds (e.g., CH₃SCN) was observed. The presented data respects before using the capacitor with such electrolyte at a voltage above 4V.

One-step assembly of metal-ion capacitors using redox-active electrolytes

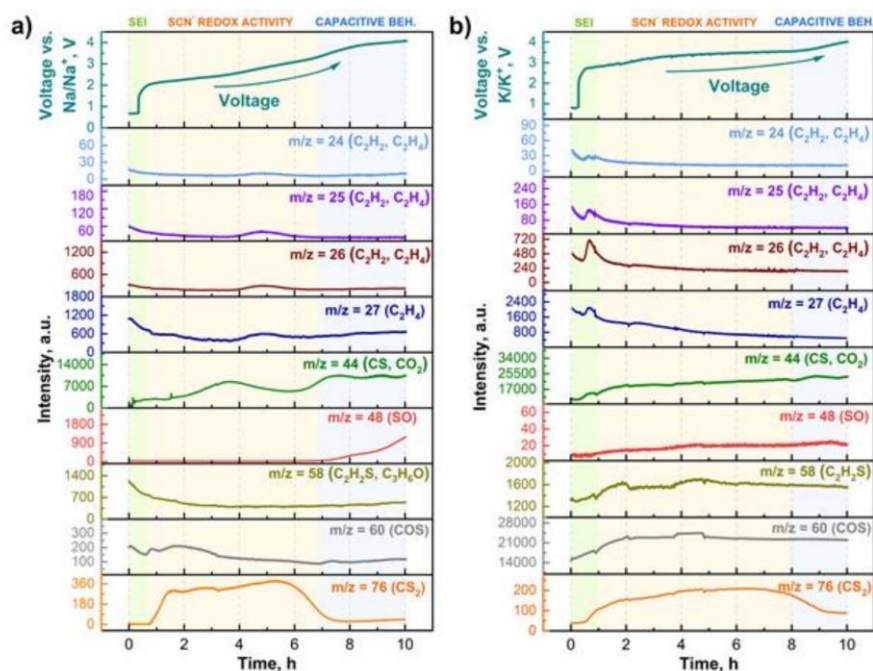


Figure S17. Operando GCMS of a) sodium-ion capacitor and b) potassium-ion capacitor assembled using one-step approach – main masses.

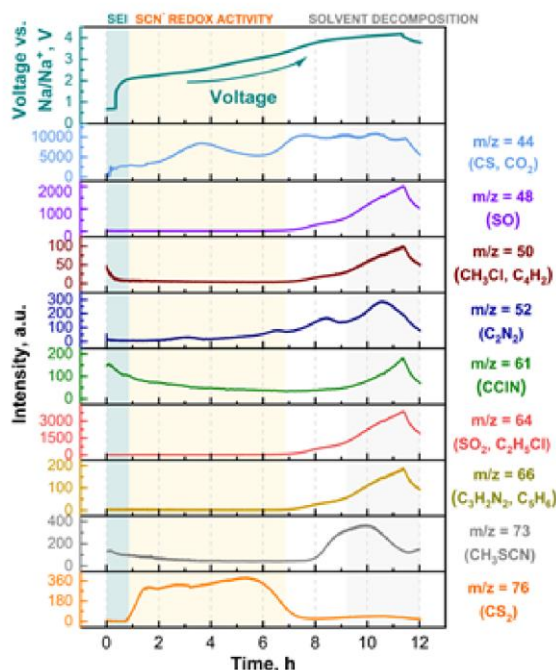


Figure S18. Operando GCMS of sodium-ion capacitor assembled using one-step approach – characteristic masses for the sodium-ion capacitor.

One-step assembly of metal-ion capacitors using redox-active electrolytes

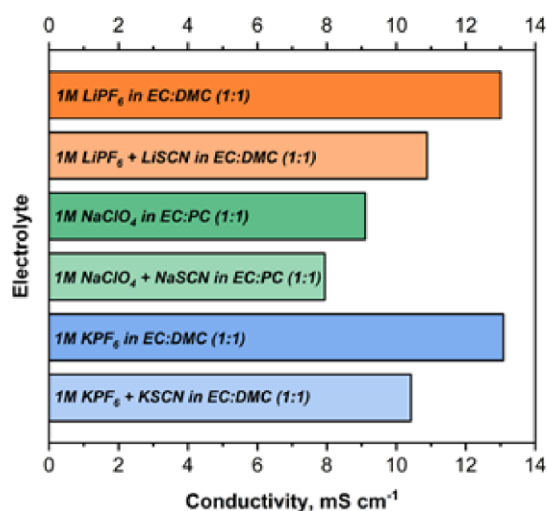


Figure S19. Conductivity summary of investigated electrolytes.

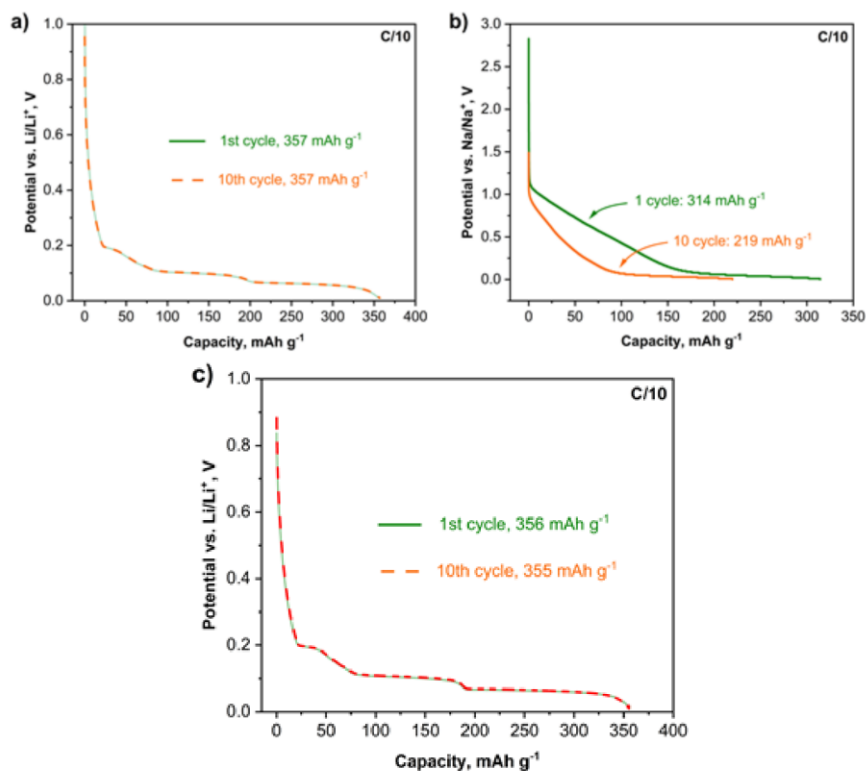


Figure S20. Galvanostatic charging and discharging of investigated negative electrodes in half-cells a) graphite in 1 mol L⁻¹ LiPF₆ EC:DMC (1:1), b) hardcarbon in 1 mol L⁻¹ NaClO₄ EC:PC (1:1), c) graphite in 1 mol L⁻¹ KPF₆ EC:DMC (1:1).

Manuscript 1

Li-ion capacitor exploiting a redox-active electrolyte

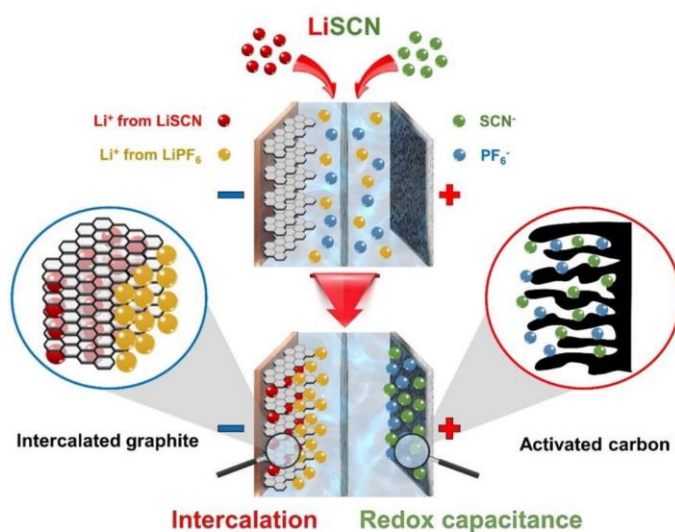
Adam Maćkowiak¹, Paweł Jeżowski¹, Adam Ślesiński¹, Yukiko Matsui², Kazunari Soeda²,
Masashi Ishikawa^{2,*}, Krzysztof Fic^{1,2,*}

¹Poznan University of Technology, Institute of Chemistry and Technical Electrochemistry,
Berdychowo 4, 60-965, Poznan, Poland

²Kansai University, Department of Chemistry and Materials Engineering, Faculty of Chemistry,
Materials and Bioengineering, 3-3-35 Yamate-cho, Suita 564-8680, Japan

*Corresponding authors: krzysztof.fic@put.poznan.pl; masaishi@kansai-u.ac.jp

Keywords: hybrid Li-ion capacitor; one-step prelithiation; organic redox-active electrolyte; electrochemical capacitor.



Abstract

In this work, we propose a novel kind of electrolyte for Li-ion capacitors (LICs) that allows full intercalation of Li^+ ions from the electrolytic solution into the negative (graphite)

electrode. Thus, no auxiliary electrode, no external prelithiation or no additives that might impact the power and mass-related metrics are necessary. In our approach, the redox-active lithium salt dissolved in 1 mol L⁻¹ lithium hexafluorophosphate in ethylene carbonate and dimethyl carbonate (LiPF₆ in EC:DMC) electrolyte serves as a charge-balancer and Li⁺ source for prelithiation. As the redox-active anion is coupled with Li⁺, its concentration in the electrolyte remains unchanged. Electrochemical tests, including cyclic voltammetry, galvanostatic charge/discharge, electrochemical impedance spectroscopy, self-discharge and constant power discharge tests, were carried out to describe and characterize this new concept. Furthermore, optimal LIC operating conditions, i.e., voltage (2.2–4.2 V) and current density (0.2 A g⁻¹), were determined. Within this voltage regime, the cell could operate at high power values (1000 W kg⁻¹), ensuring an astonishingly high specific energy of ca. 100 Wh kg⁻¹. The system was compared with commercial products available on the market. The capacitor cycle life and effect of inorganic salt addition on the conductivity were investigated. Furthermore, detailed analysis was conducted using *operando* mass spectrometry coupled with gas chromatography (GC–MS), scanning electron microscopy and energy-dispersive spectroscopy (SEM/EDS), X-ray photoelectron spectroscopy (XPS), Raman spectroscopy and infrared spectroscopy.

Introduction

Advancements in the field of electric energy generation are driving the modern world towards finding perfect energy storage systems. Currently, two energy storage technologies appear to be the most popular: electric double-layer capacitors (EDLCs) and Li-ion batteries (LIBs) [1-3]. EDLCs store energy using nonfaradaic processes, which means storage by accumulating electrostatic charge at the electrode/electrolyte interface [4-7]. The drawback of EDLCs is that they cannot provide high energy density, which significantly limits their application [8-10]. In the case of LIBs, energy storage is related to faradaic processes, based on Li insertion [11]. Due to their charge storage mechanism, LIBs demonstrate high energy densities, but they suffer from a shorter lifespan and power values lower than EDLCs [12, 13]. Given that, combining both energy storage mechanisms in one compact device, the so-called Li-ion capacitor (LIC), seems to be a reasonable solution [14-16].

The hybrid energy storage system exploits the intercalation and deintercalation of lithium ions into/from the negative electrode, which is usually made of graphite; for the positive electrode, charge is usually stored electrostatically, on the surface of the porous material, e.g., activated carbon [17, 18]. The hybridization of energy storage mechanisms allows reaching higher energy densities than in EDLCs while maintaining high specific power and

the long cycle life [19]. Thus, why are these devices not used on a larger scale? The reason is the necessity for prelithiation of the negative electrode.

LICs were first constructed using metal oxides as the negative electrode, such as $\text{Li}_4\text{Ti}_5\text{O}_{12}$ or WO_2 [20-22]. However, this kind of material could operate within the 1.2 V to 3.2 V voltage range, which results in slightly higher energy values than EDLCs [20]. Another approach is to use an auxiliary metallic lithium electrode to prelithiate the graphite electrode [23, 24]. The use of metallic lithium as a source of lithium ions is feasible at the lab-scale level; however, the additional electrode complicates cell construction and increases the cost and weight of the device (additional current collectors, separators and electrolyte), thus, its implementation in industrial process is too complicated and very costly. Another strategy uses two-step assembly, where in the first step, the negative electrode is prelithiated vs. a metallic lithium disk, and then, in the second step, the metallic lithium disk is removed from the cell and replaced by the activated carbon electrode. However, this is again very costly and complex method, as all manipulations are performed under an inert gas atmosphere. Moreover, the use of metallic lithium can lead to the formation of dendrites and thermal runaway, which might cause severe safety issues and makes the process industrially difficult [24, 25].

A different approach for prelithiation is to use lithium ions coming from a composite positive electrode [26, 27]. This method involves the mixture of lithium metal oxide with activated carbon, which constitutes a composite material. During the first charge of the cell, lithium ions are released into the electrolyte, enabling prelithiation of the graphite electrode. Despite the full intercalation process, the metal oxide remains in the system, which may constitute a dead mass deteriorating the cell performance [27]. The first composite materials consisted of Li_2MoO_3 [26], Li_2RuO_3 [27] or Li_5FeO_4 [28] mixed with activated carbon. However, all of these positive electrodes require 4.7 V vs. Li/Li^+ to intercalate the graphite, which is above the safe working potential for the electrolyte (ca. 4.5 V vs. Li/Li^+ for 1 mol L^{-1} LiPF_6 ethylene carbonate (EC):dimethyl carbonate (DMC)). Additionally, approximately 30% of lithium ions may be reinserted into the cathode material and thus cause perturbations in the operation of the LIC. A solution to these problems was found by using lithium cobalt oxide (Li_6CoO_4) [29]. Having a high irreversible capacity (600 mAh g^{-1}), the procedure with Li_6CoO_4 is completed at a lower potential (4.3 V vs. Li/Li^+) than that with the other oxides. As a result of the lack of side reactions during the prelithiation process, the LIC cycle life is increased. However, the dead mass problem remains and needs to be solved.

The next method uses so-called sacrificial salts [27, 29-32], which are part of the positive composite electrode. The role of the sacrificial material is to provide the lithium ions necessary during prelithiation of the negative electrode. Unfortunately, most of these salts after electrochemical oxidation form a dead mass (a part of the electrode that does not contribute to charge storage), which can hinder the electrochemical performance of the cell [27, 29, 30]. However, several sacrificial materials that do not contribute to the dead mass, or their amount is negligible, have been reported in the literature [19].

The last method of prelithiation was presented by Beguin *et al.* [33], where lithium ions from the electrolyte (2 mol L⁻¹ LiTFSI in EC:DMC) were used. Lithium ions were, to a certain degree (namely, intercalation stage), introduced into the graphite structure through pulses of a C/10 current to barely reach a third stage of intercalation. One of the main problems that appeared during this method was the consumption of lithium ions from the electrolyte, which reduced the electrolytic conductivity of the solution, and thus, both the power and energy of the system decreased [33, 34].

Nevertheless, the use of electrolytes as a source of lithium ions necessary for prelithiation of negative electrodes is a fascinating idea. To overcome the issues related to the conductivity decrease and partial intercalation in the negative electrode, a new and improved concept should be proposed. One of the possible solutions is the use of active electrochemical species that can be dissolved in the electrolyte. Indeed, the concept of redox-active electrolytes used to increase the energy of electrochemical capacitors has been studied by researchers [35, 36]. The use of iodides or bromides in water has proven to be a cost-effective and environmentally sustainable method of developing a new generation of high-performance capacitors [37-39]. Furthermore, the synthesis of electroactive ionic liquids (ILs) (e.g., [EMIm][SeCN] [40] or [BMPyrr][SCN] [41]) is a synergetic technique for increasing the energy by increasing both the voltage and capacitance [42]. Nonetheless, concentrating on a wide panel of redox-active electrolytes to discover conditions for converting electrochemical cells into hybrid capacitors with the best results is worthwhile [43].

Nevertheless, it has to be said that in our approach, redox-active electrolytes have been used for entirely different purpose. This article proposes the use of a novel solution for prelithiation of LICs using a redox-active lithium thiocyanate salt dissolved in 1 mol L⁻¹ LiPF₆ in EC:DMC as the electrolyte. Lithium ions derived from the redox-active thiocyanate salt can mitigate the concentration fluctuation during graphite prelithiation. Furthermore, thiocyanate-based salts are used, which are recognized as inexpensive and highly conductive electrolytic solutions displaying attractive redox activity and enhancing

the energy of the device [44]. The presented approach is innovative and could compete with known prelithiation techniques in the future.

Methods

Electrolyte

Lithium thiocyanate hydrate was purchased from Sigma Aldrich. Before use, the salt was dried at 120°C for one week to remove water contamination. LiPF₆ EC:DMC (1 mol·L⁻¹, V:V, 1:1) was purchased from BASF. The electrolyte preparation consisted of mixing the two components in a volumetric flask. A specific amount of solid lithium thiocyanate was added to the flask, which was then filled with liquid 1 mol L⁻¹ LiPF₆ EC:DMC to make a 0.25 mol L⁻¹ solution. The molar concentration of the LiSCN additive is dictated by the mass and capacity of the negative electrode, in our case graphite (with a theoretical capacity of 372 mAh g⁻¹). According to calculations, to obtain full intercalation, the LiSCN mass in the electrolyte should constitute 0.9 of the active mass of the graphite electrode. Five hundred microlitres of received electrolyte was added to soak the separators during electrochemical cell preparation. All reagents were stored in an MBraun glovebox to ensure inert environmental conditions. The conductivity of 1 mol L⁻¹ LiPF₆ EC:DMC was 10.83 mS cm⁻¹, and that of 0.25 mol L⁻¹ LiSCN in 1 mol L⁻¹ LiPF₆ EC:DMC was 9.18 mS cm⁻¹. Both values were measured at 25°C using a 2-electrode Swagelok system with a spacer and the impedance spectroscopy method.

Electrode material

The negative electrode of the hybrid LIC was made of copper foil (thickness = 10 μm) covered with a mixture of graphite, polyvinylidene fluoride (PVdF) and carbon black (total thickness = 57 μm) provided by MTI Corporation. The positive electrode was made of Kuraray YP80F (80%), polytetrafluoroethylene (PTFE) (5%) (60% suspension in water, Sigma–Aldrich®) and carbon black C65 (15%) (total thickness = 182 μm). The active mass ratio of the electrodes was approximately 1:1. The two electrodes were separated by two Whatman® GF/D separators. The reference electrode was made of metallic lithium. Additionally, during the preparation of half-cells with activated carbon or graphite, the counter and reference electrodes constituted metallic lithium discs (d = 16 mm). Round discs (d = 18 mm) of glass fibre filters (GF/D, Whatman®) were used as separators. The microtextural characteristics of the material were determined by using the Brunauer–Emmett–Teller (BET) isotherm method (77 K) with N₂ as an adsorbate (ASAP 2460, Micromeritics, USA). The surface area of the positive electrode equalled 1558 m² g⁻¹ [45]. Before the adsorption/desorption steps, samples were flushed at 350°C for 12 h under continuous helium flow and further degassed at 25°C for 5 h (vacuum). Round-shaped electrodes (d = 16 mm, A = 2 cm²) were cut from both electrode materials using an EL-Cut

provided by EL-CELL®. All cells were prepared using a glovebox (MBraun), which ensured negligible amounts of water and oxygen (<0.1 ppm).

Spectroscopic methods

The electrolyte infrared spectrum was taken with a spectrometer (Nicolet™ iS5 FT-IR) in the 500–4000 cm⁻¹ wavelength range. Examination of the electrodes after ageing was performed with a Raman DXR microscope (Thermo Fisher Scientific). The laser power (DXR 532 nm) was 4 mW, and the exposure time was 3x20 s. Spectra were taken for both the positive and negative electrodes from three different places. Gas chromatography with mass spectrometry (GC–MS) analysis was conducted using an EVOQ GC-TQ™ MS, Bruker. Apparatuses were connected with a PAT-Cell-Gas made by EL-CELL®. The temperature of the injector was 175°C, the column temperature was 150°C, and the mass spectrometer temperature was 220°C. The morphology of the solids was determined with a Hitachi S-3400N scanning electron microscope coupled with a DS Thermo Scientific adapter for energy-dispersive spectroscopy (EDS). X-ray photoelectron spectroscopy (XPS) analyses were carried out with a PHI VersaProbeII Scanning XPS system using monochromatic Al K α (1486.6 eV) X-rays focused to a 100 μ m spot and scanned over an area of 400 μ m x 400 μ m.

Electrochemical investigation

Electrochemical measurements were made with ECC-Ref systems made by EL-CELL®. LICs were assembled using a graphite electrode (on copper foil) and activated carbon electrodes, between which soaked separators were placed. The reference metallic lithium pin was introduced into the ECC-Ref by using ECC-RefLoad. Electrochemical measurements were carried out on a multichannel galvanostat/potentiostat (VMP-3 BioLogic®), and the temperature control was provided by a thermostatic chamber.

Results and discussion

The charge consumed by the SCN⁻ redox reaction during the intercalation of lithium ions into the graphite structure was hypothesized to inhibit the increase in the positive electrode potential, which would enable a further decrease in the negative electrode potential and thus enable intercalation of lithium ions into the graphite structure. The confirmation of this hypothesis could constitute an important claim, as there would be no need to use auxiliary metallic lithium electrodes [46] or sacrificial materials in the positive electrode [47]. The electrochemical performance of LiSCN at high operating voltages has not yet been studied in sufficient detail. Therefore, an electrochemical capacitor with the addition of LiSCN salts was first made. The system was first charged to 4.5 V vs. Li/Li⁺ to

One-step assembly of metal-ion capacitors using redox-active electrolytes

identify possible redox peaks (scan rate of 0.06 mV s^{-1}). In the voltammogram (Figure 1), two peaks originating from the redox reactions of the LiSCN salt are observed.

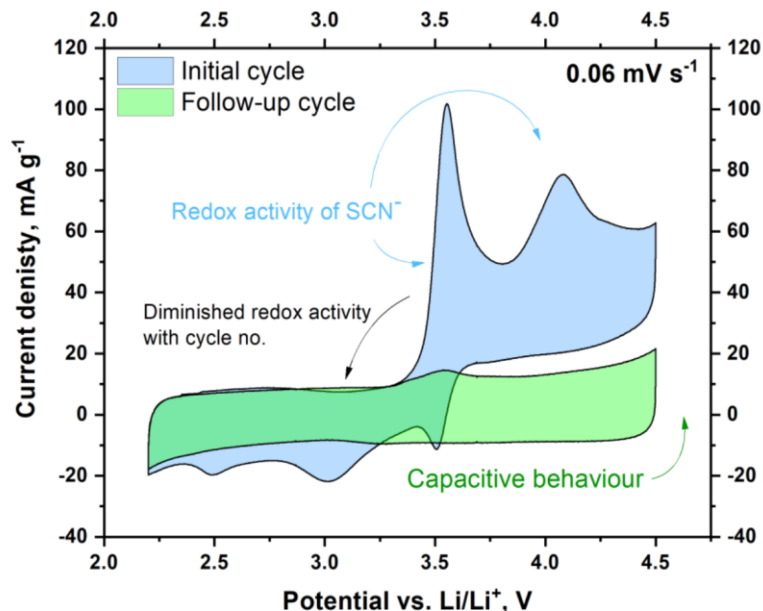


Figure 1 Cyclic voltammogram of activated carbon vs. metallic lithium system with 0.25 mol L^{-1} LiSCN in 1 mol L^{-1} LiPF₆ EC:DMC (1:1).

The literature does not specify exactly what these reactions might be, so, an attempt was made to identify the reaction products. The resulting voltammograms show the first redox reaction at approximately 3.5 V and the second at ca. 4.1 V vs. Li/Li⁺. The redox activity of SCN⁻ ions induces oxidation reactions mainly at the positive electrode, while the negative electrode continues to operate within its range. There is a significant decrease in the redox peaks with the subsequent charge and discharge cycles. The character of the redox reactions is partially irreversible, as the anodic and cathodic current values decrease with every cycle. After 6 cycles, the SCN⁻ ions are no longer electrochemically active in the presented range of potentials, and the activated carbon electrode starts to behave as an EDLC material. Another test was performed to determine how many cycles are required to almost consume the redox-active reagent. A system with activated carbon and metallic lithium was constructed to perform cyclic voltammetry with a scan rate equal to 1 mV s^{-1} (Figure 1 SI). Almost 35 cycles of charging and discharging were required to fully react the SCN⁻ ions.

In the next stage, a graphite-metallic lithium half-cell was constructed with the classic electrolyte used in LIBs. This measurement enables us to compare possible differences in the intercalation curve of the negative electrode. The system was electrochemically tested

One-step assembly of metal-ion capacitors using redox-active electrolytes

using the $C/20$ current (the current value that enables full intercalation in the graphite electrode in 20 hours) for electrolytes without the addition of LiSCN salt (Figure 2a) and with the addition of LiSCN salt (Figure 2b) to compare the intercalation processes.

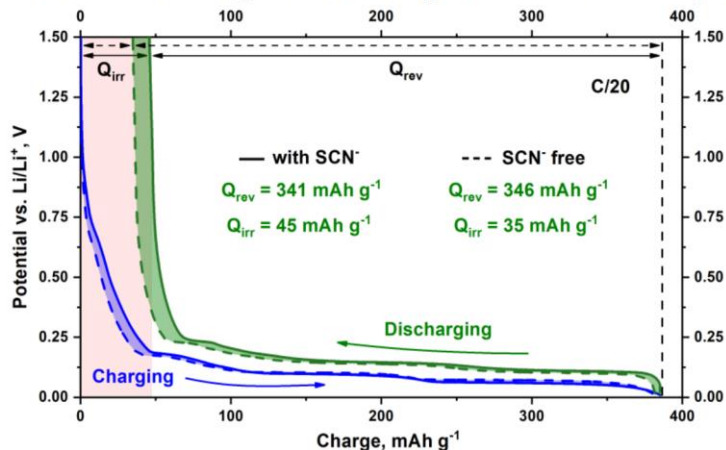


Figure 2. Graphite intercalation at $C/20$ (C corresponds to the theoretical capacity of graphite, 372 mAh g^{-1}) where the electrolyte in the cell **a**) included SCN^- ions and **b**) did not include SCN^- ions.

In the comparison, no significant differences are observed in the capacities between the systems with and without SCN^- ions, which suggests no damage to the system during intercalation of SCN^- ions. The similar reversible charges (346 mAh g^{-1} and 341 mAh g^{-1}) indicate that the same amounts of lithium ions are intercalated in both systems. Notably, the irreversible capacity is slightly higher for the cell with SCN^- (45 mAh g^{-1} compared to 35 mAh g^{-1}), which could be the result of more charge being used for the creation of the solid electrolyte interphase (SEI). The SEI layer likely includes additional decomposition compounds from SCN^- . This process also depends on changes in the electrolyte properties (slight decline in the conductivity), which are caused by adding LiSCN salt to the electrolyte. However, the addition of LiSCN salt does not significantly affect the intercalation process or the reversibility of the system.

After positive results for tests related to prelithiation of the graphite electrode (Figure 2b) and the assumed hypothesis of a slowing of the increase in the potential of the positive electrode (Figure 1), the hybrid system - LIC - was assembled. The constructed system consisted of graphite as the negative electrode, activated carbon as the positive electrode, and metallic lithium as the reference electrode. Between the electrodes, two separators were placed, which were soaked with 0.25 mol L^{-1} LiSCN in 1 mol L^{-1} LiPF_6 EC:DMC. Figure 3 shows the results of the intercalation.

One-step assembly of metal-ion capacitors using redox-active electrolytes

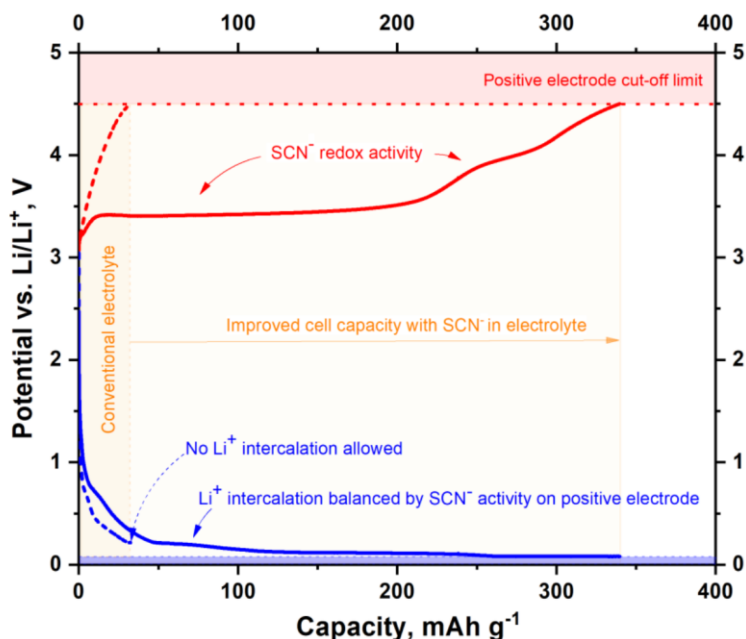


Figure 3. Prelithiation of LICs with and without 0.25 mol L^{-1} LiSCN salt addition.

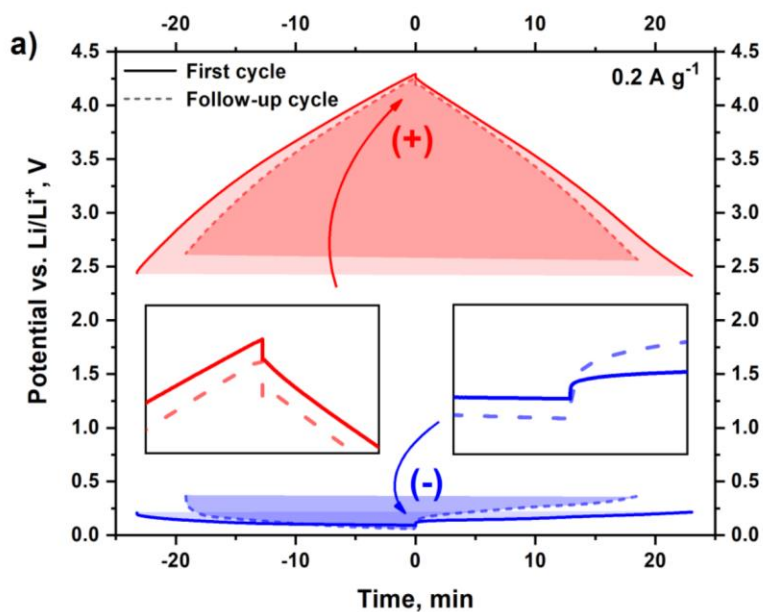
The process of full system intercalation was completed. At the negative electrode, all the steps responsible for intercalation of the appropriate amount of lithium ions into the graphite structure were noticed. Additionally, the positive electrode showed two plateaus, one longer at a potential ca. 3.4 V and the other at approximately 4 V vs. Li/Li⁺. Due to the presence of two redox reactions, which "held" the positive electrode against the potential increase, the negative electrode could intercalate lithium ions. The obtained prelithiation results (Figure 3) confirm the previously formed hypothesis regarding the inhibition of the increase in the potential of the positive electrode and the possible intercalation in the graphite electrode of lithium ions coming from the electrolyte. Notably, the lithium ions from the electrolyte were intercalated with the LiSCN additive, which was specifically calculated to leave as little dead mass in the electrolyte as possible and, more importantly, not change the conductivity of the electrolyte. Figure 3 also shows a comparison with the system consisting of the classic electrolyte without the addition of LiSCN, where we cannot observe intercalation. The maximum potential was determined to be 4.5 V, above which irreversible electrolyte decomposition processes might occur.

The C/20 current was chosen for the prelithiation process to create a thick and tight SEI layer [16], [48]. The system operating voltage range was set from 2.2 to 4.2 V vs. Li/Li⁺. The minimum potential was high enough to prevent metallic lithium plating. The maximum potential ensured no decomposition reactions of the electrolyte. Then, the appropriate value of the charge and discharge current was determined. Due to the need to use the

One-step assembly of metal-ion capacitors using redox-active electrolytes

highest possible currents to increase the power of the system in a given voltage range, a current density of 0.2 A g^{-1} was chosen (Figure 2 SI). At this current density, the negative electrode works slightly above 0 V vs. Li/Li^+ , which is a critical value below which lithium plating can occur. All subsequent tests were performed with this current value.

In the following phase, three-electrode tests were performed to observe the potential profiles of individual electrodes. The electrode charts are shown in Figure 4a. Notably, during the first cycle operation, residues of redox reactions can be observed. The negligible Ohmic drop, both before and after cycling, proves that the resistance is insignificant and that the capacitance decrease is not connected with the system construction. The working range of the negative electrode is 0.2 V to 0.5 V , and that of the positive electrode is 2.5 to $4.25 \text{ V vs. Li/Li}^+$. The work of the electrodes before and after the electrochemical operation is presented. After more than a thousand cycles of galvanostatic charging and discharging, a decrease in the system capacity compared to the initial capacity is noticed, which is assumed to not be related to the electrochemical operation. The working electrode shows a low resistance and works within the given range, while the negative electrode approaches the potential for producing metallic lithium on the electrode surface (plating). However, the deterioration of the system is not shown by plating. Later in the article, our attempt to find possible reaction products is described. An impedance spectroscopy study (Figure 4b) was also performed before and after the electrochemical operation of the system. The equivalent distributed resistance (EDR) is better after cycling because the graphite is better intercalated; however, the curve shape suggests problems with the diffusive layer resistance related to the electrochemical operation.



**One-step assembly of metal-ion capacitors using
redox-active electrolytes**

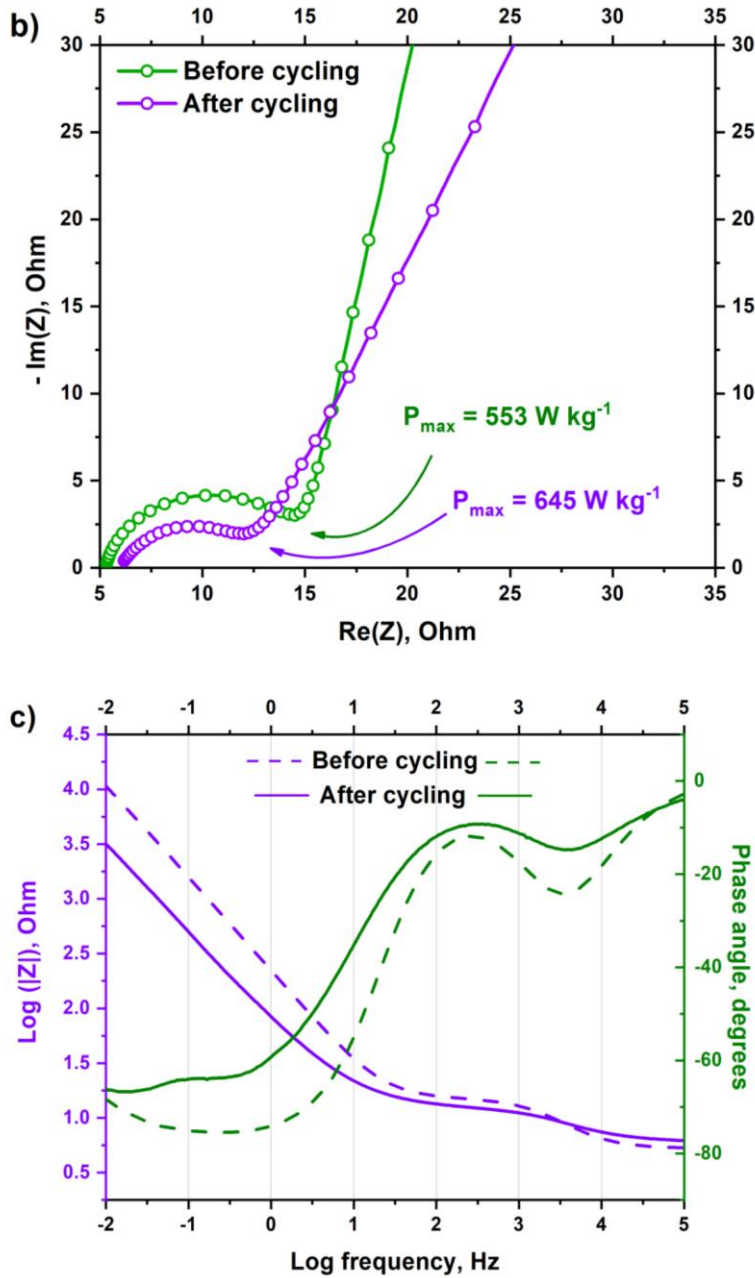


Figure 4. a) Potential distribution during cell operation with SCN^- ions before and after cycling. b) Nyquist plot.

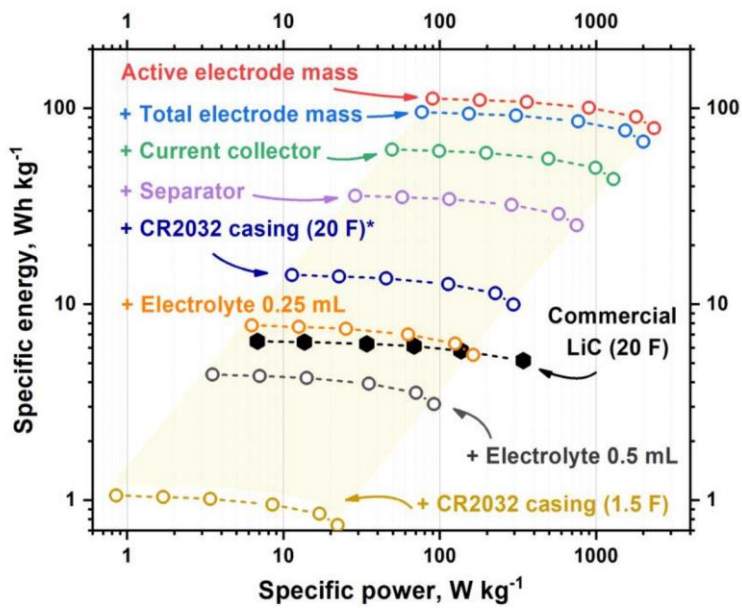
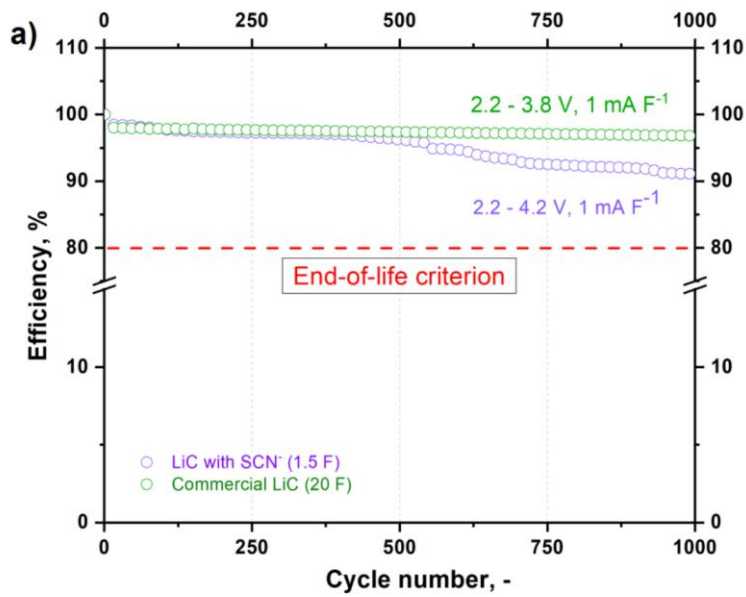
A hybrid LIC with LiSCN addition was compared to a commercial LIC in terms of cycle life (Figure 5a) and the power-energy dependence on capacitance (Figure 5b). During cycle life comparison, the commercial system was charged and discharged following the manufacturer's recommendations of 2.2 V - 3.8 V, while our capacitor was operated in the range of 2.2 V - 4.2 V. Notably, the first 500 cycles are very similar, but then breakdown occurs, which causes our system capacitance to decrease.

There is a noticeable second plateau after the decline, which may indicate a similar course as for Li-S batteries. This would mean that during electrochemical operation, sulphur compounds or elemental sulphur are formed, which may clog the pores and deteriorate the system capacitance.

When comparing two different energy storage systems, the most common representation is the Ragone diagram. In this case, however, comparing power and energy in terms of mass could be unfair, as commercial systems are made of the lightest possible materials, reducing the weight of the system to a minimum. In contrast, our measuring system (ECC-REF) is made from a large piece of stainless steel, so it is much heavier than a commercial aluminium casing. Therefore, we decided to show the dependence in terms of the system capacitance. The obtained LIC with SCN^- ions can store approximately 1.5 F, while the commercial LIC can store 20 F. The relationship is shown in Figure 5b. For lower power values, the LIC with SCN^- ions shows higher energy values. However, a significant drop can be seen with a power of 0.03 W F^{-1} . This is probably due to the acceleration of unfavourable processes in the electrochemical system, which will be clarified in more detail later in the article.

The next step was to compare the self-discharge of the obtained system with that of commercial energy storage devices. For this purpose, the compared systems were charged to the operating voltage limit (4.2 V for the LIC with SCN^- , 3.8 V for the commercial LIC and 2.7 V for the commercial EDLC), held for 2 hours, and then left for 12 hours for self-discharge while recording the voltage drop of the system. The largest decrease was expected for the commercial EDLC due to the way energy is stored only through nonfaradaic electrostatic attraction [49]. LICs should exhibit a smaller self-discharge drop than EDLCs because in addition to storing energy in a nonfaradaic manner, there are faradaic reactions that last longer [50]. Additionally, the system we presented was charged to a higher voltage, which could affect the self-discharge rate and increase the system specific energy [51]. In the presented comparison, the commercial system presents a negligible voltage drop (0.02 V). However, as mentioned before, the commercial system is composed of thin and contiguous components. Our work aimed to show the principle of operation, not present a commercial system. Nevertheless, the lower voltage drop compared to EDLCs is optimistic and suggests that when assembling a commercial system with the proposed electrolyte, the self-discharge value would be comparable to that of other commercial LICs.

One-step assembly of metal-ion capacitors using redox-active electrolytes



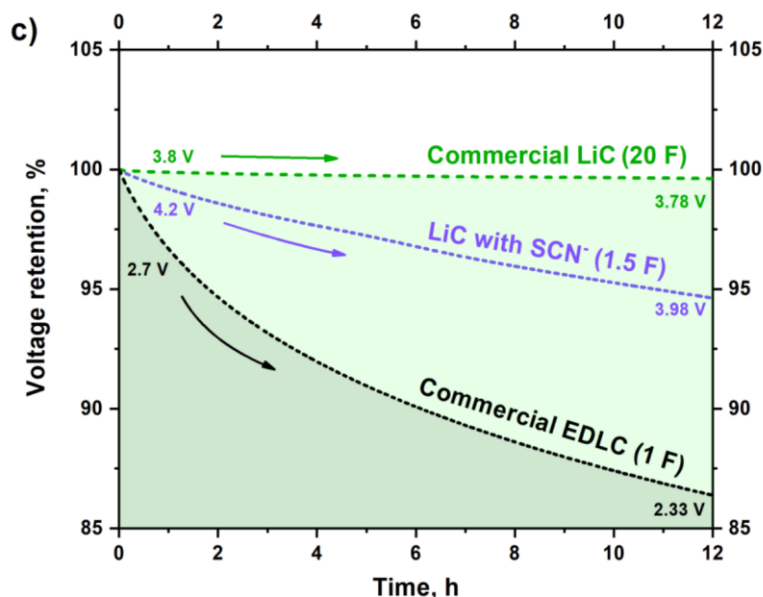


Figure 5. Comparison of the LIC with $0.25 \text{ mol L}^{-1} \text{ LiSCN}$ in $1 \text{ mol L}^{-1} \text{ LiPF}_6 \text{ EC:DMC}$ as the electrolyte and a commercial LIC in terms of the a) cyclability, b) Ragone plot modified to farads and c) self-discharge rate along with those of a commercial supercapacitor.

After electrochemical tests, an attempt was made to identify compounds formed during electrochemical cycling. After cyclic operation, a yellow precipitate was deposited on the positive electrode, which may cause clogging of the pores, change the electrolyte viscosity or constitute dead mass in the system. The cause of the deterioration of the operating system was explored. For this purpose, several instrumental analysis studies were performed, and infrared spectroscopy was employed first.

To identify signals derived from LiSCN salt, the system without SCN⁻ ions, i.e., the classic $1 \text{ mol L}^{-1} \text{ LiPF}_6$ in EC:DMC (1:1), was first investigated. Then, three additional concentrations of LiSCN salt were sequentially studied: 0.085 , 0.125 and 0.25 mol L^{-1} . Figure 6a shows the obtained spectra for the electrolytes. The addition of LiSCN manifests as signals with a wavelength from $1500\text{-}1700 \text{ cm}^{-1}$. However, the most characteristic signal is observed at 2072 cm^{-1} . This signal is mainly attributed to SCN⁻ ions. A proportional relationship between the increase in this signal and the increase in the concentration of thiocyanate in the electrolyte is observed. The obtained spectra fully confirm the chemical composition of the electrolytes.

Then, whether SCN⁻ ions are present in the electrolyte solution after electrochemical operation was investigated. Additionally, new signals indicating the presence of functional groups of compounds resulting from the decay of the electrolyte were searched for. For this

purpose, the system after 1000 galvanostatic charge and discharge cycles was disassembled in an inert atmosphere, and the electrolyte was squeezed out of the separator and then subjected to infrared spectroscopy. The obtained spectrum was compared with the spectrum of the same electrolyte before electrochemical operation, as presented in Figure 6b. The electrolyte after cyclic operation did not show any signals from SCN^- ions; in particular, attention was given to the signal at 2072 cm^{-1} . Moreover, no additional signals were observed in the spectrum. Therefore, SCN^- ions were assumed to undergo a chemical transformation during electrochemical cycling, and the resulting compound precipitated on one of the electrodes or evaporated.

Raman spectroscopy is a complementary technique to infrared spectroscopy, and it allows us to observe changes in the structure of activated carbon during electrochemical testing of the LIC. The spectrum acquired during Raman spectroscopy (Figure 3 SI) shows no additional signals from impurities. The fully developed D-band and G-band signals in comparison with the electrode before electrochemical operation show no change in the structure of the electrode after operation. Thus, the substances contained in the electrolyte and its decay products do not cause structural distortion of the morphology of the positive electrode.

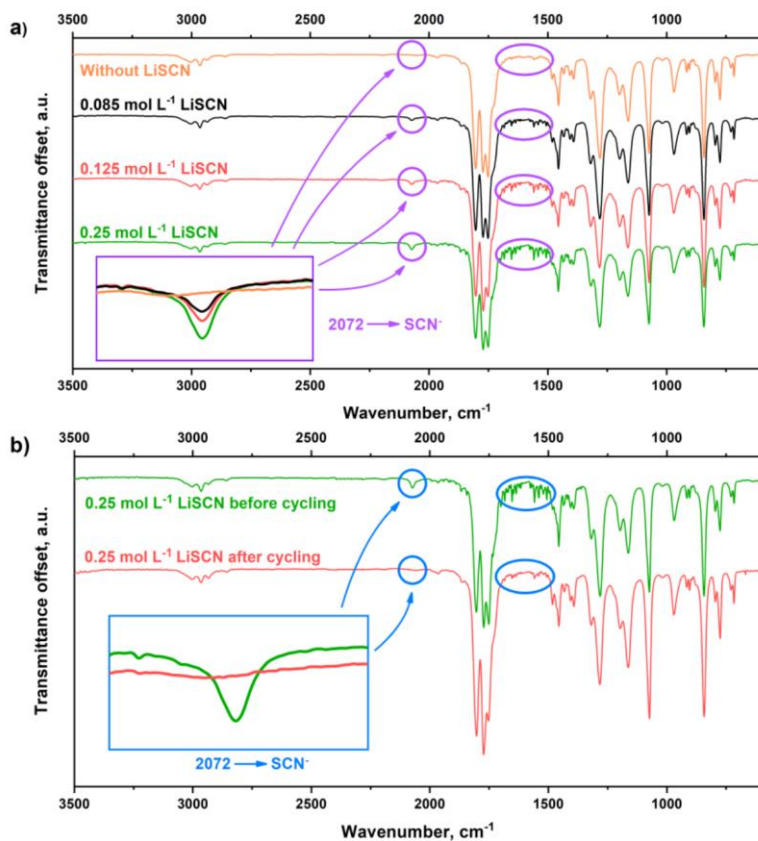
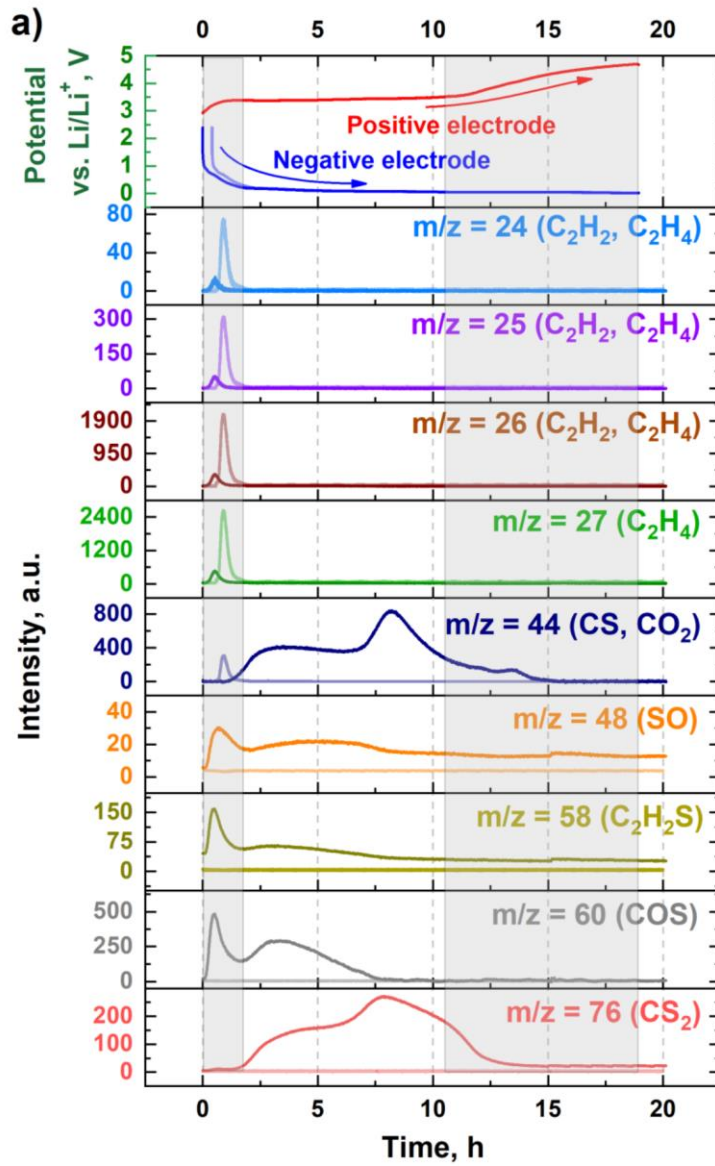


Figure 6. Infrared spectra of electrolytes **a)** with different LiSCN concentrations and **b)** before and after electrochemical cycling of the LIC with SCN^- ions.

Scanning electron microscopy (SEM) was then performed. The photos were taken at several locations for the positive electrode to observe its structure and possible changes on the surface (Figure 4a and b SI). An unknown chemical compound is deposited on the surface. For a more detailed analysis of the unexplained substance, an EDS study was performed (Figure 4c and d SI). From the conducted research, the compound released during electrochemical operation is concluded to mainly consist of sulphur or simply be elemental sulphur. The results obtained may suggest a reduction of SCN^- to CS_2 or elemental sulphur.

An XPS study was carried out to analyse the obtained samples in more detail. The spectra of the positive and negative electrodes and separator were obtained after electrochemical operation. All obtained XPS spectra confirm the composition of the electrolyte and electrode materials. The positive electrode was then examined in detail for nitrogen and sulphur. Detailed nitrogen analysis shows the presence of $-\text{C}=\text{N}-$, NH_2 or SCN^- groups. Detailed sulphur analysis shows the presence of $(\text{SCN})_x$ or thiol- $\text{SC}-$ groups. From the infrared spectra, we can reject the presence of SCN^- or $(\text{SCN})_x$. The presence of thiol groups confirms the presence of CS_2 on the positive electrode. Unfortunately, elemental sulphur is not observed. Since the tests were performed in ultrahigh vacuum, the sulphur most likely evaporated, and only unnoticeable traces remained.



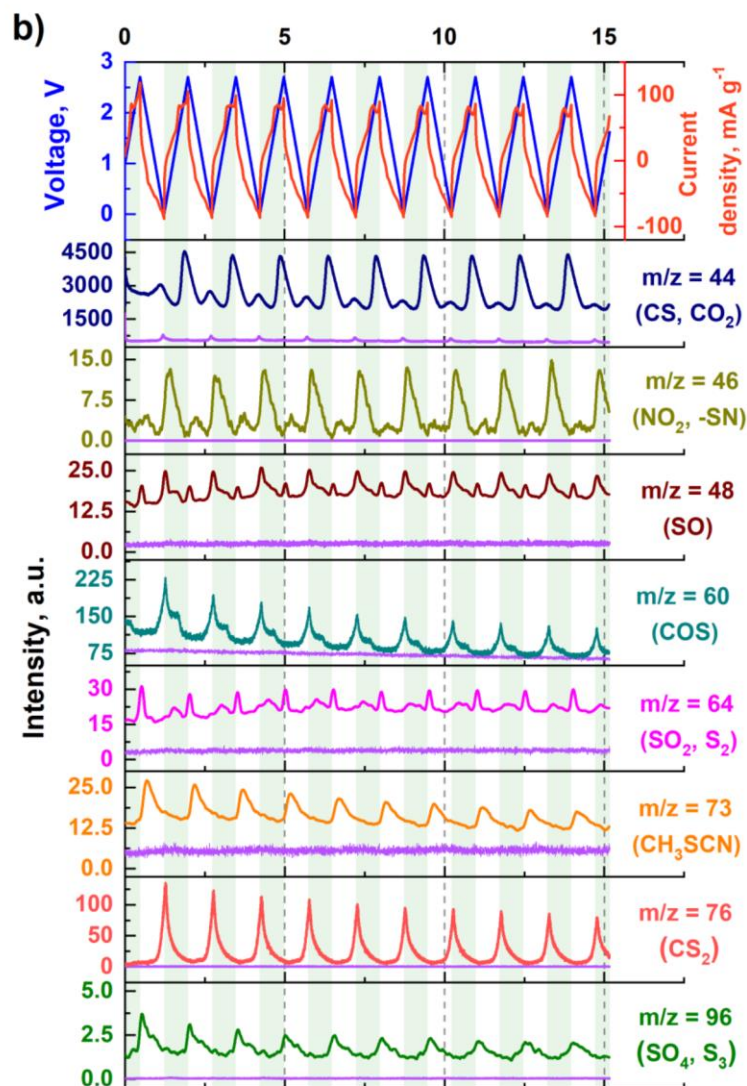


Figure 7. Mass spectra of important masses during a) prelithiation of the LICs with LiSCN salt and without LiSCN salt (lighter curve shade); b) cyclic voltammetry curves of EDLC with and without LiSCN salt (violet lines).

In the final stage of this work, GC–MS operando measurements were performed. In particular, the intercalation process with and without SCN^- ions, both in a two-electrode and a three-electrode system, was investigated. Figure 7a shows the result of the intercalation study. Clear peaks from masses 24, 25, 26 and 27 are observed. The masses obtained are characteristic of gases evolving during the formation of the SEI layer, mainly C_2H_2 and C_2H_4 [52–54]. During the analysis of the results, there was concern about the possibility of decomposition of SCN^- ions into CN^- compounds that are extremely harmful to health [43, 55]. Thus, a half-cell consisting of a graphite electrode and a lithium metal electrode, which were the counter and reference electrodes, was tested (Figure 7a). In this

system, a similar intensity ratio of masses 24, 25, 26 and 27 was obtained as for the system with LiSCN salt. This observation led to the conclusion that CN^- ions most likely do not form during the formation of the SEI layer, and the signals obtained come mostly from acetylene and ethylene. The SEI layer has a different composition than that in the classic electrolyte due to the presence of masses such as 48, 58, or 60. The masses mentioned correspond to sulphur compounds derived from the SCN^- group, which arise from reactions at the negative electrode. A particularly important signal of mass 76 is observed after SEI formation, which is assumed to be a signal from carbon disulphide. Its formation occurs when the positive electrode reaches the potential of 3.4 V vs. Li/Li^+ , i.e., the potential of the redox reaction. The products of this redox reaction can therefore be concluded to only be CS_2 because its production ends with the end of the redox reaction. During the further course of prelithiation, no evolution of other gases is observed. Notably, during the formation of the SEI layer, there are also small signals at 34 (H_2S), 44 (CO_2), 28 (CO , N_2) and 16 (CH_4).

For a more detailed analysis of the electrolyte, the systems in the classic electrolyte with and without thiosulfate ions were compared. For this purpose, two EDLCs consisting of activated carbon as the electrode material were constructed. The systems were tested during cyclic voltammetry at a scan rate of 1 mV s^{-1} . The presence of clear peaks originating from the electrolyte or products of electrochemical operation, such as CO_2 , which are common to both systems, is noticed. However, only the most important masses that constitute the difference between the compared systems are presented in Figure 7b. By carefully analysing the obtained result, we can see at which point the given gases are released (during charging or discharging). We observe an increase in masses 46, 48, 60, and 76 during discharging and masses 64, 73, and 96 during charging. Masses 64 and 96 may come either from the precipitated elemental sulphur or from the gaseous products of the oxidation of SO_2 and SO_4 . The following question should be asked: what is the source of so much oxygen in the system that the abovementioned gases can be produced in such amounts? The oxygen most likely comes from the breakdown of EC or DMC electrolytes. A small amount may also come from the helium cylinder used to flush the system. Compared to the LIC without thiosulfate ions, SCN^- ions in the form of CH_3SCN are present in the system with thiosulfate ions due to the lower operating voltage. However, notably, even at lower voltages, SCN^- ions decompose to form carbon sulphide. As seen in the subsequent cycles, carbon sulphide can also decompose into elemental sulphur.

One-step assembly of metal-ion capacitors using redox-active electrolytes

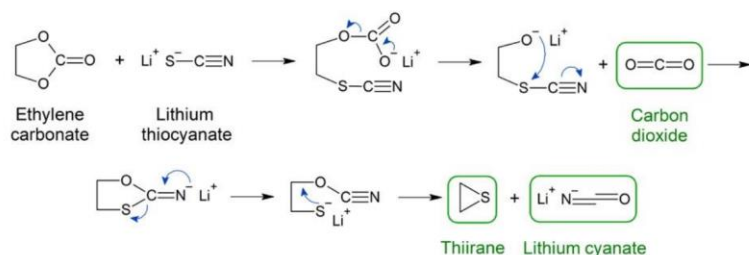
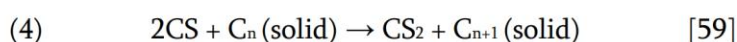
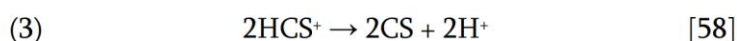
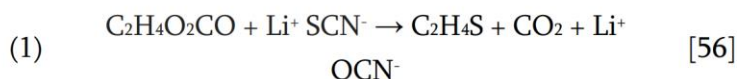


Figure 8. Proposed mechanism of the lithium thiocyanate reaction with EC during prelithiation, based on [56].

Proposed SCN⁻ reaction pathway



Indicating the proper mechanism of ion activity in the working cell system with SCN⁻ is challenging. However, based on the use of gas chromatography with mass spectrometry and an exhaustive literature review, we propose a reaction pathway. According to Figure 7a, SEI formation delivers a significant amount of masses 58 and 60, which are assumed to correspond to thiirane and thiirane (or carbonyl sulphide). Their formation is caused by the presence of an organic solvent, which is shown by the reduced SEI formation signal masses (24, 25, 26 or 27; Figure 7a). Therefore, the initial reaction is related to SCN⁻ ions along with one of the solvents – EC (Figure 8, reaction 1). During the interaction of the mentioned molecules, thiirane, carbon dioxide and lithium cyanate are the products. However, the GC–MS analysis results (Figure 7a) show a lack of CO₂ molecules in the initial stage of LiC operation, even during the SEI formation process. The abovementioned observation may lead to the conclusion that carbon dioxide is not produced. At one stage of the mechanism, the oxygen and carbon molecules react with another electrolyte decay product (e.g., CH₃^{*} from DMC), resulting in a solid or a compound with a mass masked by a stronger signal in GC–MS. Another byproduct is LiOCN. The produced lithium cyanate could take the lithium ion from the electrolyte, which may cause a decrease in the conductivity and thus deterioration of the system. In the later stage of the LIC operation, thiirane or thiirane decomposes into HCS⁺ and CH₃⁻ (reaction 2). Thioformyl, as a highly unstable molecule, further reacts with carbon sulphide (CS). However, carbon sulphide is

also an unstable compound; it polymerizes in the presence of solid carbon (activated carbon electrode) to form carbon disulphide (CS₂). These three reactions combined may be responsible for the redox activity of the electrolyte. Confirmation of the abovementioned hypothesis might be provided by comparing signals from masses 44 (HCS⁺, CS) and 76 (CS₂) during prelithiation (Figure 9). When redox activity occurs on the positive electrode, the signal from mass 44 starts to increase. HCS⁺ or CS formation appears, causing an increase in the mass 76 signal attributable to CS₂, which may be confirmed by the slight delay in the mass 76 signal response.

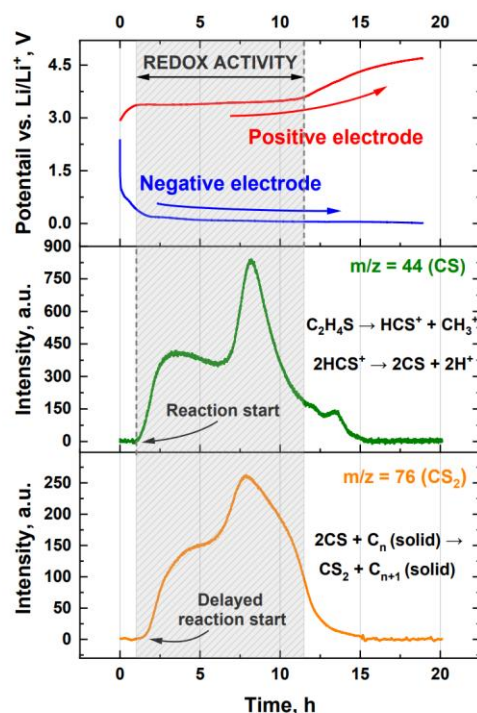
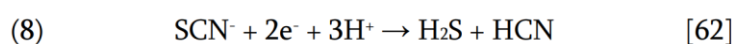
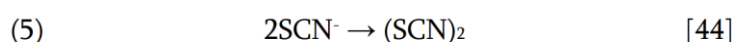


Figure 9. Mass spectra of important masses related to redox activity during prelithiation of the LIC with LiSCN salt.

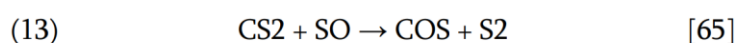
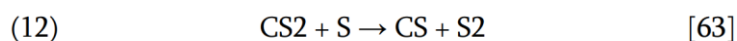
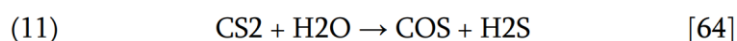
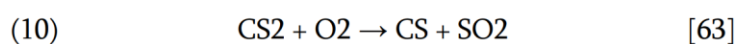
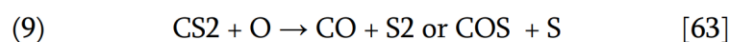
Nevertheless, the presented reactions are only the beginning of LIC operation. During further charging and discharging, many processes could occur, causing deterioration of the system. Carbon sulphide and carbon disulphide are moderately reactive molecules. They can react with oxygen, hydrogen, water, decomposition products of electrolytes and even each other, producing various compounds. Some of those reactions we classified as possible and are further listed in the text. Most of them lead to the production of elemental sulphur, which, as we assumed before, may deteriorate the system operation by clogging the pores. There are also other thiocyanate reactions that can occur in the obtained system. SCN⁻ can polymerize and thus produce carbon sulphide, elemental sulphur and carbon nitride (reactions 5, 6). Thiocyanate anions could also react with the low water contamination

(reaction 7). However, no noticeable signal from ammonia or its derivatives is observed. Extremely poisonous hydrogen cyanide could also be produced (reaction 8). However, the obtained signal ratio for masses 26 and 27 was compared with that of the intercalated system without SCN^- , and they were the same, indicating no HCN production.

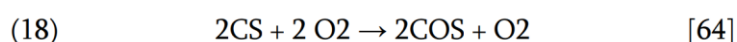
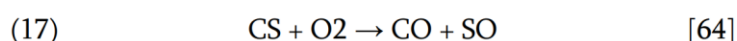
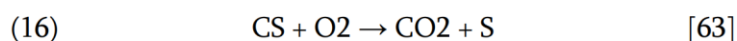
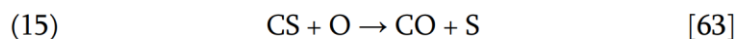
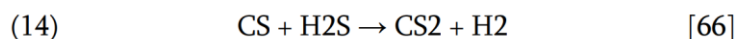
Other possible SCN^- reactions



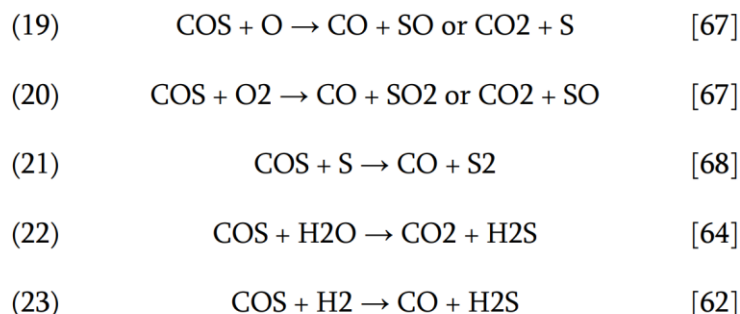
Possible CS_2 reactions



Possible CS reactions



Possible COS reactions



Conclusions and future prospects

The presented work displays an attempt to perform a prelithiation process for LICs using lithium ions from the electrolyte. For this purpose, a redox-active thiocyanate salt was added to the electrolyte to inhibit the rapid increase in the potential of the positive electrode. The experiment was successful - the graphite electrode was fully intercalated with lithium ions from the electrolyte. The hybrid system works properly with a very high capacitance and a low resistance. However, a problem is the decline in the accumulated charge of the system over time, which shows that the presented solution needs to be improved. A series of spectroscopic analyses were performed, such as IR spectroscopy, Raman spectroscopy, XPS, SEM/EDS, and operando GC-MS, to explain the changes occurring in the system. The evolution of a yellow precipitate was noted on the surface of the positive electrode. SCN^- ions were confirmed to undergo an electrochemical reaction and form CS_2 ca. 3.4 V vs. Li/Li^+ . During cyclic operation, CS_2 oxidizes into elemental sulphur, which is responsible for clogging of the pores of the positive electrode. Sulphur, by blocking the access of the electrolyte and limiting the capacitance, affects the cycle life of the system.

A future solution seems to be replacing LiSCN salt with other electroactive species that will not cause dead mass problems but will enhance the system energy. However, completing full intercalation of the system using lithium from the electrolyte is a large step forwards. The presented approach is innovative and could compete with current prelithiation techniques, but a few adjustments are still needed for full implementation in the commercial market. This achievement marks the beginning of a new, promising method, the application of which may provide serious competition for LIBs in the future.

Conflicts of interest

The authors do not declare any conflicts of interest.

Acknowledgements

This work was financially supported by the **European Research Council** within the Starting Grant project (GA 759603) under European Unions' Horizon 2020 research and innovation programme.

PJ would like to acknowledge the Foundation for Polish Science and START 2019 programme.

References

- [1] M.R. Lukatskaya, B. Dunn, Y. Gogotsi, Multidimensional materials and device architectures for future hybrid energy storage, *Nat Commun* 7(1) (2016) 12647.
- [2] N. Hirota, K. Okuno, M. Majima, A. Hosoe, S. Uchida, M. Ishikawa, High-performance lithium-ion capacitor composed of electrodes with porous three-dimensional current collector and bis(fluorosulfonyl) imide-based ionic liquid electrolyte, *Electrochimica Acta* 276 (2018) 125-133.
- [3] U. Gulzar, S. Goriparti, E. Miele, T. Li, G. Maidecchi, A. Toma, F. De Angelis, C. Capiglia, R.P. Zaccaria, Next-generation textiles: from embedded supercapacitors to lithium ion batteries, *Journal of Materials Chemistry A* 4(43) (2016) 16771-16800.
- [4] L.P. Yu, G.Z. Chen, Supercapatteries as High-Performance Electrochemical Energy Storage Devices, *Electrochemical Energy Reviews* 3(2) (2020) 271-285.
- [5] A. Balducci, Electrolytes for high voltage electrochemical double layer capacitors: A perspective article, *J Power Sources* 326 (2016) 534-540.
- [6] P. Galek, A. Mackowiak, P. Bujewska, K. Fic, Three-Dimensional Architectures in Electrochemical Capacitor Applications - Insights, Opinions, and Perspectives, *Frontiers in Energy Research* 8 (2020).
- [7] M. Yamagata, S. Ikebe, K. Soeda, M. Ishikawa, Ultrahigh-performance nonaqueous electric double-layer capacitors using an activated carbon composite electrode with alginate, *Rsc Advances* 3(4) (2013) 1037-1040.
- [8] F. Beguin, V. Presser, A. Balducci, E. Frackowiak, Carbons and electrolytes for advanced supercapacitors, *Adv Mater* 26(14) (2014) 2219-51, 2283.
- [9] J.R. Miller, Perspective on electrochemical capacitor energy storage, *Applied Surface Science* 460 (2018) 3-7.
- [10] K. Fic, G. Lota, M. Meller, E. Frackowiak, Novel insight into neutral medium as electrolyte for high-voltage supercapacitors, *Energy & Environmental Science* 5(2) (2012) 5842-5850.
- [11] M. Goktas, C. Bolli, E.J. Berg, P. Novák, K. Pollok, F. Langenhorst, M.v. Roeder, O. Lenchuk, D. Mollenhauer, P. Adelhelm, Graphite as Cointercalation Electrode for Sodium-Ion Batteries: Electrode Dynamics and the Missing Solid Electrolyte Interphase (SEI), *Advanced Energy Materials* 8(16) (2018) 1702724-n/a.
- [12] M. Soltani, S.H. Beheshti, A comprehensive review of lithium ion capacitor: development, modelling, thermal management and applications, *Journal of Energy Storage* 34 (2021) 102019.
- [13] K. Naoi, S. Ishimoto, J. Miyamoto, W. Naoi, Second generation 'nanohybrid supercapacitor': Evolution of capacitive energy storage devices, *Energy & Environmental Science* 5(11) (2012) 9363-9373.

- [14] B. Babu, C. Neumann, M. Enke, A. Lex-Balducci, A. Turchanin, U.S. Schubert, A. Balducci, Aging processes in high voltage lithium-ion capacitors containing liquid and gel-polymer electrolytes, *J Power Sources* 496 (2021) 229797.
- [15] F. Sun, J. Gao, Y. Zhu, X. Pi, L. Wang, X. Liu, Y. Qin, A high performance lithium ion capacitor achieved by the integration of a Sn-C anode and a biomass-derived microporous activated carbon cathode, *Sci Rep* 7(1) (2017) 40990.
- [16] P. Jeżowski, K. Fic, O. Crosnier, T. Brousse, F. Béguin, Lithium rhenium(vii) oxide as a novel material for graphite pre-lithiation in high performance lithium-ion capacitors, *Journal of Materials Chemistry A* 4(32) (2016) 12609-12615.
- [17] S. Ahn, Y. Haniu, H. Nara, T. Momma, W. Sugimoto, T. Osaka, Synthesis of Stacked Graphene-Sn Composite as a High-Performance Anode for Lithium-Ion Capacitors, *Journal of the Electrochemical Society* 167(4) (2020) 40519.
- [18] P. Simon, Y. Gogotsi, Materials for electrochemical capacitors, *Nat Mater* 7(11) (2008) 845-54.
- [19] P. Jeżowski, O. Crosnier, E. Deunf, P. Poizot, F. Béguin, T. Brousse, Safe and recyclable lithium-ion capacitors using sacrificial organic lithium salt, *Nat Mater* 17(2) (2018) 167-173.
- [20] G.G. Amatucci, F. Badway, A. Du Pasquier, T. Zheng, An asymmetric hybrid nonaqueous energy storage cell, *Journal of the Electrochemical Society* 148(8) (2001) A930-A939.
- [21] B. Zhao, R. Ran, M.L. Liu, Z.P. Shao, A comprehensive review of Li₄Ti₅O₁₂-based electrodes for lithium-ion batteries: The latest advancements and future perspectives, *Materials Science & Engineering R-Reports* 98 (2015) 1-71.
- [22] T.F. Zhang, F. Zhang, L. Zhang, Y.H. Lu, Y. Zhang, X. Yang, Y.F. Ma, Y. Huang, High energy density Li-ion capacitor assembled with all graphene-based electrodes, *Carbon* 92 (2015) 106-118.
- [23] T. Aida, K. Yamada, M. Morita, An advanced hybrid electrochemical capacitor that uses a wide potential range at the positive electrode, *Electrochemical and Solid State Letters* 9(12) (2006) A534-A536.
- [24] V. Khomenko, E. Raymundo-Pinero, F. Béguin, High-energy density graphite/AC capacitor in organic electrolyte, *J Power Sources* 177(2) (2008) 643-651.
- [25] L.M. Jin, C. Shen, A. Shellikeri, Q. Wu, J.S. Zheng, P. Andrei, J.G. Zhang, J.P. Zheng, Progress and perspectives on pre-lithiation technologies for lithium ion capacitors, *Energy & Environmental Science* 13(8) (2020) 2341-2362.
- [26] M.S. Park, Y.G. Lim, J.H. Kim, Y.J. Kim, J. Cho, J.S. Kim, A Novel Lithium-Doping Approach for an Advanced Lithium Ion Capacitor, *Advanced Energy Materials* 1(6) (2011) 1002-1006.
- [27] M.S. Park, Y.G. Lim, J.W. Park, J.S. Kim, J.W. Lee, J.H. Kim, S.X. Dou, Y.J. Kim, Li₂RuO₃ as an Additive for High-Energy Lithium-Ion Capacitors, *Journal of Physical Chemistry C* 117(22) (2013) 11471-11478.
- [28] M.S. Park, Y.G. Lim, S.M. Hwang, J.H. Kim, J.S. Kim, S.X. Dou, J. Cho, Y.J. Kim, Scalable integration of Li₅FeO₄ towards robust, high-performance lithium-ion hybrid capacitors, *ChemSusChem* 7(11) (2014) 3138-44.
- [29] Y.G. Lim, D. Kim, J.M. Lim, J.S. Kim, J.S. Yu, Y.J. Kim, D. Byun, M. Cho, K. Cho, M.S. Park, Anti-fluorite Li₆CoO₄ as an alternative lithium source for lithium ion capacitors: an experimental and first principles study, *Journal of Materials Chemistry A* 3(23) (2015) 12377-12385.
- [30] P. Jeżowski, K. Fic, O. Crosnier, T. Brousse, F. Béguin, Use of sacrificial lithium nickel oxide for loading graphitic anode in Li-ion capacitors, *Electrochimica Acta* 206 (2016) 440-445.
- [31] P. Jeżowski, A. Chojnacka, X. Pan, F. Béguin, Sodium amide as a “zero dead mass” sacrificial material for the pre-sodiation of the negative electrode in sodium-ion capacitors, *Electrochimica Acta* 375 (2021) 137980.
- [32] P. Jeżowski, O. Crosnier, T. Brousse, Sodium borohydride (NaBH₄) as a high-capacity material for next-generation sodium-ion capacitors, *Open Chemistry* 19(1) (2021) 432-441.
- [33] C. Decaux, G. Lota, E. Raymundo-Pinero, E. Frackowiak, F. Béguin, Electrochemical performance of a hybrid lithium-ion capacitor with a graphite anode preloaded from lithium bis(trifluoromethane)sulfonimide-based electrolyte, *Electrochimica Acta* 86 (2012) 282-286.

- [34] Z. Lin, E. Goikolea, A. Balducci, K. Naoi, P.L. Taberna, M. Salanne, G. Yushin, P. Simon, Materials for supercapacitors: When Li-ion battery power is not enough, *Mater Today* 21(4) (2018) 419-436.
- [35] E. Frackowiak, M. Meller, J. Menzel, D. Gastol, K. Fic, Redox-active electrolyte for supercapacitor application, *Faraday Discuss* 172 (2014) 179-98.
- [36] W. Qin, N. Zhou, C. Wu, M. Xie, H. Sun, Y. Guo, L. Pan, Mini-Review on the Redox Additives in Aqueous Electrolyte for High Performance Supercapacitors, *ACS Omega* 5(8) (2020) 3801-3808.
- [37] J. Eskusson, A. Janes, A. Kikas, L. Matisen, E. Lust, Physical and electrochemical characteristics of supercapacitors based on carbide derived carbon electrodes in aqueous electrolytes, *J Power Sources* 196(8) (2011) 4109-4116.
- [38] X. Wang, R.S. Chandrabose, S.E. Chun, T. Zhang, B. Evanko, Z. Jian, S.W. Boettcher, G.D. Stucky, X. Ji, High Energy Density Aqueous Electrochemical Capacitors with a KI-KOH Electrolyte, *ACS Appl Mater Interfaces* 7(36) (2015) 19978-85.
- [39] K. Fic, S. Morimoto, E. Frackowiak, M. Ishikawa, Redox Activity of Bromides in Carbon-Based Electrochemical Capacitors, *Batteries & Supercaps* 3(10) (2020) 1080-1090.
- [40] K. Fic, B. Gorska, P. Bujewska, F. Beguin, E. Frackowiak, Selenocyanate-based ionic liquid as redox-active electrolyte for hybrid electrochemical capacitors, *Electrochimica Acta* 314 (2019) 1-8.
- [41] S.D. Cho, J.K. Im, H.K. Kim, H.S. Kim, H.S. Park, Functionalization of reduced graphene oxides by redox-active ionic liquids for energy storage, *Chem Commun (Camb)* 48(51) (2012) 6381.
- [42] A. Brandt, S. Pohlmann, A. Varzi, A. Balducci, S. Passerini, Ionic liquids in supercapacitors, *Mrs Bull* 38(7) (2013) 554-559.
- [43] B. Gorska, E. Frackowiak, F. Beguin, Redox active electrolytes in carbon/carbon electrochemical capacitors, *Current Opinion in Electrochemistry* 9 (2018) 95-105.
- [44] B. Gorska, P. Bujewska, K. Fic, Thiocyanates as attractive redox-active electrolytes for high-energy and environmentally-friendly electrochemical capacitors, *Phys Chem Chem Phys* 19(11) (2017) 7923-7935.
- [45] K. Fic, A. Platek, J. Piwek, E. Frackowiak, Sustainable materials for electrochemical capacitors, *Mater Today* 21(4) (2018) 437-454.
- [46] G. Madabattula, B. Wu, M. Marinescu, G. Offer, How to Design Lithium Ion Capacitors: Modelling, Mass Ratio of Electrodes and Pre-lithiation, *Journal of the Electrochemical Society* 167(1) (2019) 13527.
- [47] X.X. Pan, A. Chojnacka, P. Jezowski, F. Beguin, Na₂S sacrificial cathodic material for high performance sodium-ion capacitors, *Electrochimica Acta* 318 (2019) 471-478.
- [48] P. Verma, P. Maire, P. Novak, A review of the features and analyses of the solid electrolyte interphase in Li-ion batteries, *Electrochimica Acta* 55(22) (2010) 6332-6341.
- [49] A. Lewandowski, P. Jakobczyk, M. Galinski, M. Biegun, Self-discharge of electrochemical double layer capacitors, *Phys Chem Chem Phys* 15(22) (2013) 8692-9.
- [50] B. Babu, A. Balducci, Self-discharge of lithium-ion capacitors, *Journal of Power Sources Advances* 5 (2020) 100026.
- [51] X.Z. Sun, Y.B. An, L.B. Geng, X. Zhang, K. Wang, J.Y. Yin, Q.H. Huo, T.Z. Wei, X.H. Zhang, Y.W. Ma, Leakage current and self-discharge in lithium-ion capacitor, *Journal of Electroanalytical Chemistry* 850 (2019) 113386.
- [52] T. Liu, L. Lin, X. Bi, L. Tian, K. Yang, J. Liu, M. Li, Z. Chen, J. Lu, K. Amine, K. Xu, F. Pan, In situ quantification of interphasial chemistry in Li-ion battery, *Nat Nanotechnol* 14(1) (2019) 50-56.
- [53] G.M. Hobold, A. Khurram, B.M. Gallant, Operando Gas Monitoring of Solid Electrolyte Interphase Reactions on Lithium, *Chemistry of Materials* 32(6) (2020) 2341-2352.
- [54] A.P. Wang, S. Kadam, H. Li, S.Q. Shi, Y. Qi, Review on modeling of the anode solid electrolyte interphase (SEI) for lithium-ion batteries, *Npj Computational Materials* 4(1) (2018) 1-26.
- [55] J.J.V. Mediavilla, B.F. Perez, M.C.F. Cordoba, J.A. Espina, C.O. Ania, Photochemical Degradation of Cyanides and Thiocyanates from an Industrial Wastewater, *Molecules* 24(7) (2019) 1373.
- [56] S. Searles, E.F. Lutz, A New Synthesis of Small Ring Cyclic Sulfides, *Journal of the American Chemical Society* 80(12) (1958) 3168-3168.

- [57] J.J. Butler, T. Baer, Photoionization study of the heat of formation of HCS+, *Journal of the American Chemical Society* 104(19) (2002) 5016-5018.
- [58] R.I. Kaiser, C. Ochsenfeld, M. Head-Gordon, Y.T. Lee, The formation of HCS and HCSH molecules and their role in the collision of comet Shoemaker-Levy 9 with Jupiter, *Science* 279(5354) (1998) 1181-4.
- [59] E.K. Moltzen, K.J. Klabunde, A. Senning, Carbon Monosulfide - a Review, *Chemical Reviews* 88(2) (1988) 391-406.
- [60] T.S. Miller, A. d'Aleo, T. Suter, A.E. Aliev, A. Sella, P.F. McMillan, Pharaoh's Serpents: New Insights into a Classic Carbon Nitride Material, *Zeitschrift Fur Anorganische Und Allgemeine Chemie* 643(21) (2017) 1572-1580.
- [61] Y. Katayama, Y. Narahara, Y. Inoue, F. Amano, T. Kanagawa, H. Kuraishi, A thiocyanate hydrolase of *Thiobacillus thioparus*. A novel enzyme catalyzing the formation of carbonyl sulfide from thiocyanate, *J Biol Chem* 267(13) (1992) 9170-5.
- [62] M.E. Rasche, L.C. Seefeldt, Reduction of thiocyanate, cyanate, and carbon disulfide by nitrogenase: kinetic characterization and EPR spectroscopic analysis, *Biochemistry* 36(28) (1997) 8574-85.
- [63] D.L. Singleton, R.J. Cvetanović, Evaluated Chemical Kinetic Data for the Reactions of Atomic Oxygen O(³P) with Sulfur Containing Compounds, *Journal of Physical and Chemical Reference Data* 17(4) (1988) 1377-1437.
- [64] M. Abián, M. Cebrián, Á. Millera, R. Bilbao, M.U. Alzueta, CS₂ and COS conversion under different combustion conditions, *Combustion and Flame* 162(5) (2015) 2119-2127.
- [65] W.P. Wood, J. Hecklen, Kinetics and mechanism of the carbon disulfide-oxygen explosion, *The Journal of Physical Chemistry* 75(7) (2002) 861-866.
- [66] P. Glarborg, B. Halaburt, P. Marshall, A. Guillory, J. Troe, M. Thellefsen, K. Christensen, Oxidation of reduced sulfur species: carbon disulfide, *J Phys Chem A* 118(34) (2014) 6798-809.
- [67] P. Glarborg, P. Marshall, Oxidation of Reduced Sulfur Species: Carbonyl Sulfide, *International Journal of Chemical Kinetics* 45(7) (2013) 429-439.
- [68] C.W. Lu, Y.J. Wu, Y.P. Lee, R.S. Zhu, M.C. Lin, Experimental and theoretical investigation of rate coefficients of the reaction S(³P)+OCS in the temperature range of 298-985 K, *J Chem Phys* 125(16) (2006) 164329.

Chapter IV

Investigation of lithium intercalation process using SPECS

Article 2: *Impact of lithium bis(fluorosulfonyl)imide (LiFSI) concentration on lithium intercalation into graphite monitored with step potential electrochemical spectroscopy (SPECS)*

Manuscript 2: *Unravelling the effects of redox-active electrolytes on carbon electrodes of Li-ion capacitor*

Article 2:

**Impact of lithium bis(fluorosulfonyl)imide (LiFSI)
concentration on lithium intercalation into graphite
monitored with Step Potential ElectroChemical
Spectroscopy (SPECS)**

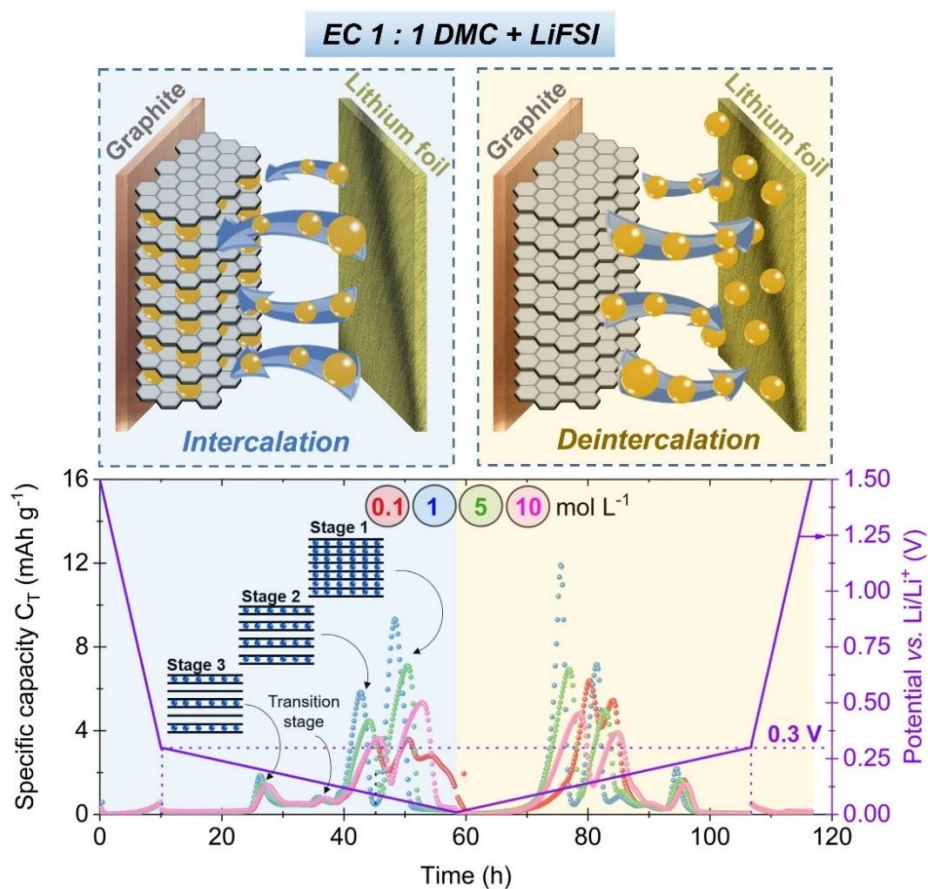
Authors: **Adam Maćkowiak**, Przemysław Galek, Paweł Jeżowski,
Krzysztof Fic

Journal: *Electrochimica Acta*, **2023**, 463, 142796

DOI: <https://doi.org/10.1016/j.electacta.2023.142796>

Licence: The content is available under CC BY 4.0

Contribution: Conceptualization, data curation, formal analysis, investigation,
methodology, visualization, writing – original draft.



Manuscript 2:

**Unravelling the effects of redox-active electrolytes on
carbon electrodes of Li-ion capacitor**

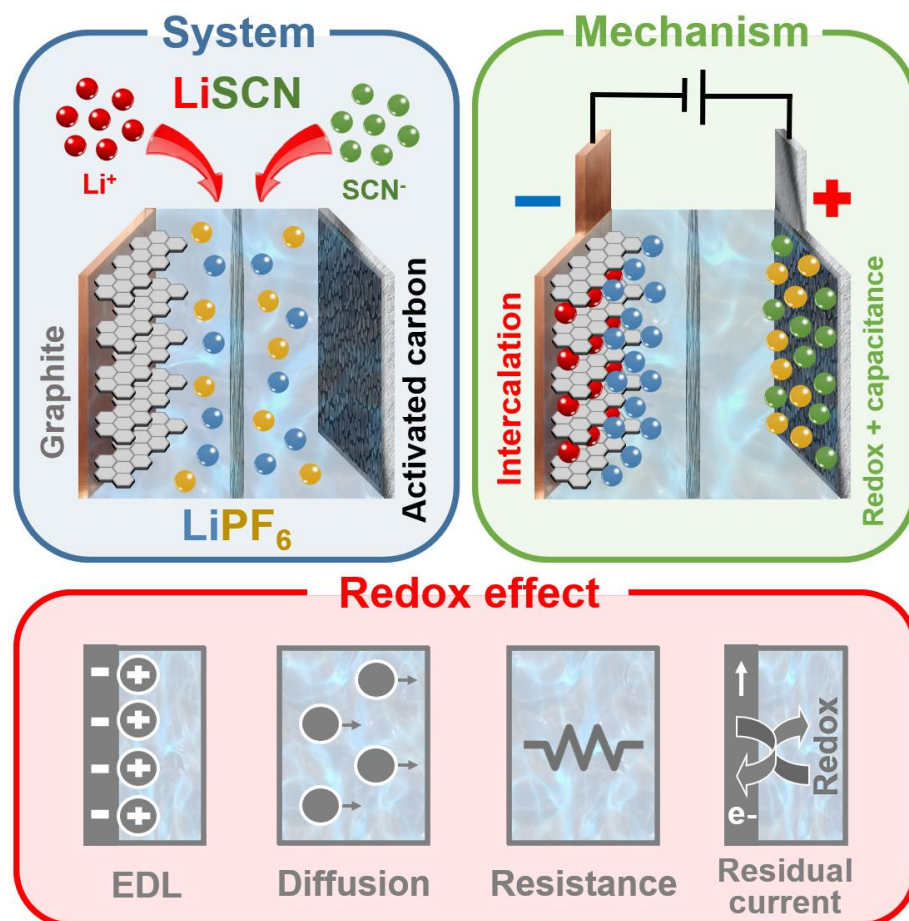
Authors: **Adam Maćkowiak**, Przemysław Galek, Paweł Jeżowski,
Krzysztof Fic

Journal: Unpublished data

DOI:

Licence: Restricted data

Contribution: Conceptualization, data curation, formal analysis, investigation,
methodology, visualization, writing – original draft.



Context of the research and summary

Due to the successful pre-insertion process in metal-ion capacitors using the one-step assembly technique with a redox electrolyte, it was decided to take a closer look at the influence of thiocyanate salts on the intercalation process itself. Several questions were raised, including:

- What technique should be used to study the influence of electroactive compounds on intercalation?
- Does the concentration of electrolyte ions affect the intercalation process?
- What impact do electroactive compounds have on the intercalation process?
- How does the additional reaction influence the ion diffusion process?
- How does the resistance of the electric double-layer change during the reaction of electroactive compounds?
- Does the addition of an electroactive compound improve the conductivity of the electrolyte?

To comprehensively study the effect of redox additives on the electrolyte, many electrochemical studies would need to be conducted, often disassembling and reassembling the system, which could disrupt the obtained data. Therefore, a search for a comprehensive solution began, which would allow obtaining plenty of data from the system with a single electrochemical test. Recently, a new technique called SPECS has emerged among electrochemical capacitors, allowing the acquisition of many data points from a single electrochemical test [262, 263]. Therefore, it was decided to investigate whether the SPECS technique could be used for comprehensive studies of metal-ion capacitors with a redox electrolyte.

However, before proceeding to study redox electrolytes, it was necessary to check whether the SPECS technique, mainly used for measurements in electrochemical capacitors, could be applied to battery systems with an intercalated graphite electrode. Therefore, **Article 2** presents SPECS studies conducted in half-cells of graphite vs. metallic lithium with four different concentrations of LiFSI salt electrolyte in an EC:DMC mixture. These studies aim

One-step assembly of metal-ion capacitors using redox-active electrolytes

to prove that the electrolyte concentration significantly affects the intercalation process and to demonstrate that the SPECS technique allows for comprehensive measurements of Faradaic systems.

Therefore, the study began by assembling half-cells of graphite vs. metallic lithium with four different electrolyte concentrations: 0.1M, 1M, 5M, and 10M. Next, three cycles of galvanostatic charging and discharging were performed to obtain a stable SEI, which at this stage of the study could interfere with the obtained SPECS results. Then, a SPECS measurements were conducted, maintaining a potential step of 10 mV and a rest time of 5 minutes from a potential of 1.5 V to 0.3 V vs. Li/Li⁺, and then the potential step was reduced to 1 mV and the rest time increased to 10 minutes in the intercalation range, i.e., from 0.3 V to 10 mV vs. Li/Li⁺. After measurement, the polarity was reversed, maintaining the same process conditions in the given ranges. The presented change in potential step and rest time is necessary to stabilize the current curve, enabling the SPECSFit program to calculate individual parameters. Thus, by performing calculations for such a range of operation, the program based on equations can determine resistance, currents, and capacity of the porous, geometric, and diffusive components, the capacity of the residual component, time constant, and diffusion parameter. It is worth noting that in this case, the residual current will probably be the most significant, as this component describes all reactions occurring in the system. By comparing the total capacity of each of the studied systems, one can observe the exact moment when a particular intercalation stage begins. A repeatable transitional state between stages 2 and 3 was even noticed for each system.

Evidently, the best concentration for conducting intercalation is the 1M solution due to high and narrow capacitive signals. For the 5M and 10M solutions, saturation with Li⁺ ions occurs, making diffusion difficult and delaying the transition through the appropriate intercalation stages. Nevertheless, the system with the 0.1M solution performs the worst, where the lack of lithium ions causes a very broad capacitive signal, suggesting problems with lithium diffusion. Next, the capacities for each component were compared, and as expected, the largest percentage was for the residual capacity (about 65%). However, the remaining

35 percent is mainly related to the EDL layer component, so it should also be considered in these systems.

In the final step, it was decided to ensure that the results obtained by SPECS are reliable. Therefore, it was decided to compare the characteristic curve of the diffusion parameter with the diffusion coefficient determined in a separate study using known GITT technique. Both the diffusion parameter and the diffusion component curves were similar, suggesting that SPECS is a reliable technique. The values of capacity and resistance obtained by the GITT technique were also very close to the results obtained using the SPECS technique. Thus, it was confirmed that the SPECS technique can be used to describe battery systems. Additionally, it was confirmed that electrolyte concentration has a significant impact on the intercalation process. Although intercalation could be achieved at any concentration, considering the overall performance of the system and the economic aspect, the 1M solution is the best option.

In **Manuscript 2**, the focus was on the addition of SCN to the electrolyte and its investigation using the SPECS technique. The goal was to understand the effect of the electrolyte additive on the performance of the positive electrode, the negative electrode, and the entire pre-intercalation process of the full hybrid cell. The study began with galvanostatic charging and discharging in half-cells. First, two half-cells, activated carbon vs. metallic lithium, with and without the SCN⁻ salt additive, were examined. As previously shown, the SCN⁻ salt increases capacity, matching the theoretical capacity of graphite. Next, two half-cells, graphite vs. metallic lithium, with and without the LiSCN salt additive, were tested. No significant differences were observed here, except for an increased irreversible capacity in the system with SCN⁻, suggesting its influence on the formation of the SEI layer. Then, a full cell, graphite vs. activated carbon, was tested, and a pre-intercalation attempt was made with and without the thiocyanate additive in the electrolyte. Complete intercalation was observed in the system with the electroactive compound additive, while without the additive, the individual intercalation stages were not observed, and the potential of the positive electrode was above the electrolyte decomposition potential.

One-step assembly of metal-ion capacitors using redox-active electrolytes

Before conducting the SPECS tests, electrochemical impedance spectroscopy was performed, showing that both the graphite half-cell and the full hybrid system with the thiocyanate anion had lower resistance values than the systems without the electroactive compound. The Nyquist plot curve exhibited a lower semicircle, indicating better charge transfer at the electrode/electrolyte interface. This difference may arise due to SCN^- ions causing the formation of a less resistive SEI layer.

Next, the SPECS studies were initiated. It is worth mentioning that all tests were conducted with a 1 mV potential step and a 10-minute rest time across the entire voltage range. Initially, tests were conducted on half-cells of activated carbon vs. metallic lithium with and without the SCN additive. A significant capacitive signal was observed at around 3.4 V vs. Li/Li⁺ for the system with SCN. Additionally, the resistance associated with the EDL layer was significantly lower for the SCN system, indicating that the reaction positively affects the positive electrode. There was also better ion diffusion in the system with thiocyanates. It should be noted that for the system without SCN, electrolyte decomposition occurs at around 4.3 V vs. Li/Li⁺, negatively leading to additional capacity and an increase in residual current.

In the next stage, graphite vs. metallic lithium half-cells with and without lithium thiocyanate were examined. Both systems presented very similar values, especially currents for the intercalation stages, which almost overlapped (with a slight difference at the third intercalation stage). However, the SCN system, similar to the galvanostatic charging and discharging tests, showed additional capacity. It can be observed that the current curve at around 0.8 V vs. Li/Li⁺ slightly bends, suggesting the influence of the SCN anion on SEI layer formation. But will such a relationship also be observed in a full system where actual oxidation occurs at the positive electrode? To answer this question, SPECS tests were conducted on two full-cells, graphite vs. activated carbon, with and without lithium thiocyanate. The system without lithium thiocyanate was not intercalated at all, and the obtained capacity mainly came from the electrolyte decomposition reaction. In contrast, the current curve of the hybrid with SCN^- anions clearly showed each intercalation stage. Moreover, an increase in capacity was

One-step assembly of metal-ion capacitors using redox-active electrolytes

observed in the system due to the reaction between 1 V and 0.7 V vs. Li/Li⁺, suggesting the influence of SCN on SEI layer formation. In this case, the capacity associated with EDL formation was only 10% of the total, with the rest related to system intercalation.

Next, a comparison was made between the graphite vs. metallic lithium half-cell and the hybrid electrode. Both systems contained SCN⁻ anions in the electrolyte. No significant differences were observed in terms of intercalation currents, EDL resistance, or time constants. However, the difference lay in the SEI layer formation. The hybrid with SCN showed greater capacity, suggesting that the reaction occurring at the positive electrode affects SEI layer formation and thus the performance of the entire cell. Additionally, an increase in the diffusion parameter was observed, suggesting that the SCN anion reaction at the positive electrode releases lithium ions, aiding intercalation. Therefore, it was concluded that redox electrolytes, by improving lithium ion diffusion, not only enable graphite electrode intercalation but also enhance intercalation compared to the traditional method with metallic lithium. Furthermore, it is important to study redox electrolyte systems in full cells, as the reaction at one electrode can influence the performance of the other electrode.

Finally, the obtained SPECS results were compared with those obtained using the GITT technique to confirm the assumed conclusions. The GITT study curves confirmed the validity of the SPECS results, as the diffusion curves overlapped in the intercalation region.

The obtained results confirm the effectiveness of using SPECS in systems with a battery negative electrode, as well as in full hybrid systems. It was confirmed that the presence of the SCN anion not only affects the SEI layer formation process but also improves the intercalation process by facilitating lithium ion distribution and reducing system resistance. It is also important to remember that the reaction at the positive electrode influences the performance of the negative electrode, hence the importance of studying complete cells. Despite the dominance of capacity related to the intercalation process, approximately 10% is also related to EDL layer formation, which is often overlooked by researchers.

Article 2

One-step assembly of metal-ion capacitors using redox-active electrolytes



Contents lists available at ScienceDirect

Electrochimica Acta

journal homepage: www.journals.elsevier.com/electrochimica-acta



Impact of lithium bis(fluorosulfonyl)imide (LiFSI) concentration on lithium intercalation into graphite monitored with Step Potential ElectroChemical Spectroscopy (SPECS)

Adam Maćkowiak, Przemysław Galek, Paweł Jeżowski, Krzysztof Fic*

Poznan University of Technology, Institute of Chemistry and Technical Electrochemistry, Berdychowo 4, 60-965, Poland

ARTICLE INFO

Keywords:

Lithium bis(fluorosulfonyl)imide
Lithium-graphite intercalation
Step potential electrochemical spectroscopy
Galvanostatic intermittent titration technique
Ions diffusion

ABSTRACT

Step Potential Electrochemical Spectroscopy (SPECS) analysis of lithium intercalation into graphite was performed. Four different solutions of lithium bis(fluorosulfonyl)imide (LiFSI) salt in EC:DMC solvent (1:1, v:v) with various concentrations (0.1, 1, 5 and 10 mol L⁻¹) were selected as electrolytes. SPECS allowed for calculating the capacity resulting from lithium intercalation between the graphite layers and the capacity that comes from the adsorption of ions on the outer electrode surface, resistance, as well as the diffusion coefficient. Additionally, to compare the results obtained, the galvanostatic intermittent titration technique (GITT) was performed under the same conditions. However, it turned out that initially, similar diffusion parameters are not identical in their meaning. Hence, SPECS can offer fresh insights into the lithium intercalation process in highly concentrated electrolytic solutions, enhancing existing approaches.

1. Introduction

Energy storage systems are a necessary part of a smart grid, where renewable energy sources like solar, wind, tidal, and geothermal converters play a significant role [1–4]. Furthermore, the recent automotive revolution shows how important it is to better understand energy storage mechanisms and their limitations [5,6]. Nowadays, two energy storage technologies – Li-ion batteries (LIBs) and electrochemical capacitors (ECs) – play a major role in the market [7]. On the one hand, ECs demonstrate high power density with almost infinite cycle life; on the other hand, batteries supply energy for a long time but demonstrate limited power density and cyclability, mostly because of the sluggish charge transfer kinetics [8,9].

Graphite has been the standard anode material for LIBs since the 1990s. It is recognized as the preferable anode material for LIBs based on intercalation chemistry. This process makes the graphite material benefit from low cost, electrochemical stability and electrochemical conductivity [10,11]. The mechanism of lithium intercalation between graphene layers of graphite was already presented years ago [12–14]. There are several models for describing the intercalation process; the most popular shows that, during the first charge, the potential of the graphite electrode drops sharply to the value of approx. 0.8 V, where

partial decomposition of the electrolyte occurs and is followed by the formation of the solid electrolyte interphase (SEI) layer [15]. The next drop in potential shows the characteristic three plateaus (stages). Each of them at different potentials corresponds to a different degree of filling intergraphene spaces by lithium ions. The third stage is LiC₁₈, and the second stage is LiC₁₂. When the 1st stage intercalation compound is totally formed, all interlayer spaces are occupied by lithium, which gives a composition of LiC₆, corresponding to a theoretical capacity of 372 mAh g⁻¹ [16–18]. But still, the intercalation process is not fully explored. To better understand the mechanism of energy storage and electrochemical performance, it is mandatory to use various electrochemical characterisation methods [19–22]. These techniques provide valuable information about capacity, resistance, efficiency, cyclability, and power and energy output [23,24]. Galvanostatic Intermittent Titration Technique (GITT) [25] and Potentiostatic Intermittent Titration Technique (PITT) [26], are widely used to investigate the lithium intercalation/deintercalation processes and allow detailed parameters such as exchange current densities or lithium ions diffusion coefficient to be determined [27,28]. Furthermore, GITT appears as the most widely applied and considered the most reliable method [28,29].

In our study, we take a closer look at the Step Potential Electrochemical Spectroscopy (SPECS) technique, first presented for

* Corresponding author.

E-mail address: krzysztof.fic@put.poznan.pl (K. Fic).

<https://doi.org/10.1016/j.electacta.2023.142796>

Received 1 February 2023; Received in revised form 23 May 2023; Accepted 28 June 2023

Available online 29 June 2023

0013-4686/© 2023 The Authors. Published by Elsevier Ltd. This is an open access article under the CC BY license (<http://creativecommons.org/licenses/by/4.0/>).

One-step assembly of metal-ion capacitors using redox-active electrolytes

electrochemical capacitors (ECs) by Donne et al. [30]. So far, this technique was used for the evaluation of ECs with carbon and metal oxide electrodes [31,32]. The presented study offers insight into the application of the SPECS method for lithium intercalation with a comparison of currently used techniques. Furthermore, this work tends to clarify the discussion of the impact of the salt concentration (here LiFSI) on the intercalation process. Although lithium hexafluorophosphate (LiPF_6) is the most commonly used salt for LiBs electrolytes [33] it may not be able to meet the requirements for future high-energy lithium batteries. Therefore, new lithium salts are constantly being developed. Compared to LiPF_6 , LiFSI-based electrolyte is characterised by more thermal stability and especially water insensitivity which influences the ageing performance of the cells [34,35]. A selection of diluted (0.1 mol L^{-1}), optimal (1 mol L^{-1}), concentrated (5 mol L^{-1}) and supersaturated (10 mol L^{-1}) concentrations was to see the differences between solutions and to confirm the relationship between diffusion and salt concentration.

The SPECS technique sheds some light on the graphite intercalation and electrolyte requirements. Moreover, it gives the necessary information for the construction of hybrid Li-ion capacitors, where the pre-intercalation might be realized directly from the electrolyte [36].

2. Experimental

2.1. Electrolyte

Dimethyl carbonate (DMC; 99% anhydrous; <20 ppm; Sigma Aldrich®) and ethylene carbonate (EC; 99% anhydrous; <60 ppm; Sigma Aldrich®) were mixed in a volumetric ratio of 1:1 under an inert atmosphere. Lithium bis(fluorosulfonyl)imide (LiFSI; 99.9%; Solvionic®) was added to the solvent to prepare four different solutions: 0.1, 1, 5 and 10 mol L^{-1} LiFSI in EC:DMC, with the conductivity as follows: 2.9, 13.9, 3.2 and 1.3 mS cm^{-1} . Conductivity measurements were made at room temperature (21°C) in a 2-electrode Swagelok® system with a spacer, using potentiostatic electrochemical impedance spectroscopy (PEIS). To understand the solvation of the LiFSI the molality of the solutions was also calculated respectively: 0.08 mol kg^{-1} (0.1 mol L^{-1}), 0.90 mol kg^{-1} (1 mol L^{-1}), 7.67 mol kg^{-1} (5 mol L^{-1}), $50.13 \text{ mol kg}^{-1}$ (10 mol L^{-1}).

2.2. Electrochemical cell

All electrochemical measurements were made in ECC-REF cells (EL-CELL®). The working electrode (WE) was a composite made of graphite (flake shaped; bulk density 0.07 g cm^{-3} ; particle size $5 \mu\text{m}$ at a density of 1.90 g cm^{-3} ; specific surface area $17 \text{ m}^2 \text{ g}^{-1}$; SFG-6; Imerys®) (91%), polyvinylidene fluoride (PVdF 6020; Solvay®) (8%) and carbon black (Timical Super C65) (1%) covered on copper foil (thickness $10 \mu\text{m}$; MTI®). The electrode thickness was $\sim 57 \mu\text{m}$. Round-shaped electrodes (diameter 16 mm ; surface area $\sim 2 \text{ cm}^2$) were cut using EL-Cut (EL-CELL®). Counter (CE) and reference (RE) electrodes were made of metallic lithium discs (diameter 16 mm). Both electrodes were separated by two glass fiber GF/D separators (diameter 18 mm ; thickness 0.67 mm ; Whatman®). All cells were prepared in a glovebox (MBraun®) with controlled atmosphere (water and oxygen content <0.1 ppm). The prepared electrolyte solutions were injected into the systems with a volume of $500 \mu\text{L}$. Gas chromatography with mass spectrometry (GCMS) analysis was conducted using EVOQ GC-TQ™ MS, Bruker. The apparatus was connected to PAT-Cell-Gas made by EL-CELL®. The electrochemical cell was inserted into the thermostatic chamber (25°C). The temperature of the injector was 220°C , the column was 180°C and the mass spectrometer was 220°C .

2.3. Electrochemical investigation

Electrochemical measurements were performed on a multichannel

galvanostat/potentiostat (VMP-3 Biologic®) controlled by EC-Lab® software at room temperature (21°C). To initially intercalate and work out the cells, 3 cycles of charging and discharging using galvanostatic charge potential limitation (GCPL) at C/20 (C – current density 372 mA g^{-1}) were performed until $10 \text{ mV vs. Li/Li}^+$ for intercalation, and $1.5 \text{ V vs. Li/Li}^+$ for deintercalation (Fig. S1). After that, the SPECS measurement was performed with the application of a series of potentiostatic hold periods (controlled by chronoamperometry; CA): every 10 mV to $0.3 \text{ V vs. Li/Li}^+$ for 5 minutes and every 1 mV to $0.01 \text{ V vs. Li/Li}^+$ for 10 minutes. This setting allows observing all changes occurring in the system with particular emphasis on the potential below 0.3 V , where individual intercalation/deintercalation steps take place. In addition, each of the electrochemical systems was subjected to a GITT examination to determine the diffusion coefficient. Cells were tested with the C/20 current using the GCPL technique, which consisted of a series of charging and discharging steps by delivering the current for an hour and then holding it for 1 h, to reach the capacity of 300 mAh g^{-1} . Such a limitation allowed for the desired accuracy and reproducibility of the results.

2.4. SPECS calculations description

In principle, during SPECS, the cell undergoes a sequence of equal changes in potential (steps) separated by the rest time, which must be long enough to reach the equilibrium state. The small step change allows maximum storage capabilities to be reached and provides information on different aspects of energy storage mechanisms. Total current (I_T) registered at a given potential step can be divided on currents related to electric double-layer (EDL) formation (I_{EDL}), diffusion limited processes (I_D) and residual processes (I_R) (Eq. 1) [37,38].

$$I_T = I_{EDL} + I_D + I_R \quad (1)$$

Furthermore, I_{EDL} can be divided into currents related to EDL formation in the electrode porosity (pore-related current, I_p) and at the outer electrode surface (so-called geometric current, I_G) (Eq. 2).

$$I_T = I_p + I_G + I_D + I_R \quad (2)$$

For porous materials like activated carbons (ACs), the electrode bulk consists of a porous structure; in graphite, it should rather be considered as the space accessible for ions between graphene layers. The outer electrode surface is considered a surface area easily accessible to the electrolyte, but in graphite materials, these are the edges of graphene layers.

Taking into account the rest time (t) and the potential step (ΔE), it is possible to calculate components like resistance (R_p) and differential capacitance (C_p) of intergraphite layers, resistance (R_G) and differential capacitance (C_G) of graphene edges and so-called diffusion parameter (B). I_R is the current related to additional, residual processes in the system. Having said that, the final form is as follows (Eq. 3):

$$I_T = \frac{\Delta E}{R_p} \exp\left(-\frac{t}{R_p + C_p}\right) + \frac{\Delta E}{R_G} \exp\left(-\frac{t}{R_G + C_G}\right) + \frac{B}{t^{0.5}} + I_R \quad (3)$$

All of these components provide detailed information about system operation. Therefore, SPECS is a fast and effective tool for identifying the stability of electrode materials, the ionic mobility in the electrolyte, the equivalent series resistance (ESR) of the electrode materials, and even the engineering of the cell [39,40].

2.5. Determination of diffusion coefficient using GITT

GITT is a method of applying current pulses to the system and measuring the potential response, made to estimate detailed values, such as the diffusion coefficient. An example of the response of the potential change to a given current pulse is shown in Fig. 1. It consists of the transition from the initial potential (E_0) through the voltage jump (IR

One-step assembly of metal-ion capacitors using redox-active electrolytes

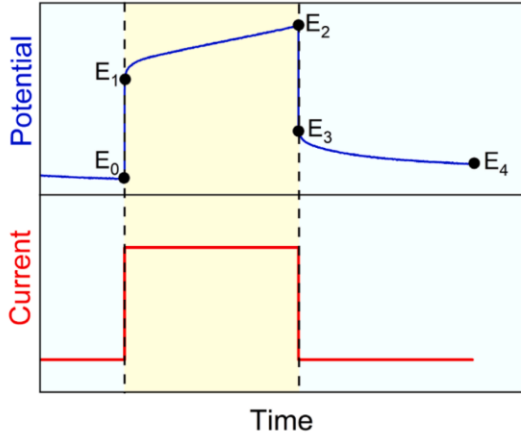


Fig. 1. Schematic representation of single galvanostatic intermittent titration technique (GITT) pulse and half-cell potential response.

drop, $E_1 - E_0$) to the increase phase ($E_2 - E_1$), then through the next IR drop ($E_3 - E_2$) to the final resting potential phase (E_4).

In 1977, Weppner and Huggins proposed a formula for estimating the diffusion coefficient by measuring the potential using the GITT measurement (Eq. 4) [41].

$$\tilde{D} = \frac{4}{\tau\pi} \left(\frac{m_B V_m}{M_B S} \right)^2 \left(\frac{\Delta E_S}{\Delta E_i} \right)^2 \text{ for } \left(\tau \ll \frac{L^2}{D} \right) \quad (4)$$

Where: \tilde{D} is the diffusion coefficient [$\text{m}^2 \text{s}^{-1}$], τ is the interval time from charging to discharging (without relaxation phase) [s], m_B is a mass of component B in the sample [g], M_B is the atomic weight of component B [g mol^{-1}], V_m is the molar volume of the sample [$\text{m}^3 \text{mol}^{-1}$], S is the area of sample-electrolyte interface [m^2], ΔE_S is the difference between the initial potential and the end potential (after relaxation time) [V], ΔE_i is the total change of the voltage cell neglecting voltage drop [V] and L is the sample thickness [m].

A series of calculations have been done over the past 45 years to simplify the obtained equation [27,29]. There are various modifications of this formula; however, to examine the diffusion coefficient for lithium ions at the graphite electrode, it was decided to use the following formula (Eq. 5) [27].

$$\tilde{D} = \frac{4}{9\pi} \left(\frac{E_4 - E_0}{E_2 - E_1} \right)^2 \frac{r_p^2}{t_p} \text{ for } \left(\tau \ll \frac{L^2}{D} \right) \quad (5)$$

According to this equation, by using the potential response values, t_p value (pulse duration) and r_p value (particle radius of the graphite electrode, $4 \mu\text{m}$) it is possible to determine the lithium diffusion coefficient.

3. Results and discussion

Four electrochemical cells with different molar solutions of LiFSI salt in the electrolyte were tested using the SPECS technique. A total capacity (C_T), at a given potential, was calculated based on the surface area under the registered current curve. To express C_T in mAh g^{-1} the charge [A s] was divided by 3600 s and also by active electrode mass [g]. In the SPECS procedure, two regimes of potential steps and time intervals were applied. In the $1.5 - 0.3 \text{ V vs. Li/Li}^+$ potential range, the accelerated SPECS procedure was used ($\Delta E = 10 \text{ mV}$; $t = 5 \text{ min.}$). Such experimental conditions were selected based on preliminary studies, where no significant current changes (in particular resulting from Li^+ intercalation) in the aforementioned potential range occurred. The

acceleration procedure allowed us to reduce the duration of the experiment. However, the applied shift was too fast in the further potential range to register current changes connected with Li^+ intercalation.

A slight increase in the registered current or C_T in 10 h (Fig. 2) indicates that the potential shift is too fast. Only the change of the time interval for 10 minutes and the potential step for 1 mV allowed for the complete occurrence of individual intercalation stages (from 10 h). Such SPECS conditions covered the $0.3 - 0.01 \text{ V vs. Li/Li}^+$ range. According to the data presented in Fig. 2, the third and second intercalation steps (regardless of electrolyte concentration) start at similar potentials (stage 3 at $0.21 \text{ V vs. Li/Li}^+$, stage 2 at $0.13 \text{ V vs. Li/Li}^+$). Peak height differences (C_T value) are associated with an optimal LiFSI concentration. For all intercalation stages, the highest C_T was obtained for 1 mol L^{-1} , then 5 mol L^{-1} , 10 mol L^{-1} and the lowest peak height was for 0.1 mol L^{-1} electrolyte. This trend is related to the intercalation stage. The system with the salt concentration of 1 mol L^{-1} is characterized by the highest conductivity (the highest mobility of ions) and the lowest resistance (R) (details of this issue are discussed later). Another difference is the potential value for which falls the C_T peak. It can be seen that with each intercalation step for 1 mol L^{-1} , the C_T peak is reached the fastest. This is due to the fast, unaffected Li^+ intercalation. A higher LiFSI concentration results in hindered wettability of the electrode (due to the high viscosity of the electrolyte [42,43]), delayed and incomplete intercalation. The efficiency of this phenomenon decreases with successive stages for electrolyte concentrations of 0.1 , 5 and 10 mol L^{-1} . This is postulated based on ever greater potential shifts for which there is a maximum of the C_T peak, concerning the potential for the 1 mol L^{-1} system peak. The peak separation for the first intercalation stage of 0.1 mol L^{-1} also seems interesting (not observable for other concentrations). The first signal is from the transition to the 1^{st} stage using lithium ions available in the solution. Because the solution is diluted, there is no sufficient amount of Li^+ ions to fill all the empty spaces between graphite layers. So process is then delayed because lithium ions have to move from the metallic electrode to the graphite surface. This transport is driven by diffusion, which increase is observed in Fig. 3e. Additionally, obtained results showed how sensitive the SPECS technique could be. The emerging signal could also indicate the decomposition of the electrolyte. However, this assumption was verified by conducting the operando gas chromatography with mass spectrometry (GCMS), which shows that no carbonate decomposition gases are formed during electrochemical work (Fig. S2). Reverse polarisation leads to the same conclusions but is linked with Li^+ deintercalation.

Before discussing processed SPECS data, it should be mentioned that the error of the fitted curves is very small and the fitting reflected a good correlation coefficient (>0.9985 , see Fig. S3). Intercalation of Li^+ , previously accumulated on the graphene edges (the outer electrode surface, called geometric), between the graphene layers results in R_p decrease (Fig. 3a). This observation applies to all intercalation stages. The introduction of Li^+ into the intergraphene layers leads to an increase in its conductivity and thus R_p decrease. The 1 mol L^{-1} system is characterized by the lowest resistance and the 0.1 mol L^{-1} by the highest. At the same time, a rapid increase in R_G was observed (Fig. 3b). This results from a partial decrease in the geometric surface conductivity, and it is related to partial Li^+ adsorption (during intercalation) from this surface to the intergraphene surface. An electrochemical spectroscopic impedance (EIS) study was also performed for two systems with an electrolyte concentration of 0.1 mol L^{-1} and 1 mol L^{-1} (Fig. S4). A characteristic feature of these cells is the changing resistance of the system during different stages of intercalation. The obtained results are comparable with the results obtained with the SPECS technique. The resistance associated with the electrode decreases to a small extent during individual stages of intercalation (Fig. 3a) and the internal resistance increases (Fig. 3b). Especially for 0.1 mol L^{-1} solution, the internal resistance increase is mainly related to the resistance of the electrolyte. This is caused by the dropping in the electrolyte conductivity because lithium ions enter between the graphite structures. For a 1 mol L^{-1}

One-step assembly of metal-ion capacitors using redox-active electrolytes

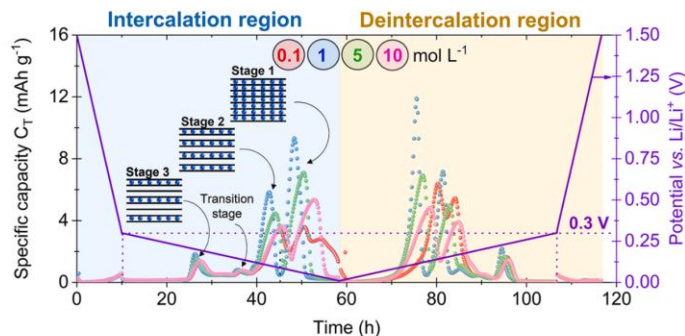


Fig. 2. Total specific capacity for lithium-graphite based systems with 0.1, 1, 5 and 10 mol L⁻¹ LiFSI in EC:DMC (1:1; v:v).

solution, the decrease in conductivity is not significant, which does not cause a relevant increase in resistance. In addition, diffusive layer resistance for both systems increases during occurring the intercalation stages, especially the 1st one which also found its reflection in SPECS (Fig. 3e). The simultaneous intercalation leads to C_p increase (Fig. 3c) and C_G decrease (Fig. 3d). The higher normalized diffusion parameter D (Fig. 3e) proves efficient Li⁺ transport and effective intercalation. Again, the highest D value corresponds to a 1 mol L⁻¹ system. The trend of residual component R (Fig. 3f) is almost identical to the trend of C_T presented earlier in Fig. 2. This proves that it has a significant influence on the total current response. This component plays a secondary role in capacitor systems and corresponds to the side reactions, e.g., pseudo-capacitive, redox or electrolyte decomposition processes. The dominant capacitance contribution comes from the current response associated with the formation of EDL. The intercalation time (time constants τ) on the considered surfaces are presented in Fig. 3g and 3h. The time of Li⁺ intercalation between the graphene layers (τ_p) increases for the subsequent intercalation stages. This is a logical observation, as it becomes more and more difficult and takes time to fill the successive layers. The time constant τ_G is comparable for the entire potential range (0.3 – 0.01 V vs. Li/Li⁺), in which adsorption at the graphene edges takes place. The slight fluctuations in τ_G appears, in the regions where the intercalation process occurs. This is due to the diffusion of previously adsorbed Li⁺ ions from the edges into the graphene layers.

By integrating the area under the individual C_T curves in the potential range of 1.5 → 0.01 V, the total C_T values for the tested systems were obtained (Fig. 4a). The differences between the C_T are small, which means all systems were properly intercalated. However, the lowest value (361 mAh g⁻¹) for the 0.1 mol L⁻¹ system makes believe that the ions concentration might be insufficient and the small loss of the capacity is regarding probably due to the uneven distribution of ions. On the other hand, the C_T values for the rest concentrations are slightly higher than the theoretical capacity of graphite (372 mAh g⁻¹).

Much greater differences were observed for C_p . In this case, for the lowest concentration, C_p is almost two times smaller compared to the 1 mol L⁻¹ solution with the highest value (128 mAh g⁻¹). The interlayer surface is much more developed than the surface of the graphite edges, therefore the C_p contribution reaches as much as 34% (for 1 mol L⁻¹) (Fig. 4b). Interestingly, the share of porous capacity in total registered capacity is so high, taking into account the small surface area of graphite; including the surface of intergraphite layers. The high C_p registered is caused by the presence of intergraphene defects [44], that favour an increase in EDL capacity [45,46]. Although it is expected from the state of the art system, that faradaic capacity will be dominant (and it is), the porous capacity has a significant contribution to the total capacity of the system. The C_G contribution is negligible for all concentrations and does not exceed 2.7% (for 10 mol L⁻¹). The C_G increases with increasing concentration from 2.7 to 10.2 mAh g⁻¹. C_D has the

lowest contribution and does not exceed 0.2% (for 1 mol L⁻¹). The values of this component depend on the resistance of the electrolyte. For 0.1 mol L⁻¹, the resistances result from the insufficient number of charge carriers, while for 5 and 10 mol L⁻¹ the resistances are due to spatial hindrances related to the abundance of ions. The dominant contribution (> 64% for 1 mol L⁻¹) of C_R is evident for battery systems. The highest value (287 mAh g⁻¹) and contribution (~80%) of this component for the 0.1 mol L⁻¹ system result from subjecting all or almost all species capable of redox transformations to their effective occurrence. In this case, the remaining small number of species (not participating in redox reactions) do not inhibit these changes. In turn, the 1 mol L⁻¹ concentration is optimal for effective intercalation (33% of C_T) between graphene layers, suppressing the redox reactions taking place (64% of C_T). The share of the individual C_T components (C_p , C_G , C_D , C_R) is presented for 1 mol L⁻¹ LiFSI in Fig. S5 in the graphical representation of specific capacity vs. time of measurement.

To compare the results of the diffusion coefficient with those of the SPECS technique, the GITT test was performed. The SPECS measurement is based on the analysis of the currents generated during the applied potential to the system, while the GITT measurement is based on the analysis of the potential differences to the applied current. Therefore, one should expect differences in the interpretation of the results. Moreover, both techniques' results are expressed in different units; in the SPECS technique, the diffusion coefficient is expressed in A s^{0.5}, and the GITT technique it is m² s⁻¹.

Since the single diffusion coefficient value can be calculated for the entire duration of the pulse, it was assumed to be the value of the current jump capacity. Therefore, there may be slight differences in the peak shifts compared to those of the SPECS technique. The GITT test was performed up to a capacity of 300 mAh g⁻¹ for each system for computational reasons (Fig. 5). Complete intercalation could be a problem in confronting the values and could result in unnecessary additional errors. Unfortunately, in this way, an important element of the system was omitted, i.e. the transition to the first intercalation stage. Such a study was also performed and presented in (Fig. S6).

When calculating the diffusion coefficient in the GITT technique, the formula was divided into three parts, component A ($\frac{d}{9\pi}$), component B ($\frac{E_A - E_0}{E_D - E_1}$) and component C ($\frac{d}{V}$). It can be noticed that component A and component C will be constant for each of the tested systems, only the values in component B will change and will determine the final shape of the curve. Component C, which contains the particle size of the electrode material (4 μm), raised to the power and further divided by the pulse time, makes the obtained values very low (~10⁻¹⁶). However, low values prove the high sensitivity of the system to the diffusion coefficient. It is worth adding that the formula does not change when the polarity of the system is modified; this is due to the mathematical equation itself, which means that only absolute values have been used in

One-step assembly of metal-ion capacitors using redox-active electrolytes

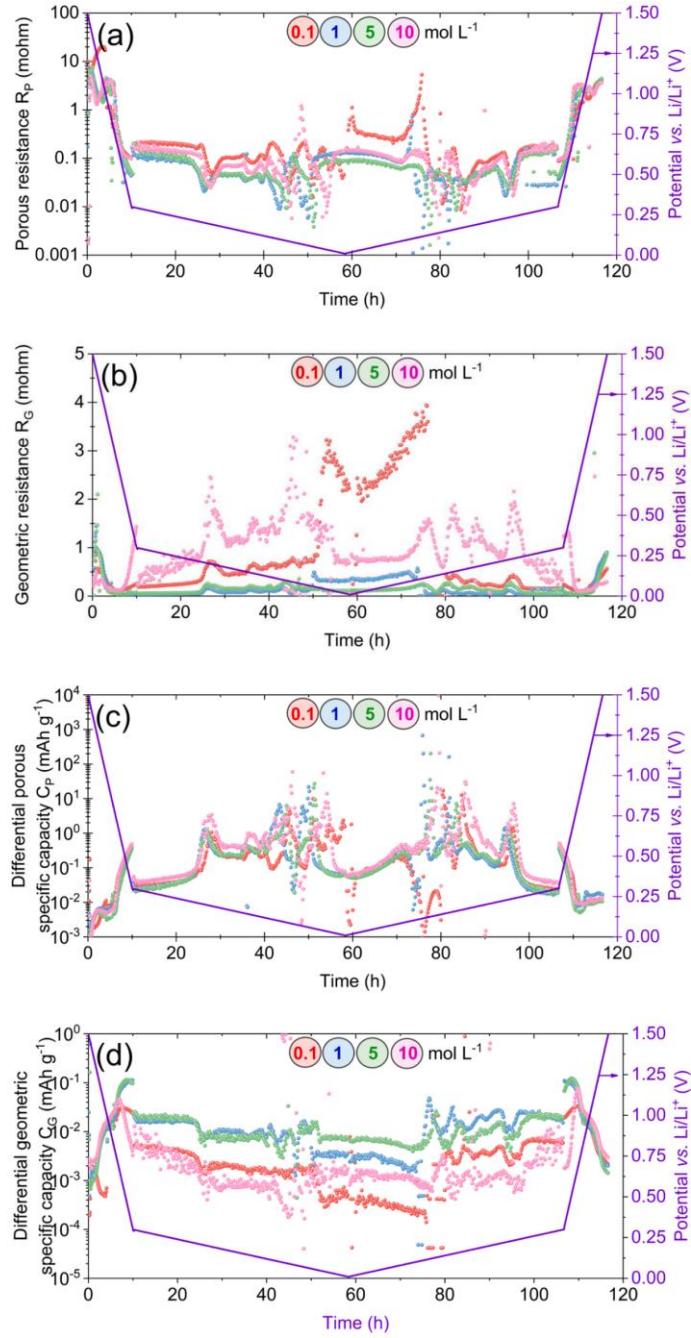


Fig. 3. SPECS results for lithium-graphite based systems with 0.1, 1, 5 and 10 mol L⁻¹ LiFSI in EC:DMC (1:1; v:v): (a, b) porous R_p and geometric R_G resistance, (c, d) differential porous C_p and geometric C_G specific capacity, (e) normalised diffusion parameter D , (f) residual current I_R and (g, h) porous τ_p and geometric τ_G time constant.

One-step assembly of metal-ion capacitors using redox-active electrolytes

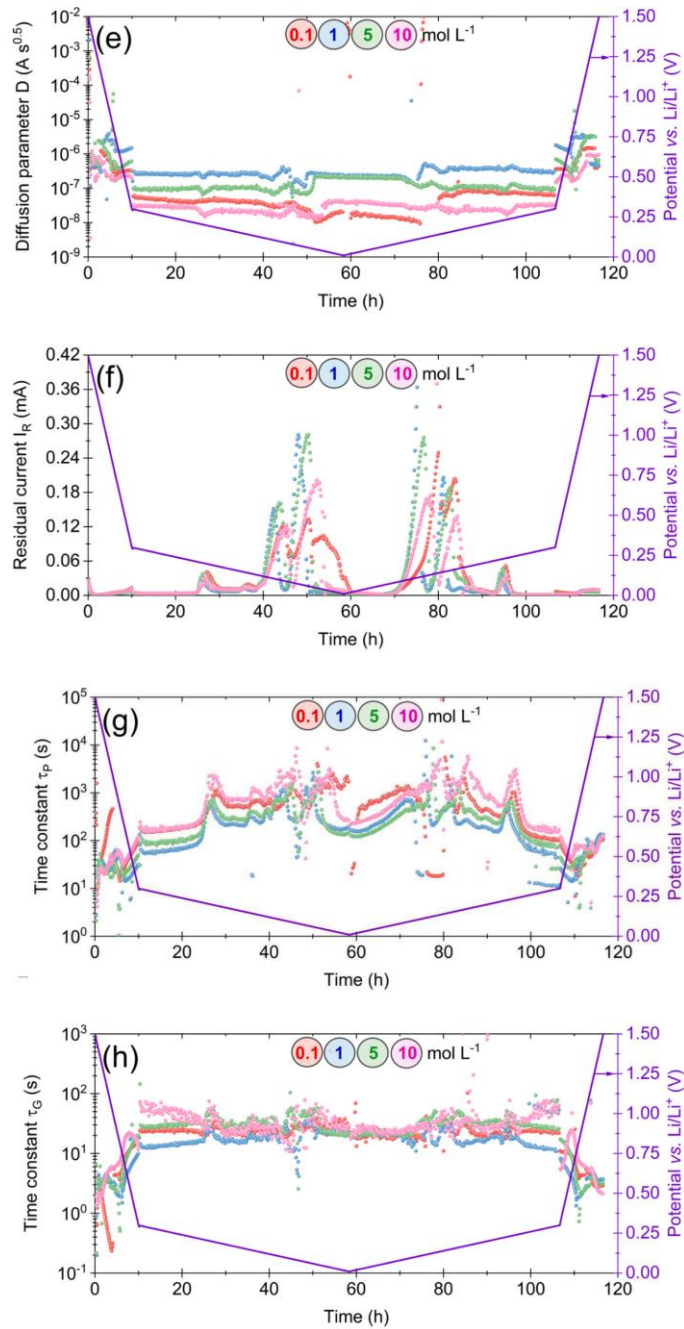


Fig. 3. (continued).

the calculations. The value of the diffusion coefficient for the lowest capacity might be slightly different because the measurement starts at the 1.5 V voltage point, which is artificially forced by the previously imposed polarisation. However, this point reflects how dynamic the

diffusion of the system is at the very beginning. When a negative polarity is applied to the system, all positive ions, mainly lithium, are first attracted to the electrode. The diffusive nature of the system indicates more capacitive features, which can be seen in the current values

One-step assembly of metal-ion capacitors using redox-active electrolytes

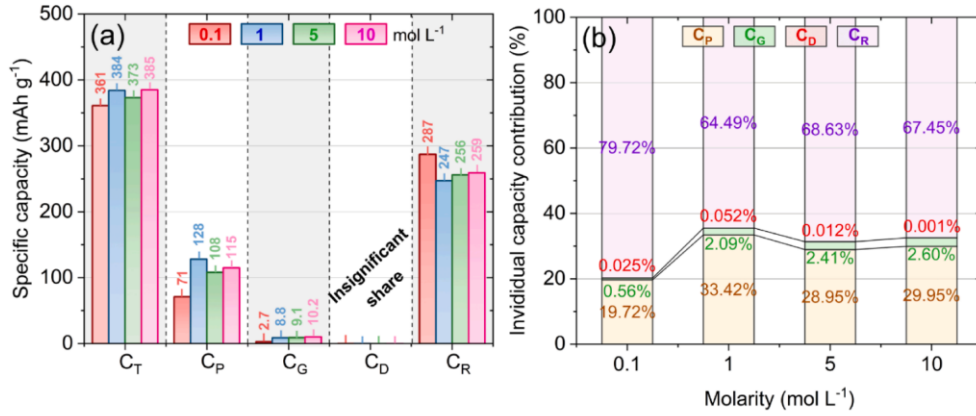


Fig. 4. (a) Specific capacity of individual SPECS components and their (b) contribution to total capacitance for lithium-graphite-based systems with 0.1, 1, 5 and 10 mol L⁻¹ LiFSI in EC:DMC (1:1; v:v).

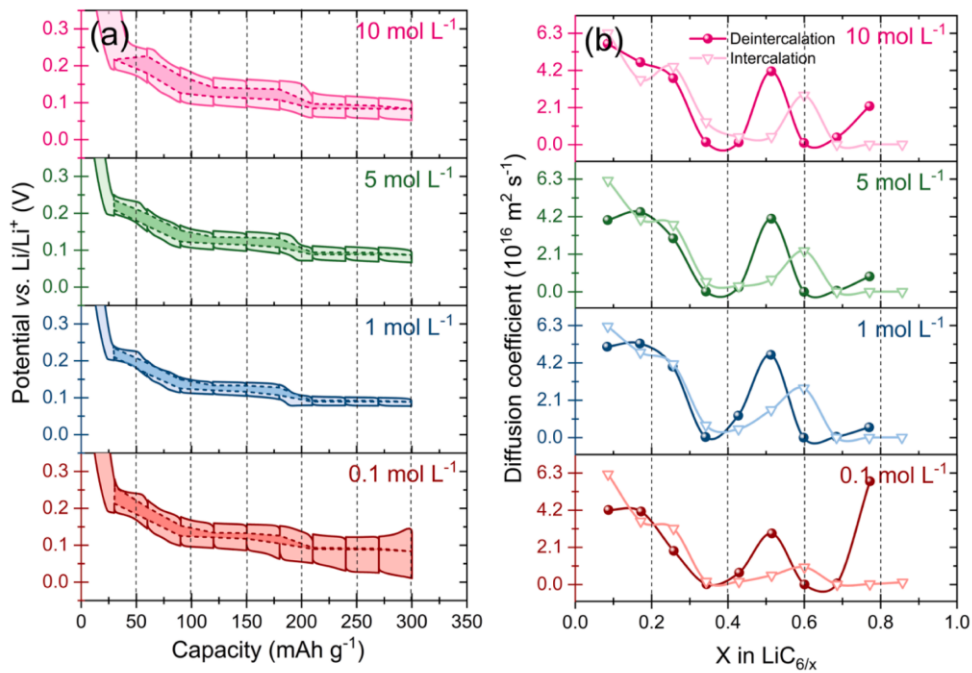


Fig. 5. Results of (a) GITT and (b) diffusion coefficient on lithium-graphite based systems capacity with 0.1, 1, 5 and 10 mol L⁻¹ LiFSI in EC:DMC (1:1; v:v) as electrolyte.

previously described at SPECS (Fig. 3c and 3d). In the case of SPECS and GITT, the diffusion coefficient at low values of the capacity of the system is the highest. The further course of the diffusion curve depends on the occurrence of individual stages of lithium intercalation into the graphite structure. As the potential decreases/increases, the diffusion coefficient changes. It is logical because based on the potential change, the diffusion coefficient is calculated in the GITT method. The data (Fig. 5b) clearly shows the transition between the 2nd and 3rd stages of intercalation. However, in the case of SPECS, there is no significant change between the stages. A slight increase preceded by a decrease in diffusion was

observed during the transition. This information provides a new outlook on the understanding of diffusion occurring in this system. This character of the curve can be explained as first the accumulation of charge on the surface and then 'waiting' for the voltage to exceed, enabling further intercalation and a temporary increase in the diffusion coefficient. In the case of GITT curves, no decrease in diffusion was observed before its increase. So, the transition between successive stages of intercalation is associated with a change in energy in the system, which makes it impossible to notice when observing the potential, while the observation of currents allows seeing such changes.

One-step assembly of metal-ion capacitors using redox-active electrolytes

When describing the values obtained from GITT, special attention should be paid to the area between the charge and discharge curves shown in Fig. 5a. They represent resistance in a system composed of several factors, including diffusion and conductivity. It can be seen that the 1 mol L⁻¹ system shows the smallest area between the intercalation and deintercalation curves. This means that the resistance values in this cell are the lowest, i.e. the diffusion and conductivity coefficients are at the optimum of the system operation. This is confirmation of the relation between different concentrations concluded from the diffusion coefficient in Fig. 5b and conductivity in Fig. S7. Another important parameter is the value of the potential difference between the charge/discharge and the resting of the system. It should be noted that the higher the potential change, the worse the charge is maintained by the electrode, which may result in the poor cyclic operation of the system. The potential difference also changes with the charge level of the working electrode. A particularly significant difference can be seen between the 0.1 and 1 mol L⁻¹ systems. An electrode that does not hold the charge well will certainly have remarkable self-discharge, which is, of course, not a good feature for the battery system.

Evaluating both the SPECS and GITT results, one should notice the shift in time/capacity of the peaks from the transition between stages depending on whether there is intercalation or deintercalation of the system. This dependence can be observed both in the SPECS current curves and in the galvanostatic curves, and the SPECS and GITT diffusion coefficients only confirm this relationship. Also, an important difference between diffusion for SPECS and GITT is the moment of polarization change. In the case of GITT, this moment causes a significant increase in the diffusion coefficient (Fig. 5b), which can be seen for each system. However, with the SPECS technique, the change in polarity makes a minor difference in diffusion. This might suggest that such a highly charged graphite electrode holds its charge until the next stage is passed.

4. Conclusions

A comparison of the systems operation with different salt concentrations shows how important it is to choose the right number of conducting ions in the system to obtain reproducible electrochemical results. Their deficiency causes difficulties in the intercalation process, a decrease in the capacity of the system and an increase in system resistance. In turn, the excess causes an increase in the resistance associated with the diffusion of ions and a decrease in conductivity, which also affects the overall performance of the system. Despite differences in nature, both SPECS and GITT analyses confirmed that there is an optimal concentration of salt to perform the intercalation process efficiently. Moreover, many factors are affected by salt concentration. In this context, for the given experimental conditions, the electrolyte with 1 mol L⁻¹ LiFSI seems to be the right (optimal) choice.

Author contributions

Adam Maćkowiak – Conceptualization, Data curation, Formal Analysis, Investigation, Methodology, Visualization, Writing – original draft.

Przemysław Galek – Conceptualization, SPECS Formal Analysis & Methodology, Visualization, Writing – review & editing.

Paweł Jeżowski – Conceptualization, Investigation, Methodology, Supervision, Validation, Writing – original draft.

Krzysztof Fic – Conceptualization, Formal Analysis, Funding acquisition, Investigation, Methodology, Project administration, Resources, Software, Supervision, Writing – review & editing.

Declaration of Competing Interest

The authors declare that they have no known competing financial interests or personal relationships that could have appeared to influence

the work reported in this paper.

Data availability

Data will be made available on request.

Acknowledgements

The authors acknowledge the funding received from the European Research Council within the Starting Grant project (GA 759603) under European Unions' Horizon 2020 research and innovation programme.

Supplementary materials

Supplementary material associated with this article can be found, in the online version, at [doi:10.1016/j.simpat.2017.03.014](https://doi.org/10.1016/j.simpat.2017.03.014).

References

- [1] P.J. Hall, E.J. Bain, Energy-storage technologies and electricity generation, *Energy Policy* 36 (12) (2008) 4352–4355.
- [2] P. Balachandra, H.S.K. Nathan, B.S. Reddy, Commercialization of sustainable energy technologies, *Renewable Energy* 35 (8) (2010) 1842–1851.
- [3] S.R. Bull, Renewable energy today and tomorrow, *Proceedings of the Ieee* 89 (8) (2001) 1216–1226.
- [4] B.P. Roberts, C. Sandberg, The Role of Energy Storage in Development of Smart Grids, *Proceedings of the Ieee* 99 (6) (2011) 1139–1144.
- [5] S.M. Lukic, J. Cao, R.C. Bansal, F. Rodriguez, A. Emadi, Energy storage systems for automotive applications, *Ieee Transactions on Industrial Electronics* 55 (6) (2008) 2258–2267.
- [6] D.P. Dubal, O. Ayyad, V. Ruiz, P. Gomez-Romero, Hybrid energy storage: the merging of battery and supercapacitor chemistries, *Chem Soc Rev* 44 (7) (2015) 1777–1790.
- [7] M. Winter, R.J. Brodd, What are batteries, fuel cells, and supercapacitors? *Chem Rev* 104 (10) (2004) 4245–4269.
- [8] B. Scrosati, History of lithium batteries, *Journal of Solid State Electrochemistry* 15 (7–8) (2011) 1623–1630.
- [9] E. Frackowiak, F. Beguin, Carbon materials for the electrochemical storage of energy in capacitors, *Carbon* 39 (6) (2001) 937–950.
- [10] R. Fong, U. Von Sacken, J.R. Dahn, Studies of lithium intercalation into carbons using nonaqueous electrochemical cells, *Journal of the Electrochemical Society* 137 (7) (1990) 2009–2013.
- [11] Y. Li, Y. Lu, P. Adelhelm, M.-M. Titirici, Y.-S. Hu, Intercalation chemistry of graphite: alkali metal ions and beyond, *Chemical Society reviews* 48 (17) (2019) 4655–4687.
- [12] H. Buqa, D. Goers, M. Holzappel, M.E. Spahr, P. Novak, High rate capability of graphite negative electrodes for lithium-ion batteries, *Journal of the Electrochemical Society* 152 (2) (2005) A474–A481.
- [13] P. Novák, F. Joho, M. Lanz, B. Rykart, J.-C. Panitz, D. Allia, R. Kötz, O. Haas, The complex electrochemistry of graphite electrodes in lithium-ion batteries, *Journal of Power Sources* 97–98 (2001) 39–46.
- [14] E. Peled, The Electrochemical Behavior of Alkali and Alkaline Earth Metals in Nonaqueous Battery Systems—The Solid Electrolyte Interphase Model, *Journal of the Electrochemical Society* 126 (12) (1979) 2047–2051.
- [15] I. Weber, B. Wang, C. Bodirsky, M. Chakraborty, M. Wachtler, T. Diemant, J. Schnaidt, R.J. Behm, Model Studies on Solid Electrolyte Interphase Formation on Graphite Electrodes in Ethylene Carbonate and Dimethyl Carbonate II: Graphite Powder Electrodes, *ChemElectroChem* 7 (23) (2020) 4794–4809.
- [16] Z.X. Shu, R.S. McMillan, J.J. Murray, Electrochemical Intercalation of Lithium into Graphite, *Journal of the Electrochemical Society* 140 (4) (1993) 922–927.
- [17] M. Qin, Z. Zeng, Q. Wu, H. Yan, M. Liu, Y. Wu, H. Zhang, S. Lei, S. Cheng, J. Xie, Dipole-dipole interactions for inhibiting solvent co-intercalation into a graphite anode to extend the horizon of electrolyte design, *Energy & environmental science* 16 (2) (2023) 546–556.
- [18] M. Winter, J.O. Besenhard, M.E. Spahr, P. Novák, Insertion Electrode Materials for Rechargeable Lithium Batteries, *Advanced materials (Weinheim)* 10 (10) (1998) 725–763.
- [19] H.M. Fellows, M. Forghani, O. Crosnier, S.W. Donne, Modelling voltametric data from electrochemical capacitors, *Journal of Power Sources* 417 (2019) 193–206.
- [20] L. Demarconnay, E. Raymundo-Pinero, F. Beguin, Adjustment of electrodes potential window in an asymmetric carbon/MnO₂ supercapacitor, *Journal of Power Sources* 196 (1) (2011) 580–586.
- [21] E. Barsoukov, J.R. Macdonald, *Impedance Spectroscopy: Theory, Experiment, and Applications*, John Wiley & Sons, Hoboken, 2005. Incorporated.
- [22] A. Lasia, *Electrochemical Impedance Spectroscopy and its Applications*, Springer, New York, 2014.
- [23] R. Kötz, M. Carlen, Principles and applications of electrochemical capacitors, *Electrochimica Acta* 45 (15–16) (2000) 2483–2498.

One-step assembly of metal-ion capacitors using redox-active electrolytes

- [24] A. Burke, R&D considerations for the performance and application of electrochemical capacitors, *Electrochimica Acta* 53 (3) (2007) 1083–1091.
- [25] B. Babu, P. Simon, A. Balducci, Fast Charging Materials for High Power Applications, *Advanced Energy Materials* 10 (29) (2020), 2001128-n/a.
- [26] M.D. Levi, E.A. Levi, D. Aurbach, The mechanism of lithium intercalation in graphite film electrodes in aprotic media. Part 2. Potentiostatic intermittent titration and in situ XRD studies of the solid-state ionic diffusion, *Journal of Electroanalytical Chemistry* 421 (1-2) (1997) 89–97.
- [27] A. Nickol, T. Schied, C. Heubner, M. Schneider, A. Michaelis, M. Bobeth, G. Cuniberti, GITT Analysis of Lithium Insertion Cathodes for Determining the Lithium Diffusion Coefficient at Low Temperature: Challenges and Pitfalls, *Journal of the Electrochemical Society* 167 (9) (2020) 90546.
- [28] J.H. Park, H. Yoon, Y. Cho, C.Y. Yoo, Investigation of Lithium Ion Diffusion of Graphite Anode by the Galvanostatic Intermittent Titration Technique, *Materials (Basel)* 14 (16) (2021) 4683.
- [29] T. Schied, A. Nickol, C. Heubner, M. Schneider, A. Michaelis, M. Bobeth, G. Cuniberti, Determining the Diffusion Coefficient of Lithium Insertion Cathodes from GITT measurements: Theoretical Analysis for low Temperatures, *Chemphyschem* 22 (9) (2021) 885–893.
- [30] M.F. Dupont, S.W. Donne, A Step Potential Electrochemical Spectroscopy Analysis of Electrochemical Capacitor Electrode Performance, *Electrochimica Acta* 167 (2015) 268–277.
- [31] M.F. Dupont, S.W. Donne, Faradaic and Non-Faradaic Contributions to the Power and Energy Characteristics of Electrolytic Manganese Dioxide for Electrochemical Capacitors, *Journal of the Electrochemical Society* 163 (6) (2016) A888–A897.
- [32] M.F. Dupont, M. Forghani, A.P. Cameron, S.W. Donne, Effect of electrolyte cation on the charge storage mechanism of manganese dioxide for electrochemical capacitors, *Electrochimica Acta* 271 (2018) 337–350.
- [33] R. Younesi, G.M. Veith, P. Johansson, K. Edström, T. Vegge, Lithium salts for advanced lithium batteries: Li-metal, Li-O₂, and Li-S, *Energy & environmental science* 8 (7) (2015) 195–1922.
- [34] S.-J. Kang, K. Park, S.-H. Park, H. Lee, Unraveling the role of LiFSI electrolyte in the superior performance of graphite anodes for Li-ion batteries, *Electrochimica Acta* 259 (2018) 949–954.
- [35] D.Y. Wang, A. Xiao, L. Wells, J.R. Dahn, Effect of Mixtures of Lithium Hexafluorophosphate (LiPF₆) and Lithium Bis(fluorosulfonyl)imide (LiFSI) as Salts in Li[Ni_{1/3}Mn_{1/3}Co_{1/3}O₂/Graphite Pouch Cells, *Journal of the Electrochemical Society* 162 (1) (2015) A169–A175.
- [36] C. Decaux, G. Lota, E. Raymundo-Pinero, E. Frackowiak, F. Beguin, Electrochemical performance of a hybrid lithium-ion capacitor with a graphite anode preloaded from lithium bis(trifluoromethane)sulfonimide-based electrolyte, *Electrochimica Acta* 86 (2012) 282–286.
- [37] M. Forghani, S.W. Donne, Duty Cycle Effects on the Step Potential Electrochemical Spectroscopy (SPECS) Analysis of the Aqueous Manganese Dioxide Electrode, *Journal of the Electrochemical Society* 165 (3) (2018) A593–A602.
- [38] M.F. Dupont, S.W. Donne, Separating Faradaic and Non-Faradaic Charge Storage Contributions in Activated Carbon Electrochemical Capacitors Using Electrochemical Methods: I. Step Potential Electrochemical Spectroscopy, *Journal of the Electrochemical Society* 162 (7) (2015) A1246–A1254.
- [39] M. Forghani, H. Mavroudis, J. McCarthy, S.W. Donne, Electroanalytical characterization of electrochemical capacitor systems using step potential electrochemical spectroscopy, *Electrochimica Acta* 332 (2020), 135508.
- [40] M. Forghani, S.W. Donne, Method Comparison for Deconvoluting Capacitive and Pseudo-Capacitive Contributions to Electrochemical Capacitor Electrode Behavior, *Journal of the Electrochemical Society* 165 (3) (2018) A664–A673.
- [41] W. Weppner, R.A. Huggins, Determination of the Kinetic Parameters of Mixed-Conducting Electrodes and Application to the System Li₃Sb, *Journal of The Electrochemical Society* 124 (10) (2019) 1569–1578.
- [42] M. Aslan, D. Weingarth, N. Jäckel, J.S. Archison, I. Grobelsek, V. Presser, Polyvinylpyrrolidone as binder for castable supercapacitor electrodes with high electrochemical performance in organic electrolytes, *Journal of Power Sources* 266 (2014) 374–383.
- [43] P. Galek, A. Slesinski, K. Fic, J. Menzel, Peculiar role of the electrolyte viscosity in the electrochemical capacitor performance, *Journal of materials chemistry. A, Materials for energy and sustainability* 9 (13) (2021) 8644–8654.
- [44] M.D. Bhatt, H. Kim, G. Kim, Various defects in graphene: a review, *RSC advances* 12 (33) (2022) 2152–21547.
- [45] Q. Xu, G. Yang, X. Fan, W. Zheng, Improving the Quantum Capacitance of Graphene-Based Supercapacitors by the Doping and Co-Doping: First-Principles Calculations, *ACS omega* 4 (8) (2019) 13209–13217.
- [46] J. Chen, Y. Han, X. Kong, X. Deng, H.J. Park, Y. Guo, S. Jin, Z. Qi, Z. Lee, Z. Qiao, R. S. Ruoff, H. Ji, The Origin of Improved Electrical Double-Layer Capacitance by Inclusion of Topological Defects and Dopants in Graphene for Supercapacitors, *Angewandte Chemie (International ed.)* 55 (44) (2016) 13822–13827.

Supplementary information

Impact of lithium bis(fluorosulfonyl)imide (LiFSI) concentration on lithium intercalation into graphite monitored with Step Potential ElectroChemical Spectroscopy (SPECS)

Adam Maćkowiak¹, Przemysław Galek¹, Paweł Jeżowski¹, Krzysztof Fic^{1*}

¹Poznan University of Technology, Institute of Chemistry and Technical
Electrochemistry, Berdychowo 4, 60965, Poland

*Corresponding author: krzysztof.fic@put.poznan.pl

One-step assembly of metal-ion capacitors using redox-active electrolytes

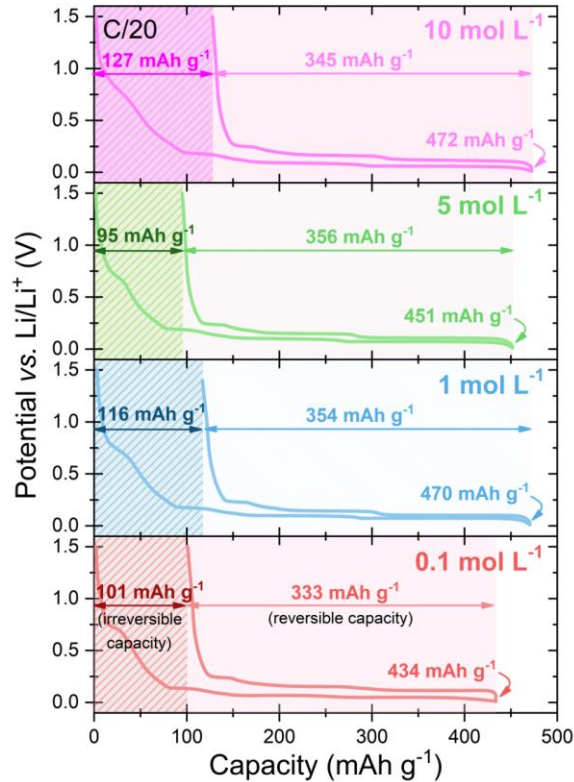


Fig. S1. Graphite intercalation and deintercalation using C/20 current (C corresponds to the theoretical capacity of graphite 372 mAh g⁻¹) with respectively 10, 5, 1 and 0.1 mol L⁻¹ LiFSI in EC:DMC (1:1, v:v) solution as electrolyte.

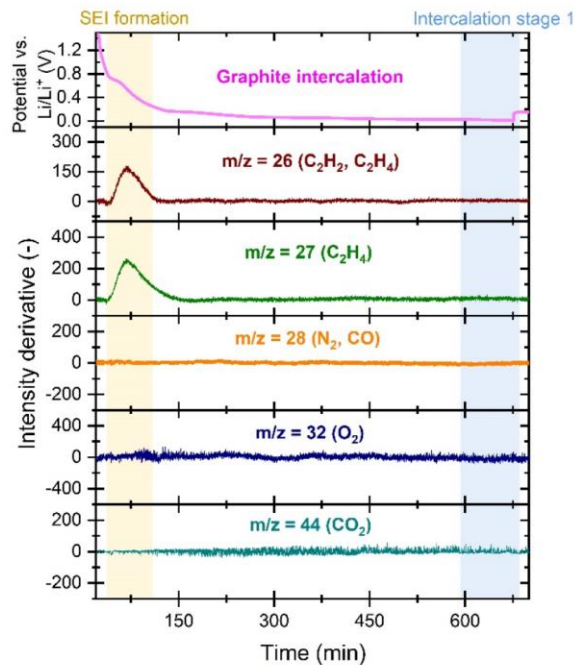


Fig. S2. Graphite intercalation using C/10 current with 0.1 mol L⁻¹ LiFSI in EC:DMC (1:1, v:v) solution as electrolyte and mass signals from carbonates decomposition gases.

One-step assembly of metal-ion capacitors using redox-active electrolytes

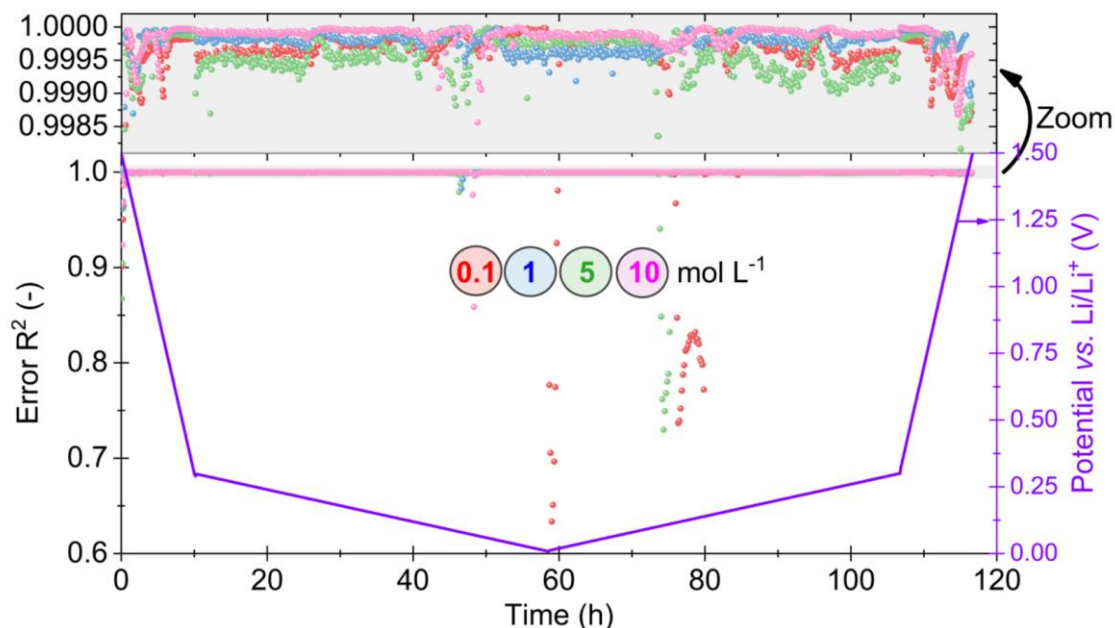


Fig. S3. Calculation error of the recorded data by the SPECS technique (lithium-graphite based system with 0.1, 1, 5 and 10 mol L⁻¹ LiFSI in EC:DMC (1:1; v:v)).

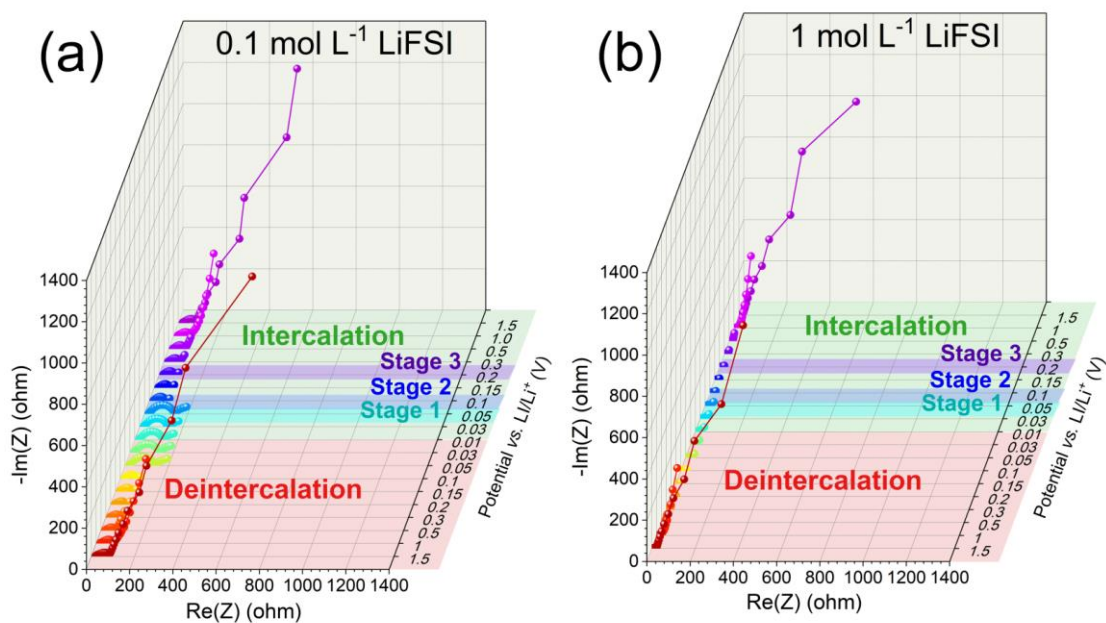


Fig. S4. Impedance spectra during graphite intercalation and deintercalation using C/20 current with (a) 0.1 mol L⁻¹ LiFSI in EC:DMC (1:1, v:v) solution and (b) 1 mol L⁻¹ LiFSI in EC:DMC (1:1, v:v) solution as electrolyte.

**One-step assembly of metal-ion capacitors using
redox-active electrolytes**

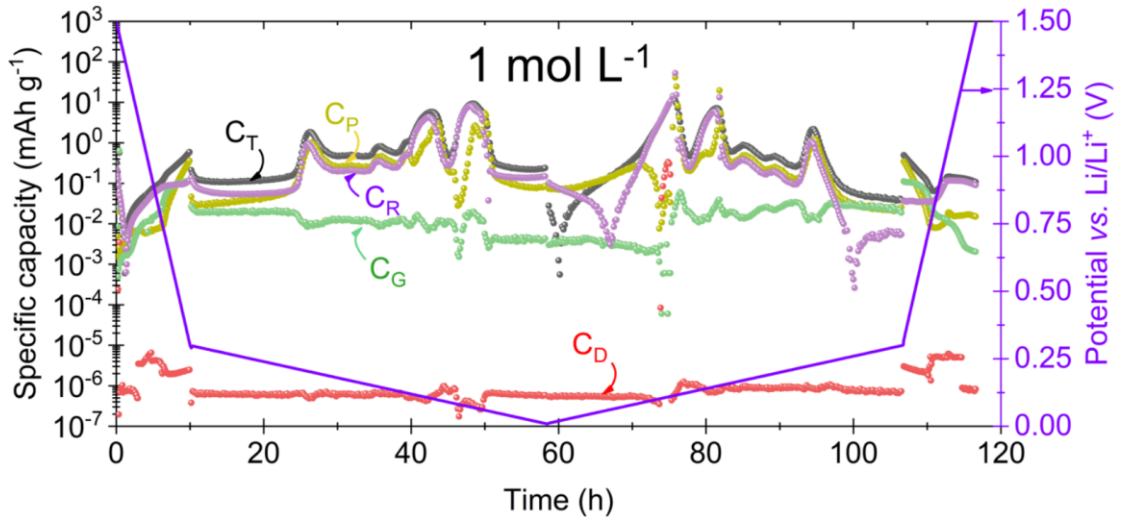


Fig. S5. Specific capacity of individual components for lithium-graphite based system with 1 mol L⁻¹ LiFSI in EC:DMC (1:1; v:v).

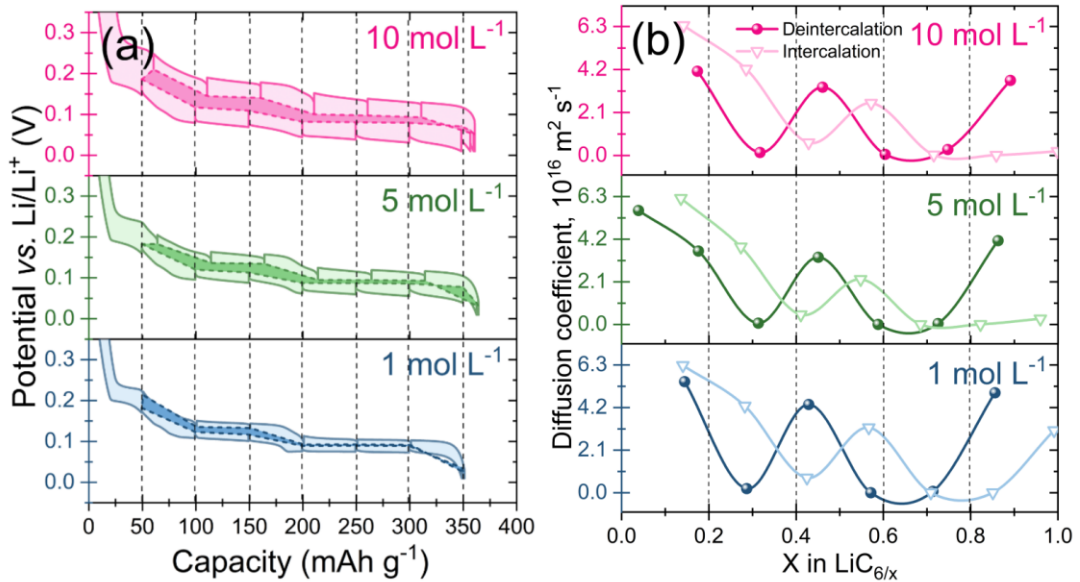


Fig. S6. Results of (a) GITT and (b) diffusion coefficient on lithium-graphite based systems capacity with 1, 5 and 10 mol L⁻¹ LiFSI in EC:DMC (1:1; v:v) as electrolyte.

One-step assembly of metal-ion capacitors using redox-active electrolytes

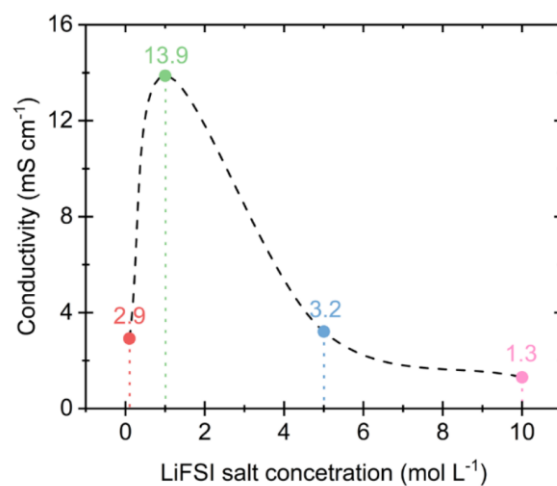


Fig. S7. Relation between the electrolyte conductivity and the LiFSI salt concentration in the EC:DMC (1:1, v:v).

Manuscript 2

Unraveling the effects of redox-active electrolytes on carbon electrodes of Li-ion capacitor

Adam Maćkowiak¹, Przemysław Galek², Paweł Jeżowski¹, Krzysztof Fic^{1*}

¹Poznan University of Technology, Institute of Chemistry and Technical Electrochemistry, Berdychowo 4, 60-965, Poznan, Poland

²Department of Inorganic Chemistry, Dresden University of Technology, Bergstraße 66, D-01069 Dresden, Germany

*Corresponding author: krzysztof.fic@put.poznan.pl

Keywords: Lithium-ion capacitor; Lithium thiocyanate; One-step pre-intercalation; Step potential electrochemical spectroscopy; Galvanostatic intermittent titration technique; Ion diffusion.

Abstract

The quest for efficient and sustainable energy storage solutions has urged significant interest in lithium-ion capacitors (LICs) due to their balanced power and energy characteristics. This study explores the performance of carbon electrodes in LICs prelithiated with a redox-active electrolyte containing lithium thiocyanate (LiSCN). Utilizing Step Potential Electrochemical Spectroscopy (SPECS) and Galvanostatic Intermittent Titration Technique (GITT), an investigation of the impact of thiocyanate on electrode performance was performed. The presence of LiSCN facilitates lithium intercalation in the negative graphite electrode, enhancing capacity and reducing resistance. The SPECS technique reveals distinct intercalation stages and improved ion diffusion, while GITT confirms these findings with diffusion coefficients. The study demonstrates the efficacy of using redox-active electrolytes in LICs, presenting a viable path for optimizing their performance in future applications.

Introduction

In the realm of energy storage, the quest for efficient and sustainable solutions continues to drive innovation and research. Electric double-layer capacitors (EDLCs), due to their high power ($\sim 10 \text{ kW kg}^{-1}$) and long lifespan (1 million cycles), find applications in areas such as automotive, electronics, renewable energy, and public transportation¹⁻⁴. However, EDLCs have significantly lower specific energy ($\sim 10 \text{ Wh kg}^{-1}$) compared to lithium-ion batteries ($\sim 250 \text{ Wh kg}^{-1}$)^{5, 6}. While lithium-ion batteries stand out as the most popular energy storage solutions currently available, their short lifespan (1000 cycles) and low specific power ($< 1 \text{ kW kg}^{-1}$) necessitate the exploration of new alternatives^{7, 8}. One such alternative is lithium-ion capacitors (LICs), characterized by optimal power (5 kW kg^{-1}) and energy ($\sim 50 \text{ Wh kg}^{-1}$) values while maintaining a long lifespan ($\sim 100,000$ cycles)^{9, 10}. LICs emerge as an

One-step assembly of metal-ion capacitors using redox-active electrolytes

attractive option for applications including automotive (regenerative braking), spacecraft power supply, renewable energy, and small portable electronics¹¹⁻¹⁴. LICs offer a promising solution poised to meet the evolving demands of modern energy storage requirements.

In the construction of LICs, carbon-based electrodes are predominantly used, which makes them lightweight and cost-efficient¹⁵. The negative electrode in capacitors can be composed of materials such as reduced graphene oxide (rGO), biomass-derived hard carbons, transition metal dichalcogenides (TMDs) and metal oxides like $\text{Li}_5\text{Ti}_5\text{O}_{12}$, TiO_2 , and Nb_2O_5 ¹⁶⁻¹⁹. Most of the mentioned materials possess a layered structure, allowing lithium ions to penetrate their structure and deposit between these layers. However, graphite, due to its flat and low Li-insertion potential of ~ 0.1 V as well as its high theoretical capacity of 372 mAh g^{-1} , is considered an ideal anode material for LICs²⁰. Positive electrodes in lithium-ion capacitors can consist of B and N co-doped carbon nanofibers, carbon nanotubes, and graphene²¹⁻²³. Activated carbon (AC) dominates as a positive electrode material in LIC research based on the energy-storage mechanism of surface adsorption, as it exhibits high surface area ($\sim 3000 \text{ m}^2 \text{ g}^{-1}$), excellent conductivity ($\sim 60 \text{ S m}^{-1}$), and good chemical stability^{24, 25}.

However, LICs face one structural obstacle - a prelithiation process must be conducted for them to function. Currently, several methods are known in the literature that enables an efficient prelithiation process, such as prelithiation using an additional lithium electrode, prelithiation utilizing sacrificial material, or prelithiation from a concentrated lithium electrolyte^{9, 26-28}. Recently, another prelithiation method using redox-active salts in the electrolyte has emerged²⁹. This approach involves oxidizing redox salts on the positive electrode during the first charging cycle, facilitating efficient intercalation of the negative electrode. It is crucial for the reaction to occur at a potential lower than the electrolyte decomposition potential and to be irreversible. The oxidation reaction of redox salts primarily occurs on the positive electrode, but how does the presence of this reaction affect the performance of the negative electrode?

There are several electrochemical techniques commonly used to assess the performance of the negative electrode, such as GCPL, CV, and PEIS³⁰⁻³². These techniques provide valuable information about capacity, resistance, efficiency, cyclability, and power and energy output³³. To determine the diffusion coefficient parameter, the most commonly chosen techniques are the Galvanostatic Intermittent Titration Technique (GITT) and the Potentiostatic Intermittent Titration Technique (PITT)^{34, 35}. However, due to the sensitivity of the lithium intercalation and deintercalation processes in the graphite structure, the use of GITT appears to be a better and more reliable solution^{36, 37}. In 2015, the application of the Step Potential Electrochemical Spectroscopy (SPECS) technique for detailed describing of energy storage systems has been demonstrated³⁸. The SPECS technique was primarily used for electrochemical capacitors³⁹. However, with appropriate reasoning, it has also been applied to provide detailed descriptions of battery systems⁴⁰. Combining the SPECS and GITT techniques represents a powerful tool for analysing processes occurring in energy storage devices.

In this article, the SPECS technique will be utilized to thoroughly investigate the processes occurring on the carbon electrodes of a lithium-ion capacitor, which will be prelithiated using an electrolyte containing a redox salt additive (**Figure 1**). This salt will consist of lithium thiocyanate (LiSCN) as the additive. The

One-step assembly of metal-ion capacitors using redox-active electrolytes

capacitor electrodes will be examined both in half-cells and in the full system configuration. Subsequently, the results obtained from SPECS will be compared with other commonly used techniques such as PEIS, GCPL, and GITT.

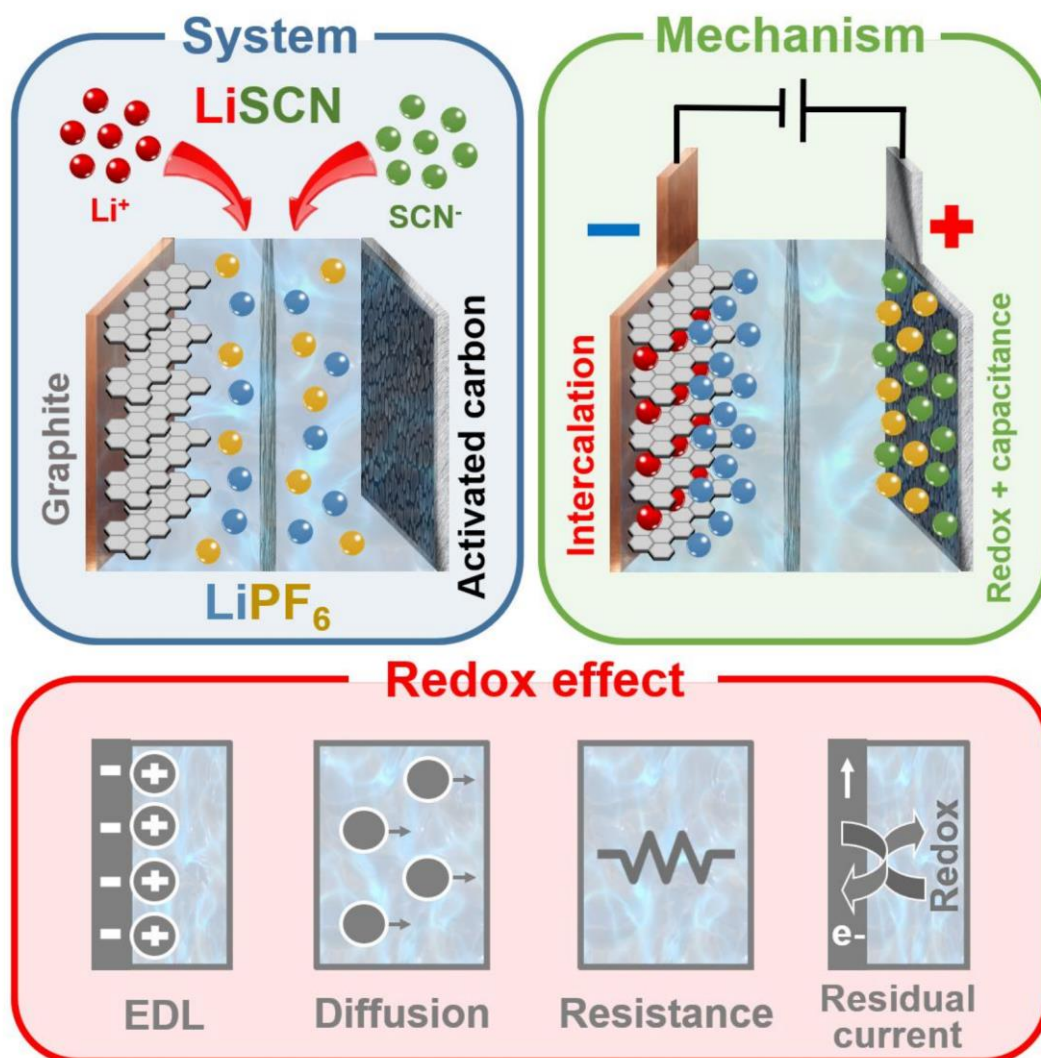


Figure 1. Schematic representation of the study with the assembly of hybrid metal-ion capacitors containing a redox-active electrolyte.

Experimental Methods

Electrolyte. Lithium hexafluorophosphate (LiPF_6) and lithium thiocyanate hydrate ($\text{LiSCN} \cdot x\text{H}_2\text{O}$) were procured from Sigma–Aldrich (Merck) and subjected to a desiccation process under vacuum at 120°C for one week. Lithium thiocyanate hydrate underwent a pre-drying procedure at 130°C employing a liquid nitrogen cold trap to remove water excess. Anhydrous solvents, ethylene carbonate (EC), and dimethyl carbonate (DMC) were obtained from Sigma–Aldrich (Merck). The electrolyte for the cells

One-step assembly of metal-ion capacitors using redox-active electrolytes

consisted of a one molar solution of LiPF_6 dissolved in a mixture of EC and DMC in a 1:1 volumetric ratio. For the redox electrolyte, a one molar solution of LiPF_6 in a mixture of EC and DMC was utilized, supplemented with a calculated amount of LiSCN salt. The quantity of thiocyanate salt added to the electrolyte was determined based on the mass of the negative electrode and its theoretical capacity. The conductivity of the electrolyte without the redox component measured 13.01 mS cm^{-1} , while the electrolyte with thiocyanate salt exhibited a conductivity of 10.88 mS cm^{-1} . Conductivity assessments were conducted at room temperature (21°C) using a 2-electrode Swagelok[®] system with a spacer, employing potentiostatic electrochemical impedance spectroscopy (PEIS). $600 \mu\text{L}$ of the prepared electrolytes were utilized to saturate the separators during the assembly of the electrochemical cells. All chemicals were stored in an MBraun glovebox to maintain an inert environment.

Electrode material. The negative electrode of the hybrid Li-ion capacitor was fabricated utilizing copper foil coated with artificial graphite (total thickness = $100 \mu\text{m}$), sourced from Customcells[®]. As for the positive electrode, a self-standing electrode composed of Kuraray YP80F (80%), polytetrafluoroethylene (PTFE) (10%), and carbon black C65 (10%) (total thickness = $114 \mu\text{m}$) was used. The positive electrode surface area is $1558 \text{ m}^2 \text{ g}^{-1}$. The microtextural properties of the positive electrode were assessed using the Brunauer–Emmett–Teller (BET) isotherm method at 77 K , employing N_2 as an adsorbate (ASAP 2460, Micromeritics, USA). Before adsorption/desorption procedures, samples underwent flushing at 350°C for 12 hours under continuous helium flow, followed by further degassing at 25°C for 5 hours under vacuum conditions⁴¹. Before the cell assembly, both negative and positive electrodes were dried for 24h at 120°C using a vacuum chamber. The reference electrode consisted of metallic lithium obtained from Sigma-Aldrich (Merck).

Cell assembly. Circular electrodes with a diameter of 16 mm and a surface area of 2 cm^2 were obtained from both positive and negative electrode materials using EL-Cut, a tool supplied by EL-CELL[®]. The active mass ratio between the electrodes was maintained at approximately 1:1. Before cell assembly, the electrolyte was freshly prepared. The positive and negative electrodes were then positioned within the ECC-REF electrochemical cell (provided by EL-CELL[®]), separated by two glass fibre discs with a diameter of 18 mm (GF/D, Whatman[®]), each saturated with $600 \mu\text{L}$ of electrolyte. The reference electrode was inserted into the reference pinhole using an ECC loader (provided by EL-CELL[®]). For half-cell measurements, the counter and reference electrodes, consisting of metallic lithium, were shaped as discs with a diameter of 16 mm . All assembly procedures were carried out within a glovebox (MBraun).

Electrochemical investigation. Electrochemical measurements were conducted using a multichannel galvanostat/potentiostat (VMP-3 Biologic[®]) under the control of EC-Lab[®] software at room temperature (21°C). The SPECS measurement involved applying a sequence of potentiostatic hold periods, controlled by chronoamperometry (CA): every 1 mV to 0.01 V vs. Li/Li^+ for 10 minutes. This protocol was designed to comprehensively monitor system changes, particularly emphasizing potential regions below 0.3 V , where individual intercalation/deintercalation events occur. Furthermore, a GITT

examination was performed on each electrochemical system to determine the diffusion coefficient. Cells underwent testing with the C/20 current using the GCPL technique, involving a series of charging and discharging steps by delivering the current for an hour followed by a 1-hour hold period to achieve complete intercalation.

Step potential electrochemical spectroscopy (SPECS). A method known as step potential electrochemical spectroscopy has recently been introduced into the realm of electric double-layer capacitors³⁸ and battery systems⁴⁰. The fundamental concept underlying SPECS involves subjecting the cell to a series of gradual changes in potential (referred to as steps), followed by periods of rest. These rest intervals are sufficiently lengthy to allow the current response to reach an equilibrium state. By employing small step changes, SPECS facilitates the completion of maximum storage capacities while simultaneously offering insights into various factors of energy storage mechanisms. The total current (I_T) recorded during a specific potential step can be divided into distinct components, namely those associated with electric double-layer (EDL) formation (I_{EDL}), diffusion-limited processes (I_D), and residual processes (I_R), as expressed by **Equation 1**⁴².

$$I_T = I_{EDL} + I_D + I_R \quad (1)$$

In the context of electrochemical capacitors, the description of electric double-layer (EDL) formation current (I_{EDL}) can be further elaborated to distinguish between the current associated with electrode porosity (referred to as pore-related current, I_P) and the current about electrode geometry, specifically the outer electrode surface (geometric current, I_G). However, in the case of battery systems, this differentiation becomes inconsequential due to the predominance of charge storage mechanisms primarily driven by redox reactions. Thus, it is clearer to simply characterize it as EDL current. Therefore, considering the influence of rest time (t) and potential step (ΔE), it becomes feasible to compute additional components such as resistance (R_{EDL}), differential capacitance (C_{EDL}), diffusion parameter (B), and residual current (I_R), culminating in the formulation of the final equation (**Eq. 2**).

$$I_T = \frac{\Delta E}{R_{EDL}} \exp\left(-\frac{t}{R_{EDL} + C_{EDL}}\right) + \frac{B}{t^{0.5}} + I_R \quad (2)$$

The residual current refers to the steady-state current that remains after a potential step is applied to the electrochemical system and the transient current has decayed. This residual current is typically constant because it represents the current flowing in the system when the electrochemical processes have reached a steady state. Nevertheless, in instances where a redox reaction transpires at a specific potential, the I_R current will proportionately escalate.

By collating the computed system components, a comprehensive depiction of system operation can be elucidated. Hence, SPECS emerges as a rapid and efficacious tool for delineating the stability of electrode materials, assessing ionic mobility within the electrolyte, quantifying the equivalent series resistance (ESR) of electrode materials, and even optimizing cell engineering^{43, 44}.

One-step assembly of metal-ion capacitors using redox-active electrolytes

Galvanostatic intermittent titration technique (GITT). Unlike SPECS, GITT is a technique in which a current pulse is applied to the system, and its potential response is measured. GITT is a well-known and commonly used technique primarily for determining the diffusion coefficient of energy storage systems³⁶. To calculate the diffusion values, the Weppner and Huggins equation is often employed⁴⁵. However, for precise determination of the lithium-ion diffusion coefficient in a system with graphite electrode, a modified equation is applied³⁷:

$$\tilde{D} = \frac{4}{9\pi} \frac{(E_4 - E_0)^2}{(E_2 - E_1)} \frac{r_p^2}{t_p} \text{ for } \left(\tau \ll \frac{L^2}{\tilde{D}} \right) \quad (3)$$

In **Equation 3**, the symbol \tilde{D} represents the diffusion coefficient [$\text{m}^2 \text{s}^{-1}$], τ is the interval time from charging to discharging (without relaxation phase) [s], and L is the sample thickness [m]. The potential response observed during GITT comprises five distinct phases: starting from the initial potential (E_0), transitioning through the voltage jump (IR drop, $E_1 - E_0$), progressing to the increment phase ($E_2 - E_1$), further proceeding through the subsequent IR drop ($E_3 - E_2$), and ultimately reaching the phase of final resting potential (E_4) (**Fig. 1**). Utilizing this equation, along with the potential response data, the values of t_p (pulse duration) and r_p (particle radius - graphite 9 μm , activated carbon 5 μm), allow the determination of the lithium diffusion coefficient.

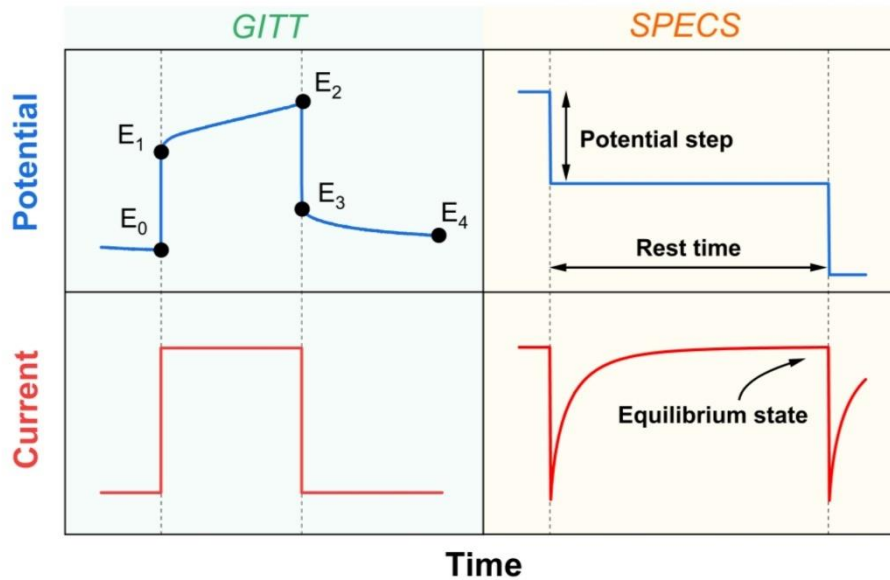


Figure 2. Schematic comparison of the single galvanostatic intermittent titration technique (GITT) pulse and step potential electrochemical spectroscopy (SPECS) pulse.

Results and discussion

Considering recent literature reports on one-step pre-intercalation in hybrid metal-ion capacitors, studies were undertaken to investigate the impact of redox-active electrolytes on the performance of individual

One-step assembly of metal-ion capacitors using redox-active electrolytes

electrodes in a lithium-ion capacitor²⁹. To thoroughly examine the effects of thiocyanates, their electrochemical behaviour during standard constant current charging and discharging of the system was first demonstrated. Figure 3a illustrates the effect of thiocyanate salt in the solution on the performance of the positive electrode. By applying a current of $C/20$ (where C corresponds to the theoretical full charge capacity of the graphite electrode, 372 mAh g^{-1}), the system without SCN^- anions exhibits a purely capacitive behaviour. The capacity for such charging up to 4.5 V is 71 mAh g^{-1} , indicating a deficit of 301 mAh g^{-1} required to fully charge the graphite electrode. To address this capacity deficiency, a precisely calculated amount of thiocyanate was added to the electrolyte, which increased the capacity to 372 mAh g^{-1} , thus matching the graphite electrode full charge capacity. The presence of thiocyanates creates a potential plateau around 3.5 V , which limits the potential increase of the positive electrode, allowing it to accumulate sufficient capacity without exceeding the cut-off potential (i.e., 4.5 V). As observed, during discharge, the curve displays a more capacitive character, suggesting that most thiocyanates underwent irreversible reactions during the initial charge.

Subsequently, the negative electrode (graphite) was studied in a half-cell configuration with and without the addition of thiocyanate salt (Figure 3b). The system with the added salt achieved a higher first-cycle capacity (399 mAh g^{-1}) compared to the system without the addition (383 mAh g^{-1}). However, a part of this capacity was utilized to form the solid electrolyte interphase (SEI) layer, resulting in a higher irreversible capacity (47 mAh g^{-1}) compared to the system without the addition (36 mAh g^{-1}). Nonetheless, both systems exhibited very similar performance, with distinct intercalation stages observed, suggesting that the SCN^- anions did not have a significant impact on the lithium intercalation process into the graphite structure.

In the subsequent phase of the study, two hybrid capacitor systems were assembled, with graphite serving as the negative electrode and activated carbon as the positive electrode. In one of these systems, LiSCN salt was added to the electrolyte. As shown in Figure 3c, the system without thiocyanate additives quickly reached the cut-off potential of the positive electrode, and the curve flattened, indicating an electrochemical reaction that decomposes the electrolyte. Meanwhile, no distinct intercalation stages were observed at the negative electrode, resulting in the system not achieving the expected capacity. The addition of SCN^- salt, as observed in the half-cell experiments, mitigated the increase in the positive electrode potential, acting as a charge-balancer and facilitating the intercalation of lithium cations into the graphite structure. Additionally, it is likely that lithium ions participated in reactions and did not adversely affect electrolyte conductivity, as the cation balance was maintained relative to a standard electrolyte. This approach confirms the effectiveness of the one-step assembly approach in lithium-ion capacitors.

Subsequently, it was decided to investigate the resistances using the potentiostatic electrochemical impedance spectroscopy (PEIS) technique for the electrodes in their fully charged state. For the positive electrodes, this was at a potential of 4.5 V , while for the negative electrodes it was at a potential of 0.01 V . Figure S1 compares the performance of the positive electrodes. The equivalent series resistance (ESR) for both systems is similar (5 ohms for the system with SCN^- anions and 6 ohms for the system without SCN^-), as both were constructed with the same electrode materials. However, the resistance

One-step assembly of metal-ion capacitors using redox-active electrolytes

represented by the semicircle size for the SCN^- system is significantly higher. This indicates an increased charge transfer resistance at the electrode/electrolyte interface, which is attributed to charge separation at the phase boundary or ion diffusion resistance in the electrolyte, particularly near the electrode surface⁴⁶. This suggests that the presence and reaction of thiocyanate anions may hinder the charge transfer at the positive electrode during the first cycle.

In contrast, for the negative electrodes (Figure 3d), the presence of SCN^- ions positively affects the resistance values in the system. This difference may be due to the reduction of some thiocyanate anions on the negative electrode surface, forming a less resistive SEI layer that facilitates the transport of lithium ions into the graphite structure. When comparing the performance of the negative electrodes in full hybrid systems, it should be noted that the response from the Stern layer in the spectra for both systems was comparable; however, the addition of SCN^- ions did not influence the thickness of the Stern layer. It should be considered that the SCN^- system was fully intercalated, which results in lower resistance values in the semicircle.

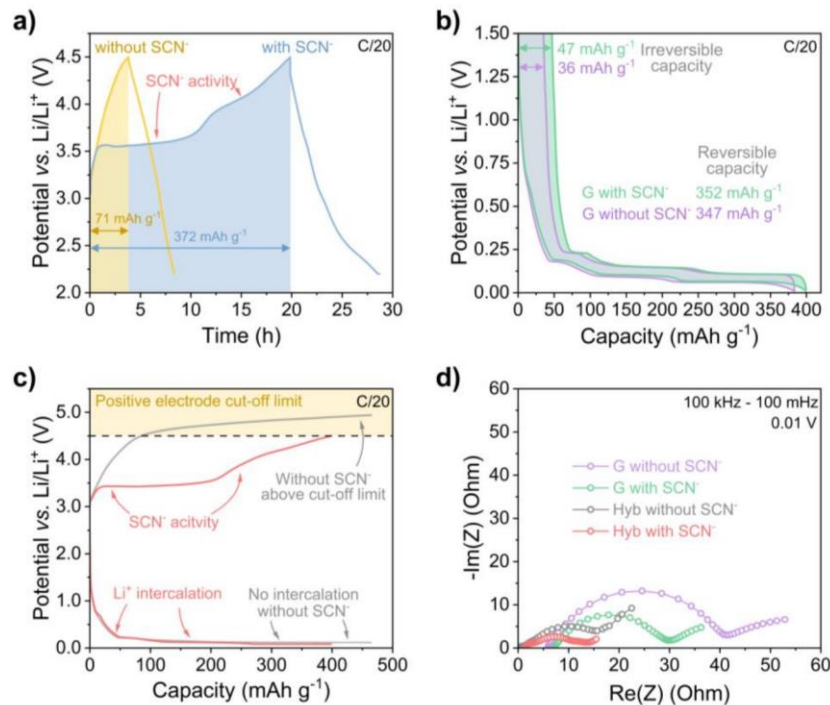


Figure 3. Comparison of charging and discharging curves for systems with and without electroactive additive in electrolyte a) half-cells with activated carbon, b) half-cells with graphite, c) full hybrid cells, d) impedance spectroscopy results for graphite electrodes in half-cells and full hybrid cells.

To effectively analyze the results obtained from the SPECS technique, it is essential first to consider the parameters that can be extracted using this powerful tool. The total current can be divided into EDL current, diffusive current, and residual current. The area under the current curves allows for the calculation of capacities attributed to EDL, diffusion, and residual effects. The SPECSfit software can further refine these equations to yield detailed values such as the diffusion parameter, time constant,

One-step assembly of metal-ion capacitors using redox-active electrolytes

and EDL layer resistance. The current associated with EDL layer formation can be further categorized into pore-related current and geometric current. In the context of electric double-layer capacitors, pore-related current relates to the formation of the EDL layer within the porous materials of the positive electrode. For graphite, this should be considered as the ion-accessible space between graphene layers. Geometric current in EDLCs refers to the outer electrode surface that is easily accessible to the electrolyte, whereas for graphite systems, it describes the edges of the graphene layers. In the studies conducted, however, the distinction between porous and geometric components was not made, to simplify the analysis by considering them as related to double-layer formation. Applying an appropriate potential step is crucial in SPECS studies. A very slow potential step was used in the experiments to achieve the most accurate current curve, with a 1 mV potential step every 10 minutes. This long interval ensures equilibrium of the current curve, though it extends the experiment duration. The 1 mV step is particularly important for capturing changes in the graphite electrode system, where potential differences between intercalation stages are marginal.

The SPECS studies began by examining half-cells with activated carbon. In this case, systems with and without the addition of LiSCN were compared, as shown in Figure 4. Initially, the total current was converted to a total specific capacity. A distinct signal from the thiocyanate reaction at a potential of 3.4 V was observed. This potential is slightly lower than the reaction potential observed in the previous galvanostatic charge study. This occurs because the SPECS study is much slower and more detailed, allowing for the capture of capacity changes much earlier. Here, it is also important to note that the electrolyte begins to decompose at around 4.3 V, making it crucial for ageing systems not to exceed this potential. Figure 4b illustrates that the specific EDL capacity is comparable for both systems above 3.6 V. However, during the SCN⁻ reaction, an increase in EDL capacity is observed, likely due to the attraction of SCN⁻ ions by the positive electrode of the cell. The residual capacity curve primarily reflects the total specific capacity, which is consistent as the faradaic reaction of the thiocyanate anion predominates here. The capacity of the diffusive layer is negligible but, as expected, is higher for the system with thiocyanates. This is due to the presence of additional ions in the system. The EDL layer resistance is higher for the system without thiocyanates, indicating a better-organized double-layer structure and less interference from Faradaic reactions in this process. The time constant curve is comparable to the EDL resistance, meaning the system requires more time to settle and adsorb ions on the surface of the positive electrode. Figures h and i compile the capacities: total capacity, EDL capacity, diffusive capacity, and residual capacity. As shown, the residual capacity has the most significant impact on the redox electrolyte system (94%), which is logical due to the electrochemical reaction. Conversely, for the system without SCN⁻, the residual capacity also has the most significant impact. This result is somewhat misleading, but closer examination of the EDL curve reveals that EDL storage predominates initially, and towards the end, when electrolyte decomposition processes occur, the capacity from the residual current increases. Figure S2 describes other parameters obtained during SPECS technique measurement. One of the more important curves is the fitting curve (Figure S2b), which shows that the error of the fitted curves is marginal, and the fitting reflected a good correlation coefficient of more than 99%.

One-step assembly of metal-ion capacitors using redox-active electrolytes

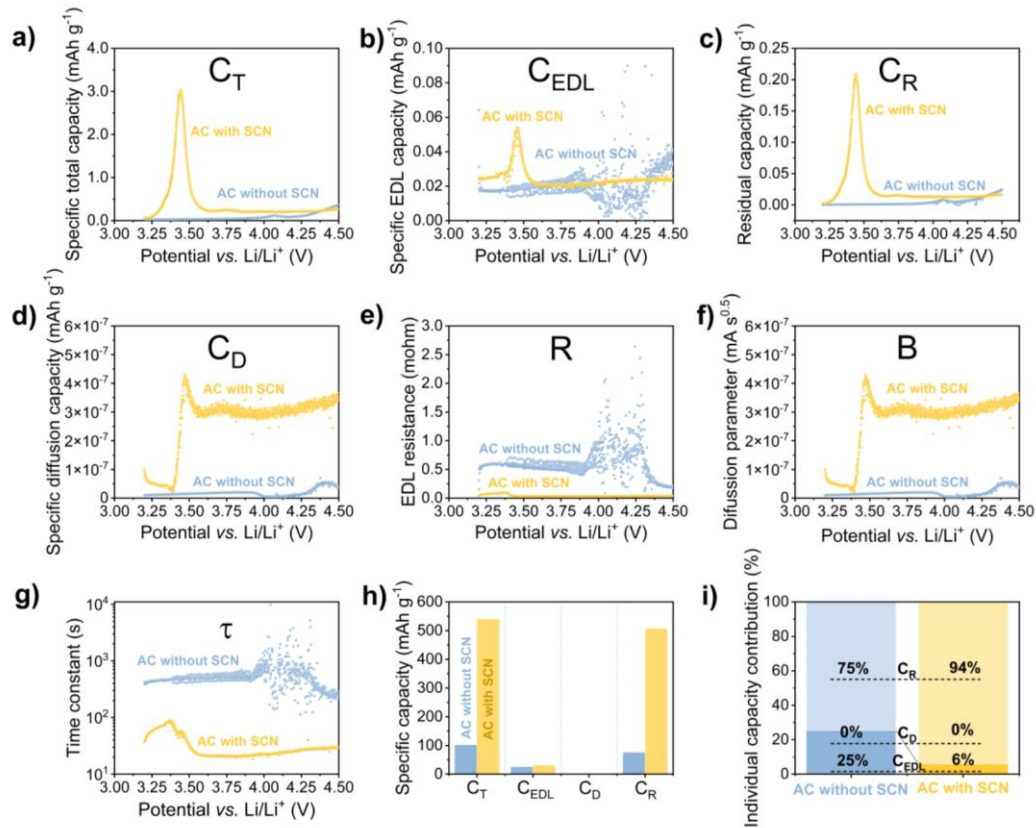


Figure 4. SPECS results of half-cells using activated carbon and activated carbon with thiocyanate salt as an electrolyte additive a) specific total capacity (C_T), b) specific EDL capacity (C_{EDL}), c) residual capacity (C_R), d) specific diffusion capacity (C_D), e) EDL resistance (R), f) diffusion parameter (B), g) time constant (τ), h) specific capacity comparison and i) individual capacity contribution.

Next, a SPECS study was conducted for two graphite systems in half-cells. Again, one system had a dissolved thiocyanate electrolyte, while the other did not. In both cases, intercalation proceeded successfully, with distinct intercalation stages visible. However, for the SCN system, the third stage is more pronounced (the signal is narrower and higher) than for the system without the electrolyte additive. Moreover, the individual intercalation stages occur slightly but at a higher potential than in a traditional lithium-graphite half-cell. Interestingly, during deintercalation, the curves of both systems overlap, suggesting changes only during the charging of the graphite electrode (Figure S3). A slight increase in capacity at a potential of about 0.75 V can also be observed, suggesting the formation of more SEI in the system with thiocyanates. The capacity of the EDL layer in this case should be negligible. Only at the beginning and end of the charging cycle, capacity originating from the electrical double-layer was observed, which is more related to the attraction of cations to the electrode surface rather than actual EDL storage due to the lack of pores and the small specific surface area of graphite (about $1 \text{ m}^2 \text{ g}^{-1}$). The capacity associated with the redox reaction is dominant here due to the lithium intercalation process, making the residual capacity curve very close to the total specific capacity curve. The diffusive capacity

One-step assembly of metal-ion capacitors using redox-active electrolytes

is, of course, marginal; however, in the beginning, diffusion is higher for the system without SCN, but from the moment reactions related to SEI formation occur, there is a significant increase in diffusion in the thiocyanate system. This is another sign suggesting that thiocyanates are responsible for the SEI layer formation. The resistance of the EDL layer follows a characteristic pattern, where initially, lithium ions diffuse towards the negative electrode, and the resistance is high (up to 18 mohm). However, as the process progresses, the electrical double-layer resistance drops practically to zero. Comparing the capacities obtained for both systems, as in the galvanostatic studies, the capacity for graphite with thiocyanates is slightly higher than for the system without. However, the percentage values in comparison between the individual components are comparable for both systems. Figure S4a shows how dominant the residual current is, and the fitting curve is also very high, above 99%.

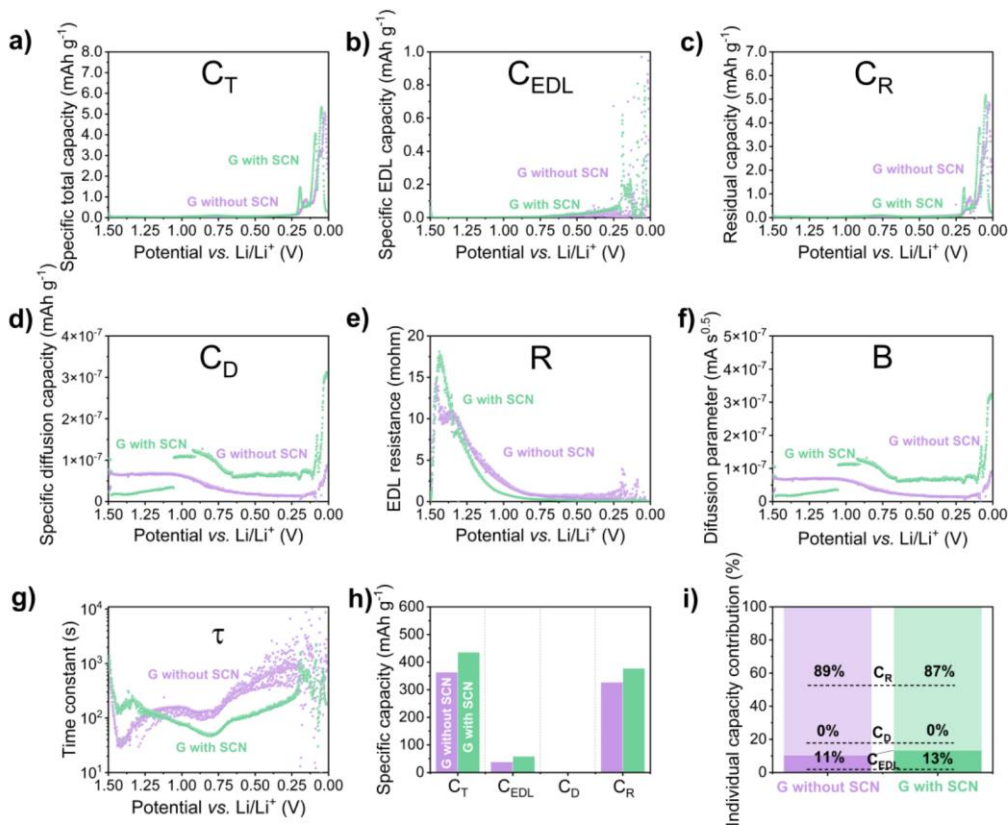


Figure 5. SPECS results of half-cells using graphite and graphite with thiocyanate salt as an electrolyte additive a) specific total capacity (C_T), b) specific EDL capacity (C_{EDL}), c) residual capacity (C_R), d) specific diffusion capacity (C_D), e) EDL resistance (R), f) diffusion parameter (B), g) time constant (τ), h) specific capacity comparison and i) individual capacity contribution.

In the next step, SPECS studies were conducted in a three-electrode system, where graphite was the negative electrode, activated carbon was the positive electrode, and metallic lithium was the reference electrode. In this case, the performance of negative electrodes in full hybrid systems with and without

One-step assembly of metal-ion capacitors using redox-active electrolytes

the addition of thiocyanates was compared. The hybrid without thiocyanates was not fully intercalated, as previously explained during the discussion of Figure 3. Nevertheless, it was decided to show the performance of this cell for comparison purposes with the hybrid assembled using the one-step assembly approach. Through the SPECS technique, the successive intercalation steps of the hybrid system with SCN (Figure 6a) can be observed. The system without thiocyanates cannot surpass the graphite potential of 0.5 V, indicating a lack of lithium intercalation process. The capacity originating from the EDL in the hybrid without SCN is negligible, while in the SCN hybrid, it increases at the end of the charging cycle and corresponds to the intercalation stages. Interestingly, the diffusion value in the hybrid system with SCN starts to increase exponentially from a potential of 0.5 V, suggesting heightened ion activity. The EDL layer resistance is similar for both systems, which is related to ion movement in the initial phase towards the negative electrode. Only later, when the appropriate energy barriers are overcome, intercalation occurs, and the resistance associated with EDL layer formation decreases. Comparing the individual capacity values, it can be noted that for the system without SCN, 98% of the capacity is related to reactions within the system, but not intercalation rather, electrolyte decomposition. In contrast, for the system with SCN, the capacity arising from the reduction reaction constitutes 90% of the individual components. However, the EDL capacity accounts for 10%, so it is important to remember that the operation of the negative electrode is not only intercalation. Figure S5 shows a very good fitting curve for the system with SCN, but for the system without thiocyanates, the error is significant. This suggests that the SPECS technique can be successfully used only for systems where no large fluctuations in potential and no violent reactions occur.

One-step assembly of metal-ion capacitors using redox-active electrolytes

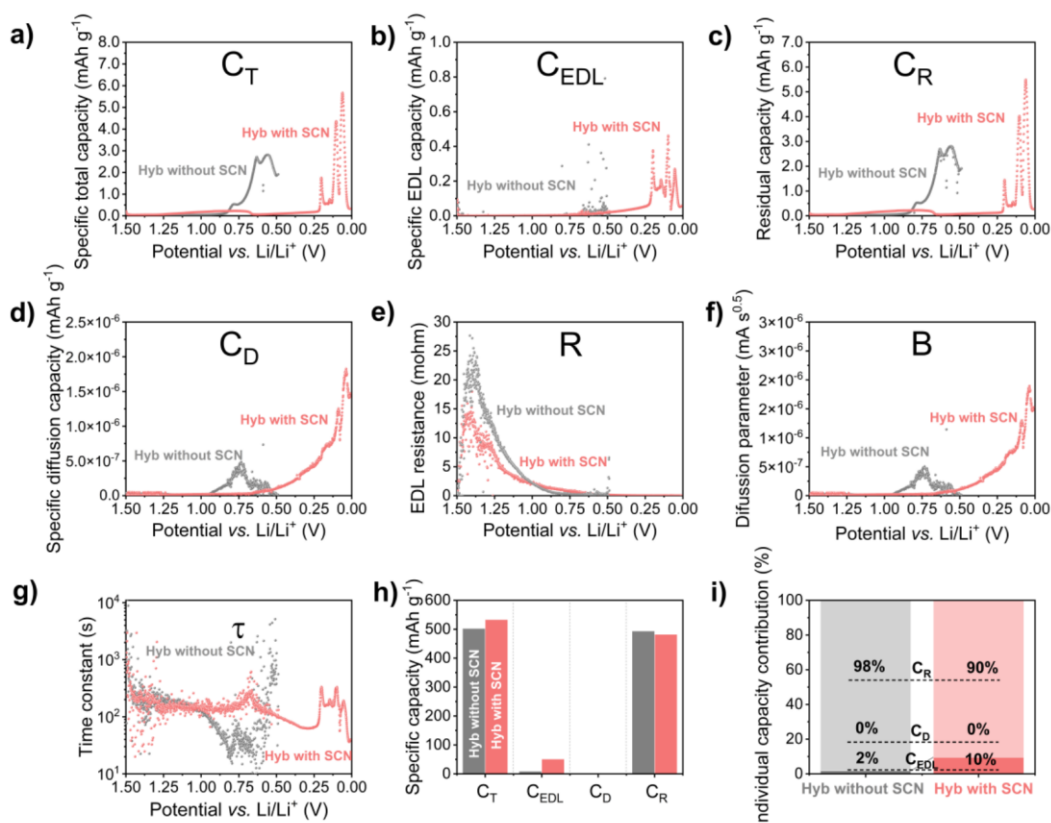


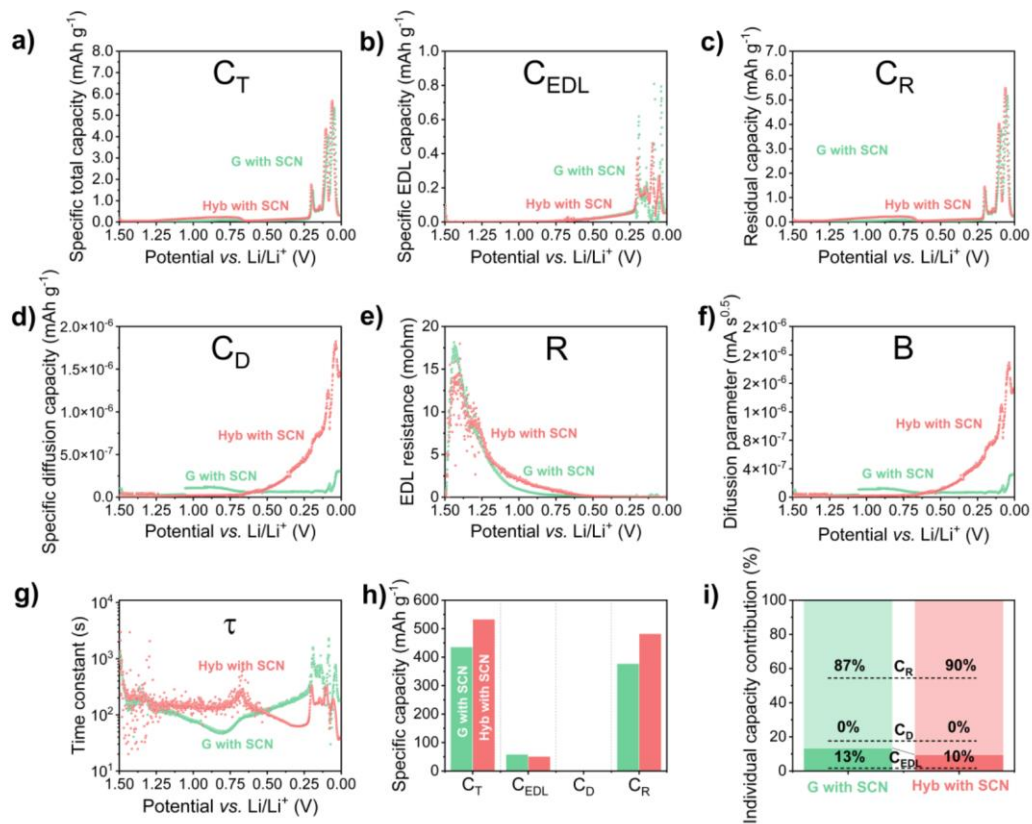
Figure 6. SPECS results of full cells using graphite and graphite with thiocyanate salt as an electrolyte additive a) specific total capacity (C_T), b) specific EDL capacity (C_{EDL}), c) residual capacity (C_R), d) specific diffusion capacity (C_D), e) EDL resistance (R), f) diffusion parameter (B), g) time constant (τ), h) specific capacity comparison and i) individual capacity contribution.

In the final comparison of SPECS results, a graphite-lithium half-cell with SCN was compared to a fully intercalated hybrid using the one-step assembly approach (Figure 7). It is common in scientific studies to test electrodes in half-cells without considering their performance in full systems which may differ. This comparison aims to highlight the differences in the performance of the graphite electrode, where theoretically the same processes should occur. But one system has a metallic electrode with constant potential as a counter electrode and the other system has an active carbon electrode with additional oxidation reactions as a counter electrode.

Comparing the total specific capacity values for both systems, the capacities responsible for individual intercalation stages overlap, suggesting that the electrodes operate in the same manner (Figure 7a). However, it should be noted that in the SCN hybrid, a much larger capacity is utilized for SEI formation. In practice, this means that the simultaneous reaction occurring at the positive electrode affects the SEI layer formation, as the oxidation of thiocyanates is not observed in the lithium electrode. The capacity associated with the double layer is comparable for both systems. However, the diffusion parameter

One-step assembly of metal-ion capacitors using redox-active electrolytes

increases exponentially during intercalation for the hybrid system, while it remains almost unchanged for the half-cell (Figure 7f). This suggests that the reaction occurring at the positive electrode influences ion diffusion at the negative electrode. Likely, during the reaction at the positive electrode, lithium ions are released, which diffuse towards the negative electrode, contributing to the intercalation process. The time constant value in the initial phase is comparable for both systems, but later it increases for the hybrid system, also suggesting interference in SEI formation. However, after the SEI layer formation, the situation reverses, and the hybrid system is characterized by lower time constant values, meaning ions move faster, confirming the relationship obtained in the diffusion parameter calculations. Overall, the presence of oxidation reactions at the positive electrode results in better ion diffusion in the electrolyte and facilitated lithium-ion intercalation. Comparing the obtained relationships of individual capacity parameters, there is no significant difference. Only in the hybrid system, there is a slightly higher contribution of redox capacity, likely due to SEI layer buildup. It is also worth noting the difference in total capacity, which is nearly 100 mAh g⁻¹. This difference is due to the SEI layer buildup, as the intercalation curves of both systems overlap (Figure S6a). In the galvanostatically charged system, there was no such difference in capacity values. Therefore, this increase in capacity mainly results from the prolonged duration of the SPECS study. In this case, thiocyanates have more time to react at the positive electrode, leading to greater overall capacity. Therefore, the numerical values for capacity obtained by the SPECS technique should be considered indicative.



One-step assembly of metal-ion capacitors using redox-active electrolytes

Figure 7. SPECS results of half-cell and full-cell using graphite with thiocyanate salt as an electrolyte additive a) specific total capacity (C_T), b) specific EDL capacity (C_{EDL}), c) residual capacity (C_R), d) specific diffusion capacity (C_D), e) EDL resistance (R), f) diffusion parameter (B), g) time constant (τ), h) specific capacity comparison and i) individual capacity contribution.

After conducting research using the SPECS technique, it was decided to compare the results using the GITT technique. For this purpose, all previously assembled systems were examined by applying 1 hour of charging and 1 hour of resting, and the results are presented in Figure 8. The applied current corresponded to a C/20 rate. Figure 8a shows the GITT results for the half-cell with activated carbon with and without the addition of thiocyanates. As shown, the system without thiocyanates quickly reaches the cut-off potential limit of the positive electrode. The system with thiocyanates, however, exhibits a visible plateau at a potential value of approximately 3.5 V, after which it reaches the maximum potential significantly later than the system without SCN, which is consistent with the galvanostatic studies (Figure 3a). Based on the obtained potential dependence over time, the diffusion coefficient of these systems was calculated and presented in Figure 8b. An increased diffusion was observed in the initial phase, followed by a plateau. Interestingly, the results do not coincide with those obtained using the SPECS technique, where the thiocyanate reaction influenced the diffusion parameter value. It should be noted, however, that the diffusion coefficient ($m^2 s^{-1}$) calculated using GITT is one of the components of the equation for the diffusion parameter ($mA s^{-1}$) calculated in SPECS. Similar values should not be expected, but a proportional response should be. It is worth mentioning that the charging time of the half-cells was significantly longer than anticipated. This occurs due to the self-discharge of the positive electrode, making the GITT technique not the best for studying systems with activated carbon.

Next, graphite half-cells with and without thiocyanate addition were examined (Figure 8c). In this case, as shown in Figure 3b, very similar performance of both systems was obtained, with the only difference being a slightly larger irreversible capacity associated with SEI formation in the SCN cell. The calculated diffusion coefficient values are characteristic of graphite systems with distinctly marked intercalation stages. The results of both systems overlap, suggesting similar electrochemical performance. However, in this case, the diffusion coefficient curve aligns with the results obtained using the SPECS technique (Figure 5f), where responses related to intercalation stages can also be observed in the same manner.

Subsequently, full hybrid systems with and without SCN salt addition were examined (Figure 8e). As confirmed by previous studies, the system without thiocyanates did not reach the target potential value (0.01 V), thus not fully intercalating. The diffusion coefficient value confirms the lack of intercalation stages, with ion movement occurring only in the initial phase, and later the diffusion coefficient being close to zero. In the case of the hybrid with SCN, the graphite electrode was correctly intercalated, and the very low potential changes during electrode resting suggest that the electrode "held" the potential better than graphite intercalated in the half-cell. This phenomenon is likely due to a more tightly formed SEI layer due to the reaction occurring at the positive electrode. In the case of the diffusion coefficient, distinct intercalation stages are visible, but they are shifted, i.e., they occur earlier than in the case of graphite intercalated in half-cells. Comparing the diffusion coefficient results with those from the SPECS

One-step assembly of metal-ion capacitors using redox-active electrolytes

technique shows a similarity in the curve's character, and the intercalation stages are also visible. However, in the case of GITT, the diffusion value between the intercalation stages is practically zero, while in SPECS, it is increasing. Both techniques provide similar, yet not identical results. This suggests that to fully understand the system characteristics, multiple techniques should be used, as there is no single universal solution.

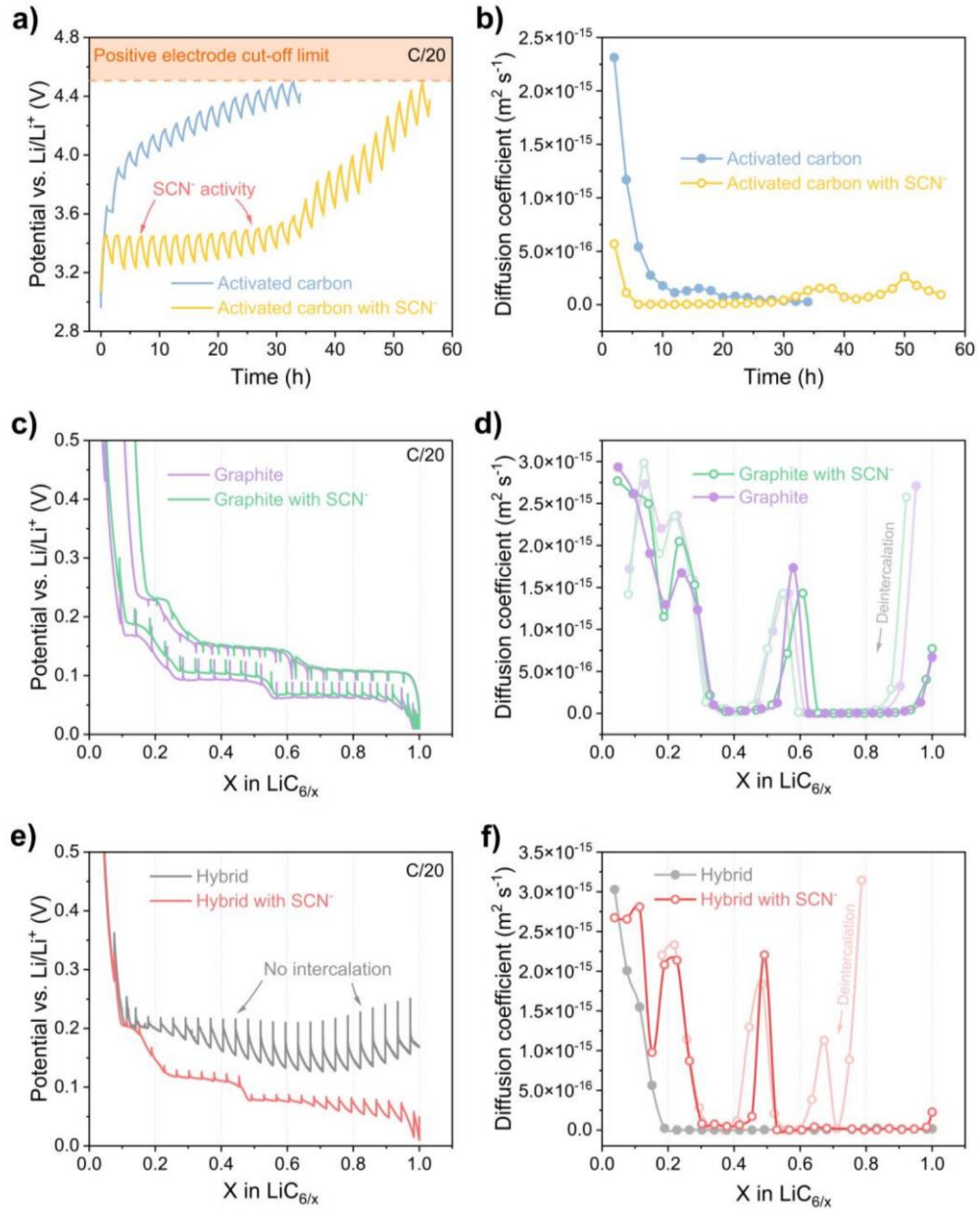


Figure 8. GITT results of half cells a) with activated carbon, c) with graphite e) graphite in full cells and b), d), f) calculated diffusion coefficients based on these results.

Conclusions

This research presents a detailed analysis of the effects of lithium thiocyanate (LiSCN) as a redox-active additive in the electrolyte of lithium-ion capacitors (LICs). The use of SPECS and GITT techniques provided comprehensive insights into the electrochemical behaviour of the system. The addition of LiSCN facilitated effective prelithiation, enhancing the capacity and performance of the graphite negative electrode. SPECS analysis showed distinct intercalation stages and improved ion diffusion in hybrid systems, while GITT confirmed these findings through characteristic diffusion coefficients. The results indicate that redox-active electrolytes, specifically those containing LiSCN, significantly enhance LIC performance by promoting better lithium intercalation and reducing electrode resistance. This study underscores the potential of redox-active additives in developing high-performance LICs, contributing to advancements in energy storage technology for automotive, renewable energy, and portable electronics applications.

Acknowledgements

This work was financially supported by the European Research Council within the Starting Grant project (GA 759603) under European Union Horizon 2020 research and innovation programme.

References

1. P. Simon and Y. Gogotsi, *Nature materials*, 2020, **19**, 1151-1163.
2. P.-y. Hung, H. Zhang, H. Lin, Q. Guo, K.-t. Lau and B. Jia, *Journal of energy chemistry*, 2022, **68**, 580-602.
3. R. T. Yadlapalli, R. R. Alla, R. Kandipati and A. Kotapati, *Journal of energy storage*, 2022, **49**, 104194.
4. P. Drabek and L. Streit.
5. J. T. Frith, M. J. Lacey and U. Ulissi, *Nature communications*, 2023, **14**, 420-420.
6. J. Zhao and A. F. Burke, *Advanced energy materials*, 2021, **11**, 2002192-n/a.
7. A. Manthiram, *ACS central science*, 2017, **3**, 1063-1069.
8. T. Kim, W. Song, D.-Y. Son, L. K. Ono and Y. Qi, *J. Mater. Chem. A*, 2019, **7**, 2942-2964.
9. P. Jeżowski, O. Crosnier, E. Deunf, P. Poizot, F. Béguin and T. Brousse, *Nat. Mater.*, 2018, **17**, 167-173.
10. M. Soltani and S. H. Beheshti, *Journal of energy storage*, 2021, **34**, 102019.
11. M. H. Nazir, A. Rahil, E. Partenie, M. Bowkett, Z. A. Khan, M. M. Hussain and S. Z. J. Zaidi, *Battery energy*, 2022, **1**, 20220022-n/a.
12. M. Uno and K. Tanaka, *IEEE transactions on aerospace and electronic systems*, 2013, **49**, 175-188.
13. S. Barcellona, F. Ciccarelli, D. Iannuzzi and L. Piegari, *Electric power components and systems*, 2016, **44**, 1248-1260.
14. V. Khomenko and V. Barsukov, *Materials today : proceedings*, 2019, **6**, 116-120.
15. G. Kothandam, G. Singh, X. Guan, J. M. Lee, K. Ramadass, S. Joseph, M. Benzigar, A. Karakoti, J. Yi, P. Kumar and A. Vinu, *Advanced science*, 2023, **10**, e2301045-n/a.
16. Y. Yao, H. Cumberbatch, D. D. Robertson, M. A. Chin, R. Lamkin and S. H. Tolbert, *Advanced functional materials*, 2023.
17. X. Wang, L. Liu and Z. Niu, *Materials chemistry frontiers*, 2019, **3**, 1265-1279.
18. S. Jayaraman, A. Jain, M. Ulaganathan, E. Edison, M. P. Srinivasan, R. Balasubramanian, V. Aravindan and S. Madhavi, *Chemical engineering journal (Lausanne, Switzerland: 1996)*, 2017, **316**, 506-513.

One-step assembly of metal-ion capacitors using redox-active electrolytes

19. R. Wang, J. Lang, P. Zhang, Z. Lin and X. Yan, *Advanced functional materials*, 2015, **25**, 2270-2278.
20. T. Insinna, E. N. Basse, K. Märker, A. Collauto, A.-L. Barra and C. P. Grey, *Chemistry of materials*, 2023, **35**, 5497-5511.
21. O. E. Eleri, F. Lou and Z. Yu, *Batteries (Basel)*, 2023, **9**, 533.
22. J. H. Lee, W. H. Shin, S. Y. Lim, B. G. Kim and J. W. Choi, *Materials for renewable and sustainable energy*, 2014, **3**, 1-8.
23. S. Zhang, C. Li, X. Zhang, X. Sun, K. Wang and Y. Ma, *ACS applied materials & interfaces*, 2017, **9**, 17136-17144.
24. A. Platek-Mielczarek, J. Conder, K. Fic and C. M. Ghimbeu, *Journal of power sources*, 2022, **542**, 231714.
25. S. D. Magar, C. Leibing, J. L. Gómez-Urbano, R. Cid, D. Carriazo and A. Balducci, *Electrochimica acta*, 2023, **446**, 142104.
26. L. Jin, C. Shen, A. Shellikeri, Q. Wu, J. Zheng, P. Andrei, J.-G. Zhang and J. P. Zheng, *Energy Environ. Sci.*, 2020, **13**, 2341-2362.
27. T. Aida, K. Yamada and M. Morita, *Electrochem. Solid-State Lett.*, 2006, **9**, A534.
28. C. Decaux, G. Lota, E. Raymundo-Piñero, E. Frackowiak and F. Béguin, *Electrochim. Acta*, 2012, **86**, 282-286.
29. A. Mackowiak, P. Jezowski, Y. Matsui, M. Ishikawa and K. Fic, *Energy Storage Mater.*, 2024, **65**, 103163.
30. E. Barsoukov and J. R. Macdonald, *Impedance Spectroscopy: Theory, Experiment, and Applications*, John Wiley & Sons, Incorporated, Hoboken, 2005.
31. L. Demarconnay, E. Raymundo-Pinero and F. Béguin, *Journal of power sources*, 2011, **196**, 580-586.
32. H. M. Fellows, M. Forghani, O. Crosnier and S. W. Donne, *Journal of power sources*, 2019, **417**, 193-206.
33. P. Galek, A. Mackowiak, P. Bujewska and K. Fic, *Frontiers in energy research*, 2020, **8**.
34. B. Babu, P. Simon and A. Balducci, *Advanced energy materials*, 2020, **10**, 2001128-n/a.
35. M. D. Levi, E. A. Levi and D. Aurbach, *Journal of electroanalytical chemistry (Lausanne, Switzerland)*, 1997, **421**, 89-97.
36. J. H. Park, H. Yoon, Y. Cho and C.-Y. Yoo, *Materials*, 2021, **14**, 4683.
37. A. Nickol, T. Schied, C. Heubner, M. Schneider, A. Michaelis, M. Bobeth and G. Cuniberti, *Journal of the Electrochemical Society*, 2020, **167**, 90546.
38. M. F. Dupont and S. W. Donne, *Electrochimica acta*, 2015, **167**, 268-277.
39. M. F. Dupont and S. W. Donne, *Journal of the Electrochemical Society*, 2016, **163**, A888-A897.
40. A. Maćkowiak, P. Galek, P. Jezowski and K. Fic, *Electrochimica acta*, 2023, **463**, 142796.
41. K. Fic, A. Platek, J. Piwek and E. Frackowiak, *Materials Today*, 2018, **21**, 437-454.
42. M. Forghani and S. W. Donne, *Journal of the Electrochemical Society*, 2018, **165**, A593-A602.
43. M. Forghani, H. Mavroudis, J. McCarthy and S. W. Donne, *Electrochimica acta*, 2020, **332**, 135508.
44. M. Forghani and S. W. Donne, *Journal of the Electrochemical Society*, 2018, **165**, A664-A673.
45. W. Weppner and R. A. Huggins, *Journal of the Electrochemical Society*, 1977, **124**, 1569-1578.
46. B.-A. Mei, J. Lau, T. Lin, S. H. Tolbert, B. S. Dunn and L. Pilon, *Journal of physical chemistry. C*, 2018, **122**, 24499-24511.

Supplementary information for

Unraveling the effects of redox-active electrolytes on
carbon electrodes of Li-ion capacitor

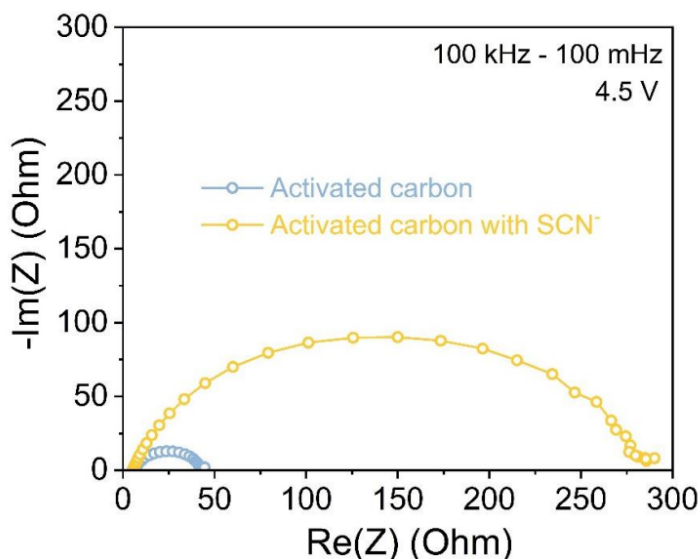


Figure S1. Impedance spectroscopy results of charged half-cells with activated carbon and activated carbon with thiocyanate salt as an electrolyte additive.

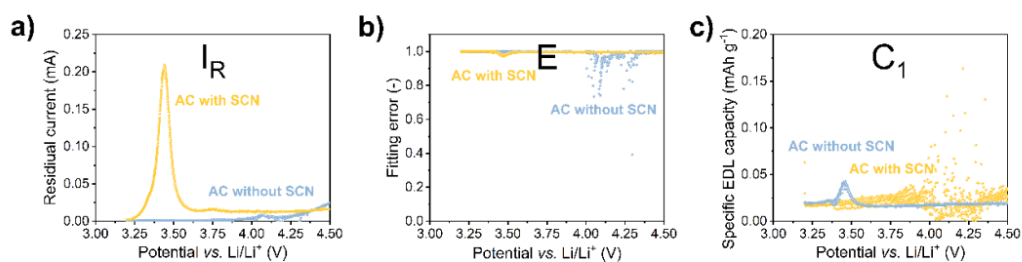


Figure S2. SPECS results of half-cells using activated carbon and activated carbon with thiocyanate salt as an electrolyte additive a) residual current (I_R) b) fitting error (E) and c) specific EDL capacity (C_1).

One-step assembly of metal-ion capacitors using redox-active electrolytes

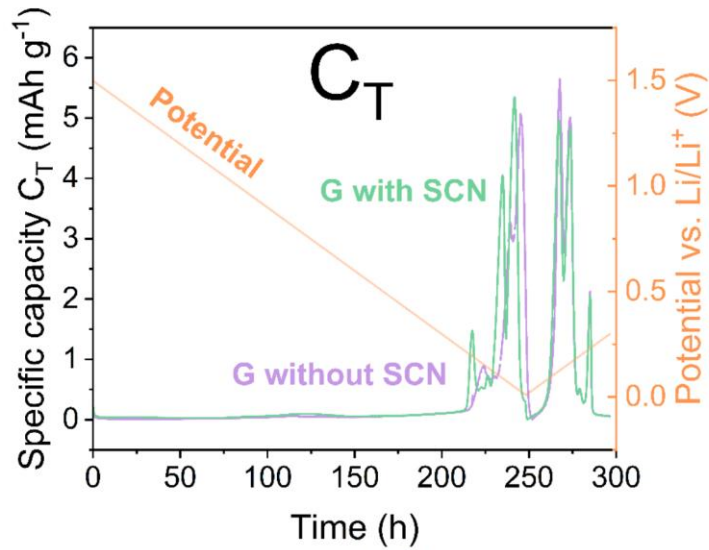


Figure S3. Total specific capacity calculated using SPECS for half-cells with graphite and graphite with thiocyanate salt as an electrolyte additive during charging and discharging.

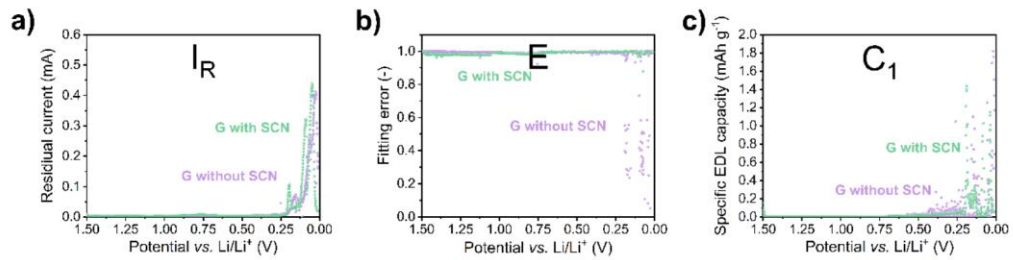


Figure S4. SPECS results of half-cells using graphite and graphite with thiocyanate salt as an electrolyte additive a) residual current (I_R) b) fitting error (E) and c) specific EDL capacity (C_1).

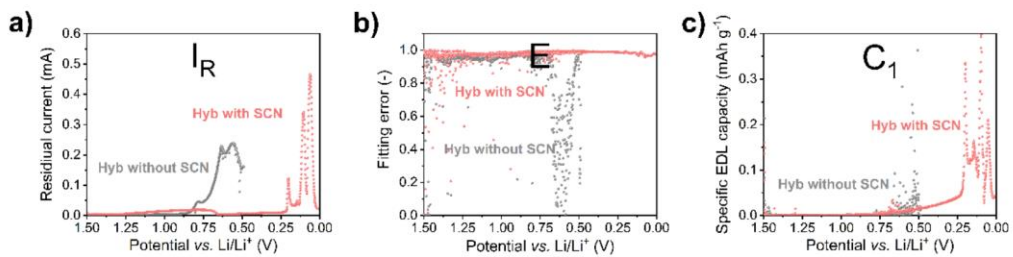


Figure S5. SPECS results of full cells using graphite and graphite with thiocyanate salt as an electrolyte additive a) residual current (I_R) b) fitting error (E) and c) specific EDL capacity (C_1).

One-step assembly of metal-ion capacitors using redox-active electrolytes

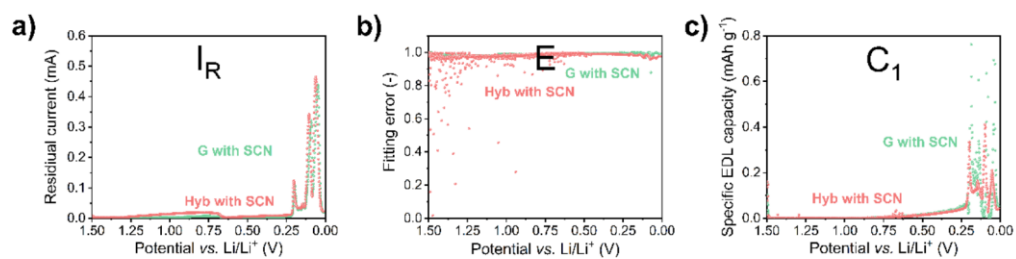


Figure S6. SPECS results of half-cell and full-cell using graphite with thiocyanate salt as an electrolyte additive a) residual current (I_R) b) fitting error (E) and c) specific EDL capacity (C_1).

Chapter V

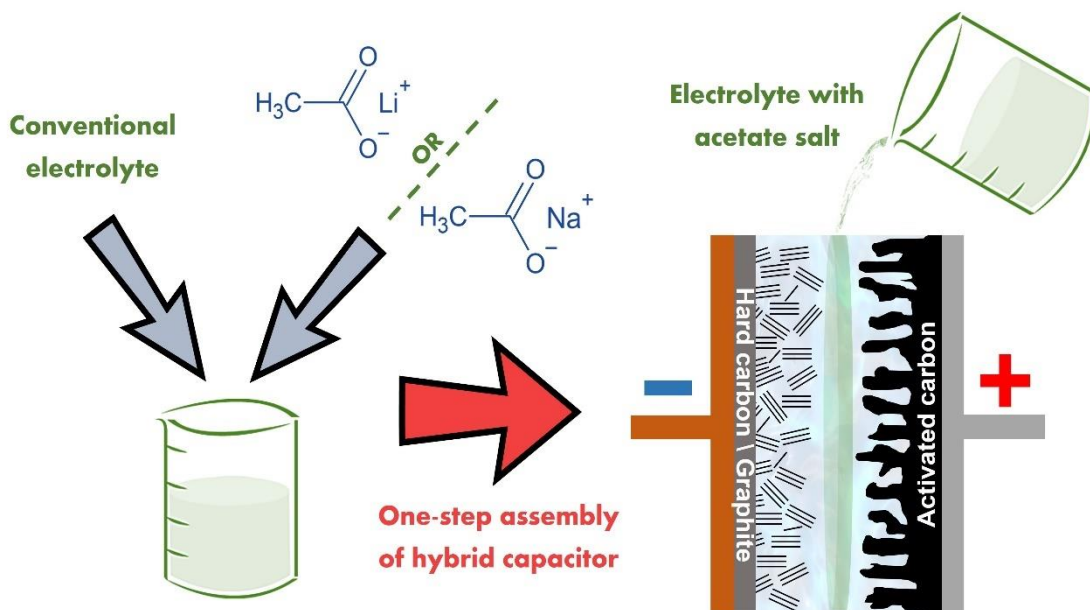
Redox-active additives to electrolyte for metal-ion capacitors

Article 3: *Unlocking the potential of acetates as electroactive additives to the electrolyte for lithium-ion and sodium-ion capacitors*

Article 3:

**Unlocking the potential of acetates as electroactive
additives to the electrolyte for lithium-ion and
sodium-ion capacitors**

Authors: **Adam Maćkowiak**, Paweł Jeżowski, Krzysztof Fic
Journal: Journal of Power Sources, **2024**, 616, 235089
DOI: doi.org/10.1016/j.jpowsour.2024.235089
Licence: The content is available under CC BY 4.0
Contribution: Writing – original draft, visualization, methodology, investigation,
formal analysis, data curation.



Context of the research and summary

The choice of a redox-active salt additive for the one-step pre-insertion approach of metal-ion capacitors is not straightforward. Such an additive must meet five criteria. The first criterion is that the salt must have a redox reaction. Without an oxidation reaction, there won't be additional capacity to balance the positive and negative electrode capacities. The second criterion is the reaction potential. This is crucial because even if the salt exhibits a reaction, if it occurs at a potential exceeding the decomposition potential of the electrolyte or electrode, it won't be applicable. Ideally, the reaction should occur significantly below the decomposition potential of the electrolyte, as different applied current densities can change the reaction potential, so it is wise to allow for a margin. The third criterion is that the reaction must be irreversible, meaning the oxidation of the electrolyte should occur. This is important because if the reaction is reversible, the positive electrode will function more like a battery than a capacitor which is not a case in this research. The fourth criterion is solubility in the electrolyte. If the salt is insoluble in the electrolyte, its reaction will either not occur or will occur to a very limited extent (with low efficiency). The final criterion is critical for the overall assessment of the cell's performance. Specifically, the theoretical capacity of the additive should be as high as possible relative to the mass of the salt. Each addition of salt increases the total mass of the system, as mentioned in **Manuscript 1**. Therefore, it is best to add a small amount of salt and achieve the highest possible capacity.

Meeting all these criteria is challenging but not impossible. Previous studies utilized thiocyanate salt (412 mAh g^{-1}), which proved effective in this approach and allowed for full intercalation of the graphite electrode and insertion of the hard carbon electrode. However, the choice of this salt was not random, as literature data indicated that thiocyanates exhibit redox activity [125], and our research group knew from experience that they could dissolve in an organic medium. It remained only to verify whether the reaction would be irreversible and if the intercalation would be possible.

One-step assembly of metal-ion capacitors using redox-active electrolytes

After the success of the studies with thiocyanate salt, the search for other redox-active additives to the electrolyte began. First, an attempt was made to use lithium carbonate (Li_2CO_3) with a theoretical capacity of 724 mAh g^{-1} . The higher theoretical capacity compared to thiocyanates was promising, as it allowed for the use of a smaller amount of salt. Additionally, it was believed that during the reaction, the lithium carbonate salt could oxidize to carbon dioxide, which could be easily removed using known techniques [211]. Thus, a half-cell of activated carbon vs. metallic lithium was assembled, and a small amount of lithium carbonate was added to the conventional electrolyte, then tested by galvanostatic charging assuming a C/20 current. As seen in **Figure 17a**, no redox reaction is observed for this salt. Moreover, with each cycle, the resistance in the system increases. The lack of reaction is most likely due to the salt not dissolving in the organic electrolyte, and its oxidation potential is probably higher than $4.5 \text{ V vs. Li/Li}^+$. Therefore, despite its enormous theoretical capacity, lithium carbonate salt is not suitable for application in the one-step assembly approach.

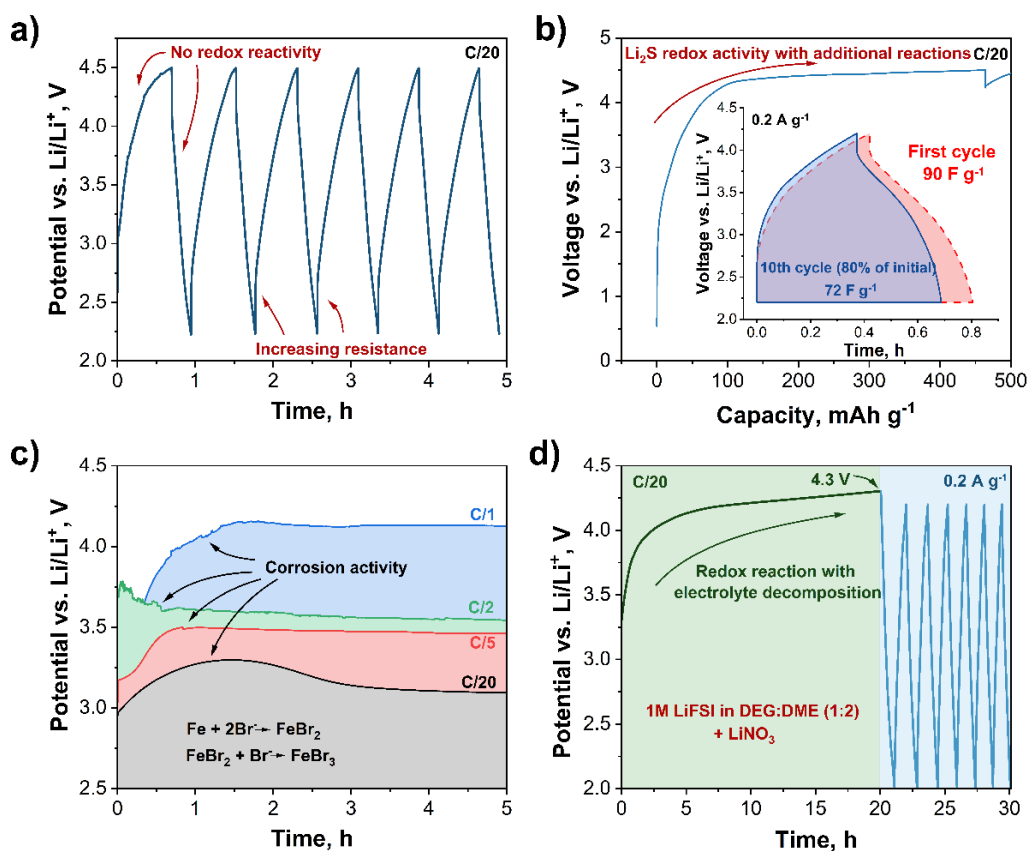


Figure 17. Electrochemical analysis of different redox-active additives to electrolyte a) Li_2CO_3 b) Li_2S c) LiBr d) LiNO_3 .

One-step assembly of metal-ion capacitors using redox-active electrolytes

The next tested additive to the electrolyte was lithium sulfide (Li_2S) salt. The theoretical capacity of lithium sulfide is 1165 mAh g^{-1} , which makes it almost three times higher than the capacity of thiocyanate salt. This allowed for a very small addition of the salt; however, despite this, it did not want to dissolve in the organic medium. Nevertheless, a half-cell of activated carbon vs. metallic lithium was first constructed, which showed additional activity at a potential of about 4.5 V vs. Li/Li^+ . Then, a full system of activated carbon vs. graphite was assembled where an attempt was made to use the one-step assembly technique (**Figure 17b**). Unfortunately, it turned out that additional capacity was obtained, probably related to the decomposition of the electrolyte. After testing the system for cyclic performance, a good capacity in the first cycle was observed, but it dropped sharply, and after 10 cycles, the system had less than 80% of the initial capacity.

Another salt tested was lithium bromide (LiBr). The capacity of this salt is 308 mAh g^{-1} ; however, it dissolves well in the organic electrolyte with EC:DMC. This compound was selected due to its known redox activity in aqueous electrolytes [124], so similar reactions were expected in an organic environment. Thus, a system of activated carbon vs. metallic lithium was assembled to check the activity of lithium bromide. Unfortunately, as shown in **Figure 17c**, the obtained capacity is significantly higher than the theoretical capacity. This is due to the corrosiveness of bromine towards metal current collectors, particularly stainless steel. Changing the collector to nickel or aluminum did not bring improvement, and protective layers made of conductive adhesives also did not protect the collectors from corrosion. Reducing the addition of bromides or using different charging currents also did not bring progress. Therefore, the use of lithium bromide was abandoned for the one-step assembly approach of metal-ion capacitors.

Next, lithium nitrate with a theoretical capacity of 388 mAh g^{-1} , similar to thiocyanates, was examined (**Figure 17d**). However, this salt completely did not dissolve in the organic electrolyte with EC:DMC. Therefore, it was decided to test the salt in another electrolyte – 1 M LiFSI in DEG:DME (1:2, v:v). Lithium nitrate dissolved fully in this electrolyte, but after assembling the half-cell, a very high reaction potential close to 4.5 V vs. Li/Li^+ was observed. For an electrolyte with

this solvent, this is relatively high, so part of the obtained capacity comes from the decomposition of the electrolyte. The additional electrolyte decomposition caused a subsequent drop in the system's capacity.

The last salt tested was lithium acetate (LiOAc), and the results obtained from the studies on this salt are presented in **Article 3**. LiOAc has a theoretical capacity of 406 mAh g⁻¹. Its organic structure was expected to aid in the solubility in the EC:DMC electrolyte. Here, similar to the case of lithium carbonate, it was anticipated that the main oxidation product would be carbon dioxide. Therefore, tests were conducted in half-cells, activated carbon vs. metallic lithium, starting with cyclic voltammetry, which confirmed the redox activity of lithium acetate at a potential of about 3.75 V vs. Li/Li⁺. This reaction is minimally reversible, disappearing completely after a few cycles. Then, galvanostatic charge and discharge tests were performed, confirming that a capacity of 342 mAh g⁻¹ was obtained in the first cycle. After a few cycles, the redox activity fades, and the electrode behaves like an electrochemical capacitor. Following the optimistic results in the half-cell, it was decided to attempt intercalation in a full cell with graphite vs. activated carbon (using metallic lithium as the reference electrode). The intercalation of the graphite electrode was successful – achieving a full one-step assembly approach in a Li-ion capacitor by using a redox-active electrolyte. The results were compared with tests without acetate additives, confirming that the presence of LiOAc is crucial for pre-intercalation. The system was then cycled, and it was noted that it easily withstood 100 charge and discharge cycles from 2.2 to 3.8 V. Following the success with LiOAc, it was decided to test sodium acetate. Similarly to lithium, the studies began with a half-cell where galvanostatic charge and discharge tests and cyclic voltammetry were conducted. In the case of cyclic voltammetry, the curve was different from lithium – a complete lack of reaction reversibility and a potential shift to 4.1 V vs. Na/Na⁺. The observed differences between the sodium and lithium systems are likely due to the varying accessibility of OAc⁻ to the activated carbon pores. The solvation shell radii of Li⁺ and Na⁺ ions in the organic medium are 4.0 and 5.7 nm, respectively. During the polarization of the positive electrode, ionic attraction pulls Li or Na ions along with the anions. Li⁺ ions have a well-defined solvation shell involving only the carbonyl

oxygens of EC molecules, while Na⁺ ions' solvation shell includes both carbonyl and ether oxygens. This allows solvated Li ions to more effectively penetrate the mesopores of the positive electrode, bringing acetate closer to the activated carbon and facilitating faster reactions. In contrast, the larger solvated Na ions cannot fully penetrate the mesopores, causing the acetate reaction to primarily occur on the electrode's outer surface. Nevertheless, a capacity of 307 mAh g⁻¹ was obtained in the first cycle, allowing for an attempt to intercalate the anode material – hard carbon. Thus, after assembling the full cell, hard carbon vs. activated carbon (with sodium metal as the reference electrode), the successful insertion of sodium ions into the negative electrode was confirmed. The system also easily withstood 100 charge and discharge cycles. Finally, the specific energy and power values were determined for the Li-ion capacitor (104 Wh kg⁻¹ and 368 W kg⁻¹) and Na-ion capacitor (89 Wh kg⁻¹ and 22 W kg⁻¹). In the next section of **Article 3**, the gases released during pre-insertion in both Li-ion and Na-ion capacitors with redox electrolyte were examined using gas chromatography with mass spectrometry. During the operation of the sodium hybrid, a significant increase in mass 44, indicating carbon dioxide, was observed as previously assumed. However, during the operation of the lithium hybrid, no increase in mass 44 was observed, suggesting a different pathway of the oxidation reaction. These studies confirm the different curves from cyclic voltammetry. This proves that the cation itself has a significant impact on the course of the reaction and the charge storage process.

Article 3

One-step assembly of metal-ion capacitors using redox-active electrolytes

Journal of Power Sources 616 (2024) 235089



Contents lists available at ScienceDirect

Journal of Power Sources

journal homepage: www.elsevier.com/locate/jpowsour



Unlocking the potential of acetates as electroactive additives to electrolytes for lithium-ion and sodium-ion capacitors

Adam Maćkowiak^a, Paweł Jeżowski^a, Krzysztof Fic^{a,b,*}

^a Poznan University of Technology, Institute of Chemistry and Technical Electrochemistry, Berdychowo 4, 60-965, Poznan, Poland

^b Lukasiewicz Research Network – Institute of Non-Ferrous Metals Division in Poznan, Central Laboratory of Batteries and Cells, Forteczna 12, 61-362 Poznan, Poland

HIGHLIGHTS

- Acetate anion demonstrates redox activity in aprotic medium.
- Redox-active electrolyte allows for facilitated assembly of hybrid capacitor.
- One-step pre-insertion is possible for various anode materials and metal ions.

ARTICLE INFO

Keywords:

Lithium-ion capacitor
Sodium-ion capacitor
One-step pre-intercalation
Lithium acetate
Sodium acetate
Metal-ion capacitor

ABSTRACT

Among energy storage systems, lithium-ion and sodium-ion capacitors have recently gained increasing attention. However, the pre-metalation stage remains a challenge in constructing and further developing these capacitors for industrial application. In this article, we report on the system with acetate salts added to the electrolyte solution to facilitate the assembly of metal-ion capacitors in a one-step process. At a specific concentration, acetate anions underwent chemical reactions, providing the charge to balance the system and enabling the negative electrode to undergo complete insertion. Two- and three-electrode studies demonstrated the performance of the full cell as well as of each electrode. The lithium-ion and sodium-ion capacitors achieved energy values of 104 Wh kg⁻¹ and 89 Wh kg⁻¹ at power densities of 368 W kg⁻¹ and 22 W kg⁻¹, respectively. The reported systems surpassed 100 cycles of charging and discharging. Moreover, *operando* gas chromatography with mass spectrometry was employed to identify the gases generated during the acetate reaction, and no toxic gases were identified. It has also been demonstrated that the hybrid cell response depends on the reaction origin (within the pores of activated carbon or on the external electrode surface). However, the acetate anions effectively serve as electrolyte additives, enabling the one-step assembly of metal-ion capacitors.

1. Introduction

Hybrid energy storage systems (HES) represent a rising and evolving category of energy storage devices that combine the inherent advantages of electrochemical double-layer capacitors (EDLCs) and lithium-ion batteries (LIBs) [1–5]. HES utilize the advantages of EDLCs, such as high power densities and extended cyclability, and also provide substantial energy density, which is characteristic of LIBs [2,6].

Graphite (with a theoretical capacity of 372 mAh g⁻¹) is commonly employed as the negative electrode in lithium-ion capacitors [7]. In contrast, in sodium-ion systems, graphite is substituted with hard carbon (~320 mAh g⁻¹) because sodium cannot intercalate into pure graphite [8,9]. Due to the concerns about lithium accessibility, recent research

has shifted towards sodium as a more cost-effective alternative resource despite its lower energy density. Consequently, there is an increasing number of papers reporting on sodium-ion capacitors [10–12]. However, a crucial pre-metalation stage is still needed, regardless of whether the capacitor is a lithium or sodium-ion capacitor [10,13]. During this stage, lithium/sodium ions are inserted into the structure of the negative electrode, enabling the maintenance of the electrode at very low potential (close to 0 V vs. Li/Li⁺ or Na/Na⁺); thus, metal plating on the surface of the electrode is prevented [14,15].

Various approaches are used to perform the pre-metalation stage, and one widely employed approach involves the use of an auxiliary metallic electrode [16]. This method exploits initial assembling a half-cell with a metallic electrode, charging it to the potential close to

* Corresponding author.

E-mail address: krzysztof.fic@put.poznan.pl (K. Fic).

<https://doi.org/10.1016/j.jpowsour.2024.235089>

Received 2 May 2024; Received in revised form 20 June 2024; Accepted 20 July 2024

Available online 31 July 2024

0378-7753/© 2024 The Author(s). Published by Elsevier B.V. This is an open access article under the CC BY license (<http://creativecommons.org/licenses/by/4.0/>).

One-step assembly of metal-ion capacitors using redox-active electrolytes

A. Maćkowiak et al.

Journal of Power Sources 616 (2024) 235089

10 mV vs. Li/Li^+ or Na/Na^+ , disassembling the cell, and subsequently reassembling it with another positive electrode, which is usually composed of activated carbon. This method has been modified over the years, and contemporary practices involve assembling a full cell with a minor addition of lithium particles, which dissolve during the initial cycle and facilitates the pre-metalation of the electrode [17]. Nonetheless, this method remains costly and carries a high risk of short-circuits due to metal dendrites, which can form easily. An alternative method involves a composite (most often positive) electrode, which combines activated carbon with a sacrificial salt [18,19]. During the initial charging, the sacrificial salt releases lithium or sodium ions into the electrolyte, allowing the negative electrode to undergo pre-metalation. Nevertheless, metal oxides often remain within the system, constituting a dead mass that can deteriorate cell performance [20]. In 2012, a new approach was introduced in which the negative electrode was intercalated directly from a concentrated electrolyte (2 mol L^{-1} lithium bis(trifluoromethane)sulfonylimide (LiTFSI) in 1:1 ethylene carbonate:dimethyl carbonate (EC:DMC) [21]. However, this method induces a decrease in the electrolyte conductivity, which affects the overall cell performance, and many challenges must be overcome to reach the 1st stage of intercalation. Therefore, selecting the appropriate electrolyte concentration is crucial for the intercalation process [22]. In a recent study, researchers modified previous approaches by incorporating a redox-active electrolyte, facilitating complete intercalation without compromising electrolyte conductivity [9]. The abovementioned approach holds considerable potential for further exploration, as the thiocyanate salt used in the study can be changed to another electro-active specimen.

Most recent research has imposed specific imperatives for all materials, electrolytes, and additives to prioritize environmental compatibility [23,24]. Acetate salts are derived from renewable sources and can be biodegradable under the right conditions [25–27]. While acetate salts have been well-characterized in aqueous electrolytes [28–30], their utilization in the organic medium is limited due to their moderate solubility. However, only small quantities of these salts are needed in the pre-metalation approach involving redox-active electrolytes; thus, the additives are less prone to inducing toxic reactions and tend to undergo oxidation to carbon dioxide [9,31]. These unique characteristics envisage acetate salts as highly viable candidates for the pre-metalation method.

This article describes the exploitation of organic salt, i.e., lithium acetate (LiOAc) and sodium acetate (NaOAc) as electrolyte additives, to facilitate a one-step pre-metalation process (Fig. 1).

The underlying hypothesis assumed that the acetate redox reaction occurs during the initial charging cycle, affecting the capacitance of the

positive electrode and its potential slope while simultaneously enabling the insertion of metal ions into the negative electrode. The acetate reaction plays a crucial role on the positive electrode by compensating the insertion charge on the negative electrode, thereby allowing complete intercalation. Notably, as acetate anion should decompose to CO_2 , the gas generated is non-toxic and can be readily eliminated [32].

2. Results and discussion

2.1. Acetate activity in the electrolyte

The main aim of this research was to perform pre-metalation of negative electrode in one step using an electrolyte with lithium or sodium salt with acetate anions. The acetate salt was expected to react on the positive electrode at potential values lower than the electrolyte decomposition, providing the charge to compensate the insertion process on the negative electrode. Additionally, the salt dissociation releases Li^+ or Na^+ cations, which are necessary for maintaining the electrolyte conductivity and the balance of the Li^+ or Na^+ concentration in the electrolyte. The acetate reaction was expected to generate a gaseous byproduct that could be removed using known cell production methods [32].

To confirm these assumptions, half-cell measurements were performed. The systems were assembled with one electrode composed of metallic lithium and another composed of activated carbon. Both electrodes were separated with a glass fibre membrane soaked with 1 M LiPF_6 , which was dissolved in a mixture of ethylene carbonate (EC) and dimethyl carbonate electrolyte (DMC) with the addition of CH_3COOLi (LiOAc). The quantity of salt was calculated based on the Faradaic law and adjusted to the theoretical capacity of graphite (see Supporting Information file). This half-cell study aimed to demonstrate that LiOAc reacts at potential values lower than the electrolyte decomposition potential. As depicted in Fig. 2a, cyclic voltammetry was conducted at 0.04 mV s^{-1} , corresponding to a C/20 current rate ($C = 372 \text{ mA g}^{-1}$).

The results revealed that the [OAc] reaction started at approximately 3.75 V vs. Li/Li^+ . Moreover, the [OAc] reaction shows a diminishing charge with each cycle, with limited reversibility observed. Thus, the observed behaviour of LiOAc suggests its applicability in electrolyte-guided intercalation methods. Subsequently, a new system was assembled in the same configuration, and galvanostatic charge/discharge tests with C/20 were conducted (Fig. 2b). Similar reactions were observed in the first cycle, resulting in a positive electrode charge of 342 mAh g^{-1} . Naturally, the presented value was estimated based on the plateau observed on the galvanostatic curve. Notably, the assumed capacity includes the charge accumulated by double-layer charging, and

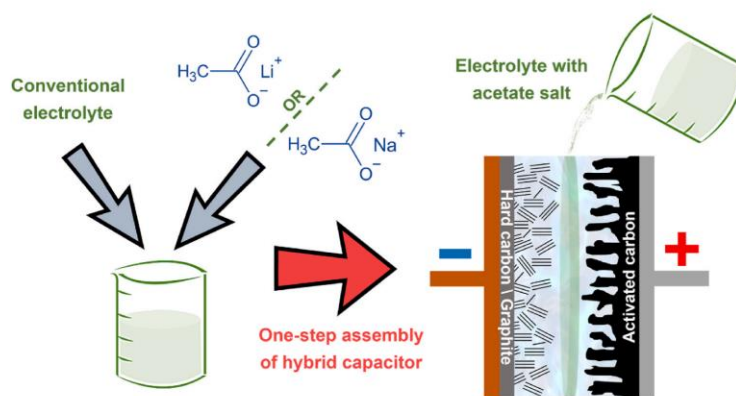


Fig. 1. Schematic representation of the assembly of hybrid metal-ion capacitors with an electrolyte containing acetate salt.

2

One-step assembly of metal-ion capacitors using redox-active electrolytes

A. Maćkowiak et al.

Journal of Power Sources 616 (2024) 235089

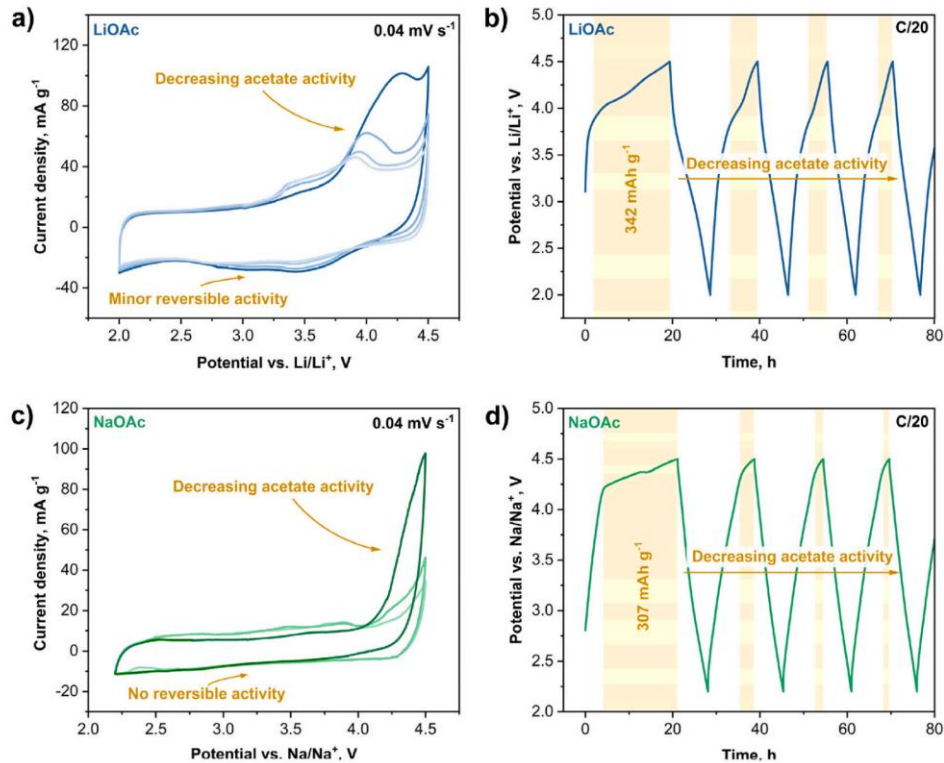


Fig. 2. Reaction of acetate anions during the measurement in the half-cell with activated carbon vs. the metallic lithium or sodium electrode: a), c) cyclic voltammetry with a scan rate of 0.04 mV s⁻¹ and b), d) galvanostatic charge/discharge with potential limitation and a current density equal to C/20.

the following cycles revealed diminishing acetate activity, indicating that the reaction was incomplete.

Later, a system with metallic sodium was assembled, and the electrolyte was switched to 1 mol L⁻¹ NaClO₄ dissolved in a mixture of EC and propylene carbonate (PC) electrolyte with a calculated addition of NaOAc (Fig. 2c). Here, a completely irreversible reaction was observed in contrast to that of the lithium-based cell. The oxidation potential was shifted towards a higher value, commencing at 4.1 V vs. Na/Na⁺. Compared to the lithium half-cell, the Na-based system underwent galvanostatic charging at a current rate of C/20 (Fig. 2d). In this context, C corresponds to the theoretical capacity of hard carbon material, specifically 320 mAh g⁻¹ [9]. The observed differences between the sodium and lithium systems most likely resulted from the different accessibility of [OAc]⁻ to the activated carbon pores. The solvation shell radii of Li⁺ and Na⁺ ions in the organic medium are 4.0 and 5.7 nm, respectively. During the polarization of the positive electrode, the ionic attraction between electrolyte molecules causes Li or Na ions to be attracted along with the anions. The well-defined first solvation shell of Li⁺ involves only carbonyl oxygens of EC molecules, whereas those of Na⁺ consist of carbonyl and ether oxygens [33,34]. Therefore, solvated Li ions can more effectively penetrate the mesopores of the positive electrode, moving [OAc]⁻ closer to the activated carbon and facilitating quicker reactions. Conversely, the solvated Na⁺ cations were too large to penetrate the mesopores fully, and the [OAc]⁻ reaction mainly occurred on the outer surface of the electrode. Notably, the potential of NaOAc oxidation might be too high and overlap with the electrolyte decomposition potential, suggesting that the carbon electrode should be further optimized to enhance Na ion accessibility. Nevertheless, both

LiOAc and NaOAc meet the requirements for potential intercalation/insertion from the electrolyte in metal-ion capacitors at the proof-of-concept stage.

2.2. Metal-ion capacitors assembled in one step

After the potential of the [OAc]⁻ reaction was established, the next objective was to determine whether this reaction facilitated the intercalation or insertion of cations into the structure of the negative electrode. For this purpose, a full cell comprising a negative electrode (graphite) and a positive electrode (activated carbon) was assembled using the electrolyte with lithium acetate, and the cell was charged with a C/20 current (Fig. 3a).

The potential slope of the positive electrode was modified by the LiOAc activity, facilitating the complete intercalation of the negative electrode. Another system lacking [OAc]⁻ ions was prepared for comparative analysis. In this scenario, the absence of a plateau region in the positive electrode response caused the potential cut-off limit to be reached quickly, impeding the intercalation process of the negative electrode. Subsequently, the charged cell underwent cycling (Fig. 3b), achieving a reasonable initial capacitance of 26 F g⁻¹. Remarkably, the initial capacitance of the system was notably efficient (exceeding 80 %) even after 100 cycles. Nonetheless, a marginal degradation of the negative electrode was observed.

The experiment was subsequently replicated for the sodium-ion capacitor. When Na-based systems are assembled, graphite is substituted with hard carbon because sodium cannot intercalate effectively into pure graphite [8]. Researchers generally believe this inability

3

One-step assembly of metal-ion capacitors using redox-active electrolytes

A. Maćkowiak et al.

Journal of Power Sources 616 (2024) 235089

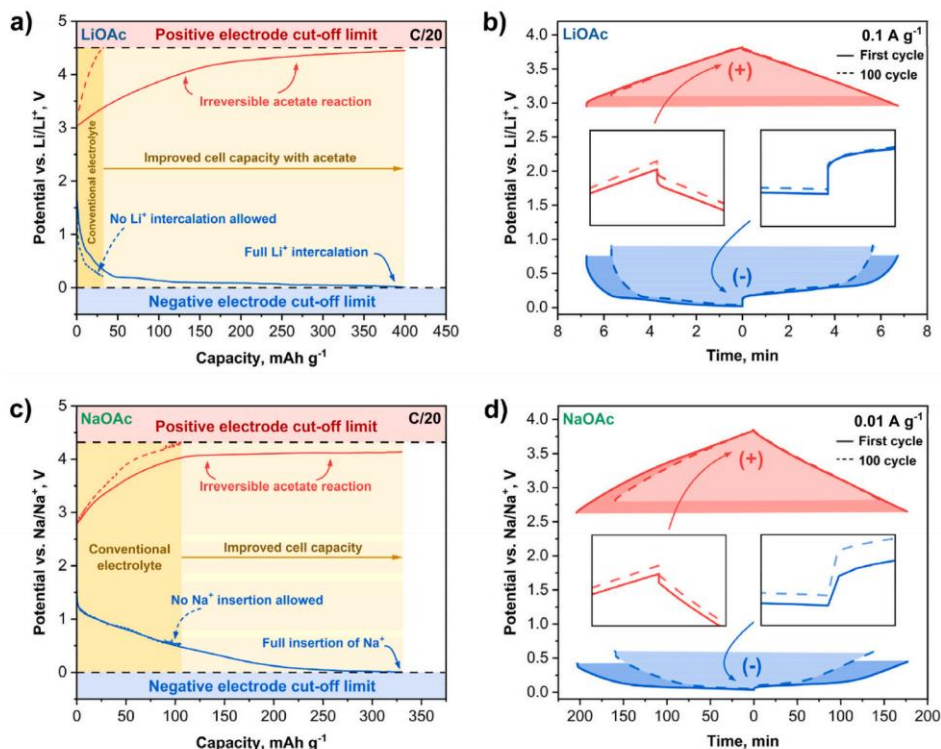


Fig. 3. Three-electrode measurements using an irreversible $[OAc]^-$ reaction to balance the negative electrode: a), c) first galvanostatic charging of the positive and negative electrodes using C/20 enabling pre-intercalation/pre-insertion of cations into the structure of the negative electrode and b), d) galvanostatic charging/discharge of the full cell; first and hundredth cycle.

stems from the mismatch in size between sodium and the interlayer spacings of graphite. Still, the primary factor involves alterations in the chemical bonding between the alkali metal ions and carbon atoms [35, 36]. Sodium-ion capacitors feature a distinct mechanism of SEI formation involving the insertion of sodium ions into the structure of hard carbon [37]. Nonetheless, the approach outlined in this study was successful, and complete sodium ion insertion into the hard carbon structure was achieved (Fig. 3c). However, full insertion was not achieved in a system without $[OAc]^-$ because the cut-off limit of the positive electrode was reached. The first and 100th cycles of the system are depicted in Fig. 3d, demonstrating that the system can provide a satisfactory capacitance of 67 F g^{-1} at a low current regime.

The initial charging was conducted up to 4.5 V vs. Li/Li^+ or vs. Na/Na^+ , which is a relatively high potential. However, the subsequent positive electrode performance was limited to 3.8 V vs. Li/Li^+ or vs. Na/Na^+ , and $[OAc]^-$ remained in the system as a dead mass due to an incomplete reaction. Therefore, the system can be enhanced by optimizing the salt additive, the size and porosity of the positive electrode or the applied current regime. Nevertheless, the provided systems work efficiently, achieving energy values of 104 Wh kg^{-1} and 89 Wh kg^{-1} at power densities of 368 W kg^{-1} and 22 W kg^{-1} for the lithium-ion and sodium-ion capacitors, respectively. The literature indicates that energy densities for Li-ion capacitors generally fall between 10 and 100 Wh kg^{-1} , with power densities ranging from 10 to 5000 W kg^{-1} [38,39]. For Na-ion capacitors, literature values suggest energy densities of 10–80 Wh kg^{-1} and power densities from 10 to $12,000 \text{ W kg}^{-1}$ [40].

The stability of the metal-ion capacitor is a crucial parameter, indicating how the capacitor maintains its performance over time.

According to literature, the stability of metal-ion capacitors can vary, depending on the specific materials and electrolytes used. For example, typical Li-ion capacitors using different electrolytes show stability ranging from 5000 to 50,000 cycles [41,42]. Na-ion capacitors often show stability between 500 and 30,000 cycles [40,43]. In the case of acetate-containing systems, the cyclability is not that high, reaching slightly more than 400 cycles for Li-based systems. Nevertheless, further investigations and optimizations could enhance the stability of these devices, potentially leading to better performance in practical applications.

2.3. Operando GC-MS investigation

In the subsequent step, various aspects were investigated, such as gases produced during cell polarization and whether $[OAc]^-$ anion converts to CO_2 , as previously hypothesized. For this purpose, full lithium-ion and sodium-ion capacitors were investigated using operando gas chromatography with mass spectrometry (GC-MS). During the initial charging cycle of the lithium-ion capacitor, the first signal observed corresponds to $m/z = 26$; these results were indicative of acetylene or ethylene, suggesting that the SEI layer is formed (Fig. 4a) [44]. Throughout the subsequent process, there was no significant increase in any of the gases, indicating that the initial reaction product must be soluble in a transitional form in the electrolyte. Interestingly, there was no significant increase in CO_2 ($m/z = 44$), and a decrease in CO_2 was observed at a later stage. Simultaneously, as the CO_2 signal decreased, the signals from fragmentary ions with masses of 42 (C_3H_6 , $\text{C}_2\text{H}_2\text{O}$), 47 (CH_3O_2^-) and 73 ($\text{C}_3\text{H}_5\text{O}_2$) increased. Therefore, the $[OAc]^-$ ion might

One-step assembly of metal-ion capacitors using redox-active electrolytes

A. Maćkowiak et al.

Journal of Power Sources 616 (2024) 235089

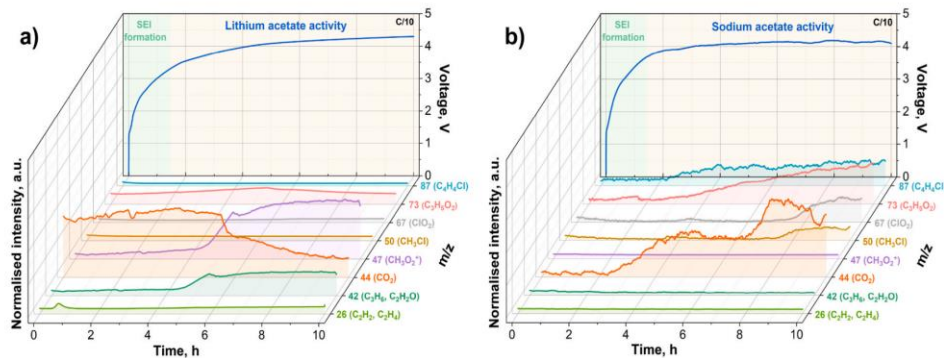


Fig. 4. Comparison of significant masses released during *operando* GC-MS of hybrid capacitors assembled using a one-step approach: a) lithium-ion capacitor and b) sodium-ion capacitor.

initially trigger oxidation to carbon dioxide, while CO_2 is immediately electrochemically reduced to numerous organic compounds. The electrochemical reduction of CO_2 is well known in aqueous electrolytes, in which CO_2 forms CO , HCOOH , HCHO , CH_3OH or CH_4 [45]. However, the electrochemical reduction product in an organic medium depends on the electrolyte used in the reaction. With this mixture of organic compounds in the electrolyte, the product of its reduction may be methane, ethylene, ethanol, formic acid and other higher hydrocarbons or oxygenates [46]. Nevertheless, the obtained compounds were believed to be soluble in the organic electrolyte, suggesting that the compounds will not significantly affect the further electrochemical operation of the system. This experiment demonstrates that the reaction differs from the typical acetate oxidation to CO_2 . The various fragmentary ions obtained from the measurements indicate that the organic substituent exerts a considerable influence; therefore, the system should be further investigated to identify the main products of the reaction.

Next, a sodium-ion capacitor with an acetate-containing electrolyte was investigated (Fig. 4b). Here, no significant GC-MS signal for SEI formation was detected because a negative electrode composed of hard carbon was utilized [9]. Interestingly, in this case, a relevant increase in CO_2 was observed. Halogens were detected because different salts were used in the electrolyte. Fragmentary ions with masses of 50 (CH_2Cl), 67 (ClO_2), and 87 ($\text{C}_4\text{H}_4\text{Cl}$) were generated from reactions associated with the decomposition of the electrolyte, i.e., the NaClO_4 salt with the solvents (PC and EC). Additionally, one of the characteristic masses was 73 ($\text{C}_3\text{H}_5\text{O}_2$), which is common for both lithium-ion and sodium-ion capacitors. Based on the increase in signal from mass 73, the mass resulted from a reaction between the solvents and carbonate salt. Despite all the masses, the rise in CO_2 was the primary reaction that occurred in the system; in contrast, CO_2 reduction most likely happened in the lithium-ion system. Therefore, a completely different chemical reaction can occur when the reaction occurs inside the pores and when the reaction occurs only on the external surface of the electrode. Moreover, the type of electrolyte used might affect the reactions; however, gas derivatives of fluorine or phosphorus were not observed in the lithium system, so the location of the reaction might play a crucial role.

Additionally, the electrochemical stability of the electrolytes was evaluated, as illustrated in Fig. S1. The lithium acetate salt presence did not impact electrolyte stability notably. This implies that the porous carbon electrode, with its large specific surface area, may play a significant role in determining the type and kinetics of acetate reactions during the charging process of the full hybrid system. Conversely, in the sodium electrolyte, the presence of acetate salt was found to reduce electrolyte stability. These stability studies support the findings from the *operando* GC-MS study, highlighting different reactions for lithium acetate and sodium acetate. Specifically, sodium acetate undergoes

electrochemical decomposition due to potential differences, while the decomposition of lithium acetate is primarily influenced by the positive electrode, resulting in a distinct reaction mechanism.

3. Conclusions

The present research demonstrated the electrochemical activity of LiOAc and NaOAc , which can be successfully implemented in the pre-metalation of lithium-ion and sodium-ion capacitors. A difference in activity potentials between the two systems was observed due to the difference in the sizes of solvated lithium acetate and sodium acetate molecules and their influence on the penetration of pores in the positive electrode. The electrolyte also affects the reactions, as confirmed by *operando* GC-MS analysis. Significant CO_2 emission was only observed for sodium acetate. With lithium-ion cells, the acetate reaction differs but remains irreversible and can be used for one-step intercalation. The electrochemical activity of the acetates was most likely molecular oxidation, and the charge obtained from this reaction fully enabled intercalation/insertion of the negative electrode. The results confirmed that $[\text{OAc}]^-$ can be used for the one-step assembly of hybrid metal-ion capacitors. The one-step assembly system can provide several advantages, such as decreased production costs, accelerated cell assembly, and the lack of metallic electrode, the use of which may be dangerous. Based on these advantages, this method shows enormous potential, and using acetates as electroactive additives to electrolytes is an example of this approach.

4. Experimental

Electrolyte. Salts: lithium hexafluorophosphate (LiPF_6), sodium perchlorate (NaClO_4), lithium acetate dihydrate ($\text{LiOAc} \cdot 2\text{H}_2\text{O}$) and sodium acetate trihydrate ($\text{NaOAc} \cdot 3\text{H}_2\text{O}$) were purchased from Sigma-Aldrich (Merck). Before use, all salts were dried under vacuum at 120°C for one week to remove water contamination. Lithium acetate dihydrate and sodium acetate trihydrate salts were predried at 100°C utilizing a liquid nitrogen cold trap to eliminate excess water. The anhydrous solvents propylene carbonate (PC), ethylene carbonate (EC) and dimethyl carbonate (DMC) were obtained from Merck. The lithium cell electrolyte was a 1:1 volumetric ratio of 1 M solution of LiPF_6 in a mixture of EC and DMC (13.45 mS cm^{-1} , 4.11 mPa s) combined with the addition of a calculated quantity of LiOAc salt (12.68 mS cm^{-1} , 4.54 mPa s). For sodium investigations, the prepared electrolyte was a 1-M solution of NaClO_4 in EC and PC mixed in a 1:1 volumetric ratio (8.7 mS cm^{-1} , 6.88 mPa s) with the addition of a calculated quantity of NaOAc salt (8.4 mS cm^{-1} , 6.95 mPa s). Detailed conductivity and viscosity results are presented in Fig. S2. The mass of acetate salts added to

5

One-step assembly of metal-ion capacitors using redox-active electrolytes

A. Maćkowiak et al.

Journal of Power Sources 616 (2024) 235089

each electrolyte was determined based on the mass of each negative electrode and its theoretical capacity. Subsequently, 650 μL of the prepared electrolyte was added to soak the separators during the electrochemical cell assembly. All reagents were stored in an MBraun glovebox under inert environmental conditions. The conductivity measurements were performed at 25 $^{\circ}\text{C}$ using a 2-electrode Swagelok system with a spacer, and the impedance spectroscopy method was used to calculate the conductivity from the resistance. Viscosity measurements were made by a plate-cone rheometer (Brookfield – model DV2T).

Electrode material. The negative electrode of the hybrid Li-ion capacitor was made of copper foil covered with artificial graphite (total thickness = 100 μm) and was provided by Customcells[®]. The negative electrode of the hybrid Na-ion capacitor was a laboratory-prepared electrode made of copper foil coated with a mixture of hard carbon (Carbotron P, Kureha), polyvinylidene fluoride (PVDF) and carbon black (total thickness = 93 μm). The positive electrode of all metal-ion capacitors was a self-standing electrode made of Kuraray YP80F (80 %), polytetrafluoroethylene (PTFE) (10 %) and carbon black C65 (10 %) (total thickness = 114 μm). The surface area of the positive electrode was 1558 $\text{m}^2 \text{g}^{-1}$ [47]. The microtextural characteristics of the positive electrode were determined by using the Brunauer–Emmett–Teller (BET) isotherm method (77 K) with N_2 as an adsorbate (ASAP 2460, Micromeritics, USA). Before the adsorption/desorption steps, the samples were flushed at 350 $^{\circ}\text{C}$ for 12 h under continuous helium flow and further degassed at 25 $^{\circ}\text{C}$ for 5 h (vacuum). The reference electrodes were made from metallic lithium (Merck) and metallic sodium (Alfa Aesar).

Cell assembly. Round electrodes (diameter = 16 mm, surface area = 2 cm^2) were cut from the positive and negative electrode materials using EL-Cut, a tool provided by EL-CELL[®]. The active mass ratio of the electrodes was maintained at approximately 1:1. The electrolyte was freshly prepared before each cell was assembled. The positive and negative electrodes were then positioned in the ECC-REF electrochemical cell (supplied by EL-CELL[®]) and separated by two glass fibre discs (diameter = 18 mm, GF/D, Whatman[®]) saturated with 650 μL of electrolyte. The reference electrode was introduced into the reference pinhole using an ECC loader (provided by EL-CELL[®]). For half-cell measurements, the counter and reference electrodes, represented by metallic lithium and metallic sodium, were shaped as discs with a diameter of 16 mm. All cell assembly procedures were conducted within a glovebox (MBraun) to maintain minimal water and oxygen levels, ensuring concentrations below 0.1 ppm.

Electrochemical investigation. Electrochemical measurements were performed using the ECC-Ref and PAT-Cell-Gas systems provided by EL-CELL[®]. Cyclic voltammetry and galvanostatic cycling with potential limitations were conducted through a multichannel galvanostat/potentiostat (VMP-3 BioLogic[®]) at room temperature (21 $^{\circ}\text{C}$). An EVOQ GC-TQ[™] MS instrument (Bruker[®]) connected to the PAT-Cell-Gas system from EL-CELL[®] was used for gas chromatography with mass spectrometry (GC-MS) analysis. The electrochemical cell was placed within a thermostatic chamber at a temperature of 25 $^{\circ}\text{C}$. The specific temperature settings for the GC-MS analysis included an injector temperature of 200 $^{\circ}\text{C}$, a column temperature of 175 $^{\circ}\text{C}$, and a mass spectrometer temperature of 220 $^{\circ}\text{C}$. The electrochemical stability tests were performed in volume cells in a three-electrode configuration, where the working electrode was glassy carbon, the counter electrode was platinum, and the reference electrode was metallic lithium or metallic sodium. The stability studies employed the linear sweep voltammetry (LSV) technique with a scan rate of 0.04 mV s^{-1} .

CRedit authorship contribution statement

Adam Maćkowiak: Writing – original draft, Visualization, Methodology, Investigation, Formal analysis, Data curation. **Paweł Jeżowski:** Writing – original draft, Validation, Supervision, Methodology, Investigation, Funding acquisition. **Krzysztof Fic:** Writing – review

& editing, Writing – original draft, Supervision, Software, Resources, Project administration, Methodology, Investigation, Funding acquisition, Formal analysis, Conceptualization.

Declaration of competing interest

The authors declare that they have no known competing financial interests or personal relationships that could have appeared to influence the work reported in this paper.

Data availability

Data will be made available on request.

Acknowledgements

This work was financially supported by the European Research Council within the Starting Grant project (GA 759603) and the Proof of Concept project (GA 101138710). P.J. would like to acknowledge the Foundation for Polish Science for the START 2019 programme as well as the Polish National Agency for Academic Exchange for the stipend PPN/BEK/2018/1/00123.

Appendix A. Supplementary data

Supplementary data to this article can be found online at <https://doi.org/10.1016/j.jpowsour.2024.235089>.

References

- [1] B. Babu, A. Balducci, Journal of Power Sources Advances 5 (2020) 100026.
- [2] Y. Sun, J. Tang, F. Qin, J. Yuan, K. Zhang, J. Li, D.-M. Zhu, L.-C. Qin, J. Mater. Chem. A 5 (2017) 13601–13609.
- [3] J. Piwek, A. Slesinski, K. Fic, S. Aina, A. Vizintin, B. Tratnik, E. Tchernychova, M. P. Lobera, M. Bernechea, R. Dominko, E. Frackowiak, Electrochim. Acta 424 (2022) 140649.
- [4] M. Granados-Moreno, G. Moreno-Fernández, R. Mysyk, D. Carriazo, Sustain. Energy Fuels 7 (2023) 965–976.
- [5] T. Kim, W. Song, D.-Y. Son, L.K. Ono, Y. Qi, J. Mater. Chem. A 7 (2019) 2942–2964.
- [6] H. Jiang, S. Wang, D. Shi, F. Chen, Y. Shao, Y. Wu, X. Hao, J. Mater. Chem. A 9 (2021) 1134–1142.
- [7] J. Aisenbauer, T. Eisenmann, M. Kuenzel, A. Kazzazi, Z. Chen, D. Bresser, Sustain. Energy Fuels 4 (2020) 5387–5416.
- [8] T. Hwang, M. Cho, K. Cho, ACS Omega 6 (2021) 9492–9499.
- [9] A. Maćkowiak, P. Jeżowski, Y. Matsui, M. Ishikawa, K. Fic, Energy Storage Mater. 65 (2024) 103163.
- [10] P. Jeżowski, A. Chojnacka, X. Pan, F. Béguin, Electrochim. Acta 375 (2021) 137980.
- [11] K. Zou, P. Cai, C. Liu, J. Li, X. Gao, L. Xu, G. Zou, H. Hou, Z. Liu, X. Ji, J. Mater. Chem. A 7 (2019) 13540–13549.
- [12] J. Ajuria, E. Redondo, M. Arnaiz, R. Mysyk, T. Rojo, E. Goikolea, J. Power Sources 359 (2017) 17–26.
- [13] L. Jin, C. Shen, A. Shellikeri, Q. Wu, J. Zheng, P. Andrei, J.-G. Zhang, J.P. Zheng, Energy Environ. Sci. 13 (2020) 2341–2362.
- [14] P. Jeżowski, K. Fic, O. Crosnier, T. Brousse, F. Béguin, J. Mater. Chem. A 4 (2016) 12609–12615.
- [15] Q. Liu, J. Chen, D. Du, S. Zhang, C. Zhu, Z. Zhang, C. Wang, L. Yin, R. Wang, J. Mater. Chem. A 11 (2023) 17491–17502.
- [16] T. Aida, K. Yamada, M. Morita, Electrochem. Solid State Lett. 9 (2006) A534.
- [17] W. Li, H. Yao, K. Yan, G. Zheng, Z. Liang, Y.M. Chiang, Y. Cui, Nat. Commun. 6 (2015) 7436.
- [18] P. Jeżowski, O. Crosnier, E. Deunf, P. Poizot, F. Béguin, T. Brousse, Nat. Mater. 17 (2017) 167–173.
- [19] M. Arnaiz, D. Shanmukaraj, D. Carriazo, D. Bhattacharjya, A. Villaverde, M. Armand, J. Ajuria, Energy Environ. Sci. 13 (2020) 2441–2449.
- [20] P. Jeżowski, K. Fic, O. Crosnier, T. Brousse, F. Béguin, Electrochim. Acta 206 (2016) 440–445.
- [21] C. Decaux, G. Lota, E. Raymundo-Piñero, E. Frackowiak, F. Béguin, Electrochim. Acta 86 (2012) 282–286.
- [22] A. Maćkowiak, P. Galek, P. Jeżowski, K. Fic, Electrochim. Acta 463 (2023) 142796.
- [23] S. Bhojate, C.K. Ranaweera, C. Zhang, T. Morey, M. Hyatt, P.K. Kahol, M. Ghimire, S.R. Mishra, R.K. Gupta, Global challenges 1 (2017) 1700063.
- [24] A. Maćkowiak, P. Galek, K. Fic, Chemosphere 265 (2021) 4028–4037.
- [25] N. Yadav, M. Hakkarainen, Chemosphere 265 (2021) 128731.
- [26] C.-Y. Zhong, Y.-P. Lv, W.-F. Wen, Q. Chen, W.-M. Zhang, ACS Sustain. Chem. Eng. 10 (2022) 6045–6056.

One-step assembly of metal-ion capacitors using redox-active electrolytes

A. Maćkowiak et al.

Journal of Power Sources 616 (2024) 235089

- [27] X. Rico, E.-M. Nuutinen, B. Gullón, V. Pihlajaniemi, R. Yáñez, *Food Bioprod. Process.* 130 (2021) 216–228.
- [28] J. Piwek, A. Platek, K. Fic, E. Frackowiak, *Electrochim. Acta* 215 (2016) 179–186.
- [29] M.R. Lukatskaya, J.I. Feldblyum, D.G. Mackanic, F. Lissel, D.L. Michels, Y. Cui, Z. Bao, *Energy Environ. Sci.* 11 (2018) 2876–2883.
- [30] J. Chen, S. Lei, S. Zhang, C. Zhu, Q. Liu, C. Wang, Z. Zhang, S. Wang, Y. Shi, L. Yin, R. Wang, *Adv. Funct. Mater.* 33 (2023) n/a.
- [31] D.F.A. Koch, R. Woods, *Electrochim. Acta* 13 (1968) 2101–2109.
- [32] R. Aalund, B. Endreddy, M. Pecht, *Frontiers in Chemical Engineering* 4 (2022).
- [33] T.A. Pham, K.E. Kweon, A. Samanta, V. Lordi, J.E. Pask, *J. Phys. Chem. C* 121 (2017) 21913–21920.
- [34] Christopher L. Berhaut, D. Lemordant, P. Porion, L. Timperman, G. Schmidt, M. Anouti, *RSC Adv.* 9 (2019) 4599–4608.
- [35] J.Y. Hwang, S.T. Myung, Y.K. Sun, *Chem. Soc. Rev.* 46 (2017) 3529–3614.
- [36] H. Moriwake, A. Kuwabara, C.A.J. Fisher, Y. Ikuhara, *RSC Adv.* 7 (2017) 36550–36554.
- [37] Y. Li, F. Wu, Y. Li, M. Liu, X. Feng, Y. Bai, C. Wu, *Chem. Soc. Rev.* 51 (2022) 4484–4536.
- [38] M. Soltani, S.H. Beheshti, *J. Energy Storage* 34 (2021) 102019.
- [39] X. Yu, C. Zhan, R. Lv, Y. Bai, Y. Lin, Z.-H. Huang, W. Shen, X. Qiu, F. Kang, *Nano Energy* 15 (2015) 43–53.
- [40] Y. Zhang, J. Jiang, Y. An, L. Wu, H. Dou, J. Zhang, Y. Zhang, S. Wu, M. Dong, X. Zhang, Z. Guo, *ChemSusChem* 13 (2020) 2522–2539.
- [41] M. Schroeder, M. Winter, S. Passerini, A. Balducci, *J. Power Sources* 238 (2013) 388–394.
- [42] J.J. Lamb, O.S. Burheim, *Energies* 14 (2021) 979.
- [43] K. Kaliyappan, M.A. Jauhar, L. Yang, Z. Bai, A. Yu, Z. Chen, *Electrochim. Acta* 327 (2019) 134959.
- [44] T. Liu, L. Lin, X. Bi, L. Tian, K. Yang, J. Liu, M. Li, Z. Chen, J. Lu, K. Amine, K. Xu, F. Pan, *Nat. Nanotechnol.* 14 (2019) 50–56.
- [45] S. Nitopi, E. Bertheussen, S.B. Scott, X. Liu, A.K. Engstfeld, S. Horch, B. Seger, I.E. L. Stephens, K. Chan, C. Hahn, J.K. Nørskov, T.F. Jaramillo, I. Chorkendorff, *Chem. Rev.* 119 (2019) 7610–7672.
- [46] A.S. Kumar, M. Pupo, K.V. Petrov, M. Ramdin, J.R. van Ommen, W. de Jong, R. Kortlever, *J Phys Chem C Nanomater Interfaces* 127 (2023) 12857–12866.
- [47] K. Fic, A. Platek, J. Piwek, E. Frackowiak, *Mater. Today* 21 (2018) 437–454.

Supplementary information for
**Unlocking the potential of acetates as
electroactive additives to electrolytes for
lithium-ion and sodium-ion capacitors**

Adam Maćkowiak, Paweł Jeżowski, Krzysztof Fic*

Poznan University of Technology, Institute of Chemistry and Technical
Electrochemistry, Berdychowo 4, 60-965, Poznan, Poland

*Corresponding author: krzysztof.fic@put.poznan.pl

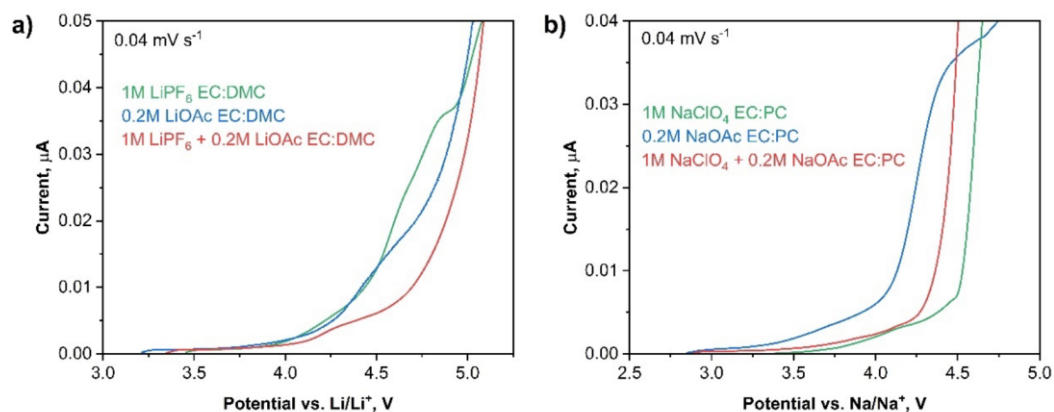


Figure S1. Stability of electrolytes with and without redox-active additive for a) Li-ion capacitor and b) Na-ion capacitor.

One-step assembly of metal-ion capacitors using redox-active electrolytes

Unlocking the potential of acetates as electroactive additives to electrolytes for lithium-ion and sodium-ion capacitors

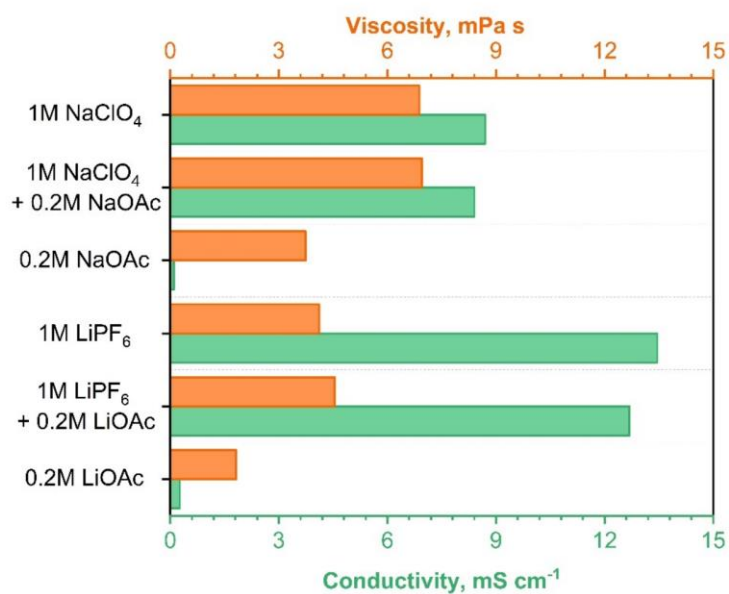


Figure S2. Viscosity and conductivity measurements of conventional electrolytes, conventional electrolytes with acetate additives and solvents (EC:DMC and EC:PC) with neat acetate salts.

One-step assembly of metal-ion capacitors using redox-active electrolytes

Unlocking the potential of acetates as electroactive additives to electrolytes for lithium-ion and sodium-ion capacitors

Acetate addition calculation:

The theoretical capacity of the LiOAc and NaOAc salts were calculated using Faraday's equation (Equation S1):

$$m = \frac{Mit}{Fz}$$

where,

m = mass of the substance, g

M = molar mass of the substance, g mol⁻¹

I = applied current, A

t = time, s

F = Faraday's constant, C mol⁻¹

z = number of electrons used in single reaction, -

The molar mass of lithium acetate is 65.98 g mol⁻¹. By substituting this value into the equation and converting the units, a capacity of approximately 406 mAh g⁻¹ can be obtained. Given the well-known exact active mass of graphite and its theoretical capacity (372 mAh g⁻¹), the required amount of LiOAc to balance the positive electrode can be calculated. The capacity of activated carbon (<50 mAh g⁻¹) is neglected here.

Similar calculations were performed for a sodium-ion capacitor, but the molar mass of sodium acetate was 82.03 mAh g⁻¹, and the theoretical capacity of hard carbon was 320 mAh g⁻¹.

Chapter VI

Summary of the results

Summary and conclusions

Five works were prepared from the conducted research for the doctoral dissertation: three published scientific articles and two manuscripts submitted to scientific journals. **Article 1** focused on confirming the main research hypothesis that it is possible to fully intercalate the negative electrode in metal-ion capacitors using a redox-active electrolyte. The novel approach for the pre-insertion of metal-ion capacitors, specifically Li-ion, Na-ion, and K-ion capacitors, was developed using thiocyanate salts. Thiocyanate salts, through an irreversible oxidation reaction at the positive electrode, inhibit the increase of the positive electrode potential, thereby enabling the insertion of metal cations into the structure of the negative electrode. The one-step assembly approach of metal-ion capacitors allows for effective pre-insertion, which, compared to currently known methods, offers benefits by reducing the time and costs associated with assembling metal-ion capacitors. Furthermore, it has been proven that using this technique results in better specific energy values than other techniques, bringing metal-ion capacitors closer to the currently popular lithium-ion batteries.

In **Manuscript 1**, it was demonstrated that the one-step assembly approach for Li-ion capacitors has the potential for commercial application due to achieving better energy values than currently produced commercial hybrid capacitors. Additionally, **Manuscript 1** attempted to explain the oxidation reaction of thiocyanates. It was proven that SCN ions first oxidize to the unstable compound CS, which then transforms into CS₂, COS, or SO compounds, but ultimately SCN is mainly converted into thiirane and lithium cyanate. More importantly, it was demonstrated that toxic hydrogen cyanide is not produced during operation.

In Chapter IV of the dissertation, **Article 2** demonstrated that the SPECS technique, previously used mainly in electrochemical capacitors, is also applicable to systems with a battery negative electrode. Thanks to the SPECS measurements, it was shown that electrolyte concentration plays a key role in the intercalation process. The obtained research results were confirmed using the GITT technique, which, when combined with the SPECS, provides a complementary description of the operation of energy storage systems. In

Manuscript 2, by using SPECS, it was verified that the SCN anion not only impacts the formation of the SEI layer but also enhances the intercalation process by aiding in lithium ion distribution and lowering system resistance. Additionally, it is crucial to consider that the reaction at the positive electrode affects the performance of the negative electrode, emphasizing the need to study complete cells. Although the capacity is largely dominated by the intercalation process, around 10% is attributed to EDL layer formation, which researchers often overlook.

In Chapter V of the dissertation, the difficulty of finding the right redox-active salt for the one-step pre-insertion approach for metal-ion capacitors is described. Examples of several salts are presented, along with reasons why their application is either impossible or simply not cost-effective. However, in **Article 3**, an acetate salt is presented as an alternative to thiocyanate salts. It is proven that they can be effectively used in the one-step assembly approach for Li-ion and Na-ion capacitors. Additionally, it is shown how significantly the type of cation affects the performance of the metal-ion capacitor. A difference in activity potentials between the two systems was observed due to the difference in the sizes of solvated lithium acetate and sodium acetate molecules and their influence on the penetration of pores in the positive electrode. The electrolyte also affects the reactions, as confirmed by *operando* GC–MS analysis where the CO₂ emission was only observed for sodium-ion capacitors.

Key findings of this dissertation include:

- Possible pre-insertion of the negative electrode using a redox-active electrolyte with thiocyanate salt
- Successful application of the redox-active electrolyte pre-insertion technique in Li-ion, Na-ion, and K-ion capacitors
- One-step pre-insertion technique results in better energy values than other techniques known in literature
- Capacitors intercalated using redox-active electrolyte achieve better specific energy values than commercially used LICs

One-step assembly of metal-ion capacitors using redox-active electrolytes

- SPECS technique can be used to describe the storage of electric charge in systems with a battery negative electrode
- Electrolyte concentration has a significant impact on the intercalation process
- The presence of redox-active electrolyte causes better diffusion of lithium ions, which positively affects the intercalation process
- Acetate salts can also be used in the one-step assembly approach of metal-ion capacitors using redox-active electrolyte
- The type of cation has a significant impact on the mechanism of electric charge storage in metal-ion capacitors.

8. Articles not included in the dissertation

Title: **Three-dimensional architectures in electrochemical capacitor applications – insights, opinions and perspectives**

Authors: Przemysław Galek, **Adam Maćkowiak**, Paulina Bujewska, Krzysztof Fic

Journal: Frontiers in Energy Research, 2020, vol. 8, 139-1 – 139-21

DOI: <https://doi.org/10.3389/fenrg.2020.00139>

Abstract

This article provides a summary of recent advancements in electrode materials with 3D structures for use in electrochemical capacitors (ECs). It categorizes these structures based on their production methods into template and non-template strategies, highlighting the pros and cons of each approach. The focus is particularly on carbon materials due to their ability to form hierarchical porous channels, as well as their high conductivity and mechanical stability. Numerous literature examples are provided for various solutions. The article concludes by discussing future challenges for these materials.



Title: **Deep eutectic solvents for high-temperature electrochemical capacitors**

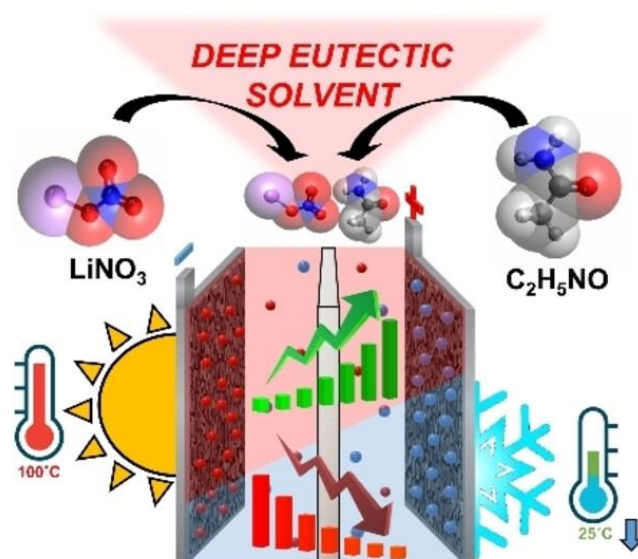
Authors: **Adam Maćkowiak**, Przemysław Galek, Krzysztof Fic

Journal: ChemElectroChem, 2021, vol. 8, 4028 – 4037

DOI: <https://doi.org/10.1002/celec.202100711>

Abstract

In this article, the authors introduce the concept of an electrochemical capacitor that operates under high-temperature conditions (100°C). The proposed solution involves an electrolyte composed of a deep eutectic mixture of lithium nitrate and acetamide. To characterize this mixture, techniques such as infrared and Raman spectroscopy, differential scanning calorimetry, and gas chromatography with mass spectrometry were employed. The electrochemical analysis covers system aging verification, self-discharge monitoring, leakage current measurement, and fundamental research to determine specific capacitance and maximum voltage. Additionally, the study includes a thorough examination of adding lithium nitrate salt and an organic solvent to the system, as well as replacing lithium ions with sodium or potassium.



One-step assembly of metal-ion capacitors using redox-active electrolytes

Title: **Redox materials for electrochemical capacitors**

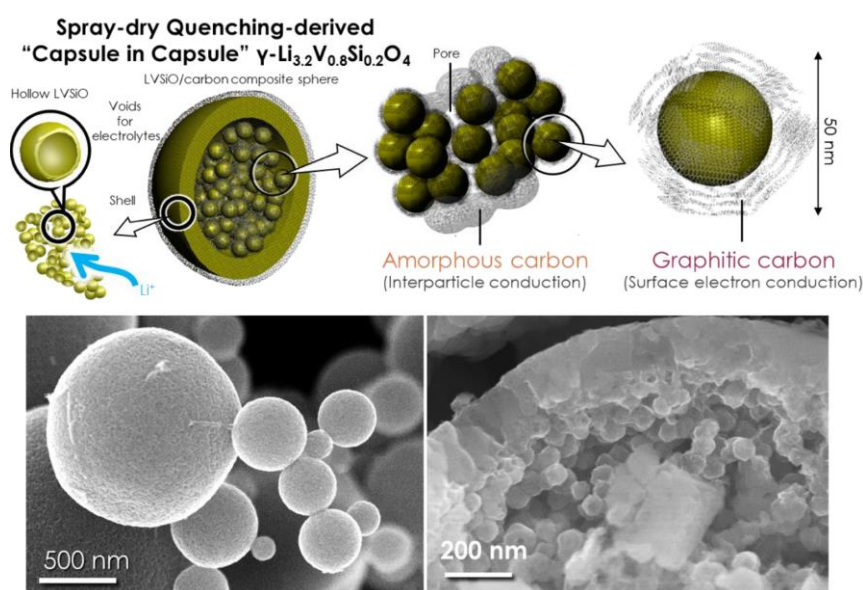
Authors: Chiku M., Abdollahifar M., Brousse T., Chen G. Z., Crosnier O., Dunn B., Fic K., Hu C. C., Jeżowski P., **Maćkowiak A.**, Naoi K., Ogihara N., Okita N., Okubo M., Sugimoto W., Wu N. Li.

Journal: Electrochemistry, 2024, vol. 92, 074002

DOI: <https://doi.org/10.5796/electrochemistry.24-70054>

Abstract

Electrochemical capacitors are renowned for their high-power density and durability, with various redox reactions being explored to enhance their energy density. Recently, a wide range of redox materials, beyond the traditionally studied transition metal oxides, have been investigated for use in these capacitors. This review provides an in-depth examination of redox materials used in electrochemical capacitors. It begins with an analysis of manganese oxides and ruthenium oxides, common metal oxides known for their pseudocapacitance. The review also covers nickel oxides used in hybrid capacitors and highlights various 0D and 2D nanomaterials. Additionally, it discusses pseudocapacitance involving nanosized complex materials and metal-organic frameworks. Electrolyte systems with redox characteristics for electrochemical capacitors are also reviewed.



List of figures and tables

Figures

Figure 1. Energy sources and methods used for its conversion	17
Figure 2. Ragone plot of popular energy storage systems	21
Figure 3. Scheme of the electric double-layer formed at the solid state – liquid interface	25
Figure 4. Schematic construction of EDLC	27
Figure 5. Electrode materials for electrochemical capacitors	28
Figure 6. Lithium-ion battery construction	35
Figure 7. Galvanostatic charging of the graphite electrode	37
Figure 8. Schematic representation of each stage during graphite intercalation process	37
Figure 9. Comparison of Li-ion batteries with different cathode materials and LTO anode material	39
Figure 10. Stages of forming SEI layer on the graphite electrode using conventional electrolyte (LiPF ₆ in EC:DMC, 1:1, v:v)	44
Figure 11. Schematic construction of lithium-ion capacitor	48
Figure 12. Schematic construction of sodium-ion capacitor	50
Figure 13. Assembly of lithium-ion capacitor using auxiliary metallic electrode approach for pre-insertion	52
Figure 14. Assembly of lithium-ion capacitor using composite materials approach for pre-insertion	54
Figure 15. Pre-insertion of graphite electrode using concentrated electrolyte approach	55
Figure 16. Scheme of electroanalytical techniques	56
Figure 17. Electrochemical analysis of different redox-active additives to electrolyte a) Li ₂ CO ₃ b) Li ₂ S c) LiBr d) LiNO ₃	174

Tables

Table 1. Comparison of EDLC, LIC and LIB23

Table 2. Advantages and disadvantages of the electrolytes used
in the ECs31

Scientific accomplishments

1. Publications

- 1) [Unlocking the potential of acetates as electroactive additives to the electrolyte for lithium-ion and sodium-ion capacitors](#)
Maćkowiak A., Jeżowski P., Matsui Y., Ishikawa M., Fic K.
Journal of Power Sources, 2024, 616, 235089 **IF = 8.100**
- 2) [Redox materials for electrochemical capacitors](#)
Chiku M., Abdollahifar M., Brousse T., Chen G. Z., Crosnier O., Dunn B., Fic K., Hu C. C., Jeżowski P., **Maćkowiak A.**, Naoi K., Ogihara N., Okita N., Okubo M., Sugimoto W., Wu N. Li.
Electrochemistry, 2024, 92, 074002 **IF = 2.700**
- 3) *Unravelling the effects of redox-active electrolytes on carbon electrodes of Li-ion capacitor*
Maćkowiak A., Galek P., Jeżowski P., Fic K.
Submitted -
- 4) *Li-ion capacitor exploiting a redox-active electrolyte*
Maćkowiak A., Jeżowski P., Ślesiński A., Matsui Y., Soeda K., Ishikawa M., Fic K.,
Submitted -
- 5) [Redox-active electrolytes as a viable approach for the one-step assembly of metal-ion capacitors](#)
Maćkowiak A., Jeżowski P., Matsui Y., Ishikawa M., Fic K.
Energy Storage Materials, 2024, 65, 103163 **IF = 20.400**
- 6) [Impact of lithium bis\(fluorosulfonyl\)imide \(LiFSI\) concentration on lithium intercalation into graphite monitored with step potential electrochemical spectroscopy \(SPECS\)](#)
Maćkowiak A., Galek P., Jeżowski P., Fic K.

**One-step assembly of metal-ion capacitors using
redox-active electrolytes**

- Electrochimica Acta, 2023, 463, 142796 **IF = 6.600**
- 7) [Deep Eutectic Solvents for High-Temperature Electrochemical Capacitors](#)
Maćkowiak A., Galek P., Fic K.,
ChemElectroChem, 2021, 8, 1-11 **IF = 4.590**
- 8) [Three-dimensional architectures in electrochemical capacitor applications – insights, opinions and perspectives](#)
Galek P., **Maćkowiak A.**, Bujewska P., Fic K.
Frontiers in Energy Research, 2020, 8, 139-1 – 139-21 **IF = 4.008**
- 9) [Synthesis and characterization of double-salt herbicidal ionic liquids comprising both 4-chloro-2-methylphenoxyacetate and trans-cinnamate anions](#)
Szymaniak D., **Maćkowiak A.**, Ciarka K., Praczyk T., Pernak J.
ChemPlusChem, 2020, 85, 2281 – 2289 **IF = 3.210**
- 10) [Herbicidal ionic liquids containing the acetylcholine cation](#)
Czuryszkiewicz D., **Maćkowiak A.**, Marcinkowska A., Borkowski A.,
Chrzanowski Ł., Pernak J.
ChemPlusChem, 2019, 84, 268 – 276 **IF = 3.210**

Total Impact Factor: 52.818

2. Patents and patent applications

Patents:

- 1) [Hybrid electrochemical capacitor \(Li-ion capacitor\)](#)
Maćkowiak A., Jeżowski P., Fic K.
Patent number Pat. 244345
- 2) [Hybrid electrochemical capacitor \(Na-ion capacitor\)](#)
Maćkowiak A., Jeżowski P., Fic K.
Patent number Pat. 244110
- 3) [Hybrid electrochemical capacitor \(K-ion capacitor\)](#)
Maćkowiak A., Jeżowski P., Fic K.
Patent number Pat. 244111
- 4) [High-temperature electrochemical capacitor](#)
Maćkowiak A., Galek P., Frąckowiak E., Fic K.
Patent number Pat. 240818
- 5) [Electrochemical capacitor](#)
Galek P., Tobis M., **Maćkowiak A.**, Foroutan Koudahi M., Bujewska P.,
Piwek J., Ślesiński A., Menzel J., Jeżowski P., Fic K.
Patent number Pat. 245531
- 6) [New ionic liquids with acetylcholine cation and herbicide anion, method of their preparation and use as herbicides](#)
Marcinkowska K., Praczyk T., **Maćkowiak A.**, Czuryzkiewicz D.,
Pernak J.
Patent number Pat. 237098
- 7) [Bisammonium salts with cinnamate and 4-chloro-2-methylphenoxyacetate anion, their preparation and use as herbicides](#)
Marcinkowska K., Praczyk T., Czuryzkiewicz D., **Maćkowiak A.**,
Pernak J.
Patent number Pat. 236683

Patent applications:

- 1) Hybrid lithium-ion capacitor
Maćkowiak A., Jeżowski P., Fic K.
P. 447463
- 2) Hybrid sodium-ion capacitor
Maćkowiak A., Jeżowski P., Fic K.
P. 447466
- 3) Hybrid potassium-ion capacitor
Maćkowiak A., Jeżowski P., Fic K.
P. 447465

3. Scientific conferences

3.1. Oral presentations

- 1) *Redox-active electrolyte for one-step assembly of sodium-ion capacitors*
Maćkowiak A., Jeżowski P., Matsui Y., Ishikawa M., Fic K.
7th International Conference on Advanced Capacitors (ICAC),
Kamakura, Japan, 26-29.09.2023
- 2) *One-step assembly of sodium-ion capacitors using the redox-active electrolyte*
Maćkowiak A., Jeżowski P., Matsui Y., Ishikawa M., Fic K.
74th Annual Meeting of the International Society of Electrochemistry (ISE),
Lyon, France, 3-8.09.2023
- 3) *In-depth investigation of lithium intercalation into the graphite layers using step potential electrochemical spectroscopy (SPECS)*
Maćkowiak A., Galek P., Jeżowski P., Fic K.
73rd Annual Meeting of the International Society of Electrochemistry (ISE),
Online meeting, 12-16.09.2022
- 4) *A step potential electrochemical spectroscopy (SPECS) investigation of the lithium intercalation process*
Maćkowiak A., Galek P., Jeżowski P., Fic K.
1st Regional Meeting of the International Society of Electrochemistry (ISE),
Prague, Czech Republic, 15-19.08.2022
- 5) *Hybrid electrochemical capacitor with redox-active electrolyte*
Fic K., **Maćkowiak A.**, Jeżowski P., Matsui Y., Soeda K., Ishikawa M.
7th International Symposium on Enhanced Electrochemical Capacitors
(ISEECap), Bologna, Italy, 11-15.07.2022
- 6) *Novel type of Li-ion capacitor with improved energy/power performance*
Maćkowiak A., Jeżowski P., Soeda K., Matsui Y., Ishikawa M., Fic K.
240th Electrochemical Society Meeting (ECS),
Orlando, USA, 10-14.10.2021
- 7) *Novel concept for hybrid Li-ion capacitor*
Maćkowiak A., Jeżowski P., Matsui Y., Soeda K., Ishikawa M., Fic K.
72nd Annual Meeting of the International Society of Electrochemistry (ISE)

Jeju, South Korea, 29.08 – 3.09.2021

- 8) *Synthesis and characterization of double-salt herbicidal ionic liquids comprising both 4-chloro-2-methylphenoxyacetate and trans-cinnamate anions*

Maćkowiak A., Czuryżkiewicz D., Ciarka K., Praczyk T., Pernak J.

62 Zjazd naukowy Polskiego Towarzystwa Chemicznego

Warsaw, Poland, 2-6.09.2019

3.2. Poster presentations

- 1) *A step potential electrochemical spectroscopy (SPECS) investigation of the lithium intercalation process*

Maćkowiak A., Galek P., Jeżowski P., Fic K.

8th International Symposium on Enhanced Electrochemical Capacitors (ISEECap), Vitoria-Gasteiz, Spain, 8-12.07.2024

- 2) *A step potential electrochemical spectroscopy (SPECS) investigation of the lithium intercalation process*

Maćkowiak A., Galek P., Jeżowski P., Fic K.

7th International Conference on Advanced Capacitors (ICAC),
Kamakura, Japan, 26-29.09.2023

- 3) *Redox-active electrolytes for pre-lithiation of graphite electrode in lithium-ion capacitors*

Maćkowiak A., Jeżowski P., Matsui Y., Soeda K., Ishikawa M., Fic K.

7th International Symposium on Enhanced Electrochemical Capacitors (ISEECap), Bologna, Italy, 11-15.07.2022

- 4) *Deep eutectic solvents based on lithium nitrate and acetamide as electrolytes in high-temperature electric double-layer capacitors*

Maćkowiak A., Galek P., Fic K.

12th European Symposium on Electrochemical Engineering (ESEE),
Leeuwarden, The Netherlands, 14-17.06.2021

- 5) *Deep eutectic solvent based on lithium nitrate and acetamide as electrolyte in high-temperature electric double-layer capacitors*

Maćkowiak A., Galek P., Fic K.

**One-step assembly of metal-ion capacitors using
redox-active electrolytes**

71st Annual Meeting of the International Society of Electrochemistry (ISE),
Belgrade, Serbia, 31.08 – 4.09.2020

6) *Herbicidal ionic liquids containing the acetylcholine cation*

Maćkowiak A., Czuryzkiewicz D., Marcinkowska A., Praczyk T., Pernak J.

III Szczecińskie Sympozjum Młodych Chemików

Szczecin, Poland, 8.05.2018

4. Awards

- 1) **3rd place in EUNICE Imagine Innovation Cup**
for the project titled: *AndanteCaps – Future Energy*
Issued by The European University for Customized Education (EUNICE)
Santander, Spain, 07.2024
- 2) **Scholarship for young researchers from the Poznan scientific community**
Issued by Poznan City Hall
Poznan, Poland, 06.2024
- 3) **Santander award for students and PhD students of the Poznan University of Technology**
Issued by Santander Consumer Bank
Poznan, Poland, 06.2024
- 4) **Main award for best original creative work by PhD student in 2023**
For article titled: *Redox-active electrolytes as a viable approach for the one-step assembly of metal-ion capacitors*
Issued by the Polish Academy of Sciences
Poznan, Poland, 06.2024
- 5) **1st place in the PUT START UP competition for the best business idea**
for the project titled: *AndanteCaps – Future Energy*
Issued by Academic Business Incubator of the Poznan University of Technology
Poznan, Poland, 12.2023
- 6) **STER – Mobility scholarship**
for the project titled: *Electroactive ionic liquids as electrolyte additives for metal-ion capacitors*
Issued by National Agency for Academic Exchange
Poznan, Poland, 11.2023
- 7) **French Government Scholarship for a research stay in France**
for the project titled: *Metal-ion capacitors as the future of energy storage*
Issued by French Government
Paris, France, 12.2021

8) ***Cover picture of ChemElectroChem magazine***

For the article titled: *Deep eutectic solvents for high-temperature electrochemical capacitors*

Issued by Wiley

Poznan, Poland, 09.2021

9) ***Rector medal for outstanding contribution to university life***

Issued by Poznan University of Technology

Poznan, Poland, 07.2019

5. Research projects

- 1) **Researcher in European Research Council (ERC)** within the **Proof of Concept** project titled: *It yet remains to see...'* – *Hybrid electrochemical energy storage system of high power and improved cycle life*
Poznan, Poland, 05.2024 – 08.2024
- 2) **Researcher in Marie Skłodowska-Curie Actions** within the project titled: *ENERCAP – European Network to Empower Research on CAPacitors*
Poznan, Poland, 11.2023 – 05.2023
- 3) **Principal investigator in National Agency for Academic Exchange** within the **STER – Mobility IV** project titled: *Electroactive ionic liquids as electrolyte additives for metal-ion capacitors*
Montreal, Canada, 01.2024 – 04.2024
- 4) **Researcher in European Research Council (ERC)** within the **Starting Grant** project titled: *If immortality unveil...'* – *development of the novel types of energy storage systems with excellent long-term performance*
Poznan, Poland, 11.2019 – 09.2023
- 5) **Principal investigator in Poznan University of Technology** project titled: *Synthesis and application of a novel group of ionic liquids in electrochemical capacitors*
Poznan, Poland, 01.2023 – 11.2023
- 6) **Principal investigator in French Government** within the **BGF SSHN** project titled: *Metal-ion capacitors as the future of energy storage devices*
Mulhouse, France, 04.2022 – 06.2022

6. Memberships and trainings

Memberships:

- 1) **International Society of Electrochemistry**
09.2020 – 01.2024
- 2) **Council of doctoral students of the Faculty of Chemical Technology at the Poznan University of Technology**
11.2022 – 07.2024
- 3) **Council of doctoral students of the Poznan University of Technology**
02.2023 – 10.2023
- 4) **Supervisor of the badminton section of the Poznan University of Technology**
10.2018 – 07.2024

Trainings:

- 1) **Elsevier Reviewer Recognition**
Issued by Elsevier, 02.2024
- 2) **Battery Energy Storages in Smart Grids**
Issued by University of Vaasa, 08.2022
- 3) **ASAP 2460 Gas Adsorption training**
Issued by Micromeritics Instrument Corporation, 04.2022
- 4) **Statistica software „DOE – Computer aided planning and statistical analysis of innovative research”**
Issued by StatSoft Polska, 05.2021
- 5) **Communication in intercultural setting**
Issued by Poznan University of Technology, 02.2021
- 6) **Effective time and work management**
Issued by National Agency for Academic Exchange, 12.2020

Literature

- [1] D. Larcher, J.M. Tarascon, *Nature Chemistry*, 7 (2015) 19-29.
- [2] J.C. Steckel, R.J. Brecha, M. Jakob, J. Strefler, G. Luderer, *Ecological Economics*, 90 (2013) 53-67.
- [3] J. Wang, W. Azam, *Geoscience Frontiers*, 15 (2024) 101757.
- [4] A. Raihan, M.I. Pavel, D.A. Muhtasim, S. Farhana, O. Faruk, A. Paul, *Innovation and Green Development*, 2 (2023) 100035.
- [5] Y. Teff-Seker, O. Berger-Tal, Y. Lehnardt, N. Teschner, *Renewable & Sustainable Energy Reviews*, 168 (2022) 112801.
- [6] X.E. Zhao, Q.Z. Ye, S. Candel, D. Vignon, R. Guillaumont, *Engineering*, 26 (2023) 159-172.
- [7] T. Sharmin, N.R. Khan, M.S. Akram, M.M. Ehsan, *International Journal of Thermofluids*, 18 (2023) 100323.
- [8] T. Egeland-Eriksen, A. Hajizadeh, S. Sartori, *International Journal of Hydrogen Energy*, 46 (2021) 31963-31983.
- [9] M. Irfan, S. Deilami, S.J. Huang, B.P. Veettil, *Energies*, 16 (2023) 7248.
- [10] H. Li, X.W. Cao, Y. Liu, Y.B. Shao, Z.L. Nan, L. Teng, W.S. Peng, J. Bian, *Energy Reports*, 8 (2022) 6258-6269.
- [11] A. Czerwiński, *Akumulatory, baterie, ogniwa*, Wydawnictwo komunikacji i łączności, Warszawa, 2018.
- [12] A.S. Mohd Razif, N.F. Ab Aziz, M.Z.A. Ab Kadir, K. Kamil, *Energy Strategy Reviews*, 52 (2024) 101346.
- [13] A. Aghmadi, O.A. Mohammed, *Batteries-Basel*, 10 (2024) 141.
- [14] M.S. Guney, Y. Tepe, *Renewable & Sustainable Energy Reviews*, 75 (2017) 1187-1197.
- [15] M.L. Yue, H. Lambert, E. Pahon, R. Roche, S. Jemei, D. Hissel, *Renewable & Sustainable Energy Reviews*, 146 (2021) 111180.
- [16] R.G. Bodkhe, R.L. Shrivastava, V.K. Soni, R.B. Chadge, *International Journal of Electrochemical Science*, 18 (2023) 100108.
- [17] M. Waseem, M. Amir, G.S. Lakshmi, S. Harivardhagini, M. Ahmad, *Green Energy and Intelligent Transportation*, 2 (2023) 100121.
- [18] F. Rahim Malik, H.-B. Yuan, J.C. Moran, N. Tippayawong, *Engineering Science and Technology, an International Journal*, 43 (2023) 101452.
- [19] Q. Hassan, I.D.J. Azzawi, A.Z. Sameen, H.M. Salman, *Sustainability*, 15 (2023) 11501.
- [20] J. Nyangon, A. Darekar, *Innovation and Green Development*, 3 (2024) 100149.
- [21] T. Xu, X. Zheng, B. Ji, Z. Xu, S. Bao, X. Zhang, G. Li, J. Mei, Z. Li, *Separation and Purification Technology*, 330 (2024) 125501.

One-step assembly of metal-ion capacitors using redox-active electrolytes

- [22] W.H.H. Zhu, Y. Zhu, Z. Davis, B.J. Tatarchuk, *Applied Energy*, 106 (2013) 307-313.
- [23] M.A. Abraham, *Encyclopedia of sustainable technologies*, Second edition, Elsevier, Amsterdam, 2024.
- [24] A.R. Dehghani-Sani, E. Tharumalingam, M.B. Dusseault, R. Fraser, *Renewable & Sustainable Energy Reviews*, 104 (2019) 192-208.
- [25] J.R. Garche, C.K. Dyer, *Encyclopedia of electrochemical power sources*, Academic Press, Amsterdam, 2009.
- [26] P. Chen, K. Zhang, D. Tang, W. Liu, F. Meng, Q. Huang, J. Liu, *Front Chem*, 8 (2020) 372.
- [27] G. Nazir, A. Rehman, J.H. Lee, C.H. Kim, J. Gautam, K. Heo, S. Hussain, M. Ikram, A.A. AlObaid, S.Y. Lee, S.J. Park, *Nano-micro Letters*, 16 (2024) 138.
- [28] Y.W. Zhong, B. Liu, Z.Q. Zhao, Y.H. Shen, X.R. Liu, C. Zhong, *Energies*, 14 (2021) 2607.
- [29] M.D. Hossain, M.M. Islam, M.J. Hossain, S. Yasmin, S.R. Shingho, N.A. Ananna, C.M. Mustafa, *Journal of Energy Storage*, 27 (2020) 101108.
- [30] D. Pavlov, V. Naidenov, S. Ruevski, *Journal of Power Sources*, 161 (2006) 658-665.
- [31] A. Townsend, R. Gouws, *Energies*, 15 (2022) 4930.
- [32] J. Garche, P.T. Moseley, E. Karden, Lead–acid batteries for hybrid electric vehicles and battery electric vehicles, in: *Advances in Battery Technologies for Electric Vehicles*, Elsevier, 2015, 75-101.
- [33] J.C. Barbosa, R. Gonçalves, C.M. Costa, S. Lanceros-Mendez, *Energies*, 14 (2021) 3145.
- [34] K. Itani, A. De Bernardinis, H. Zhang, *Energies*, 16 (2023) 7530.
- [35] Y. Sato, S. Takeuchi, K. Kobayakawa, *Journal of Power Sources*, 93 (2001) 20-24.
- [36] S.J. An, J.L. Li, C. Daniel, D. Mohanty, S. Nagpure, D.L. Wood, *Carbon*, 105 (2016) 52-76.
- [37] M. Dubarry, A. Devie, *ECS Meeting Abstracts*, MA2016-02 (2016) 13-13.
- [38] P. Greim, A.A. Solomon, C. Breyer, *Nat Commun*, 11 (2020) 4570.
- [39] L.A. Zhao, T. Zhang, W. Li, T. Li, L. Zhang, X.G. Zhang, Z.Y. Wang, *Engineering*, 24 (2023) 172-183.
- [40] R.K. Gupta, T.A. Nguyen, *Smart Multifunctional nano-links*, Elsevier, United States, 2022.
- [41] J. Both, *IEEE Electrical Insulation Magazine*, 31 (2015) 22-29.
- [42] H. Schrangner, F. Barzegar, Q. Abbas, *Current Opinion in Electrochemistry*, 21 (2020) 167-174.
- [43] J. Zhang, M. Gu, X. Chen, *Micro and Nano Engineering*, 21 (2023) 100229.
- [44] N.P.D. Ngidi, A.F. Koekemoer, S.S. Ndlela, *Journal of Energy Storage*, 89 (2024) 111638.
- [45] P. Simon, Y. Gogotsi, *Nature Materials*, 7 (2008) 845-854.
- [46] M. Czagany, S. Hompoth, A.K. Keshri, N. Pandit, I. Galambos, Z. Gacsi, P. Baumli,

One-step assembly of metal-ion capacitors using redox-active electrolytes

Materials (Basel), 17 (2024) 702.

[47] A. Lewandowski, P. Jakobczyk, M. Galinski, M. Biegun, Phys Chem Chem Phys, 15 (2013) 8692-8699.

[48] E. Pipitone, G. Vitale, Journal of Power Sources, 448 (2020) 227368.

[49] P. Galek, A. Mackowiak, P. Bujewska, K. Fic, Frontiers in Energy Research, 8 (2020).

[50] Y. Shao, M.F. El-Kady, J. Sun, Y. Li, Q. Zhang, M. Zhu, H. Wang, B. Dunn, R.B. Kaner, Chem Rev, 118 (2018) 9233-9280.

[51] G.G. Njema, R.B.O. Ouma, J.K. Kibet, P. V, Journal of Renewable Energy, 2024 (2024) 1-35.

[52] Y.Q. Chen, Y.Q. Kang, Y. Zhao, L. Wang, J.L. Liu, Y.X. Li, Z. Liang, X.M. He, X. Li, N. Tavajohi, B.H. Li, Journal of Energy Chemistry, 59 (2021) 83-99.

[53] J. Xie, Y.C. Lu, Nat Commun, 11 (2020) 2499.

[54] M. Soltani, S.H. Beheshti, Journal of Energy Storage, 34 (2021) 102019.

[55] M. Canal-Rodríguez, M. Arnaiz, N. Rey-Raap, A. Arenillas, J. Ajuria, Electrochimica Acta, 463 (2023) 142809.

[56] J.J. Lamb, O.S. Burheim, Energies, 14 (2021) 979.

[57] O.E. Eleri, F.L. Lou, Z.X. Yu, Batteries-Basel, 9 (2023) 533.

[58] X.J. Wang, L.L. Liu, Z.Q. Niu, Materials Chemistry Frontiers, 3 (2019) 1265-1279.

[59] B. Babu, P. Simon, A. Balducci, Advanced Energy Materials, 10 (2020) 2001128.

[60] T. Wilberforce, Z. El-Hassan, F.N. Khatib, A. Al Makky, A. Baroutaji, J.G. Carton, A.G. Olabi, International Journal of Hydrogen Energy, 42 (2017) 25695-25734.

[61] I. Becker Howard, Patent number US2800616A (1957).

[62] M. Pershaanaa, S. Bashir, S. Ramesh, K. Ramesh, Journal of Energy Storage, 50 (2022) 104599.

[63] N.S. Shaikh, S.B. Ubale, V.J. Mane, J.S. Shaikh, V.C. Lokhande, S. Praserttham, C.D. Lokhande, P. Kanjanaboos, Journal of Alloys and Compounds, 893 (2022) 161998.

[64] P.K. Panda, A. Grigoriev, Y.K. Mishra, R. Ahuja, Nanoscale Adv, 2 (2020) 70-108.

[65] G.G. Amatucci, F. Badway, A. Du Pasquier, T. Zheng, Journal of the Electrochemical Society, 148 (2001) A930-A939.

[66] J. Nakayama, H. Zhou, J. Izumi, K. Watanabe, K. Suzuki, F. Nemoto, N.L. Yamada, R. Kanno, M. Hirayama, Advanced Materials Interfaces, 11 (2023).

[67] G. Bussetti, K. Wandelt, Encyclopedia of solid-liquid interfaces, Elsevier, Amsterdam, 2024.

[68] A. Alizadeh, W.L. Hsu, M. Wang, H. Daiguji, Electrophoresis, 42 (2021) 834-868.

[69] K. Salari, P. Zarafshan, M. Khashehchi, G. Chegini, H. Etezadi, H. Karami, J. Szulzyk-Cieplak, G. Lagod, Membranes (Basel), 12 (2022) 459.

One-step assembly of metal-ion capacitors using redox-active electrolytes

- [70] B.B. Damaskin, O.A. Petrii, *Journal of Solid State Electrochemistry*, 15 (2011) 1317-1334.
- [71] S.B. Davey, A.P. Cameron, K.G. Latham, S.W. Donne, *Electrochimica Acta*, 386 (2021) 138416.
- [72] A. Chu, P. Braatz, *Journal of Power Sources*, 112 (2002) 236-246.
- [73] A.K. Shukla, A. Banerjee, M.K. Ravikumar, A. Jalajakshi, *Electrochimica Acta*, 84 (2012) 165-173.
- [74] S. Sharma, P. Chand, *Results in Chemistry*, 5 (2023) 100885.
- [75] Y. Maletin, N. Stryzhakova, S. Zelinsky, S. Chernukhin, D. Tretyakov, S. Tychina, D. Drobny, *Green*, 4 (2014) 9-17.
- [76] K. Yang, Q. Fan, C. Song, Y. Zhang, Y. Sun, W. Jiang, P. Fu, *Green Energy and Resources*, 1 (2023) 100030.
- [77] S.S. Shah, M.A. Aziz, *Journal of Chemistry and Environment*, (2024) 1-45.
- [78] R. Heimbockel, F. Hoffmann, M. Froba, *Phys Chem Chem Phys*, 21 (2019) 3122-3133.
- [79] A. Ajina, D. Isa, *Institute of Electrical and Electronic Engineers*, (2010) 335-339.
- [80] H.L. Qi, Z. Bo, S.L. Yang, L.P. Duan, H.C. Yang, J.H. Yan, K.F. Cen, K. Ostrikov, *Energy Storage Materials*, 16 (2019) 607-618.
- [81] P. Sinha, K.K. Kar, A.K. Naskar, *Advanced Materials Technologies*, 7 (2022).
- [82] P. Qin, X. Li, B. Gao, J. Fu, L. Xia, X. Zhang, K. Huo, W. Shen, P.K. Chu, *Nanoscale*, 10 (2018) 8728-8734.
- [83] L.N. Khandare, D.J. Late, N.B. Chaure, *Front Chem*, 11 (2023) 1166544.
- [84] H.H. Wang, J.Y. Lin, Z.X. Shen, *Journal of Science-Advanced Materials and Devices*, 1 (2016) 225-255.
- [85] M. Tobis, S. Sroka, E. Frackowiak, *Frontiers in Energy Research*, 9 (2021).
- [86] Z.W. Li, S. Gao, H.Y. Mi, C.C. Lei, C.C. Ji, Z.L. Xie, C. Yu, J.S. Qiu, *Carbon*, 149 (2019) 273-280.
- [87] J. Liang, H.T. Zhao, L.C. Yue, G.Y. Fan, T.S. Li, S.Y. Lu, G. Chen, S.Y. Gao, A.M. Asiri, X.P. Sun, *Journal of Materials Chemistry A*, 8 (2020) 16747-16789.
- [88] J.H. Wee, Y.A. Kim, C.M. Yang, *Microporous and Mesoporous Materials*, 310 (2021) 110595.
- [89] M.E. Plonska-Brzezinska, L. Echegoyen, *Journal of Materials Chemistry A*, 1 (2013) 13703-13714.
- [90] M. Tobis, J. Piwek, A.P. Platek-Mielczarek, L. Przypis, D. Janas, E. Frackowiak, *Electrochimica Acta*, 492 (2024) 144386.
- [91] R.S. Costa, O.S.G.P. Soares, R. Vilarinho, J.A. Moreira, M.F.R. Pereira, A. Pereira, C. Pereira, *Carbon Trends*, 5 (2021) 100137.
- [92] T.P. Mofokeng, Z.N. Tetana, K.I. Ozoemena, *Carbon*, 169 (2020) 312-326.

One-step assembly of metal-ion capacitors using redox-active electrolytes

- [93] Q.Q. Ke, J. Wang, *Journal of Materiomics*, 2 (2016) 37-54.
- [94] Y. Quintero, S. Herrera, Z. Zapata-Benabithé, A. Manzano-Ramírez, L. Cruz, *ECS Advances*, 2 (2023) 41001.
- [95] Z.Y. Gao, C. Chen, J.L. Chang, L.M. Chen, D.P. Wu, F. Xu, K. Jiang, *Electrochimica Acta*, 260 (2018) 932-943.
- [96] D. Zhang, C. Tan, W. Zhang, W. Pan, Q. Wang, L. Li, *Molecules*, 27 (2022) 716.
- [97] X.H. Long, W. Setyawan, K.P. Tai, Y. Liu, M.S. Yu, Z.Q. Wang, N. Gao, X.L. Wang, *Carbon*, 191 (2022) 350-361.
- [98] L.W. Le Fevre, J. Cao, I.A. Kinloch, A.J. Forsyth, R.A.W. Dryfe, *ChemistryOpen*, 8 (2019) 418-428.
- [99] D.G. Papageorgiou, I.A. Kinloch, R.J. Young, *Progress in Materials Science*, 90 (2017) 75-127.
- [100] Q. Abbas, P.A. Shinde, M.A. Abdelkareem, A.H. Alami, M. Mirzaeian, A. Yadav, A.G. Olabi, *Materials (Basel)*, 15 (2022) 7804.
- [101] B. Krüner, C. Odenwald, A. Tolosa, A. Schreiber, M. Aslan, G. Kickelbick, V. Presser, *Sustainable Energy & Fuels*, 1 (2017) 1588-1600.
- [102] C.S. Wang, B. Yan, J.J. Zheng, L. Feng, Z.Z. Chen, Q. Zhang, T. Liao, J.Y. Chen, S.H. Jiang, C. Du, S.J. He, *Advanced Powder Materials*, 1 (2022) 100018.
- [103] A. Halama, B. Szubzda, G. Pasciak, *Electrochimica Acta*, 55 (2010) 7501-7505.
- [104] P. Kossyrev, *Journal of Power Sources*, 201 (2012) 347-352.
- [105] Z.B. Zhang, C. Jiang, D.W. Li, Y.Q. Lei, H.M. Yao, G.Y. Zhou, K. Wang, Y.L. Rao, W.G. Liu, C.L. Xu, X.X. Zhang, *Carbon*, 170 (2020) 567-579.
- [106] C. Bouchelta, M.S. Medjram, O. Bertrand, J.P. Bellat, *Journal of Analytical and Applied Pyrolysis*, 82 (2008) 70-77.
- [107] J.A. Maciá-Agulló, B.C. Moore, D. Cazorla-Amorós, A. Linares-Solano, *Carbon*, 42 (2004) 1367-1370.
- [108] F. Beguin, E. Frackowiak, *Supercapacitors : materials, systems, and applications*, Wiley-VCH, Weinheim, 2013.
- [109] K. Fic, A. Platek, J. Piwek, J. Menzel, A. Slesinski, P. Bujewska, P. Galek, E. Frackowiak, *Energy Storage Materials*, 22 (2019) 1-14.
- [110] Q. Gou, S. Zhao, J. Wang, M. Li, J. Xue, *Nano-micro Letters*, 12 (2020) 98.
- [111] M. Mirzaeian, Q. Abbas, A. Ogwu, P. Hall, M. Goldin, M. Mirzaeian, H.F. Jirandehi, *International Journal of Hydrogen Energy*, 42 (2017) 25565-25587.
- [112] K. Jurewicz, R. Pietrzak, P. Nowicki, H. Wachowski, *Electrochimica Acta*, 53 (2008) 5469-5475.
- [113] M. Khademi, D.P.J. Barz, *Langmuir*, 36 (2020) 4250-4260.
- [114] H.Y. Lee, J.B. Goodenough, *Journal of Solid State Chemistry*, 144 (1999) 220-223.

One-step assembly of metal-ion capacitors using redox-active electrolytes

- [115] G. Lota, J. Tyczkowski, R. Kapica, K. Lota, E. Frackowiak, *Journal of Power Sources*, 195 (2010) 7535-7539.
- [116] K. Fic, G. Lota, M. Meller, E. Frackowiak, *Energy & Environmental Science*, 5 (2012) 5842-5850.
- [117] F. Wang, C. Hu, M. Zhou, K.L. Wang, J.L. Lian, J. Yan, S.J. Cheng, K. Jiang, *Science Bulletin*, 61 (2016) 451-458.
- [118] S. Zallouz, L. Dentzer, C.M. Ghimbeu, *ACS Applied Energy Materials*, 7 (2024) 1448-1460.
- [119] M.S. El Halimi, A. Zanelli, F. Soavi, T. Chafik, *World*, 4 (2023) 431-449.
- [120] J. Park, J. Kim, S. Lee, J.H. Kim, M.-H. Yoon, D. Lee, S.J. Yoo, *Energy Storage Materials*, 65 (2024) 103137.
- [121] P. Galek, E. Frackowiak, K. Fic, *Electrochimica Acta*, 334 (2020) 135572.
- [122] S.T. Senthilkumar, R.K. Selvan, J.S. Melo, *Journal of Materials Chemistry A*, 1 (2013) 12386-12394.
- [123] G. Lota, E. Frackowiak, *Electrochemistry Communications*, 11 (2009) 87-90.
- [124] K. Fic, S. Morimoto, E. Frackowiak, M. Ishikawa, *Batteries & Supercaps*, 3 (2020) 1080-1090.
- [125] B. Gorska, P. Bujewska, K. Fic, *Phys Chem Chem Phys*, 19 (2017) 7923-7935.
- [126] G. Feng, J. Huang, B.G. Sumpter, V. Meunier, R. Qiao, *Phys Chem Chem Phys*, 12 (2010) 5468-5479.
- [127] Y. Chen, S.Z. Liu, Z.X. Bi, Z. Li, F.Y. Zhou, R.F. Shi, T.C. Mu, *Green Energy & Environment*, 9 (2024) 966-991.
- [128] R.R. Galimzyanov, S.V. Stakhanova, I.S. Krechetov, A.T. Kalashnik, M.V. Astakhov, A.V. Lisitsin, A.Y. Rychagov, T.R. Galimzyanov, F.S. Tabarov, *Journal of Power Sources*, 495 (2021) 229442.
- [129] A. Jänes, T. Thomberg, J. Eskusson, E. Lust, *ECS Transactions*, 64 (2015) 31-40.
- [130] N.S. Nadiah, F.S. Omar, A. Numan, Y.K. Mahipal, S. Ramesh, K. Ramesh, *International Journal of Hydrogen Energy*, 42 (2017) 30683-30690.
- [131] K. Chiba, T. Ueda, H. Yamamoto, *Electrochemistry*, 75 (2007) 668-671.
- [132] E. Pamaté, F. Beguin, *Electrochimica Acta*, 389 (2021) 138687.
- [133] V.L. Martins, R.M. Torresi, *Current Opinion in Electrochemistry*, 9 (2018) 26-32.
- [134] Q.W. Yang, K. Yu, H.B. Xing, B.G. Su, Z.B. Bao, Y.W. Yang, Q.L. Ren, *Journal of Industrial and Engineering Chemistry*, 19 (2013) 1708-1714.
- [135] J. Pereira, R. Souza, A. Moreira, A. Moita, *Ionics*, 30 (2024) 4343-4385.
- [136] R. Palm, H. Kurig, K. Tönurist, A. Jänes, E. Lust, *Electrochemistry Communications*, 22 (2012) 203-206.

One-step assembly of metal-ion capacitors using redox-active electrolytes

- [137] N.A. Shamsuri, M.H. Hamsan, M.F. Shukur, Y. Alias, S.N.A. Halim, S.B. Aziz, A.H. Jahidin, M. Sulaiman, L. Yuwana, S.O.J. Siong, N.M. Sarih, M.F.Z. Kadir, *Journal of Energy Storage*, 75 (2024) 109559.
- [138] Y. Wei, W. Chen, X.Y. Ge, J.Y. Liang, Z. Xing, Q.G. Zhang, Z.X. Wang, *Polymer*, 289 (2023) 126501.
- [139] N. Sarfraz, N. Kanwal, M. Ali, K. Ali, A. Hasnain, M. Ashraf, M. Ayaz, J. Ifthikar, S. Ali, A. Hendi, N. Baig, M.F. Ehsan, S.S. Shah, R. Khan, I. Khan, *Energy Storage Materials*, 71 (2024) 103619.
- [140] K. Funke, *Sci Technol Adv Mater*, 14 (2013) 043502.
- [141] P.V. Wright, *Electrochimica Acta*, 43 (1998) 1137-1143.
- [142] S.K. Tripathi, A. Kumar, S.A. Hashmi, *Solid State Ionics*, 177 (2006) 2979-2985.
- [143] Q. Chen, X.M. Li, X.B. Zang, Y.C. Cao, Y.J. He, P.X. Li, K.L. Wang, J.Q. Wei, D.H. Wu, H.W. Zhu, *Rsc Advances*, 4 (2014) 36253-36256.
- [144] N.C. Adak, S. Lim, G.H. Lee, W. Lee, *Front Chem*, 12 (2024) 1330655.
- [145] L.P. Yue, J. Ma, J.J. Zhang, J.W. Zhao, S.M. Dong, Z.H. Liu, G.L. Cui, L.Q. Chen, *Energy Storage Materials*, 5 (2016) 139-164.
- [146] J.K. Wang, L. Wang, H. Xu, L. Sheng, X.M. He, *Green Energy & Environment*, 9 (2024) 454-472.
- [147] M.V. Reddy, A. Mauger, C.M. Julien, A. Paoletta, K. Zaghib, *Materials (Basel)*, 13 (2020) 1884.
- [148] M.S. Whittingham, *Nature Energy*, 6 (2021) 214-214.
- [149] Y. Huang, *Interdisciplinary Materials*, 1 (2022) 323-329.
- [150] B. Mand Khan, W. Chun Oh, P. Nuengmatch, K. Ullah, *Materials Science and Engineering: B*, 287 (2023) 116141.
- [151] J.-L. Brédas, J.M. Buriak, F. Caruso, K.-S. Choi, B.A. Korgel, M.R. Palacín, K. Persson, E. Reichmanis, F. Schüth, R. Seshadri, M.D. Ward, *Chemistry of Materials*, 31 (2019) 8577-8581.
- [152] J.P. Pender, G. Jha, D.H. Youn, J.M. Ziegler, I. Andoni, E.J. Choi, A. Heller, B.S. Dunn, P.S. Weiss, R.M. Penner, C.B. Mullins, *ACS Nano*, 14 (2020) 1243-1295.
- [153] N. Recham, J.N. Chotard, L. Dupont, C. Delacourt, W. Walker, M. Armand, J.M. Tarascon, *Nature Materials*, 9 (2010) 68-74.
- [154] C.F. Liu, Z.G. Neale, G.Z. Cao, *Materials Today*, 19 (2016) 109-123.
- [155] P.U. Nzereogu, A.D. Omah, F.I. Ezema, E.I. Iwuoha, A.C. Nwanya, *Applied Surface Science Advances*, 9 (2022) 100233.
- [156] R. Borah, F.R. Hughson, J. Johnston, T. Nann, *Materials Today Advances*, 6 (2020) 100046.
- [157] J. Asenbauer, T. Eisenmann, M. Kuenzel, A. Kazzazi, Z. Chen, D. Bresser, *Sustainable Energy & Fuels*, 4 (2020) 5387-5416.

One-step assembly of metal-ion capacitors using redox-active electrolytes

- [158] W. Zhou, P.H. Sit, ACS Omega, 5 (2020) 18289-18300.
- [159] C. Uhlmann, J. Illig, M. Ender, R. Schuster, E. Ivers-Tiffée, Journal of Power Sources, 279 (2015) 428-438.
- [160] A. Tomaszewska, Z.Y. Chu, X.N. Feng, S. O'Kane, X.H. Liu, J.Y. Chen, C.Z. Ji, E. Endler, R.H. Li, L.S. Liu, Y.L. Li, S.Q. Zheng, S. Vetterlein, M. Gao, J.Y. Du, M. Parkes, M.G. Ouyang, M. Marinescu, G. Offer, B. Wu, Etransportation, 1 (2019) 100011.
- [161] V.M. Leal, E.L.D. Coelho, M.B.J.G. Freitas, Journal of Energy Chemistry, 79 (2023) 118-134.
- [162] A.K. Mishra, Monika, B.S. Patial, Materials Today Electronics, 7 (2024) 100089.
- [163] M. Zybert, H. Ronduda, A. Szczesna, T. Trzeciak, A. Ostrowski, E. Zero, W. Wieczorek, W. Raróg-Pilecka, M. Marcinek, Solid State Ionics, 348 (2020) 115273.
- [164] S.H. Farjana, N. Huda, M.A.P. Mahmud, Journal of Sustainable Mining, 18 (2019) 150-161.
- [165] R.M. Salgado, F. Danzi, J.E. Oliveira, A. El-Azab, P.P. Camanho, M.H. Braga, Molecules, 26 (2021) 3188.
- [166] S. Suttison, K. Pengpat, U. Intatha, J. Fan, W. Zhang, S. Eitssayeam, Elsevier, (2022) 2347-2350.
- [167] M. Şen, M. Özcan, Y.R. Eker, Next Sustainability, 3 (2024) 100036.
- [168] G.B. Berhe, W.N.E. Su, L.H. Abrha, H.K. Bezabh, T.M. Hagos, T.T. Hagos, C.J. Huang, N.A. Sahalie, B.A. Jote, B. Thirumalraj, D. Kurniawan, C.H. Wang, B.J. Hwang, Journal of Materials Chemistry A, 8 (2020) 14043-14053.
- [169] H.P. Gao, D. Tran, Z. Chen, Current Opinion in Electrochemistry, 31 (2022) 100875.
- [170] S. Babu Sanker, R. Baby, Journal of Energy Storage, 50 (2022) 104606.
- [171] Z.F. Tang, D.D. Feng, Y.L. Xu, L. Chen, X.D. Zhang, Q. Ma, Batteries-Basel, 9 (2023) 156.
- [172] F.I. Saaid, M.F. Kasim, T. Winie, K.A. Elong, A. Azahidi, N.D. Basri, M.K. Yaakob, M.S. Mastuli, S.N. Amira Shaffee, M.Z. Zolkiffly, M.R. Mahmood, Heliyon, 10 (2024) e23968.
- [173] C.Y. Mao, M. Wood, L. David, S.J. An, Y.P. Sheng, Z.J. Du, H.M. Meyer, R.E. Ruther, D.L. Wood, Journal of the Electrochemical Society, 165 (2018) A1837-A1845.
- [174] L. Wang, J. Yu, S.Y. Li, F.S. Xi, W.H. Ma, K.X. Wei, J.J. Lu, Z.Q. Tong, B. Liu, B. Luo, Energy Storage Materials, 66 (2024) 103243.
- [175] X. Kong, Z. Xi, L. Wang, Y. Zhou, Y. Liu, L. Wang, S. Li, X. Chen, Z. Wan, Molecules, 28 (2023) 2079.
- [176] Z.L. Wang, Z.M. Mao, L.F. Lai, M. Okubo, Y.H. Song, Y.J. Zhou, X. Liu, W. Huang, Chemical Engineering Journal, 313 (2017) 187-196.
- [177] T.S. Mu, L.Z. Xiang, X. Wan, S.F. Lou, C.Y. Du, P.J. Zuo, G.P. Yin, Energy Storage Materials, 53 (2022) 958-968.
- [178] E.J. Moon, J.K. Hong, S.K. Mohanty, M. Yang, K. Ihm, H. Lee, H.D. Yoo, Journal of Power

One-step assembly of metal-ion capacitors using redox-active electrolytes

Sources, 559 (2023) 232657.

[179] D. Farhat, F. Ghamouss, J. Maibach, K. Edström, D. Lemordant, (2017).

[180] M. Soltani, S.B. Vilsen, A.I. Stroe, V. Knap, D.I. Stroe, *Journal of Energy Storage*, 68 (2023) 107745.

[181] I. Belharouak, G.M. Koenig, K. Amine, *Journal of Power Sources*, 196 (2011) 10344-10350.

[182] S. Kainat, J. Anwer, A. Hamid, N. Gull, S.M. Khan, *Materials Chemistry and Physics*, 313 (2024) 128796.

[183] Q. Li, J.E. Chen, L. Fan, X.Q. Kong, Y.Y. Lu, *Green Energy & Environment*, 1 (2016) 18-42.

[184] T.X. Wu, *International Journal of Electrochemical Science*, 17 (2022) 221171.

[185] S. Sarkar, M.J. Lefler, B.S. Vishnugopi, R.B. Nuwayhid, C.T. Love, R. Carter, P.P. Mukherjee, *Cell Reports Physical Science*, 4 (2023) 101356.

[186] S. Uchida, T. Kiyobayashi, *Journal of Power Sources*, 511 (2021) 230423.

[187] D.M. Seo, D. Chalasani, B.S. Parimalam, R. Kadam, M.Y. Nie, B.L. Lucht, *Ecs Electrochemistry Letters*, 3 (2014) A91-A93.

[188] L.H. Chen, J. Shu, Y.B. Huang, Z.P. Shi, H. Luo, Z.P. Liu, C. Shen, *Applied Surface Science*, 598 (2022) 153740.

[189] H. Du, Y. Kang, C. Li, Y. Zhao, Y. Tian, J. Lu, Z. Chen, N. Gao, Z. Li, J. Wozny, T. Li, L. Wang, N. Tavajohi, F. Kang, B. Li, *Carbon Neutralization*, 2 (2023) 416-424.

[190] A. Šimek, T. Kazda, J. Báňa, O. Čech, *Monatshefte für Chemie - Chemical Monthly*, 155 (2024) 313-317.

[191] S.S. Zhang, K. Xu, T.R. Jow, *Journal of the Electrochemical Society*, 149 (2002) A586-A590.

[192] Z. Li, L. Wang, X. Huang, X. He, *Advanced Functional Materials*, (2024).

[193] S.-Y. Ha, J.-G. Han, Y.-M. Song, M.-J. Chun, S.-I. Han, W.-C. Shin, N.-S. Choi, *Electrochimica Acta*, 104 (2013) 170-177.

[194] Y.H. Zhang, W. Lu, L.N. Cong, J. Liu, L.Q. Sun, A. Mauger, C.M. Julien, H.M. Xie, J. Liu, *Journal of Power Sources*, 420 (2019) 63-72.

[195] K.V. Kravchyk, D.T. Karabay, M.V. Kovalenko, *Sci Rep*, 12 (2022) 1177.

[196] L. Zhang, X. Zhang, G. Tian, Q. Zhang, M. Knapp, H. Ehrenberg, G. Chen, Z. Shen, G. Yang, L. Gu, F. Du, *Nat Commun*, 11 (2020) 3490.

[197] Y.X. Li, J. Yang, X.Z. Zhang, X.M. Cui, Q.M. Pan, *Journal of Materials Chemistry A*, 11 (2023) 9029-9038.

[198] K.M. Abraham, H.S. Choe, D.M. Pasquariello, *Electrochimica Acta*, 43 (1998) 2399-2412.

[199] L. El Ouatani, R. Dedryvère, C. Siret, P. Biensan, D. Gonbeau, *Journal of The Electrochemical Society*, 156 (2009).

One-step assembly of metal-ion capacitors using redox-active electrolytes

- [200] X. Zhou, P. Li, Z.H. Tang, J.L. Liu, S.W. Zhang, Y.K. Zhou, X.H. Tian, *Energies*, 14 (2021) 7467.
- [201] F. Wu, A. Mullaliu, T. Diemant, D. Stepien, T.N. Parac-Vogt, J.K. Kim, D. Bresser, G.T. Kim, S. Passerini, *InfoMat*, 5 (2023).
- [202] E.G. Shim, T.H. Nam, J.G. Kim, H.S. Kim, S.I. Moon, *Journal of Power Sources*, 172 (2007) 919-924.
- [203] Z.D. Li, Y.C. Zhang, H.F. Xiang, X.H. Ma, Q.F. Yuan, Q.S. Wang, C.H. Chen, *Journal of Power Sources*, 240 (2013) 471-475.
- [204] X.X. Zuo, J.H. Wu, M.K. Zhao, C.Y. Wang, J.S. Liu, J.M. Nan, *Ionics*, 22 (2016) 201-208.
- [205] S. Basu, G.S. Hwang, *Acta Materialia*, 235 (2022) 118077.
- [206] H. Adenusi, G.A. Chass, S. Passerini, K.V. Tian, G.H. Chen, *Advanced Energy Materials*, 13 (2023).
- [207] E. Peled, S. Menkin, *Journal of the Electrochemical Society*, 164 (2017) A1703-A1719.
- [208] Y.B. He, M. Liu, Z.D. Huang, B. Zhang, Y. Yu, B.H. Li, F.Y. Kang, J.K. Kim, *Journal of Power Sources*, 239 (2013) 269-276.
- [209] G.V. Zhuang, K. Xu, H. Yang, T.R. Jow, P.N. Ross, Jr., *J Phys Chem B*, 109 (2005) 17567-17573.
- [210] C. Groher, D.M. Cupid, A. Mautner, E. Rosenberg, J. Kahr, *Journal of Power Sources*, 605 (2024) 234481.
- [211] R. Aalund, B. Endreddy, M. Pecht, *Frontiers in Chemical Engineering*, 4 (2022).
- [212] S.K. Heiskanen, J. Kim, B.L. Lucht, *Joule*, 3 (2019) 2322-2333.
- [213] M. Soto, K. Fink, C. Zweifel, P.J. Weddle, E.W.C. Spotte-Smith, G.M. Veith, K.A. Persson, A.M. Colclasure, B.J. Tremolet de Villers, *J Chem Eng Data*, 69 (2024) 2236-2243.
- [214] B. Jagger, M. Pasta, *Joule*, 7 (2023) 2228-2244.
- [215] U.S. Meda, L.B. Lal, M. Sushantha, P. Garg, *Journal of Energy Storage*, 47 (2022) 103564.
- [216] Y. Zhang, J. Jiang, Y. An, L. Wu, H. Dou, J. Zhang, Y. Zhang, S. Wu, M. Dong, X. Zhang, Z. Guo, *ChemSusChem*, 13 (2020) 2522-2539.
- [217] S.S. Zhao, X.Z. Sun, N.F. Wang, C. Li, Y.B. An, Y.N. Xu, K. Wang, X. Zhang, Y.W. Ma, *Acs Applied Energy Materials*, (2024).
- [218] A. Chojnacka, F. Beguin, *Electrochemistry Communications*, 139 (2022) 107305.
- [219] A.K. Samantara, S. Ratha, *Metal-Ion Hybrid Capacitors for Energy Storage*, 2020, Springer, Cham, Switzerland
- [220] N. Omar, J. Ronsmans, Y. Firozu, M. Monem, A. Samba, H. Gualous, O. Hegazy, J. Smekens, T. Coosemans, P. Van den Bossche, J. Van Mierlo, *World Electric Vehicle Journal*, 6 (2013) 484-494.
- [221] M. Akshay, S. Jyothilakshmi, Y.S. Lee, V. Aravindan, *Small*, 20 (2024) e2307248.

One-step assembly of metal-ion capacitors using redox-active electrolytes

- [222] J.M. Jiang, P. Nie, B. Ding, Y.D. Zhang, G.Y. Xu, L.Y. Wu, H. Dou, X.G. Zhang, *Journal of Materials Chemistry A*, 5 (2017) 23283-23291.
- [223] A. Teasdale, L. Ishaku, C.V. Amaechi, I. Adelusi, A. Abdelazim, *World Electric Vehicle Journal*, 15 (2024) 326.
- [224] G. Mandic, A. Nasiri, E. Ghotbi, E. Muljadi, *Ieee Journal of Emerging and Selected Topics in Power Electronics*, 1 (2013) 287-295.
- [225] V. Khomenko, V. Barsukov, *Materials Today-Proceedings*, 6 (2019) 116-120.
- [226] F. Ciccarelli, A. Del Pizzo, D. Iannuzzi, *Ieee Transactions on Power Electronics*, 29 (2014) 275-286.
- [227] K.M. Abraham, *ACS Energy Letters*, 5 (2020) 3544-3547.
- [228] P. Jeżowski, A. Chojnacka, X. Pan, F. Béguin, *Electrochimica Acta*, 375 (2021) 137980.
- [229] K.Y. Zou, P. Cai, C. Liu, J.Y. Li, X. Gao, L.Q. Xu, G.Q. Zou, H.S. Hou, Z.M. Liu, X.B. Ji, *Journal of Materials Chemistry A*, 7 (2019) 13540-13549.
- [230] J. Ajuria, E. Redondo, M. Arnaiz, R. Mysyk, T. Rojo, E. Goikolea, *Journal of Power Sources*, 359 (2017) 17-26.
- [231] T. Hwang, M. Cho, K. Cho, *ACS Omega*, 6 (2021) 9492-9499.
- [232] H. Moriwake, A. Kuwabara, C.A.J. Fisher, Y. Ikuhara, *RSC Advances*, 7 (2017) 36550-36554.
- [233] J.Y. Hwang, S.T. Myung, Y.K. Sun, *Chem Soc Rev*, 46 (2017) 3529-3614.
- [234] S.K. Saju, S. Chattopadhyay, J.N. Xu, S. Alhashim, A. Pramanik, P.M. Ajayan, *Cell Reports Physical Science*, 5 (2024).
- [235] K. Kuratani, M. Yao, H. Senoh, N. Takeichi, T. Sakai, T. Kiyobayashi, *Electrochimica Acta*, 76 (2012) 320-325.
- [236] D. Morales, L.G. Chagas, D. Paterno, S. Greenbaum, S. Passerini, S. Suarez, *Electrochimica Acta*, 377 (2021) 138062.
- [237] A. Ponrouch, E. Marchante, M. Courty, J.M. Tarascon, M.R. Palacín, *Energy & Environmental Science*, 5 (2012) 8572-8583.
- [238] C. del Mar Saavedra Rios, A. Beda, L. Simonin, C. Matei Ghimbeu, *Hard Carbon for Na-ion Batteries: From Synthesis to Performance and Storage Mechanism*, in: *Na-ion Batteries*, John Wiley & Sons, United States, 2021, 101-146.
- [239] Y.J. Wu, Y.J. Sun, Y. Tong, X. Liu, J.F. Zheng, D.X. Han, H.Y. Li, L. Niu, *Energy Storage Materials*, 41 (2021) 108-132.
- [240] L.P. Wang, J.Y. Yang, J. Li, T. Chen, S.L. Chen, Z.R. Wu, J.L. Qiu, B.J. Wang, P. Gao, X.B. Niu, H. Li, *Journal of Power Sources*, 409 (2019) 24-30.
- [241] B. Babu, C. Neumann, S. Muench, M. Enke, L. Medenbach, C. Leibing, A. Lex-Balducci, A. Turchanin, U.S. Schubert, A. Balducci, *Energy Storage Materials*, 56 (2023) 342-350.
- [242] N. Li, D. Su, *Carbon Energy*, 1 (2019) 200-218.

One-step assembly of metal-ion capacitors using redox-active electrolytes

- [243] G. Vardhini, S. Suriyakumar, M.M. Shaijumon, *Acs Applied Energy Materials*, 5 (2022) 9595-9604.
- [244] J.M. Jiang, Z.W. Li, Z.T. Zhang, S.J. Wang, H. Xu, X.R. Zheng, Y.X. Chen, Z.C. Ju, H. Dou, X.G. Zhang, *Rare Metals*, 41 (2022) 3322-3335.
- [245] T. Aida, I. Murayama, K. Yamada, M. Morita, *Electrochemical and Solid State Letters*, 10 (2007) A93-A96.
- [246] M.S. Park, Y.G. Lim, J.H. Kim, Y.J. Kim, J. Cho, J.S. Kim, *Advanced Energy Materials*, 1 (2011) 1002-1006.
- [247] C. Decaux, G. Lota, E. Raymundo-Piñero, E. Frackowiak, F. Béguin, *Electrochimica Acta*, 86 (2012) 282-286.
- [248] K. Kato, M.T.E. Rodrigues, G. Babu, P.M. Ajayan, *Electrochimica Acta*, 324 (2019) 134871.
- [249] T. Aida, K. Yamada, M. Morita, *Electrochemical and Solid State Letters*, 9 (2006) A534-A536.
- [250] N. Yasuda, K. Okada, T. Chiba, K. Hiraiwa, Patent number WO2011JP70559 (2012).
- [251] M.S. Park, Y.G. Lim, J.W. Park, J.S. Kim, J.W. Lee, J.H. Kim, S.X. Dou, Y.J. Kim, *Journal of Physical Chemistry C*, 117 (2013) 11471-11478.
- [252] M.S. Park, Y.G. Lim, S.M. Hwang, J.H. Kim, J.S. Kim, S.X. Dou, J. Cho, Y.J. Kim, *ChemSusChem*, 7 (2014) 3138-3144.
- [253] Y.G. Lim, D. Kim, J.M. Lim, J.S. Kim, J.S. Yu, Y.J. Kim, D. Byun, M. Cho, K. Cho, M.S. Park, *Journal of Materials Chemistry A*, 3 (2015) 12377-12385.
- [254] K. Su, Y. Wang, B. Yang, X. Zhang, W. Wu, J. Lang, X. Yan, *Energy & Environmental Materials*, 6 (2023).
- [255] P. Jezowski, O. Crosnier, E. Deunf, P. Poizot, F. Béguin, T. Brousse, *Nat Mater*, 17 (2018) 167-173.
- [256] M. Arnaiz, M. Canal-Rodríguez, D. Carriazo, A. Villaverde, J. Ajuria, *Electrochimica Acta*, 437 (2023) 141456.
- [257] M. Walter, M.V. Kovalenko, K.V. Kravchyk, *New Journal of Chemistry*, 44 (2020) 1677-1683.
- [258] J. Barón-Jaimez, M.R. Joya, J. Barba-Ortega, *Journal of Physics: Conference Series*, 466 (2013) 12023-12024.
- [259] N. Elgrishi, K.J. Rountree, B.D. McCarthy, E.S. Rountree, T.T. Eisenhart, J.L. Dempsey, *Journal of Chemical Education*, 95 (2018) 197-206.
- [260] R. Suarez-Hernandez, G. Ramos-Sánchez, I. González, *Journal of Energy Storage*, 73 (2023) 109120.
- [261] A.C. Lazanas, M.I. Prodromidis, *ACS Meas Sci Au*, 3 (2023) 162-193.
- [262] M.F. Dupont, S.W. Donne, *Electrochimica Acta*, 167 (2015) 268-277.
- [263] M.F. Dupont, M. Forghani, A.P. Cameron, S.W. Donne, *Electrochimica Acta*, 271 (2018)

One-step assembly of metal-ion capacitors using redox-active electrolytes

337-350.

[264] M.F. Dupont, S.W. Donne, *Journal of the Electrochemical Society*, 163 (2016) A888-A897.

[265] M. Forghani, S.W. Donne, *Journal of the Electrochemical Society*, 165 (2018) A664-A673.

[266] M. Forghani, H. Mavroudis, J. McCarthy, S.W. Donne, *Electrochimica Acta*, 332 (2020) 135508.

[267] W. Weppner, R.A. Huggins, *Journal of The Electrochemical Society*, 124 (2019) 1569-1578.

[268] A. Nickol, T. Schied, C. Heubner, M. Schneider, A. Michaelis, M. Bobeth, G. Cuniberti, *Journal of the Electrochemical Society*, 167 (2020) 90546.

[269] M. Arnaiz, J. Ajuria, *Batteries & Supercaps*, 4 (2021) 733-748.

[270] B. Gorska, E. Frackowiak, F. Beguin, *Current Opinion in Electrochemistry*, 9 (2018) 95-105.

One-step assembly of metal-ion capacitors using redox-active electrolytes

Copyrights



Redox-active electrolytes as a viable approach for the one-step assembly of metal-ion capacitors

Author: Adam Maćkowiak, Paweł Jeżowski, Yukiko Matsui, Masashi Ishikawa, Krzysztof Fic

Publication: Energy Storage Materials

Publisher: Elsevier

Date: February 2024

© 2023 The Authors. Published by Elsevier B.V.

Creative Commons

This is an open access article distributed under the terms of the [Creative Commons CC-BY](#) license, which permits unrestricted use, distribution, and reproduction in any medium, provided the original work is properly cited.

You are not required to obtain permission to reuse this article.

To request permission for a type of use not listed, please contact [Elsevier](#) Global Rights Department.

Are you the [author](#) of this Elsevier journal article?



Impact of lithium bis(fluorosulfonyl)imide (LiFSI) concentration on lithium intercalation into graphite monitored with Step Potential ElectroChemical Spectroscopy (SPECS)

Author: Adam Maćkowiak, Przemysław Galek, Paweł Jeżowski, Krzysztof Fic

Publication: Electrochimica Acta

Publisher: Elsevier

Date: 20 September 2023

© 2023 The Authors. Published by Elsevier Ltd.

Creative Commons

This is an open access article distributed under the terms of the [Creative Commons CC-BY](#) license, which permits unrestricted use, distribution, and reproduction in any medium, provided the original work is properly cited.

You are not required to obtain permission to reuse this article.

To request permission for a type of use not listed, please contact [Elsevier](#) Global Rights Department.

Are you the [author](#) of this Elsevier journal article?



Unlocking the potential of acetates as electroactive additives to electrolytes for lithium-ion and sodium-ion capacitors

Author: Adam Maćkowiak, Paweł Jeżowski, Krzysztof Fic

Publication: Journal of Power Sources

Publisher: Elsevier

Date: 1 October 2024

© 2024 The Author(s). Published by Elsevier B.V.

Creative Commons

This is an open access article distributed under the terms of the [Creative Commons CC-BY](#) license, which permits unrestricted use, distribution, and reproduction in any medium, provided the original work is properly cited.

You are not required to obtain permission to reuse this article.

To request permission for a type of use not listed, please contact [Elsevier](#) Global Rights Department.

Are you the [author](#) of this Elsevier journal article?

Co-authorship statements



POLITECHNIKA POZNAŃSKA

Mgr inż. Adam Maćkowiak

Institute of Chemistry and Technical Electrochemistry
Poznan University of Technology, Berdychowo 4
61-131 Poznan, tel.: +48 (61) 665-3977
e-mail: adam.mackowiak@put.poznan.pl



Poznan, 18.07.2024

Declaration of individual contribution in publications

As the co-author of the following paper, I hereby declare that my contribution to this work was:

Article: Redox-active electrolytes as a viable approach for the one-step assembly of metal-ion capacitors

Authors: **Adam Maćkowiak**, Paweł Jeżowski, Yukiko Matsui, Masashi Ishikawa, Krzysztof Fic

Journal: Energy Storage Materials

DOI: doi.org/10.1016/j.ensm.2023.103163

Contribution: Conceptualization, data curation, formal analysis, investigation, methodology, visualization, writing – original draft

Signature

One-step assembly of metal-ion capacitors using redox-active electrolytes



POLITECHNIKA POZNAŃSKA

Mgr inż. Adam Maćkowiak

Institute of Chemistry and Technical Electrochemistry
Poznan University of Technology, Berdychowo 4
61-131 Poznań, tel.: +48 (61) 665-3977
e-mail: adam.mackowiak@put.poznan.pl



Poznan, 18.07.2024

Declaration of individual contribution in publications

As the co-author of the following paper, I hereby declare that my contribution to this work was:

Article: Impact of lithium bis(fluorosulfonyl)imide (LiFSI) concentration on lithium intercalation into graphite monitored with step potential electrochemical spectroscopy (SPECS)

Authors: **Adam Maćkowiak**, Przemysław Galek, Paweł Jeżowski, Krzysztof Fic

Journal: Electrochimica Acta

DOI: doi.org/10.1016/j.electacta.2023.142796

Contribution: Conceptualization, data curation, formal analysis, investigation, methodology, visualization, writing – original draft.

Signature

One-step assembly of metal-ion capacitors using redox-active electrolytes



POLITECHNIKA POZNAŃSKA

Mgr inż. Adam Maćkowiak

Institute of Chemistry and Technical Electrochemistry
Poznan University of Technology, Berdychowo 4
61-131 Poznań, tel.: +48 (61) 665-3977
e-mail: adam.mackowiak@put.poznan.pl



Poznan, 18.07.2024

Declaration of individual contribution in publications

As the co-author of the following paper, I hereby declare that my contribution to this work was:

Article: Unlocking the potential of acetates as electroactive additives to electrolytes for lithium-ion and sodium-ion capacitors

Authors: **Adam Maćkowiak**, Paweł Jeżowski, Krzysztof Fic

Journal: Journal of Power Sources

DOI: doi.org/10.1016/j.jpowsour.2024.235089

Contribution: Data curation, formal analysis, investigation, methodology, visualization, writing – original draft.

Adam Maćkowiak

Signature

One-step assembly of metal-ion capacitors using redox-active electrolytes



POLITECHNIKA POZNAŃSKA

Mgr inż. Adam Maćkowiak

Institute of Chemistry and Technical Electrochemistry
Poznan University of Technology, Berdychowo 4
61-131 Poznań, tel.: +48 (61) 665-3977
e-mail: adam.mackowiak@put.poznan.pl



Poznan, 26.09.2024

Declaration of individual contribution in publications

As the co-author of the following paper, I hereby declare that my contribution to this work was:

Article: Li-ion capacitor exploiting a redox-active electrolyte

Authors: **Adam Maćkowiak**, Paweł Jeżowski, Adam Ślesiński, Yukiko Matsui, Kazunari Soeda, Masashi Ishikawa, Krzysztof Fic

Journal: Submitted

DOI: -

Contribution: Conceptualization, data curation, formal analysis, investigation, methodology, visualization, writing – original draft

Signature

One-step assembly of metal-ion capacitors using redox-active electrolytes



POLITECHNIKA POZNAŃSKA

Mgr inż. Adam Maćkowiak

Institute of Chemistry and Technical Electrochemistry
Poznan University of Technology, Berdychowo 4
61-131 Poznań, tel.: +48 (61) 665-3977
e-mail: adam.mackowiak@put.poznan.pl



Poznan, 26.09.2024

Declaration of individual contribution in publications

As the co-author of the following paper, I hereby declare that my contribution to this work was:

Article: Unravelling the effects of redox-active electrolytes on carbon electrodes of Li-ion capacitor

Authors: **Adam Maćkowiak**, Przemysław Galek, Paweł Jeżowski, Krzysztof Fic

Journal: Submitted

DOI: -

Contribution: Conceptualization, data curation, formal analysis, investigation, methodology, visualization, writing – original draft

Signature

One-step assembly of metal-ion capacitors using redox-active electrolytes

Dresden, 22.07.2024

Declaration of individual contribution in publications

As the co-author of the following paper, I hereby declare that my contribution to this work was:

Article: Impact of lithium bis(fluorosulfonyl)imide (LiFSI) concentration on lithium intercalation into graphite monitored with step potential electrochemical spectroscopy (SPECS)

Authors: Adam Maćkowiak, **Przemysław Gałek**, Paweł Jeżowski, Krzysztof Fic

Journal: Electrochimica Acta

DOI: doi.org/10.1016/j.electacta.2023.142796

Contribution: Conceptualization, SPECS formal analysis and methodology, visualization, writing – review and editing.



Signature

One-step assembly of metal-ion capacitors using redox-active electrolytes

Dresden, 22.07.2024

Declaration of individual contribution in publications

As the co-author of the following paper, I hereby declare that my contribution to this work was:

Article: Unravelling the effects of redox-active electrolytes on carbon electrodes of Li-ion capacitor

Authors: Adam Maćkowiak, **Przemysław Galek**, Paweł Jeżowski, Krzysztof Fic

Journal: Submitted

DOI: -

Contribution: Conceptualization, SPECS formal analysis and methodology, visualization, writing – review and editing.



Signature

One-step assembly of metal-ion capacitors using redox-active electrolytes



POLITECHNIKA POZNAŃSKA

Dr inż. Paweł Jeżowski

Institute of Chemistry and Technical Electrochemistry
Poznan University of Technology, Berdychowo 4
61-131 Poznań, tel.: +48 (61) 665-3663
e-mail: pawel.jezowski@pul.poznan.pl



Poznan, 22.07.2024

Declaration of individual contribution in publications

As the co-author of the following paper, I hereby declare that my contribution to this work was:

Article: Redox-active electrolytes as a viable approach for the one-step assembly of metal-ion capacitors

Authors: Adam Maćkowiak, **Paweł Jeżowski**, Yukiko Matsui, Masashi Ishikawa, Krzysztof Fic

Journal: Energy Storage Materials

DOI: doi.org/10.1016/j.ensm.2023.103163

Contribution: Conceptualization, funding acquisition, investigation, methodology, supervision, validation, writing – original draft.


Signature

One-step assembly of metal-ion capacitors using redox-active electrolytes



POLITECHNIKA POZNAŃSKA

Dr inż. Paweł Jeżowski

Institute of Chemistry and Technical Electrochemistry
Poznan University of Technology, Berdychowo 4
61-131 Poznań, tel.: +48 (61) 665-3663
e-mail: pawel.jezowski@put.poznan.pl



Poznan, 22.07.2024

Declaration of individual contribution in publications

As the co-author of the following paper, I hereby declare that my contribution to this work was:

Article: Impact of lithium bis(fluorosulfonyl)imide (LiFSI) concentration on lithium intercalation into graphite monitored with step potential electrochemical spectroscopy (SPECS)

Authors: Adam Maćkowiak, Przemysław Galek, **Paweł Jeżowski**, Krzysztof Fic

Journal: Electrochimica Acta

DOI: doi.org/10.1016/j.electacta.2023.142796

Contribution: Conceptualization, investigation, methodology, supervision, validation, writing – original draft.


Signature

One-step assembly of metal-ion capacitors using redox-active electrolytes



POLITECHNIKA POZNAŃSKA

Dr inż. Paweł Jeżowski

Institute of Chemistry and Technical Electrochemistry
Poznan University of Technology, Berdychowo 4
61-131 Poznań, tel.: +48 (61) 665-3663
e-mail: pawel.jezowski@put.poznan.pl



Poznan, 20.09.2024

Declaration of individual contribution in publications

As the co-author of the following paper, I hereby declare that my contribution to this work was:

Article: Unlocking the potential of acetates as electroactive additives to electrolytes for lithium-ion and sodium-ion capacitors

Authors: Adam Maćkowiak, **Paweł Jeżowski**, Krzysztof Fic

Journal: Journal of Power Sources

DOI: doi.org/10.1016/j.jpowsour.2024.235089

Contribution: Writing – original draft, validation, supervision, methodology, investigation, funding acquisition


Signature

One-step assembly of metal-ion capacitors using redox-active electrolytes



POLITECHNIKA POZNAŃSKA

Dr inż. Paweł Jeżowski

Institute of Chemistry and Technical Electrochemistry
Poznan University of Technology, Berdychowo 4
61-131 Poznań, tel.: +48 (61) 665-3663
e-mail: pawel.jezowski@put.poznan.pl



Poznan, 20.09.2024

Declaration of individual contribution in publications

As the co-author of the following paper, I hereby declare that my contribution to this work was:

Article: Unravelling the effects of redox-active electrolytes on carbon electrodes of Li-ion capacitor

Authors: Adam Maćkowiak, Przemysław Galek, **Paweł Jeżowski**, Krzysztof Fic

Journal: Submitted

DOI: -

Contribution: Writing – original draft, validation, supervision, methodology, investigation, funding acquisition, conceptualization


Signature

One-step assembly of metal-ion capacitors using redox-active electrolytes



POLITECHNIKA POZNAŃSKA

Dr inż. Paweł Jeżowski

Institute of Chemistry and Technical Electrochemistry
Poznan University of Technology, Berdychowo 4
61-131 Poznań, tel.: +48 (61) 665-3663
e-mail: pawel.jezowski@put.poznan.pl



Poznan, 20.09.2024

Declaration of individual contribution in publications

As the co-author of the following paper, I hereby declare that my contribution to this work was:

Article: Li-ion capacitor exploiting a redox-active electrolyte

Authors: Adam Maćkowiak, **Paweł Jeżowski**, Adam Ślesiński, Yukiko Matsui, Kazunari Soeda, Masashi Ishikawa, Krzysztof Fic

Journal: Submitted

DOI: -

Contribution: Writing – original draft, validation, supervision, methodology, investigation, funding acquisition, conceptualization


Signature

One-step assembly of metal-ion capacitors using redox-active electrolytes



POLITECHNIKA POZNAŃSKA

Dr inż. Adam Ślesinski

Institute of Chemistry and Technical Electrochemistry
Poznan University of Technology, Berdychowo 4
61-131 Poznań, tel.: +48 (61) 665-3977
e-mail: adam.slesinski@put.poznan.pl



Poznan, 20.09.2024

Declaration of individual contribution in publications

As the co-author of the following paper, I hereby declare that my contribution to this work was:

Article: Li-ion capacitor exploiting a redox-active electrolyte

Authors: Adam Maćkowiak, Paweł Jeżowski, **Adam Ślesinski**, Yukiko Matsui, Kazunari Soeda, Masashi Ishikawa, Krzysztof Fic

Journal: Submitted

DOI: -

Contribution: Writing – original draft, supervision, methodology, formal analysis, writing – review and editing

Ślesinski

Signature

One-step assembly of metal-ion capacitors using redox-active electrolytes

Osaka, 20.09.2024

Declaration of individual contribution in publications

As the co-author of the following paper:

Article: Redox-active electrolytes as a viable approach for the one-step assembly of metal-ion capacitors

Authors: Adam Maćkowiak, Paweł Jeżowski, Yukiko Matsui, **Masashi Ishikawa**, Krzysztof Fic

Journal: Energy Storage Materials

DOI: doi.org/10.1016/j.ensm.2023.103163

I hereby declare that my contribution to this work was:

Contribution: Writing – review and editing, writing – original draft, supervision, methodology, funding acquisition, conceptualization.



Signature

One-step assembly of metal-ion capacitors using redox-active electrolytes

Osaka, 20.09.2024

Declaration of individual contribution in publications

As the co-author of the following paper:

Article: Li-ion capacitor exploiting a redox-active electrolyte

Authors: Adam Maćkowiak, Paweł Jeżowski, Adam Ślesiński, Yukiko Matsui,
Kazunari Soeda, **Masashi Ishikawa**, Krzysztof Fic

Journal: Submitted to "Small"

DOI: -

I hereby declare that my contribution to this work was:

Contribution: Writing – review and editing, writing – original draft, supervision,
methodology, funding acquisition, conceptualization.



Signature

One-step assembly of metal-ion capacitors using redox-active electrolytes

Osaka, 20.09.2024

Declaration of individual contribution in publications

As the co-author of the following paper,

Article: Redox-active electrolytes as a viable approach for the one-step assembly of metal-ion capacitors
Authors: Adam Maćkowiak, Paweł Jeżowski, **Yukiko Matsui**, Masashi Ishikawa, Krzysztof Fic
Journal: Energy Storage Materials
DOI: doi.org/10.1016/j.ensm.2023.103163

I hereby declare that my contribution to this work was:

Contribution: Writing – original draft, supervision, methodology, formal analysis

Yukiko Matsui

Signature

One-step assembly of metal-ion capacitors using redox-active electrolytes

Osaka, 20.09.2024

Declaration of individual contribution in publications

As the co-author of the following paper,

Article: Li-ion capacitor exploiting a redox-active electrolyte

Authors: Adam Maćkowiak, Paweł Jeżowski, Adam Ślesieński, **Yukiko Matsui**,
Kazunari Soeda, Masashi Ishikawa, Krzysztof Fic

Journal: Submitted to "Small"

DOI: -

I hereby declare that my contribution to this work was:

Contribution: Writing – original draft, supervision, methodology, formal analysis,
writing – review and editing

Yukiko Matsui

Signature

One-step assembly of metal-ion capacitors using redox-active electrolytes

Osaka, 20.09.2024

Declaration of individual contribution in publications

As the co-author of the following paper:

Article: Li-ion capacitor exploiting a redox-active electrolyte

Authors: Adam Maćkowiak, Paweł Jeżowski, Adam Ślesiński, Yukiko Matsui,
Kazunari Soeda, Masashi Ishikawa, Krzysztof Fic

Journal: Submitted to "Small"

DOI: -

I hereby declare that my contribution to this work was:

Contribution: discussion, supervision, methodology revision.


Signature

One-step assembly of metal-ion capacitors using redox-active electrolytes



POLITECHNIKA POZNAŃSKA

Dr hab. inż. Krzysztof Fic, prof. PP

Institute of Chemistry and Technical Electrochemistry
Poznan University of Technology, Berdychowo 4
61-131 Poznań, tel.: +48 (61) 665-3303
e-mail: Krzysztof.fic@put.poznan.pl



Poznan, 20.09.2024

Declaration of individual contribution in publications

As the co-author of the following paper,

Article: Redox-active electrolytes as a viable approach for the one-step assembly of metal-ion capacitors

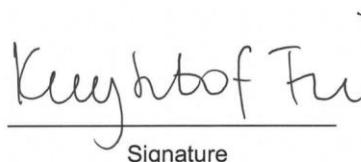
Authors: Adam Maćkowiak, Paweł Jeżowski, Yukiko Matsui, Masashi Ishikawa,
Krzysztof Fic

Journal: Energy Storage Materials

DOI: doi.org/10.1016/j.ensm.2023.103163

I hereby declare that my contribution to this work was:

Contribution: Writing – review and editing, writing – original draft, supervision,
project administration, methodology, funding acquisition, software,
conceptualization, formal analysis, investigation, resources.



Signature

One-step assembly of metal-ion capacitors using redox-active electrolytes



POLITECHNIKA POZNAŃSKA

Dr hab. Inż. Krzysztof Fic, prof. PP

Institute of Chemistry and Technical Electrochemistry
Poznan University of Technology, Berdychowo 4
61-131 Poznań, tel.: +48 (61) 665-3303
e-mail: Krzysztof.fic@put.poznan.pl



Poznan, 20.09.2024

Declaration of individual contribution in publications

As the co-author of the following paper,

Article: Impact of lithium bis(fluorosulfonyl)imide (LiFSI) concentration on lithium intercalation into graphite monitored with step potential electrochemical spectroscopy (SPECS)

Authors: Adam Maćkowiak, Przemysław Galek, Paweł Jeżowski, **Krzysztof Fic**

Journal: Electrochimica Acta

DOI: doi.org/10.1016/j.electacta.2023.142796

I hereby declare that my contribution to this work was:

Contribution: Conceptualization, formal analysis, funding acquisition, investigation, methodology, project administration, resources, software, supervision, writing – review and editing.


Signature

One-step assembly of metal-ion capacitors using redox-active electrolytes



POLITECHNIKA POZNAŃSKA

Dr hab. Inż. Krzysztof Fic, prof. PP

Institute of Chemistry and Technical Electrochemistry
Poznan University of Technology, Berdychowo 4
61-131 Poznań, tel.: +48 (61) 665-3303
e-mail: Krzysztof.fic@put.poznan.pl



Poznan, 20.09.2024

Declaration of individual contribution in publications

As the co-author of the following paper,

Article: Unlocking the potential of acetates as electroactive additives to electrolytes for lithium-ion and sodium-ion capacitors

Authors: Adam Maćkowiak, Paweł Jeżowski, **Krzysztof Fic**

Journal: Journal of Power Sources

DOI: doi.org/10.1016/j.jpowsour.2024.235089

I hereby declare that my contribution to this work was:

Contribution: Writing – review and editing, writing – original draft, supervision, project administration, methodology, funding acquisition, software, conceptualization, formal analysis, investigation, resources.

Signature

One-step assembly of metal-ion capacitors using redox-active electrolytes



POLITECHNIKA POZNAŃSKA

Dr hab. Inż. Krzysztof Fic, prof. PP

Institute of Chemistry and Technical Electrochemistry

Poznań University of Technology, Berdychowo 4

61-131 Poznań, tel.: +48 (61) 665-3303

e-mail: Krzysztof.fic@put.poznan.pl



Poznań, 20.09.2024

Declaration of individual contribution in publications

As the co-author of the following paper,

Article: Li-ion capacitor exploiting a redox-active electrolyte

Authors: Adam Maćkowiak, Paweł Jeżowski, Adam Ślesiński, Yukiko Matsui, Kazunari Soeda, Masashi Ishikawa, **Krzysztof Fic**

Journal: Submitted to "Small"

DOI: -

I hereby declare that my contribution to this work was:

Contribution: Writing – review and editing, writing – original draft, supervision, project administration, methodology, funding acquisition, software, conceptualization, formal analysis, investigation, resources.

Signature

One-step assembly of metal-ion capacitors using redox-active electrolytes



POLITECHNIKA POZNAŃSKA

Dr hab. Inż. Krzysztof Fic, prof. PP

Institute of Chemistry and Technical Electrochemistry
Poznan University of Technology, Berdychowo 4
61-131 Poznań, tel.: +48 (61) 665-3303
e-mail: Krzysztof.fic@put.poznan.pl



Declaration of individual contribution in publications

As the co-author of the following paper,

Article: Unravelling the effects of redox-active electrolytes on carbon electrodes of Li-ion capacitor

Authors: Adam Maćkowiak, Przemysław Galek, Paweł Jeżowski, **Krzysztof Fic**

Journal: Submitted to "Sustainable Materials"

DOI: -

I hereby declare that my contribution to this work was:

Contribution: Writing – review and editing, writing – original draft, supervision, project administration, methodology, funding acquisition, software, conceptualization, formal analysis, investigation, resources.

Signature